

Aus der Klinik und Poliklinik für Hals-, Nasen- und Ohrenheilkunde der Ludwig-
Maximilians-Universität München

Direktor: Prof. Dr. med. Alexander Berghaus

Leiter der HNO Forschung: Prof. Dr. rer. nat. Olivier Gires

“Expression and function of the tumor associated antigen
EpCAM in early esophageal carcinoma”

Dissertation zum Erwerb des Doktorgrades der Naturwissenschaften

an der Medizinischen Fakultät

der Ludwig-Maximilians-Universität München



vorgelegt von

Heidi Kremling

aus Rodewisch

März 2014

Gedruckt mit Genehmigung der Medizinischen Fakultät der Ludwig-Maximilians-Universität
München.

Betreuer: Prof. Dr. rer. nat. Olivier Gires

Zweitgutachter/in: Prof. Dr. rer. nat. Mechthild Stöckelhuber

Dekan: Prof. Dr. med. Dr. h.c. Maximilian Reiser, FACR, FRCR

Tag der mündlichen Prüfung: 12.11.2014

Eidesstattliche Versicherung

Heidi Kremling

Name, Vorname

Ich erkläre hiermit an Eides statt,
dass ich die vorliegende Dissertation mit dem Thema

“Expression and function of the tumor associated antigen
EpCAM in early esophageal carcinoma”

selbständig verfasst, mich außer der angegebenen keiner weiteren Hilfsmittel bedient und alle Erkenntnisse, die aus dem Schrifttum ganz oder annähernd übernommen sind, als solche kenntlich gemacht und nach ihrer Herkunft unter Bezeichnung der Fundstelle einzeln nachgewiesen habe.

Ich erkläre des Weiteren, dass die hier vorgelegte Dissertation nicht in gleicher oder in ähnlicher Form bei einer anderen Stelle zur Erlangung eines akademischen Grades eingereicht wurde.

München, den 19.11.2014

Ort, Datum

Unterschrift Doktorand/in

TABLE OF CONTENTS

| | |
|---|-----------|
| TABLE OF CONTENTS..... | I |
| 1 INTRODUCTION..... | 1 |
| 1.1 Mechanisms in cancer progression | 2 |
| 1.1.1 Basic steps of carcinogenesis | 2 |
| 1.1.2 Epithelial-to-mesenchymal transition (EMT)..... | 6 |
| 1.1.2.1 EMT in development and tissue regeneration..... | 7 |
| 1.1.2.2 EMT and cancer progression..... | 8 |
| 1.1.2.3 TGF β signaling and its role in cancer progression..... | 11 |
| 1.1.3 Mesenchymal-to-epithelial transition (MET)..... | 15 |
| 1.2 The epithelial cell adhesion molecule (EpCAM)..... | 17 |
| 1.2.1 The <i>EPCAM</i> gene | 17 |
| 1.2.2 The EpCAM protein | 19 |
| 1.2.3 Proteolytic cleavage and signaling of EpCAM | 22 |
| 1.2.4 Expression pattern of EpCAM | 25 |
| 1.2.4.1 EpCAM expression in normal tissue..... | 25 |
| 1.2.4.2 EpCAM expression in stem cells and regenerating tissue | 26 |
| 1.2.4.3 EpCAM expression in cancer cells | 26 |
| 1.2.5 Functions of EpCAM | 28 |
| 1.2.5.1 EpCAM - the cell adhesion molecule | 28 |
| 1.2.5.2 EpCAM - the cell signaling molecule | 29 |
| 1.2.5.3 EpCAM - the prognostic and therapeutic marker | 30 |
| 1.2.6 EpCAM in esophageal carcinomas..... | 31 |
| 1.3 Aim of the present study | 33 |
| 2 MATERIAL..... | 35 |
| 2.1 Chemicals..... | 35 |
| 2.2 Buffer | 37 |
| 2.2.1 Cell culture | 37 |
| 2.2.2 Flow cytometry..... | 37 |
| 2.2.3 Adhesion assay | 37 |
| 2.2.4 Membrane assay | 38 |
| 2.2.5 SDS-PAGE and western blot..... | 38 |
| 2.3 Molecular kits..... | 39 |

| | | |
|-------------|--|-----------|
| 2.4 | Antibodies | 39 |
| 2.5 | Oligonucleotids | 40 |
| 2.5.1 | qRT-PCR primer | 40 |
| 2.5.2 | siRNA | 41 |
| 2.5.3 | shRNA | 41 |
| 2.6 | Plasmids | 41 |
| 2.7 | Cell lines | 42 |
| 2.8 | Consumables | 43 |
| 2.9 | Equipment | 44 |
| 2.10 | Software | 46 |
| 3 | METHODS | 47 |
| 3.1 | Cell culture | 47 |
| 3.1.1 | Passaging of cells | 47 |
| 3.1.2 | Counting of cells..... | 47 |
| 3.1.3 | Freezing and thawing of cells..... | 47 |
| 3.1.4 | Transfection of cells | 48 |
| 3.1.4.1 | Transient transfection with MATra..... | 48 |
| 3.1.4.2 | Generation of stable cell lines | 49 |
| 3.1.5 | Flow cytometry..... | 49 |
| 3.1.5.1 | Flow cytometry analysis of membrane proteins | 49 |
| 3.1.5.2 | Flow cytometry analysis of YFP expressing cells | 50 |
| 3.1.6 | Cytospin..... | 50 |
| 3.1.7 | TGF β assay | 51 |
| 3.1.8 | Scratch assay..... | 51 |
| 3.1.8.1 | Scratch assay with Kyse 520 ^{high} and Kyse 520 ^{low} cells..... | 51 |
| 3.1.8.2 | Scratch assay with siRNA transfected Kyse 30 cells..... | 53 |
| 3.1.8.3 | Fluorescence staining of Kyse 30 and Kyse 520 ^{low} scratch assays | 53 |
| 3.1.9 | Spheroid formation | 54 |
| 3.1.9.1 | Basic spheroid formation | 54 |
| 3.1.9.2 | Spheroid invasion assay | 54 |
| 3.1.10 | Adhesion assay | 55 |
| 3.1.10.1 | Cell-matrix adhesion assay w/o calcium..... | 55 |
| 3.1.10.2 | Cell-cell adhesion assay w/o calcium..... | 56 |
| 3.2 | Molecular methods | 57 |

| | | |
|------------|--|-----------|
| 3.2.1 | Isolation of mRNA | 57 |
| 3.2.2 | Reverse transcription polymerase chain reaction (RT-PCR) | 57 |
| 3.2.3 | Quantitative Real-Time PCR (qRT-PCR) | 58 |
| 3.3 | Biochemical methods | 59 |
| 3.3.1 | Membrane assay | 59 |
| 3.3.2 | Preparation of whole cell lysates | 60 |
| 3.3.3 | Determination of protein concentration (BCA-assay)..... | 61 |
| 3.3.4 | Sodium dodecyl sulfate polyacrylamide gel electrophoresis (SDS-PAGE)..... | 61 |
| 3.3.5 | Immunoblotting (western blot)..... | 62 |
| 3.4 | Cell labeling and staining methods..... | 63 |
| 3.4.1 | Immunofluorescence | 63 |
| 3.4.2 | Immunohistochemistry | 64 |
| 3.5 | Mouse experiments | 65 |
| 3.6 | Statistical analysis | 65 |
| 4 | RESULTS | 66 |
| 4.1 | Cellular systems | 67 |
| 4.1.1 | Esophageal cancer cell lines Kyse 30 and Kyse 520..... | 67 |
| 4.1.2 | Non small lung cancer cell line A459 | 69 |
| 4.1.3 | Cell lines stably overexpressing EpCAM..... | 71 |
| 4.2 | EpCAM is cleaved in esophageal cancer cell lines..... | 75 |
| 4.3 | EpCAM increases proliferation in esophageal cancer cell lines..... | 76 |
| 4.3.1 | Knock-down of EpCAM decreases proliferation in esophageal cancer cells | 76 |
| 4.3.2 | Kyse 520 ^{high} cells proliferate faster than Kyse 520 ^{low} cells..... | 78 |
| 4.4 | EpCAM expression enhances tumor growth <i>in vivo</i>..... | 79 |
| 4.5 | Reduction of EpCAM correlates with mesenchymal traits | 82 |
| 4.5.1 | EpCAM is downregulated in migrating cells | 82 |
| 4.5.2 | Downregulation of EpCAM is associated with increased migration velocity and gain of mesenchymal markers | 85 |
| 4.5.2.1 | Kyse 30 cells migrate faster and show increased vimentin levels upon depletion of EpCAM | 85 |
| 4.5.2.2 | Kyse 520 ^{low} cells migrate faster and show higher levels of mesenchymal markers than Kyse 520 ^{high} cells | 87 |
| 4.5.2.3 | Migration velocity is enhanced in Kyse 520 ^{low} cells transfected with EpCAM-specific siRNA | 89 |
| 4.5.3 | Kyse 520 cells with lower levels of EpCAM show higher invasion capacity.... | 91 |

| | | |
|--|---|------------|
| 4.6 | EpCAM is decreased upon induced EMT | 93 |
| 4.6.1 | TGFβ treatment of A549 cells | 93 |
| 4.6.2 | TGFβ treatment of esophageal cancer cell lines..... | 95 |
| 4.6.2.1 | Effects of TGFβ treatment in Kyse 30 cells..... | 95 |
| 4.6.2.2 | Effects of TGFβ treatment in Kyse 520 ^{low} cells..... | 97 |
| 4.7 | Overexpression of EpCAM is not sufficient to prevent effects of TGFβ..... | 99 |
| 4.7.1 | EpCAM overexpression does not prevent TGFβ-induced EMT in A549 cells.. | 99 |
| 4.7.2 | EpCAM overexpression does not prevent TGFβ-induced EMT in Kyse 30 cells | 101 |
| 4.8 | How does EpCAM sustain the epithelial/ proliferative phenotype? | 104 |
| 4.8.1 | Analysis of the signaling function of EpCAM | 104 |
| 4.8.1.1 | EpCAM depletion does not activate the TGFβ pathway in A549 cells | 105 |
| 4.8.1.2 | EpCAM depletion does not activate the TGFβ pathway in Kyse 30 cells | 107 |
| 4.8.2 | Analysis of the adhesive function of EpCAM..... | 109 |
| 4.8.2.1 | Cell adhesion is not weakened in EpCAM-depleted Kyse 30 cells | 109 |
| 4.8.2.2 | EpCAM depletion impacts on cell-matrix but not cell-cell adhesion in Kyse 520 cells..... | 112 |
| 5 | DISCUSSION | 114 |
| 5.1 | EpCAM expression correlates with increased proliferation and formation of larger tumors..... | 116 |
| 5.2 | Loss of EpCAM leads to traits of EMT in esophageal cancer cells..... | 119 |
| 5.3 | The mechanism behind – How does EpCAM sustain the epithelial phenotype? | 126 |
| 5.4 | Conclusion | 131 |
| 6 | SUMMARY | 135 |
| 7 | ZUSAMMENFASSUNG (German summary)..... | 137 |
| APPENDIX | 139 | |
| ABBREVIATIONS | 139 | |
| LIST OF FIGURES AND TABLES..... | 142 | |
| Table list..... | 142 | |
| Figure list..... | 142 | |
| REFERENCES..... | 144 | |
| PUBLICATIONS | 162 | |
| ACKNOWLEDGEMENTS | 163 | |

1 INTRODUCTION

Cancer is a leading cause of death, affecting more and more people all over the world (World-Health-Organization 2013). In fact, according to current data provided by the World Health Organization, after cardiovascular and infection diseases, cancer is the third leading cause of death worldwide (World-Health-Organization 2008; World-Health-Organization 2013). Cancer is characterized by a malignant transformation of cells, enabling them to proliferate and give rise to primary tumors. During further cancer progression, tumor cells start to loosen from the primary tumor, travel through the body and eventually give rise to metastases, which represent the major reason for cancer-related deaths (Chaffer and Weinberg 2011). The increasing cancer burden, especially in the economically developed countries, is mainly due to population aging and growth as well as to a cancer-related lifestyle, including cigarettes, alcohol, rich diets and physical inactivity (Sankpal *et al.* 2012; Maziak 2013; Pericleous *et al.* 2013; World-Health-Organization 2013). Besides environmental causes, genetic abnormalities as well as certain bacteria and viruses are associated with an increased risk to develop tumors. The first gene which was found and described to be associated with tumor formation was breast cancer 1 (BRCA 1) (Hall *et al.* 1990) in 1990. In 1994 a second breast cancer associated gene, BRCA 2, was described (Wooster *et al.* 1994) and up to now there are hundreds of genes known to be associated with cancer formation and progression, including the tumor suppressor genes p53 (Jiang *et al.* 2013; Akeno *et al.* 2014), retinoblastoma protein (RB) (Manning and Dyson 2012; Dick and Rubin 2013) and phosphatase and tensin homologue (PTEN) (Sansal and Sellers 2004; Song *et al.* 2012), as well as genes involved in cell cycle regulation like cyclins and cyclin-dependent kinases (CDKs) (Gallorini *et al.* 2012; Mishra 2013). Furthermore, there is growing evidence that also non-coding regions of the genome are associated with cancer formation. Small, non-coding RNAs with a length of approximately 18-25 nucleotides, so called micro RNAs (miRNAs), were recently found to play an important role in tumorigenesis and are thereby of growing interest for researchers aiming to identify processes involved in cancer formation and progression (Lujambio and Lowe 2012; Kala *et al.* 2013; Takahashi *et al.* 2014). As already mentioned, bacterial or viral infections can act as inducers or promoters of tumorigenesis. This includes infection by hepatitis B virus (HBV), which was found to be associated with the formation of hepatocellular carcinomas (Tan 2011; Fallot *et al.* 2012), human papillomavirus (HPV), which associates with oropharyngeal and cervical carcinomas (Amirian *et al.* 2013; Panwar *et al.* 2014) and Epstein-Barr virus (EBV), which was found to be involved in the

formation of Burkitt's lymphoma as well as nasopharyngeal and gastric carcinomas (Iizasa *et al.* 2012; Fu *et al.* 2013). One example for a tumor associated bacteria, is the gram-negative bacterium *Helicobacter pylori*, which can populate the stomach and was found to be associated with gastric and lung cancer (Deng *et al.* 2013; Wroblewski and Peek 2013).

Taken together, cancer formation can be the result of a multitude of different causative agents, whereby often interplay of two or more cancer promoting effects is necessary to enable tumor growth. During the last decades scientists obtained deeper insights into how different environmental and genetic processes contribute to tumorigenesis, enabling society to provide cancer patients with innovative and more efficient treatment strategies. However, deeper understanding of cancer-related processes also disclosed the huge complexity and the intricate interplay of numerous molecular mechanisms. This complexity, as well as the fact that each tumor has its very own peculiarities, makes it so far impossible to find a treatment strategy efficiently targeting all types of cancer at all points of tumor progression.

1.1 Mechanisms in cancer progression

As this study focuses on the role of the epithelial protein EpCAM (see 1.2), the following descriptions refer to the processes involved in the formation and progression of carcinomas, a special subtype of tumors, which derive per definition from epithelial cells. However, the basic steps of tumorigenesis, including formation of a primary tumor, cell scattering by migration and invasion, circulation of cells, homing of tumor cells to secondary sites, and outgrowth of metastasis, can be observed in every type of solid cancer (Vanharanta and Massague 2013; National Cancer Institute 2014).

1.1.1 Basic steps of carcinogenesis

Formation of metastases is the major reason for cancer related deaths. 90% of patients, which die because of tumor diseases, die due the effects of metastases (Chaffer and Weinberg 2011). During the last decades scientific efforts were challenging the question how metastases form and which mechanisms are involved in this process. However, despite its high impact on prognosis and survival of patients, metastatic spread is a comparably poorly understood mechanism in cancer progression (Chaffer and Weinberg 2011).

The outgrowth of a metastasis is the endpoint of a complex set of different processes, many of them still not finally understood. Indeed, until now not even the formation of primary

tumors is comprehensively elucidated. Currently there are two hypotheses (see Fig. 1.1). The clonal evolution model is based on the assumption that tumors form from body cells, which acquired a set of mutations, either by genetic predisposition, spontaneous mutation or environmental influences like cigarette smoke, sunlight or radiation, providing them with a malignant phenotype, which eventually leads to a clonal expansion of these cells. According to this hypothesis it is assumed that all cells of a tumor are similar and have the same abilities to induce cancer formation (Foulds 1954; Nowell 1976; Greaves and Maley 2012). The second hypothesis also assumes that normal body cells mutate to cancer cells by genetic alterations, enabling them to form a primary tumor. However, this hypothesis postulates that cells of the primary tumor fundamentally differ from each other, whereby only a small cell population inherits the ability to induce cancer formation. These so-called cancer stem cells (CSCs) or tumor-inducing cells (TICs) give rise to the other tumor cells, the so-called tumor bulk, which add to tumor growth and size but are not capable to induce tumor formation by themselves. The idea of this “cancer stem cell” hypothesis was already discussed by Virchow in 1881, but first evidence that such cells really exist and play a role in cancer progression was first published in 1994 in a study by Lapidot *et al.* concerning acute myeloid leukemia (Lapidot *et al.* 1994). Since then, more and more findings supported this hypothesis (Tan *et al.* 2006; O’Flaherty *et al.* 2012; Yu *et al.* 2012). Still, until now it is not completely clarified which one of the abovementioned hypotheses reflects the processes actually taking place in tumor formation, or if both scenarios exist in different subtypes of cancer. Depending on which hypothesis actually takes place, treatment strategies would differ. In case of the clonal evolution model, every cancer cell needs to be removed in order to stop cancer progression. In contrast, in the cancer stem cell model, only the CSCs need to be eradicated, as only these cells can drive cancer progression (see Fig. 1.1).

In the next step of cancer progression, tumor cells start to loosen from the primary tumor bulk and migrate into the surrounding tissue. In carcinomas, this requires a basic modification of the cancer cells, as the epithelial cells from which the tumors derive normally form tight connections, including tight junctions, adherence junctions, desmosomes and hemidesmosomes, with neighbouring cells and the basement membrane (Chaffer and Weinberg 2011; Tiwari *et al.* 2012; Guillot and Lecuit 2013). To enable cell movement, these contacts first have to be abrogated and cells need to undergo severe morphological and molecular changes. Invasive cells were found to change their phenotype from cobblestone-like to spindle-shaped and express a set of genes involved in extracellular matrix remodeling. In other words, cells undergo phenotypic changes from epithelial to mesenchymal, which is

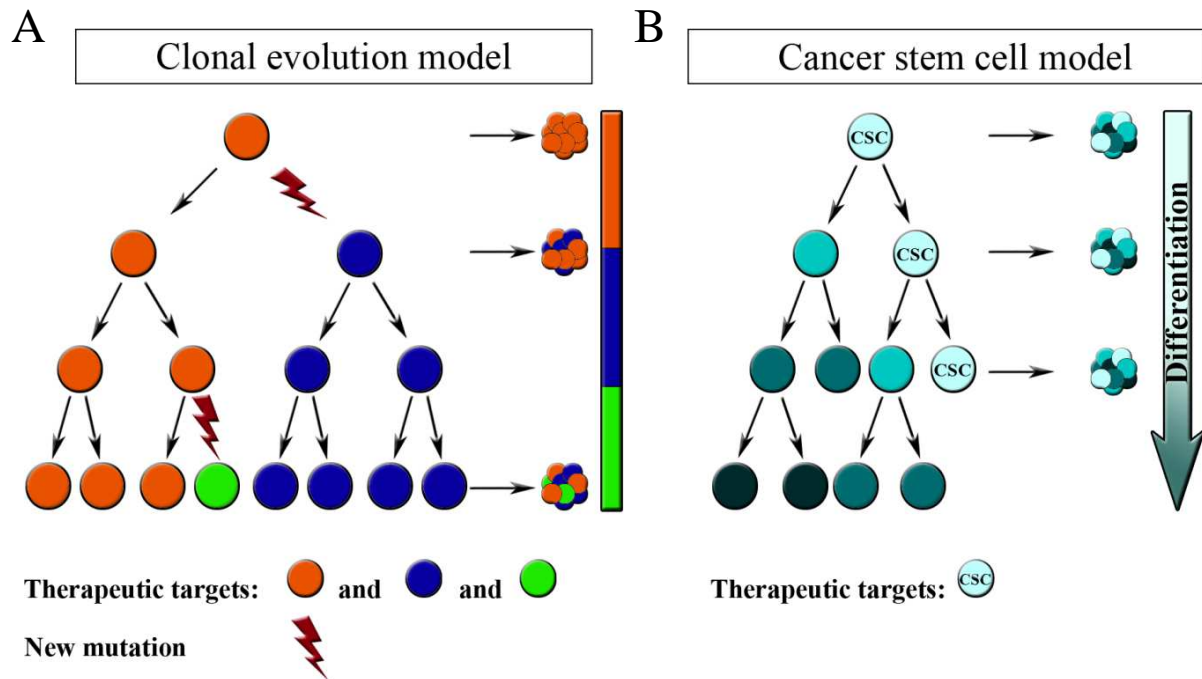


Figure 1. 1: Schematic illustration of the current cancer formation models.

Currently, two major hypotheses attempt to explain primary tumor formation. (A) The clonal evolution model proposes that tumors derive from a mutated cell, which divides and thereby gives rise to other cells with the same abilities. Differences between cancer cells are only due to new mutations and all cells are capable of tumor formation. In consequence, to get rid of a tumor, all cancer cells need to be eradicated. (B) The cancer stem cell model hypothesizes that cells in a primary tumor significantly differ in their characteristics. In this model only a subtype of cells, termed cancer stem cells (CSCs) can induce tumor formation. Accordingly, only CSCs need to be eradicated to prevent cancer progression. (Modified picture from Laks *et al.* (Laks *et al.* 2010).)

achieved in a process called epithelial-to-mesenchymal transition (EMT) (Thiery *et al.* 2009; Mathias *et al.* 2012; Tiwari *et al.* 2012) (see 1.1.2). The activation of this process in cancer cells often depends on EMT-inducing signals released from surrounding stromal cells (Yang and Weinberg 2008; Barron and Rowley 2012; Semenza 2013). Interestingly, it was found that cancer cells themselves can recruit stromal cells, including fibroblasts, myo-fibroblasts, granulocytes, macrophages, mesenchymal stem cells and lymphocytes (Chaffer and Weinberg 2011; Hanahan and Coussens 2012). After changing their phenotype, cancer cells have the ability to leave the primary tumor, locally invade into the surrounding tissue and intravasate into the blood or lymph stream, by which they get transported to secondary sites of the patient's body. The occurrence of these so-called circulating tumor cells (CTCs) was found to be correlated with increased metastatic burden, aggressiveness of cancer, decreased relapse time, decreased survival and overall bad prognosis (Chaffer and Weinberg 2011; Groot Koerkamp *et al.* 2013; Krawczyk *et al.* 2013; Tjensvoll *et al.* 2014).

Eventually, CTCs get lodged at the vascular wall of a foreign tissue, either by mechanical trapping, chemoattraction or site-specific adhesion (Abdel-Ghany *et al.* 2001; Brown and Ruoslahti 2004; Alix-Panabieres *et al.* 2008), and leave the capillary system. To do so, cells either extravasate and subsequently invade into the surrounding tissue, or they proliferate intraluminally, eventually leading to the rupture of the vascular wall (Ito *et al.* 2001; Wong *et al.* 2002; Sahai 2007; Chaffer and Weinberg 2011). Although, tumor cells deriving from different organs basically display differences in their predominant metastasation sites (Vanharanta and Massague 2013; National Cancer Institute 2014), the bone marrow has emerged as common homing organ for many different cancer subtypes, including breast, gastric, lung and prostate carcinomas (Alix-Panabieres *et al.* 2008). This might be due to the composition of the capillaries in this tissue, which are formed by only one single layer of endothelial cells, making it a rather inefficient barrier (Kopp *et al.* 2005). After homing, cancer cells, which are now termed disseminated tumor cells (DTCs), need to regain their ability to proliferate in order to give rise to overt metastases. Therefore, processes involved in EMT, which were a prerequisite for the cells to reach secondary sites of the body, at least partially need to be reversed in a process called mesenchymal-to-epithelial transition (MET) (Bonnomet *et al.* 2010; Wendt *et al.* 2012). However, although a deeper knowledge about how DTCs regain their epithelial phenotype and re-start proliferation would provide a huge step towards the understanding of the metastatic process, this step in cancerogenesis remained so far poorly investigated. This is mainly due to the experimental challenges of studying dormancy and single cells in vastly larger tissues, especially as there is so far a lack of appropriate model systems (Goss and Chambers 2010; Chaffer and Weinberg 2011).

Taken together, the process of carcinogenesis can be subdivided into four main parts: 1) formation of a primary tumor; 2) single tumor cells leaving the primary tumor and invading into blood or lymph stream; 3) homing of tumor cells to secondary sites of the body and 4) outgrowth of metastases. These steps are schematically depicted in Figure 1.2.

Globally seen, metastases formation is a highly inefficient process, as most of the tumor cells leaving a primary tumor die on their way to a secondary homing side or during the colonisation of distant organs due to stress, lack of survival signals, a hostile environment and/or reactions of the innate immune system (Luzzi *et al.* 1998; Chambers *et al.* 2002; Vanharanta and Massague 2013). However, as soon as a metastasis is formed, consequences are typically fatal as metastatic growth is associated with destruction of the affected organ, eventually leading to organ failure and usually death of the cancer patient. It is therefore

essential to understand the mechanisms leading to metastatic spread in order to prevent this process.

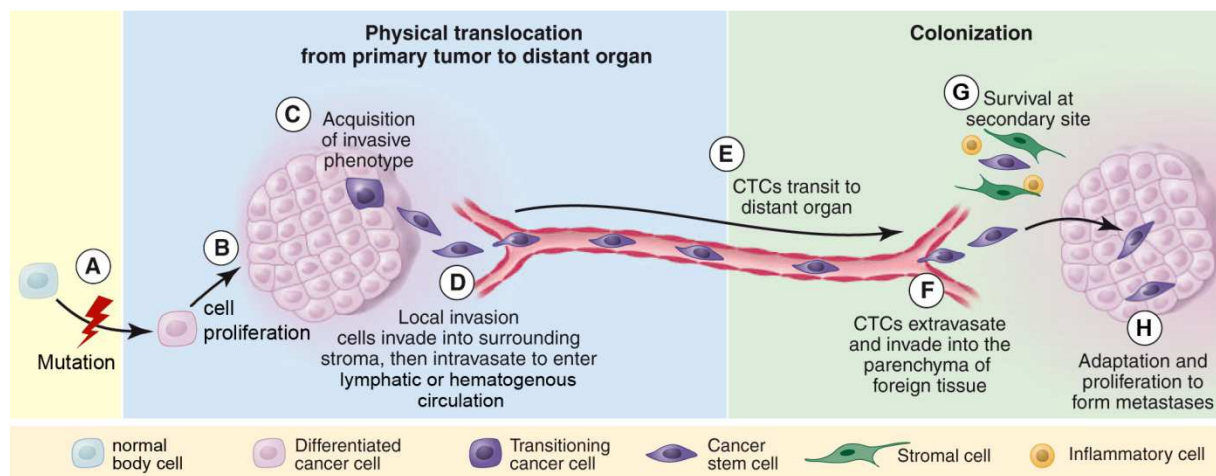


Figure 1. 2: Schematic illustration of basic mechanisms involved in carcinogenesis.

(A) Tumor formation starts with the generation of malignant cells upon single or cumulative mutations. (B) The transformed cell proliferates and eventually gives rise to a primary tumor. (C) Certain cells from the primary tumor undergo phenotypic changes enabling them to leave the primary tumor and (D) invade into the lymphoid or hematological system. (E) Via the blood and/or lymph stream the tumor cells (at this stage termed circulating tumor cells, CTCs) are transported to secondary sites of the body. (F) CTCs extravasate and invade into the surrounding tissue. (G) The cancer cells (at this stage termed disseminated tumor cells, DTCs) need to survive in the new environment. (H) In order to enable formation and outgrowth of metastases, DTCs have to adapt to the microenvironment and reactivate the proliferative phenotype. (Modified picture from Chaffer *et al.* (Chaffer and Weinberg 2011).)

1.1.2 Epithelial-to-mesenchymal transition (EMT)

Epithelial-to-mesenchymal transition (EMT) is a cellular process during which polarized epithelial cells undergo multiple biochemical changes allowing them to adopt a mesenchymal phenotype. This process is accompanied with a loss of epithelial markers as E-cadherin, cytokeratins, laminin-1 and desmoplakin, an increase of mesenchymal markers like N-cadherin, vimentin, fibronectin and TWIST and a gain of mesenchymal morphology and characteristics. These characteristics include migratory and invasive capacity, increased resistance to apoptosis and the ability to re-model the extracellular matrix (see Fig. 1.3) (Kalluri and Weinberg 2009). EMT is essential in various processes including embryogenesis, development and tissue regeneration, but is also involved in organ fibrosis and cancer progression (Kalluri and Weinberg 2009; Thiery *et al.* 2009; Ansieau *et al.* 2011).

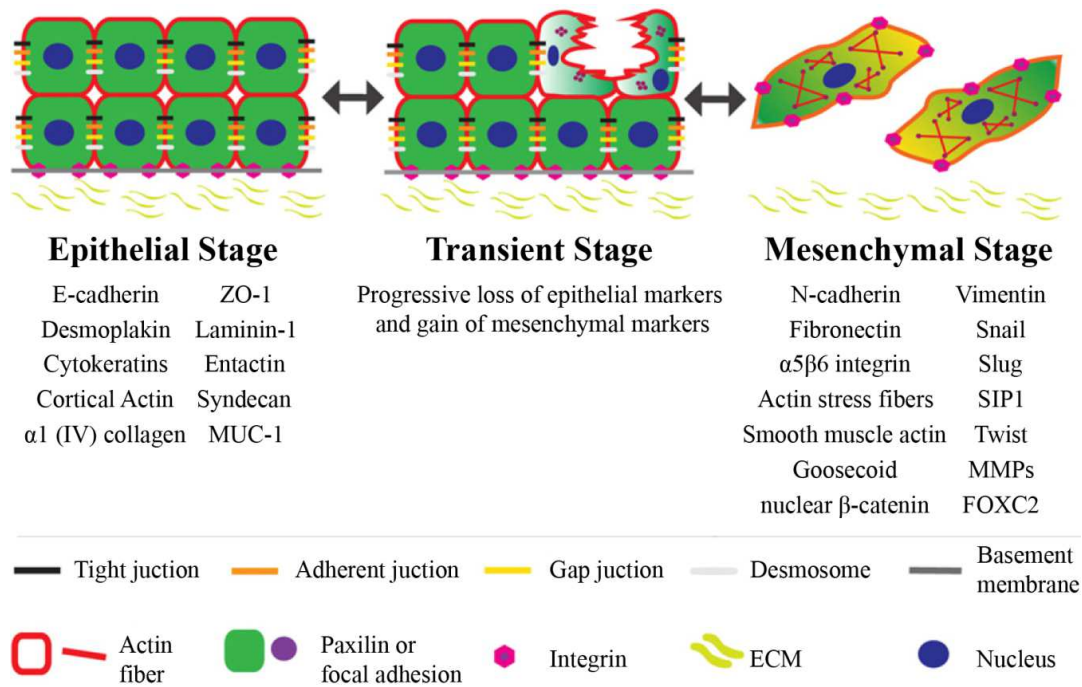


Figure 1. 3: Schematic illustration of epithelial-to-mesenchymal transition (EMT).

During EMT, polarized, epithelial cells lose their epithelial phenotype and adopt a mesenchymal phenotype. This is associated with a loss of cell adhesions and tissue integrity, but provides the cells with mesenchymal characteristics like migratory and invasive capacity, and increased resistance towards apoptosis. The process is accompanied by a substantial change of cellular markers. Listed are here accepted markers of EMT-associated changes. Co-localisation of these markers defines an intermediate phenotype, marking cells that have passed only partly through an EMT. ZO-1, Zona occludens 1; MUC-1, mucin-1, SIP1, survival of motor neuron protein interacting protein 1; MMPs, matrix metalloproteinases; FOXC2, forkhead box C2. (Modified picture from Kalluri *et al.* and Tiwari *et al.* (Kalluri and Weinberg 2009; Tiwari *et al.* 2012).)

1.1.2.1 EMT in development and tissue regeneration

The process of epithelial-to-mesenchymal transition was first described in 1995 by the pioneer work of Elizabeth Hay in a model of chick primitive streak formation (Hay 1995). During development, EMT is involved in gastrulation, neural crest formation and organ development (Thiery *et al.* 2009). Thereby EMT is not irreversible. It is rather the case that several rounds of EMT and its reversal process, the mesenchymal-to-epithelial transition (MET), are necessary for the formation of specific cell types and the complex three-dimensional structure of organs. According to these rounds of alternating EMT and MET, it is distinguished between primary, secondary and tertiary EMT (Thiery *et al.* 2009). Primary EMT processes are involved in gastrulation, including the formation and internalisation of mesodermal cells (Nakaya and Sheng 2008; Nakaya *et al.* 2008), and formation of the neural crest (Kerosuo and Bronner-Fraser 2012; Strobl-Mazzulla and Bronner 2012). Secondary and

tertiary EMT are amongst others essential for the formation of somites (Dale *et al.* 2006; Morales *et al.* 2007), palate (Ahmed *et al.* 2007; Dudas *et al.* 2007), pancreas (Villasenor *et al.* 2010), liver (Bort *et al.* 2006; Si-Tayeb *et al.* 2010) and reproductive tracts (Timms 2008), as well as for heart development (Nakajima *et al.* 2000; Person *et al.* 2005).

Processes similar to EMT are also involved in tissue regeneration in form of a physiological response to injury. Thereby keratinocytes at the boarder of the wound recapitulate parts of EMT (Thiery *et al.* 2009), which allows them to loosen cell-cell contacts, become motile and remodel the extracellular matrix around them by secreting proteases. This eventually re-establishes the function of the epithelial layer as mechanical and hydration barrier (Leopold *et al.* 2012). EMT is also involved in the tissue repairing process during postovulatory wound healing in the ovarian surface epithelium (Ahmed *et al.* 2006).

Besides the essential role during development and tissue repair, EMT is also an important element in disease-related processes. Accordingly, it was revealed that the formation of myofibroblast cells, which cause excessive collagen deposition in organs, leading to organ failure, is mainly caused by EMT and is not as originally thought due to pathological activation of interstitial fibroblasts (Iwano *et al.* 2002; Thiery *et al.* 2009). Indeed, EMT has been identified as a cause for organ fibrosis in kidney, liver, lung, heart, eye and intestine (Kim *et al.* 2006; Zeisberg *et al.* 2007; Kalluri and Weinberg 2009; Thiery *et al.* 2009). The involvement of EMT in carcinogenesis will be discussed in the following.

1.1.2.2 EMT and cancer progression

As already mentioned, tumor cells have different requirements throughout cancer progression with a phenotypic change of cancer cells from proliferative to migratory during metastatic spread (see 1.1.1). EMT is nowadays considered as the major process involved in this step of carcinogenesis (Mathias *et al.* 2012; Tiwari *et al.* 2012; Wendt *et al.* 2012). However, this was not always the case, for though EMT processes were well documented in cancer cells *in vitro*, the significance of this process for cancer progression *in vivo* was long doubted, mainly due to the lack of convincing evidence for EMT in clinical samples (Thiery *et al.* 2009). The mechanisms taking place during EMT in cancer progression are the same than those involved in development, including the reconstruction of the cytoskeleton, secretion of EMT-promoting cytokines and growth factors, remodeling of the extracellular matrix and disassembly of cell junctions (Moustakas *et al.* 2002; Zavadil and Bottinger 2005; Moustakas and Heldin 2012; Tiwari *et al.* 2012; Wendt *et al.* 2012). In most cases, induction

of EMT in malignant cells requires signaling between the cancer cells and their surrounding stromal cells, which provide tumor cells with a variety of cytokines and growth factors (Chaffer and Weinberg 2011; Tiwari *et al.* 2012), including fibroblast growth factor 2 (FGF2), epidermal growth factor (EGF), hepatocellular growth factor (HGF), platelet derived growth factor (PDGF), insulin-like growth factor (IGF), tumor necrosis factor α (TNF α) and the transforming growth factor β (TGF β) (Savagner *et al.* 1997; Strutz *et al.* 2002; Zavadil and Bottinger 2005; Yang *et al.* 2006; Lo *et al.* 2007; Tiwari *et al.* 2012). All these molecules are capable to activate the expression of EMT-promoting transcription factors like SNAIL, SLUG, TWISTs and ZEBs by activating one or more EMT-inducing pathways. This includes the mitogen-activated protein kinase (MAPK), phosphatidylinositol-3 kinase (PI3K), Wnt/ β -catenin, nuclear factor 'kappa-light-chain-enhancer' of activated B-cells (NF κ B), Notch- and Hippo/Warts pathways (Thiery 2002; Lo *et al.* 2007; Medici *et al.* 2008; Park *et al.* 2008). Figure 1.4 provides an overview on the pathways involved in EMT and shows how they are interconnected. Besides growth factor signaling, also genetic modifications can lead to EMT induction. Fibroblast growth factor receptor 2 (FGFR2) was the first gene in which alternative splicing was found to be associated with activation of EMT. Here, alternative splicing of the third Ig-like domain results in the occurrence of two receptor isoforms, which either do or do not induce EMT due to different ligand-binding specificities (Savagner *et al.* 1994). The Cadherin-Associated Protein Delta 1 (CTNND1), ENAH1 and CD44 are further genes in which alternative splicing was found to be associated with the regulation of EMT and cancer progression (Keirsebilck *et al.* 1998; Pino *et al.* 2008; Brown *et al.* 2011). In addition, the RNA binding proteins epithelial splicing regulatory protein 1 and 2 (ESRP1/2) were recently found to inhibit EMT by promoting the splicing of the epithelial-specific forms of the abovementioned genes (Warzecha *et al.* 2009; Warzecha *et al.* 2010). Also DNA and histone modifications can contribute to EMT. One example is the DNA methylation of the E-cadherin promoter and its concomitantly lower expression which can be observed in nearly all epithelial cancers (Graff *et al.* 1995; Tiwari *et al.* 2012). In addition, proteins which are a part of the chromatin remodeling polycomb repression complexes (PRC) 1 and 2 were found to be involved in EMT. BMI-1, a part of the PRC1 (Wu and Yang 2011) activates EMT by repressing the tumor suppressor gene PTEN, subsequently leading to the activation of the PI3K pathway, stabilisation of SNAIL and downregulation of E-cadherin (Song *et al.* 2009). In contrast, EZH2, a part of the PRC2 (Schuettengruber *et al.* 2007), directly inhibits E-cadherin expression by adding repressive H3K27me3 (trimethylation of lysine 27 in histone 3) marks to its promoter region (Cao *et al.* 2008).

1.1.2.3 TGF β signaling and its role in cancer progression

Among all pathways that contribute to EMT, the transforming growth factor (TGF β) pathway is one of the major and also the best examined one (Yang and Weinberg 2008; Wendt *et al.* 2012). TGF β is an ubiquitously expressed cytokine which plays a role in many different cellular processes, including development, differentiation, cell growth, survival, migration and tissue homeostasis (Moustakas and Heldin 2012; Wendt *et al.* 2012). Furthermore, it inhibits the proliferation of epithelial, endothelial and hematopoietic cell lineages by arresting them in G1-phase (Sheen *et al.* 2013). However, because of its involvement in multiple cellular processes it is also implicated in several pathological conditions, like autoimmune and cardiovascular diseases, and cancer (Gordon and Blobel 2008). Interestingly, TGF β signaling in primary carcinomas is associated with tumor repression as it inhibits cell proliferation and induces apoptosis (Sheen *et al.* 2013). The effect of TGF β on proliferation is due to the induction of the cyclin dependent kinase (CDK) inhibitors p21Cip and p15Ink4b, and the suppression of proteins correlated with enhanced proliferation, like c-Myc and ID-1,2,3 (Katz *et al.* 2013). In contrast, induction of apoptosis is provided upon the activation of pro-apoptotic caspases and members of the BCL2 family (Padua and Massague 2009). In addition, TGF β plays a role in maintaining genomic stability in cancer cells and modulation of the tumor surrounding stroma (Katz *et al.* 2013). However, it is a hallmark of tumor cells in advanced stages of carcinogenesis to develop a resistance towards the tumor suppressive function of TGF β , eventually transforming the signals provided by this cytokine into cancer-promoting ones. This functional switch is called “the TGF β paradox” (Moustakas and Heldin 2012; Wendt *et al.* 2012) and as soon as tumor cells passed it, TGF β signaling provides them with pro-survival traits including immune suppressive functions and the ability to stimulate angiogenesis. In addition TGF β induces EMT, which provides cells with the ability to leave the primary tumor, thereby enabling metastatic spread (Padua and Massague 2009; Katz *et al.* 2013; Sheen *et al.* 2013).

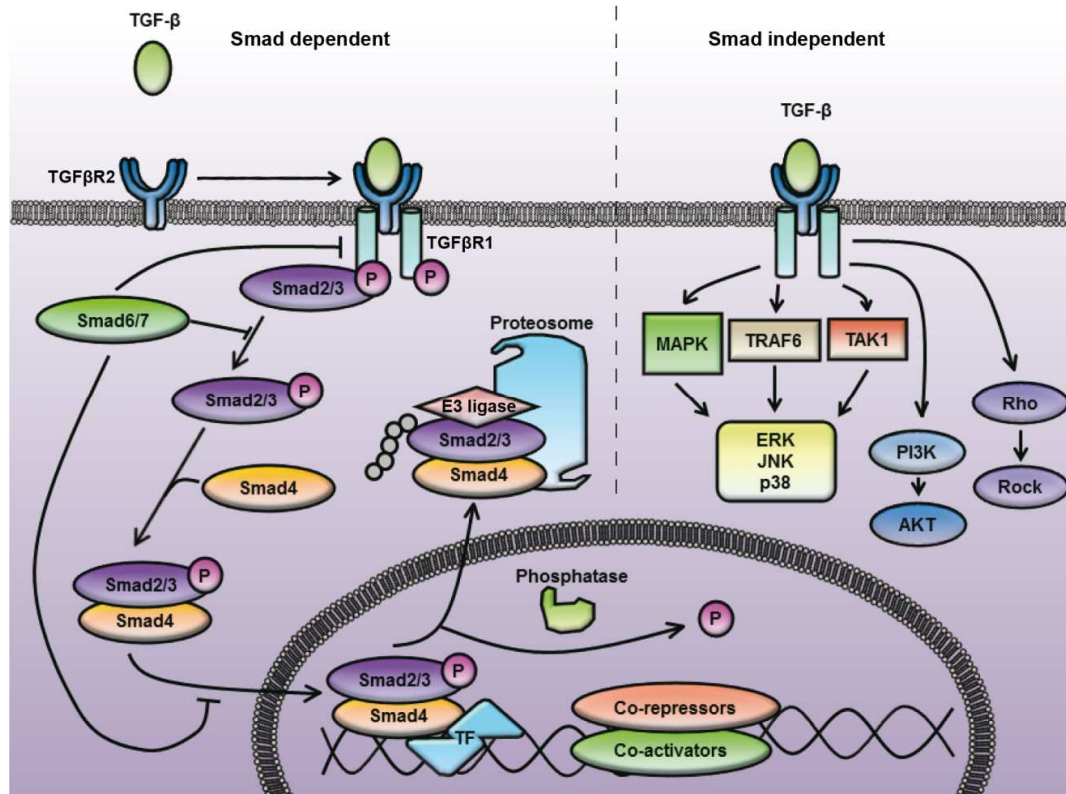


Figure 1. 5: TGFβ signaling.

TGFβ can activate SMAD-dependent and SMAD-independent pathways. For SMAD-dependent signaling, TGFβ binds and activates TGFβ-receptors I and II (TGFβR1/2), which subsequently activate SMAD 2 and 3 proteins by phosphorylation. SMAD 2/3 binds to SMAD 4 and the complex translocates into the nucleus where it activates TGFβ-specific genes. The pathway can be inhibited by SMAD 6/7. In addition, TGFβ can activate SMAD-independent signaling pathways, including the MAPK, TRAF6, PI3K and RhoA pathways. (Modified picture from Sheen *et al.* (Sheen *et al.* 2013).)

TGFβ signaling starts with the activation of the TGFβ receptors type I and II (TGFβR1/ TGFβR2), which are both transmembrane serine/threonine kinases. Thereby, TGFβ first binds and activates TGFβR2, which subsequently activates TGFβR1 upon phosphorylation. Activation of TGFβR1 then initiates canonical SMAD signaling by phosphorylating the receptor-associated SMADs (R-SMADs) SMAD2 and SMAD3. Phosphorylated SMADs then form a complex with SMAD 4. This complex translocates into the nucleus where it binds to SMAD-binding elements and activates TGFβ-specific genes. The pathway is negatively regulated by SMAD6/7 which can inhibit TGFβ signaling either by binding to activated TGFβR1, thereby preventing the phosphorylation of SMAD2/3, or by inducing the proteasomal degradation of SMAD2/3 by recruiting a specific E3 ubiquitin ligase (Moustakas and Heldin 2012; Sheen *et al.* 2013). Besides the SMAD-dependent signal pathway, TGFβ can also activate SMAD-independent signal mechanism, including the PI3K, MAPK, RhoA-ROCK and TRAF6-TAK1 pathways (Derynck and Zhang 2003) (see Fig. 1.5).

Regarding EMT, TGF β signaling results in the activation of the most important EMT promoting transcription factors, which are the E-box binding zinc finger proteins SNAIL, SLUG, ZEB1 and ZEB 2, as well as the basic helix-loop-helix proteins TWIST1 and 2 (Park *et al.* 2008; Moustakas and Heldin 2012). Expression of these molecules subsequently activates various EMT programs, including the remodelling of the cytoskeleton, secretion of EMT-promoting cytokines and growth factors, like FGF2, interleukin-like EMT-inducer (ILEI), Wnt, Jagged, HGF and EGF, remodeling of the extracellular matrix and disassembly of cell junctions (Moustakas *et al.* 2002; Zavadil and Bottinger 2005; Moustakas and Heldin 2012; Wendt *et al.* 2012) (see Fig. 1.6). SNAIL, SLUG and the ZEB proteins act as transcriptional repressors of E-cadherin and other proteins associated with epithelial phenotype and functions, like the tight junction proteins occludin and CAR (coxsackie and adenovirus receptor), and induce the expression of mesenchymal genes. In contrast, TWIST 1 and 2 mainly induce expression of mesenchymal and pro-invasive genes (Vincent *et al.* 2009; Nieto 2011). Interestingly, activation of the transcription factors SNAIL and SLUG by TGF β signaling, vice versa also induces the expression of TGF β (Medici *et al.* 2008). In addition, it was found that SNAIL contributes to the upregulation of SLUG, and that induction of ZEB1 depends on the cooperation of SNAIL and TWIST 1 (Medici *et al.* 2008; Taube *et al.* 2010; Dave *et al.* 2011). The intense cross-regulation of cytokines and transcription factors is a hallmark of EMT and provides a consecutive feed-forward loop allowing the ultimate progression into the mesenchymal phenotype (Moustakas and Heldin 2012). Figure 1.6 provides an overview of various molecules and mechanisms, which are regulated upon TGF β -induced EMT, and also depicts a large number of proteins and RNAs, which were found to be involved in the regulation of these processes.

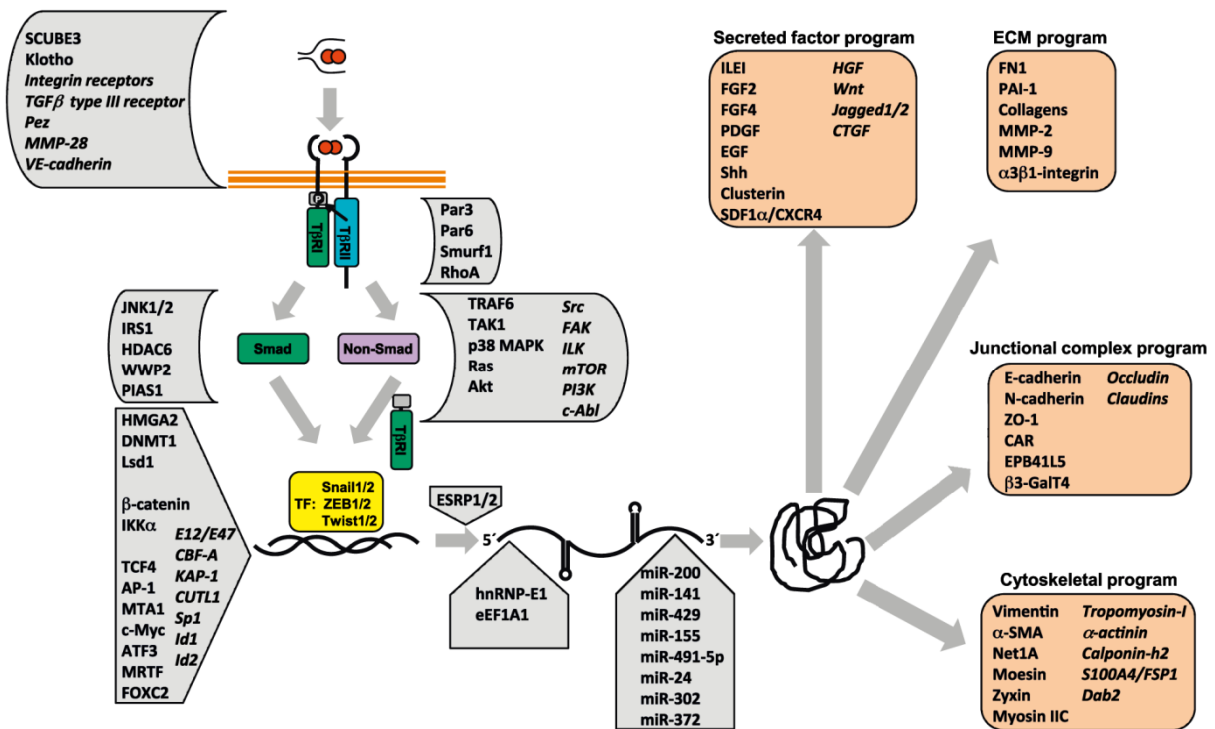


Figure 1. 6: TGFβ-dependent activation of EMT.

TGFβ induces epithelial-to-mesenchymal transition by activating EMT-promoting transcription factors upon SMAD-dependent or -independent pathways. This eventually leads to activation of various EMT programs (beige boxes). TGFβ-induced EMT is regulated by a large subset of different proteins and RNAs (grey boxes). (Modified picture from Moustakas *et al.* (Moustakas and Heldin 2012).)

As it is such a strong and important inducer of EMT, inhibition of TGFβ signaling has emerged as anti-cancer therapy approach. Current strategies can be subdivided into three groups, i.e. prevention of TGFβ expression using antisense molecules, inhibition of the ligand-receptor interaction by monoclonal antibodies or ligand traps, and inhibition of the signaling cascade by using TGFβ receptor kinase inhibitors and aptamers (Padua and Massague 2009; Sheen *et al.* 2013). For each of these approaches several molecules, which are currently either in non-clinical or early clinical trials, have been developed (Sheen *et al.* 2013). However, caution is needed when targeting TGFβ in cancer cells, as depletion of this molecule or its signaling cascade might induce mesenchymal-to-epithelial transition in certain cancer cells, thereby enabling the outgrowth of metastases (see 1.1.3).

1.1.3 Mesenchymal-to-epithelial transition (MET)

Epithelial-to-mesenchymal transition was found to be an essential progress during cancer progression, enabling cells to leave the primary tumor and translocate to secondary sites of the body. However, for the outgrowth of metastases, tumor cells need to reverse the EMT process and regain their proliferative phenotype (Bonnomet *et al.* 2010). As during development, where cycles of EMT and its reversal process mesenchymal-to-epithelial transition (MET) allow the formation of specific tissues and cell types (Yang and Weinberg 2008; Thiery *et al.* 2009), the current opinion is that the epithelial, proliferative phenotype of tumor cells is comparably reactivated by MET during cancer progression. Data supporting this idea were recently provided by Chao *et al.* and Dykxhoorn *et al.*, who showed that metastatic outgrowth of breast cancer cells in the lungs of mice is promoted by initiation of the MET program and the concomitant elevation of E-cadherin levels (Dykxhoorn *et al.* 2009; Chao *et al.* 2010).

In contrast to EMT, which was intensively studied in development and disease, relatively little is known about the induction of and the processes involved in MET (Yang and Weinberg 2008; Kalluri and Weinberg 2009). The best studied example for MET is the formation of nephron epithelium during kidney development, where mesenchymal cells start to polarize, develop cell adhesions and differentiate into epithelial cells, which form the kidney tubules (Davies 1996). This process was found to be driven by proteins like paired box 2 (PAX2), Wilms tumor 1 (WT1) and the bone morphogenic factor 1 (BMP-1) (Rothenpieler and Dressler 1993; Lipschutz 1998), which was also found to be involved in the MET process occurring during kidney regeneration (Zeisberg *et al.* 2005). Studies focusing on the role of MET on metastatic outgrowth of cancer so far revealed that inhibition of canonical SMAD-signaling by inhibition of SMAD2 or overexpression of SMAD7 (see Fig. 1.6) is sufficient to induce MET and formation of overt metastases in a breast cancer progression model (Papageorgis *et al.* 2010). Furthermore, it has been shown that overexpression of miR-200, which was found to prevent EMT and thereby helps to maintain epithelial integrity (Korpal *et al.* 2008; Mongroo and Rustgi 2010), enhances formation of macroscopic metastases in mice (Dykxhoorn *et al.* 2009). Also TGF β , a master inducer of EMT in cancer cells, is suggested to be associated with metastatic growth. Though TGF β downregulation might interfere with the formation of migrating CTCs, in DTCs already located at secondary sites such interference could rather lead to induction of metastatic outgrowth by activation of the MET program (Shipitsin *et al.* 2007; Wendt *et al.* 2012). Last but not least, as in the case of EMT, also the

microenvironment is discussed to induce MET in cancer cells, either by providing MET-activating signals or simply due to the lack of EMT-promoting signals (Kalluri and Weinberg 2009).

Although EMT and MET in cancer cells are often depicted as two straight processes allowing cells to switch from the epithelial to the mesenchymal phenotype or vice versa, the reality seems to be more subtle and complex. In many carcinomas, cells seem to undergo only partly processes of EMT, resulting in cancer cells holding both epithelial and mesenchymal markers and thereby displaying a phenotype, which is not observable in normal tissues (Yang and Weinberg 2008; Saito *et al.* 2009; Chaffer and Weinberg 2011). This kind of “intermediate phenotype” might provide cancer cells with enhanced plasticity, allowing easier switching between a more epithelial and a more mesenchymal phenotype. As both, EMT and MET, have been shown to be critical steps in carcinogenesis, a better knowledge about these processes is mandatory to efficiently interfere with cancer progression.

1.2 The epithelial cell adhesion molecule (EpCAM)

This study was performed to provide deeper insights into the specific functions of EpCAM during tumor formation and progression. The next chapter of the introduction summarizes the current knowledge on EpCAM expression and functions.

1.2.1 The *EPCAM* gene

The human *EPCAM* gene is a member of the tumor-associated antigen gene family GA-733 (Linnenbach et al. 1989; Szala et al. 1990; Alberti et al. 1994). The gene is located on chromosome 2 (location 2p21), has a size of around 17.9 kb (NCBI 2014) and is comprised of 9 coding exons, which are transcribed into a 1.5 kb long mRNA (Balzar et al. 1999b). Exons 1-6 encode the extracellular domain of the protein, including an epidermal growth factor (EGF)-like domain, a thyroglobulin (TY)-like domain and a cysteine-depleted region, as well as the signal peptide, which is later cleaved off from the protein, but is essential for its transport into the endoplasmic reticulum and the golgi-mediated transport to the cell membrane. The transmembrane domain of EpCAM is encoded by exon 7, and the exons 8-9 encode the intracellular domain of the protein (see Fig. 1.7) (Schnell et al. 2013). The *EPCAM* gene is highly conserved among different species, including mouse, rat, zebrafish and human, showing a sequence homology of 81% between human and mouse and 98% between man and gorilla (Bergsagel et al. 1992; Schnell et al. 2013).

A Chromosome 2

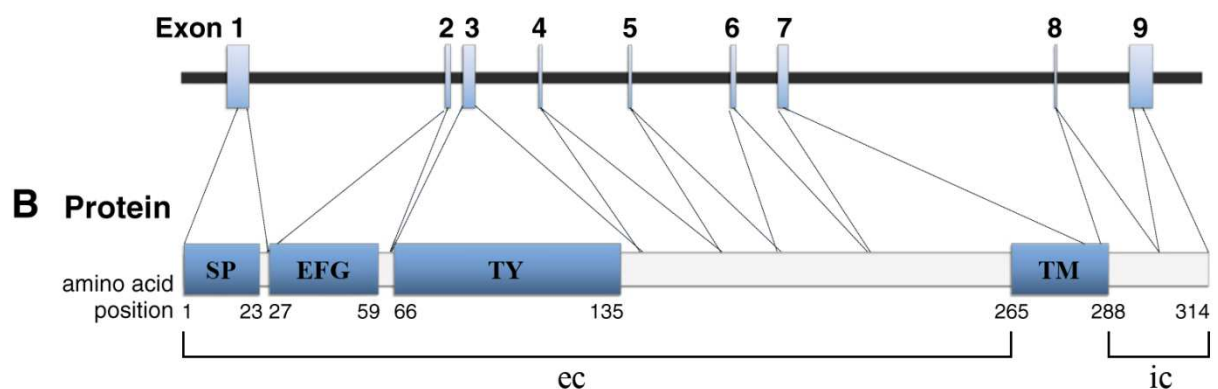


Figure 1. 7: The *EPCAM* gene.

The *EPCAM* gene (A) contains 9 exons, which encode the EpCAM protein (B) as indicated. SP, signal peptide; EGF, epidermal growth factor-like domain; TY, thyroglobulin-like domain; TM, transmembrane domain; ec, extracellular domain; ic, intracellular domain. (Modified picture from Schnell et al. (Schnell et al. 2013).)

Studies concerning the 5'-regulatory region of the *EPCAM* gene revealed a lack of a TATA and a CAAT box. Instead, other eukaryotic promoter elements such as initiator consensus sequences and GC boxes, as well as consensus binding sequences for SP-1, activator protein 1 (AP-1), activating protein 2 (AP-2), ETS, ESE-1 and E-pal-like transcription factors, which are known to play a role in epithelial specific expression, were detected (Behrens et al. 1991; Lee et al. 1996; McLaughlin et al. 2004). In addition, it was found that 177 bp of the 5'-flanking region are sufficient to obtain maximal activity of the promoter. In contrast, 687 bp of the 5'-flanking region are necessary to ensure epithelial specificity (McLaughlin *et al.* 2004). The expression of EpCAM was found to be impaired by NF κ B, TNF α und INF γ (Gires et al. 2001; Gires et al. 2003) and activated by TCF/ β -catenin (Yamashita et al. 2007).

The only mutation of the *EPCAM* gene known so far is associated with an intestinal disease called congenital tufting enteropathy (CTE). Patients suffering from this disease show a homozygous G \rightarrow A substitution at the donor splice site of exon 4, leading to a divergent EpCAM isoform, which does not localize to the plasma membrane anymore. This results in a dysplasia of the intestine, associated with a severe malfunction and high lethality (Sivagnanam et al. 2008). Similar symptoms were reported in two EpCAM knock-out mouse models (Guerra *et al.* 2012; Lei *et al.* 2012). Guerra *et al.* showed that EpCAM knock-out mice died soon after birth because of hemorrhagic diarrhea, due to intestinal defects, including intestinal tufts, villous atrophy and colon crypt hyperplasia. As all these abnormalities can also be observed in patients with CTE, Guerra *et al.* provided the first animal model for this disease (Guerra *et al.* 2012). In addition, they provided a rationale for the observed intestinal defects by showing that the loss of EpCAM leads to dysregulation of E-cadherin and β -catenin and thereby to abnormalities in the architecture and function of the intestine (Guerra *et al.* 2012). Another group found evidence that intestinal defects of EpCAM knock-out mice were due to an abnormal morphology of tight junctions (Lei *et al.* 2012). They showed that in normal intestines, EpCAM co-localizes and associates with claudin-7 to form proper cell-cell junctions. Furthermore, EpCAM was also found to form complexes with claudins-2, -3 and -15. In EpCAM-depleted cells, however, expression of all these proteins was repressed, with claudin-7 being downregulated to undetectable levels. This, in consequence led to the formation of morphologically abnormal tight junctions. Taken together, Lei *et al.* could show that EpCAM recruits claudins to cell-cell junctions and thereby contributes to the barrier function of the intestine (Lei *et al.* 2012).

1.2.2 The EpCAM protein

As its name implicates, the epithelial cell adhesion molecule (EpCAM) is part of the cell adhesion molecule (CAM)-family. It consists of 314 amino acids (AA) and can be subdivided in three main parts: a large extracellular domain, a single transmembrane domain and a small intracellular domain (Balzar *et al.* 1999b; Gires 2008) (see Fig. 1.8). The extracellular domain includes the signal peptide and consists of 265 AA. The 23 AA long signal peptide is cleaved off by signal peptidases in the endoplasmic reticulum. Thereby, signal peptidases cut primarily between alanine 23 and glutamine 24 (Strnad *et al.* 1989; Szala *et al.* 1990; Chong and Speicher 2001). However, a small proportion (around 1%) of EpCAM becomes cleaved between AA 21 and 22 (Chong and Speicher 2001). The mature extracellular domain consists of 242 AA and contains two different motifs, i.e. a EGF-like domain between AA 27-59 and a type 1a TY-like domain between AA 66-135 (Gires 2008). The TY-motif is conserved in many different proteins and plays a role as tumor suppressor as it binds and inhibits cathepsins (Meh *et al.* 2005), which are involved in tumor progression and metastases formation (Nomura and Katunuma 2005; Tan *et al.* 2013). However, a role of EpCAM as substrate or inhibitor of cathepsins was so far not described (Schnell *et al.* 2013). In 2001, Balzar *et al.* reported that the cell adhesion function of EpCAM (see 1.2.5.1) is mediated by its EGF-like and TY-like domains, which allow for the formation of EpCAM tetramers (Balzar *et al.* 2001). Thereby the TY-like domain mediates the lateral contact, whereas the EGF-like domain enables the connection of EpCAM molecules from two different cells, the so called homophilic cell-cell adhesion (Balzar *et al.* 1999a; Balzar *et al.* 1999b; Balzar *et al.* 2001). In a linear view of EpCAM's extracellular domain, this model makes sense. However, TY-domains generate a 180° bend in all proteins analyzed so far (Molina *et al.* 1996; Novinec *et al.* 2006; Mihelic and Turk 2007). Thus, it remains somewhat unclear how both domains in the extracellular part of EpCAM contribute to cell adhesion. After the TY-like domain, there is a cystein-depleted region, followed by the 23 AA long single transmembrane domain of the EpCAM protein, which was shown to be associated with the tight junction protein claudin-7 (Nubel *et al.* 2009). The transmembrane domain is followed by the 26 AA long intracellular domain of EpCAM. This domain contains two putative α -actinin binding consensus sequences, which are located between the AA 290-296 and 304-314. The binding of α -actinin was found to be essential for the adhesive function of EpCAM as α -actinin connects EpCAM with the actin cytoskeleton (Balzar *et al.* 1998).

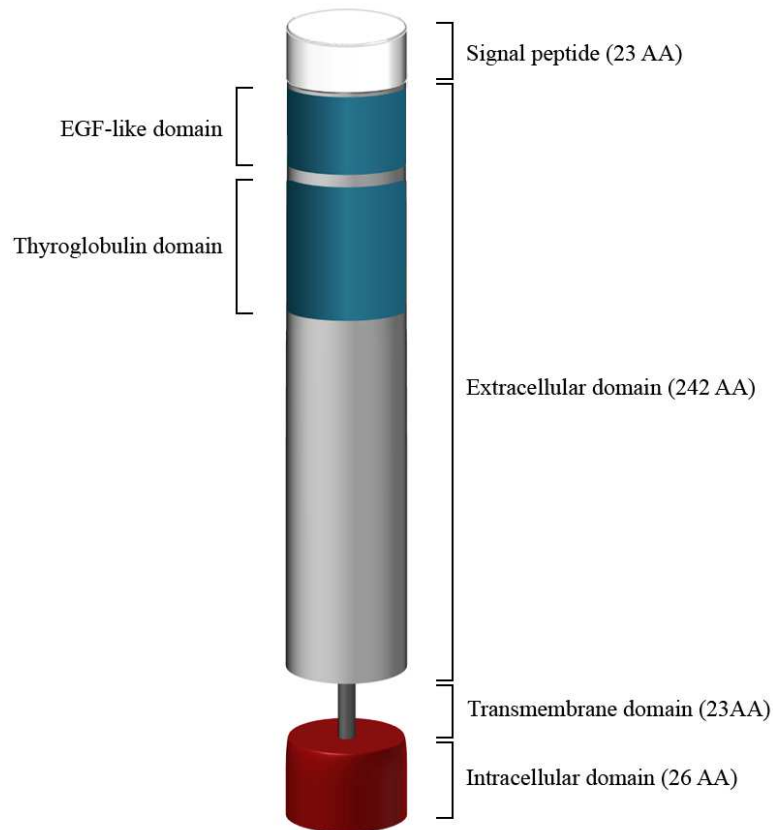


Figure 1. 8: The EpCAM protein.

EpCAM consists of 314 AA and can be subdivided in three main parts: a large extracellular domain, including the signal peptide, which gets cleaved off in the endoplasmic reticulum, a single transmembrane domain and small intracellular domain.

The extracellular domain of EpCAM contains three glycosylation sites, which are located at the asparagine residues 74, 111 and 198 (N^{74} , N^{111} , N^{198}). Various glycosylation of these sites result in EpCAM variants, which display different molecular weights of 34, 40 or 42 kDa (Thampoe et al. 1988; Schon et al. 1993; Litvinov et al. 1994b). Glycosylation of N^{198} was furthermore found to be important for the stability of EpCAM as mutation of this site from asparagine to alanine was associated with decreased overall EpCAM protein levels and shorter half-life time of the protein at the cell membrane (Munz et al. 2008). Glycosylation of EpCAM does apparently also play a role in tumor cells. It was found that EpCAM is heavily glycosylated in head and neck carcinoma cells, whereas it showed no or weak glycosylation in healthy tissues (Pauli et al. 2003). It is therefore tempting to speculate that different glycosylation of EpCAM is associated with the regulation of the stability and, consequently, of the functions of the protein in malignant and healthy tissue (Schnell *et al.* 2013). Figure 1.9 depicts a detailed illustration of the EpCAM sequence and its posttranslational modifications.

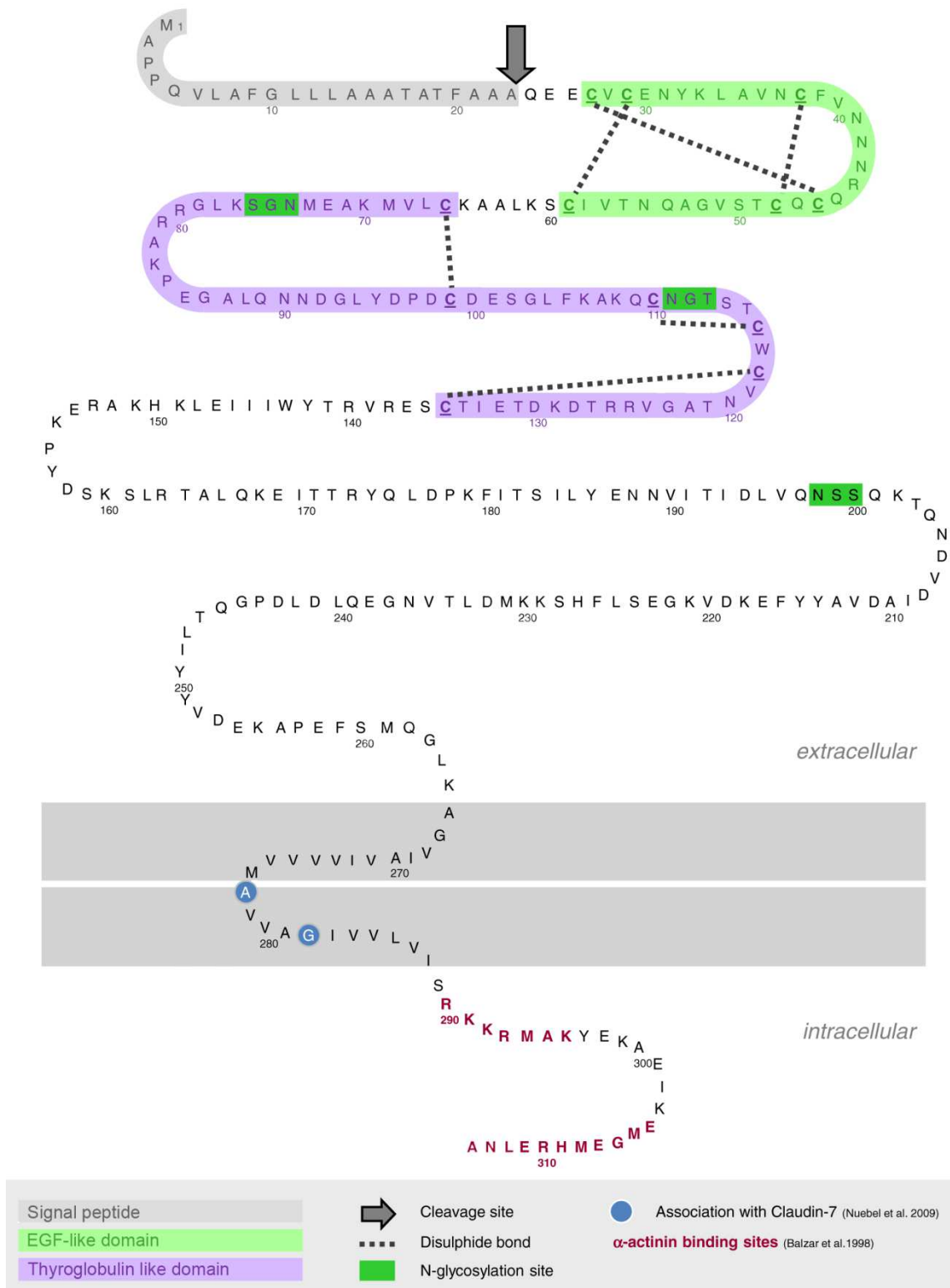


Figure 1. 9: Amino acid sequence of EpCAM.

Amino acid sequence of EpCAM with posttranslational modifications and putative binding motifs. Arrow, cleavage site of the signal peptidase. (Modified picture from Schnell *et al.* (Schnell *et al.* 2013).)

1.2.3 Proteolytic cleavage and signaling of EpCAM

Although EpCAM is studied since the late 1970s, the cleavage of EpCAM was discovered only recently in a study by Maetzel *et al.* in which the group provide evidence that EpCAM is cleaved upon regulated intramembrane proteolysis (RIP) and provide a mechanism how EpCAM signaling functions (Maetzel *et al.* 2009) (see Fig. 1.10).

Juxtacrine cell-cell interactions represent one way of the induction of EpCAM cleavage (Denzel *et al.* 2009). It is believed that cell-cell contact allows for the interaction of EpCAM molecules on opposing cells or, alternatively, for the interaction of EpCAM with a yet unknown ligand. These interactions trigger a cascade of cleavage processes termed regulated intramembrane proteolysis. In a first step, the extracellular domain of EpCAM (EpEX) is cleaved off from the remaining molecule by the tumor necrosis factor alpha-converting enzyme (TACE, ADAM17), a member of the ADAM protein family (Edwards *et al.* 2008). This is a prerequisite for the second cleavage of the c-terminal part of EpCAM (EpCAM-CTF), which is still an integral part of the plasma membrane. In addition, it was found that the soluble EpEX provides a positive feedback loop and enhances RIP of EpCAM in a paracrine way (Denzel *et al.* 2009). During the second step of RIP, EpCAM-CTF is cleaved by a γ -secretase complex, which contains presenilin-2 (PS-2). This results in the formation of cytoplasmic EpICD (the intracellular domain of EpCAM) and a small extracellular fragment of EpCAM, with a so far unknown function. Following the second cleavage, EpICD is released into the cytoplasm and forms complexes with four and a half LIM domains protein 2 (FHL-2) and β -catenin. Thereby FHL-2 was found to be the central interaction partner of EpCAM, binding to EpICD via its fourth LIM domain. As FHL-2 also binds β -catenin with its second and third LIM domain (Martin *et al.* 2002; Labalette *et al.* 2004), it was hypothesized that FHL-2 is essential for EpCAM signaling as scaffold protein (Imrich *et al.* 2012). After formation, the abovementioned complex can translocate into the nucleus and bind the transcription factor lymphoid enhancer-binding factor 1 (Lef-1) (Barolo 2006), which enables the activation of EpCAM-specific target genes, including genes involved in cell proliferation and “stemness” (Maetzel *et al.* 2009; Lu *et al.* 2010; Imrich *et al.* 2012; Chaves-Perez *et al.* 2013) (see Fig. 1.10).

Compared to tumor cells, EpCAM cleavage seems to occur to a much lower extent in normal epithelia. In addition, no EpICD signals could so far be detected in the nuclei, but only in the cytoplasm, of normal colon mucosa (Maetzel *et al.* 2009). A possible explanation for this are different expression levels of proteins involved in EpCAM signaling, like TACE,

presenilin-2 and FHL-2, in healthy and malignant tissues (Johannessen *et al.* 2006; Kenny 2007; Selkoe and Wolfe 2007). Alternatively, cleavage might occur at similar rates in normal cells, but products might be less stable or nuclear translocation impaired.

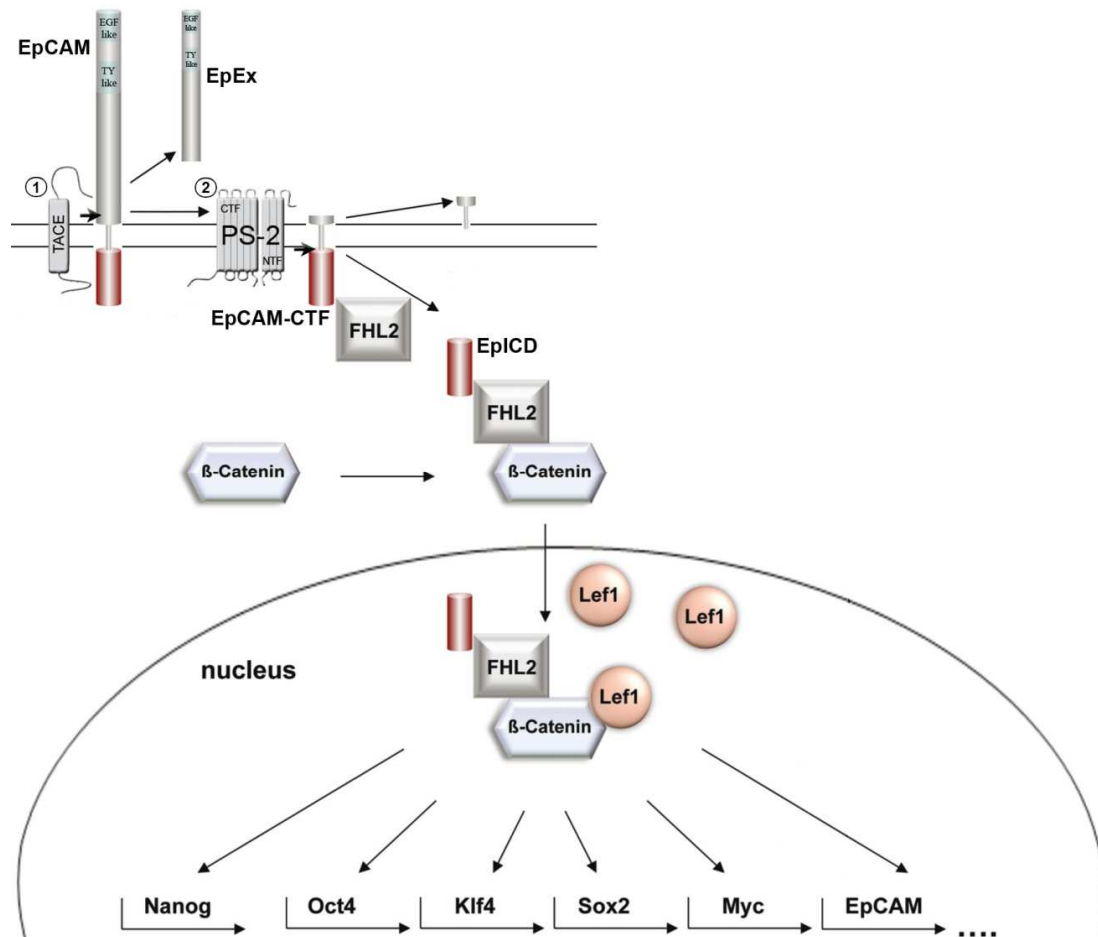


Figure 1. 10: Cleavage and signaling of EpCAM.

EpCAM is cleaved upon regulated membrane proteolysis. In a first step, EpCAM gets cleaved by TACE (1), which leads to the release of the extracellular part of EpCAM (EpEx) and is prerequisite for the second cleavage, during which the C-terminal fragment of EpCAM (EpCAM-CTF) is cleaved by a presenilin-2-containing γ -secretase complex (2). The second cleavage leads to the release of the internal part of EpCAM (EpICD) into the cytoplasm, where it forms complexes with FHL-2 and β -catenin, which eventually translocate in the nucleus, bind to Lef-1 transcription factors and activate EpCAM-specific target genes. (Modified picture from Imrich *et al.* and Maetzel *et al.* (Maetzel *et al.* 2009; Imrich *et al.* 2012).)

Recent findings by Hachmeister *et al.* revealed another protein, which is involved in the cleavage of EpCAM (Hachmeister *et al.* 2013). The β -secretase-1 (BACE-1), which also plays a central role in the generation of the pathologic A β -fragment in the neurodegenerative Alzheimer`s disease (Vassar *et al.* 2009; Ghosh *et al.* 2012; Nalivaeva and Turner 2013), was discovered as new sheddase in the RIP of murine and human EpCAM. The specificity of

BACE-1 cleavage was assured by using combinations of overexpression of BACE-1 and BACE-1-specific inhibitors, resulting in a significantly increased or reduced EpCAM processing, respectively (Hachmeister *et al.* 2013). As BACE-1 has a pH optimum of 4.5, it was hypothesized that BACE-1-based EpCAM cleavage occurs in acidic, intracellular compartments (endosomes/lysosomes) after previous endocytosis of EpCAM (Hachmeister *et al.* 2013) (see Fig. 1.11).

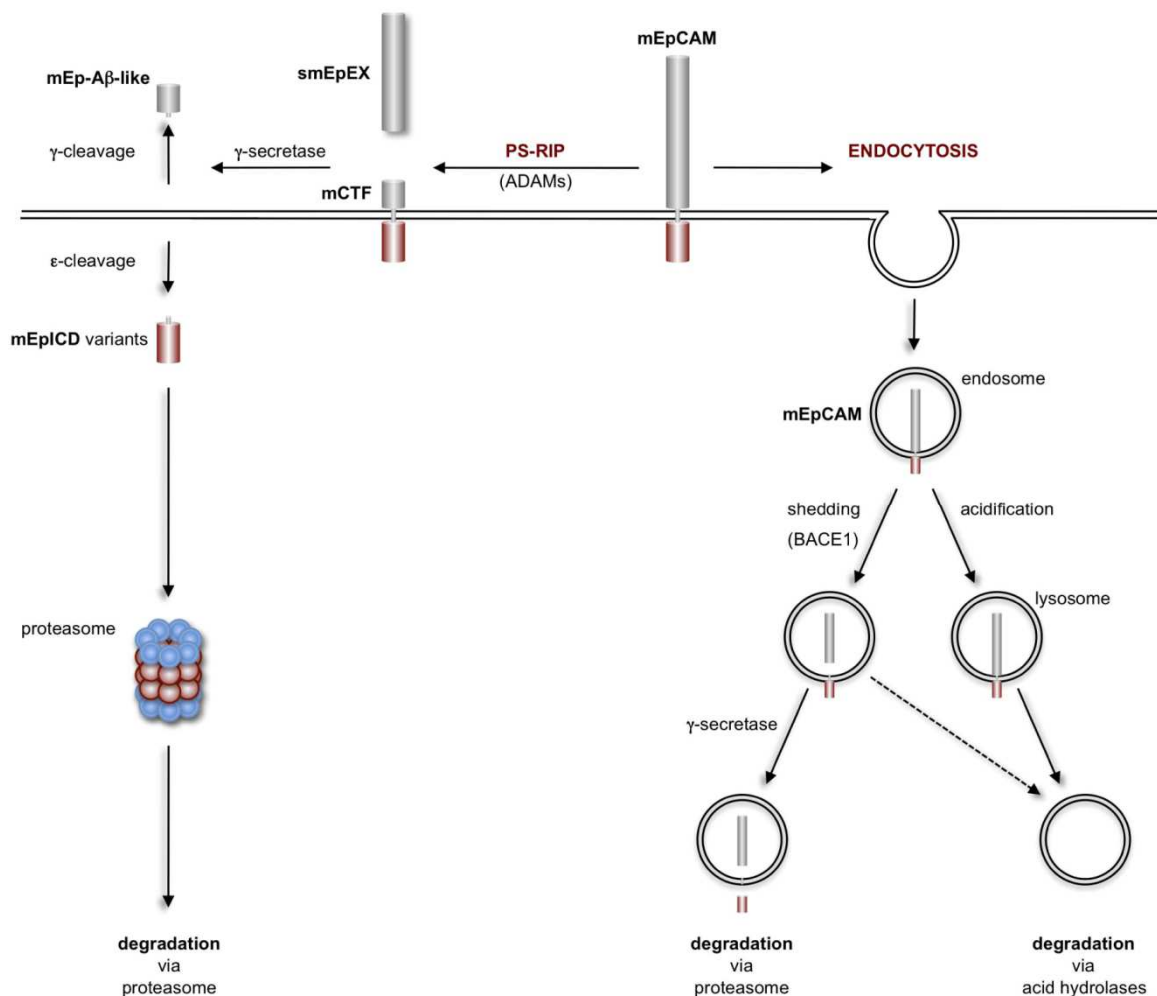


Figure 1. 11: Cleavage and processing of murine EpCAM.

The first cleavage step in the RIP of murine EpCAM (mEpCAM) can be performed by ADAMs (left pathway) or BACE-1 (right pathway). Cleavage of mEpCAM by ADAMs results in the formation of soluble EpEX (smEpEX) and EpCAM-CTF (mCTF). The subsequent cleavage of mCTF by the γ -secretase complex leads to the formation of an EpCAM-A β -like fragment (mEp-A β -like) and EpICD variants (mEpICD), which become degraded by the proteasome. BACE-1-associated RIP requires endocytosis of EpCAM. After BACE-1 cleavage, cleavage products are further processed and degraded by hydrolases or the proteasome. (Picture by Hachmeister *et al.* (Hachmeister *et al.* 2013).)

Besides the involvement of BACE-1 in EpCAM cleavage, Hachmeister *et al.* also revealed that the intracellular cleavage of murine EpCAM leads to the generation of five different forms of EpICD as well as to mEp-A β -like fragments that are similar to the A β -fragment of APP, which is associated with the progression of Alzheimer's disease (Hachmeister *et al.* 2013). However, out of the five EpICD variants only one was stable enough to be measured in mass spectroscopy with untreated cells. Most likely this variant is also the one, which can be detected in western blot. All other variants could only be detected when cells were treated with proteasome specific inhibitors or when proteasome-free membrane fractions were used as a source of proteins. In line with these findings it could be shown that the murine EpICD is prone to degradation by the proteasome, as treatment of cells expressing murine EpCAM with specific proteasome inhibitors, resulted in significant stronger EpICD signals in western blot (Hachmeister *et al.* 2013). This liability to proteasomal degradation was also found in case of human EpICD (Maetzel *et al.* 2009).

1.2.4 Expression pattern of EpCAM

1.2.4.1 EpCAM expression in normal tissue

Usually, EpCAM can only be found at the basolateral cell membrane of simple, pseudo-stratified and transitional epithelia, whereas it is not expressed in squamous epithelia, mesenchymal cells, neuroendocrine tissue, cells derived from the bone marrow and cells of lymphoid origin (Moldenhauer *et al.* 1987; Momburg *et al.* 1987; Schnell *et al.* 2013). Expression levels of EpCAM vary between different organs and cell types. Thereby, weak EpCAM expression levels can for example be found in the stomach, whereas the small intestine and the colon display intermediate and high levels of EpCAM, respectively (Moldenhauer *et al.* 1987). Also the different cell types of the skin vary according to their EpCAM expression levels, with keratinocytes and melanocytes expressing no EpCAM, whereas high levels of EpCAM can be found at the proliferative zone and the perspiratory glands (Momburg *et al.* 1987; Tsubura *et al.* 1992). Similar findings were reported for different organs of the male (prostate, testis) and female (ovary, cervix, uterus) genital tracts (Tsubura *et al.* 1992; Litvinov *et al.* 1996). Organs displaying strong EpCAM expression levels are, besides the colon, the gall bladder, the respiratory tract (including trachea, bronchia, bronchioles and alveolus) and the glands of the endocrine system, i.e. thyroid gland, pituitary gland and adrenal glands (Moldenhauer *et al.* 1987; Pauli *et al.* 2003). In addition, EpCAM is expressed in certain cells of the kidney and the pancreas as well as in cells from

the bile duct (Cirulli *et al.* 1998; Breuhahn *et al.* 2006; Trzpis *et al.* 2007b). Typically, EpCAM expression is present in tissues with increased numbers of proliferating and less differentiated cells. One example for this observation is the epithelium of the intestine in which an decreasing EpCAM gradient can be observed from crypts to villi, corresponding to high EpCAM expression in the intestinal stem cells which are located in the crypts and decreasing levels in the differentiated cells at the top of the villi (Balzar *et al.* 1999b; Schnell *et al.* 2013).

1.2.4.2 EpCAM expression in stem cells and regenerating tissue

It was postulated that EpCAM expression is essential during embryonic development and morphogenesis (Trzpis *et al.* 2007a; Trzpis *et al.* 2008). Indeed, EpCAM expression can be detected in oocytes, the two-cell state and morulas (Tarmann *et al.* 1990), as well as in human and murine embryonic stem cells (Gonzalez *et al.* 2009; Lu *et al.* 2010; Ng *et al.* 2010). However, in later developmental stages EpCAM expression varies between the different tissues formed, whereat it is still expressed in the fetal lung, liver, pancreas, kidneys, skin, mammary glands and germ cells (Kasper *et al.* 1995; Stingl *et al.* 2001; Dan *et al.* 2006). In some tissues, like the pancreas, expression of EpCAM is maintained also in the adult organ (Cirulli *et al.* 1995; Cirulli *et al.* 1998), whereas other cell types, like mature hepatoblasts entirely shut down EpCAM expression (de Boer *et al.* 1999). Although adult liver cells do not express EpCAM under normal circumstances, it was found that its expression is reactivated upon inflammatory liver diseases (Breuhahn *et al.* 2006). Furthermore, it has been shown that after liver damage the organ is regenerated by EpCAM-positive progenitor cells (de Boer *et al.* 1999). It was therefore postulated that re-expression of EpCAM is associated with a regenerative potential in the liver (Breuhahn *et al.* 2006). In addition, a potential role of EpCAM in the regulation of the stem cell phenotype in liver progenitor cells was discussed (Gires 2008; Yoon *et al.* 2011; Gires 2012).

1.2.4.3 EpCAM expression in cancer cells

EpCAM is *de novo* or overexpressed in the majority of malign and benign primary carcinomas (Went *et al.* 2004; Schnell *et al.* 2013). Especially high amounts of EpCAM can be found in carcinomas derived from colon, intestine, breast, lung and prostate (Litvinov *et al.* 1996; Spizzo *et al.* 2004; Went *et al.* 2004; Went *et al.* 2006). In addition, not only the levels but also the location of EpCAM differs between normal and transformed cells. In healthy

tissues, EpCAM can be found only at the basolateral cell membranes and sometimes in the cytoplasm, which might be due to transport of EpCAM to the membrane, EpCAM cleavage or endocytic processes. In contrast, in carcinoma cells EpCAM can be detected at the whole cell membrane, maybe due to the loss of polarity in these cells. Additionally, strong EpCAM signals can also be detected in their cytoplasm and nuclei (Ralhan *et al.* 2010a; Ralhan *et al.* 2010b; Kunavisarut *et al.* 2012). In most carcinomas subtypes, the overexpression of EpCAM correlates with enhanced cancer progression and worsened clinical outcome (see 1.2.5.3) (van der Gun *et al.* 2010).

Despite the broad knowledge about EpCAM in primary tumors, studies dealing with the expression of EpCAM in CTCs, DTCs and metastases remain so far inconclusive. Kuhn *et al.* found that liver metastases deriving from colorectal cancer showed the same high EpCAM expression level as primary tumors (Kuhn *et al.* 2007). Similar findings were made by Jojovic *et al.* in large lung metastases of colon carcinomas (Jojovic *et al.* 1998). In contrast, Takes *et al.* showed that metastases derived from head and neck carcinomas in most cases display lower EpCAM levels than the cognate primary tumors (Takes *et al.* 2001). As EpCAM in these days is the most frequently used marker to retrieve CTCs from blood and detect DTCs in lymph nodes (see 1.2.5.3), it is assumed that those cells are also EpCAM-positive. Indeed there is evidence that EpCAM is expressed in the majority of DTCs in thyroid cancer (Ensinger *et al.* 2006) and in CTCs deriving from breast cancer (Tewes *et al.* 2009; Aktas *et al.* 2011). However, an increasing set of data, including studies from colon and breast carcinomas, reports on the loss of EpCAM in CTCs and DTCs (Jojovic *et al.* 1998; Rao *et al.* 2005; Gorges *et al.* 2012).

1.2.5 Functions of EpCAM

EpCAM was identified as tumor-associated antigen already in 1979 as it triggered a cancer-related immune response in mice (Herlyn *et al.* 1979). Until today various functions of EpCAM were described, including a role in cell adhesion and cell signaling, as well as a prognostic and therapeutic marker in carcinomas.

1.2.5.1 EpCAM - the cell adhesion molecule

EpCAM (epithelial cell adhesion molecule) obtained its name from the findings that it is primarily expressed in epithelial cells (see 1.2.4) and that it is involved in cell adhesion. Although EpCAM is structurally not related to any of the four major families of cell adhesion molecules (CAMs), i.e. cadherins, integrins, immunoglobulins (Ig) and selectins (Balzar *et al.* 1998), its role in cell adhesion was described in studies by Litvinov *et al.* already in 1994. The group showed that overexpression of EpCAM enhances cell aggregation by the calcium independent formation of homophilic cell-cell contacts in cells expressing no relevant amount of other cell adhesion molecules. Vice versa, they also provided evidence that treatment of cells with an EpCAM-specific antibody inhibits the formation of intercellular contacts (Litvinov *et al.* 1994a; Litvinov *et al.* 1994b). Subsequent studies revealed that besides the extracellular domain, which enables the homophilic interaction of EpCAM molecules, also the intracellular of EpCAM is essential in cell adhesion as its binding to α -actinin provides the connection to the actin cytoskeleton (Balzar *et al.* 1998). However, although ectopic EpCAM expression was found to increase cell adhesion in cells expressing (almost) no CAMs, in epithelial, E-cadherin-expressing cells its influence on cell adhesion was shown to be of rather modulating nature. It was reported that EpCAM modulates and abrogates strong cadherin-mediated junctions and subsequently replaces them by its own comparatively weak cell-cell adhesions (Litvinov *et al.* 1997). Phosphatidylinositol 3-kinase (PI3K) was identified as mediator of this process. Thereby PI3K binds to α -catenin, which connects the cadherin adhesion complexes to the actin cytoskeleton, and abrogates the interactions between α -catenin and actin, resulting in contact loss of the adhesion complexes to the cytoskeleton (Winter *et al.* 2007). It was hypothesized that the substitution of the strong cell-cell contacts, mediated by E-cadherin, by the relatively weak cell interactions provided by EpCAM, leads to enhanced cell plasticity in epithelial tissues which in consequence promotes proliferation and cell movement during development, morphogenesis and carcinogenesis (Schnell *et al.* 2013). More recent studies revealed an effect of EpCAM on the formation and composition of tight

junctions (TJ). EpCAM knock-out mice displayed a strong depletion of proteins from the claudin family. The downregulation of these proteins, which play an essential role in the formation of TJ (Angelow *et al.* 2008), resulted in severe intestinal defects, more often than not leading to the death of the mice (Lei *et al.* 2012). Furthermore, it has been shown that EpCAM contributes to the formation of functional tight junctions and epithelial integrity by interacting with different claudin proteins (Lei *et al.* 2012; Wu *et al.* 2013).

1.2.5.2 EpCAM - the cell signaling molecule

Besides its role as cell adhesion molecule, EpCAM was also found to be involved in cell signaling in cancer as well as in stem cells (Imrich *et al.* 2012). EpCAM signaling is mediated by the internal part of EpCAM (EpICD), which is released upon regulated intramembrane proteolysis (see 1.2.3) and was found to be mandatory for the signaling function of the molecule (Munz *et al.* 2004; Maetzel *et al.* 2009). In carcinoma cells, EpCAM signaling was found to be associated with the regulation of genes involved in different cellular processes. Transcriptome analyses conducted in lung and colon carcinoma cell lines, which were treated with or without an EpCAM-specific antibody, revealed that most genes regulated by EpCAM signaling are involved in cell cycle regulation, proliferation, cell growth, apoptosis and cancer related processes. Some of the genes which were found to be induced upon treatment of the cells with EpCAM-specific antibody were the cell cycle activators LATS2 and FOSL2 and the anti-apoptotic genes GADD45 and PIM1. In contrast, expression of the pro-apoptotic gene DIDO1 was found to be repressed (Maaser and Borlak 2008). Further studies provided evidence that also the proliferation inducing genes c-Myc and cyclin A, D and E are upregulated upon EpCAM signaling (Maetzel *et al.* 2009; Chaves-Perez *et al.* 2013). In addition, the fatty acid binding protein 5 (EFABP) and matrix metalloproteinase 7 (MMP-7) were identified as EpCAM target genes (Munz *et al.* 2005; Denzel *et al.* 2012).

In tumor cells deriving from the colon, EpCAM was found to be associated with the tetraspanin CD9 (Le Naour *et al.* 2006), a protein of the tetraspanin web, which is involved in many different biological processes, including cell signaling, motility and adhesion, as well as tumor initiation, progression and metastasis (Hemler 2001; Yunta and Lazo 2003; Hemler 2013). It has been shown that in combination with the tetraspanin web and claudin-7, which is also involved in the formation of EpCAM-mediated tight junctions (see 1.2.5.1), EpCAM activates metastatic processes in colon carcinoma (Kuhn *et al.* 2007). Additionally, it was

found that claudin-7 induces EpCAM cleavage by associating with presenilin-2, thereby leading to enhanced tumor cell proliferation (Thuma and Zoller 2013).

A positive correlation between EpCAM and cell proliferation has been observed in a set of different *in vitro* and *in vivo* studies. Already in 1994, Schön *et al.* revealed a positive correlation of EpCAM expression with cell proliferation in several transformed epithelial cell lines. Thereby the group also showed that blocking of specific epitopes of EpCAM using antibodies decreases proliferation of cells (Schon *et al.* 1994). Two years later, Litvinov *et al.* could correlate the expression of EpCAM in cervical intraepithelial neoplasia to an increased expression of the proliferation marker Ki67 (Litvinov *et al.* 1996). Since then, increasing evidence from numerous different studies showed that EpCAM expression enhances proliferation in many different cell types, including breast, gastric and pharyngeal carcinoma cell lines and human embryonic kidney cells. Consequently, EpCAM depletion was correlated with decreased proliferation in the tested cells (Munz *et al.* 2004; Osta *et al.* 2004; Maetzel *et al.* 2009; Wenqi *et al.* 2009; Chaves-Perez *et al.* 2013).

In embryonic stem cells (ES cells), EpCAM was found to play a role in the maintenance of the stem cell phenotype, whereat EpCAM knock-down was associated with a disturbance of ES cell characteristics in human as well as in murine stem cells (Gonzalez *et al.* 2009; Ng *et al.* 2010). Currently it is hypothesized that EpCAM sustains the stem cell phenotype by regulating stemness genes like *OCT4*, *KLF4*, *SOX2* and *NANOG* (Lu *et al.* 2010; Imrich *et al.* 2012).

1.2.5.3 EpCAM - the prognostic and therapeutic marker

Due to its strong *de novo* or overexpression in almost all cancer entities compared to the cognate healthy tissues (Winter *et al.* 2003b; Schnell *et al.* 2013), EpCAM until now is used as prognostic and therapeutic marker in cancer (Moldenhauer *et al.* 1987; Baeuerle and Gires 2007; Imrich *et al.* 2012). In addition, it is the most frequently used antigen to detect and retrieve CTCs and DTCs in cancer patients (Cohen *et al.* 2006; Criscitiello *et al.* 2010; Weissenstein *et al.* 2012). In most carcinoma types, including lung, breast, prostate, bladder and pancreas carcinomas, EpCAM expression is correlated with increased tumor growth, enhanced cancer progression, and/or shorter overall/disease free survival (Piyathilake *et al.* 2000; Spizzo *et al.* 2004; Brunner *et al.* 2008; Scheunemann *et al.* 2008; Ni *et al.* 2013). Only in renal and thyroid carcinomas EpCAM was described to have a tumor suppressive role. In addition, there is a subset of cancer entities, including gastric and oral carcinomas, in which

tumor promoting and suppressive functions of EpCAM are described (Ensinger *et al.* 2006; Klatte *et al.* 2009; van der Gun *et al.* 2010).

As therapeutic marker, EpCAM was already used in a set of different anti-cancer approaches, including the development of tumor specific antibodies (Riesenberg *et al.* 2001), the fusion of EpCAM-specific antibody fragments to toxins (Di Paolo *et al.* 2003; Patriarca *et al.* 2012; Flatmark *et al.* 2013) or the tumor necrosis factor-related apoptosis-inducing ligand (TRAIL) (Bremer *et al.* 2004a; Bremer *et al.* 2004b) and vaccination (Mosolits *et al.* 2004). Different chimeric (chimeric Edrecolomab), humanized (3622W94), human engineered (ING-1) and fully humanized (Adecatumumab) EpCAM-specific antibodies with different binding epitopes were already developed (Imrich *et al.* 2012). The first EpCAM antibody, which was tested in humans, was Edrecolomab (Panorex). But although first clinical studies associated the treatment with Edrecolomab with reduced tumor recurrence and reduced death of patients suffering from metastasized colorectal cancer, these finding could not be reproduced in larger clinical trials (Riethmuller *et al.* 1994; Riethmuller *et al.* 1998; Fields *et al.* 2009). In addition, already low concentrations of EpCAM-specific high affinity antibodies, like ING-1 and 3622W94, were associated with acute pancreatitis in clinical trials (LoBuglio *et al.* 1997; Goel *et al.* 2007). In contrast, the application of Adecatumumab, which displayed an intermediate binding affinity, only led to minor side effects, like nausea, chill, fatigue and diarrhea, when used in higher doses, in a clinical phase II study. Additionally, in this particular study the treatment with Adecatumumab was associated with a good prognosis in terms of overall survival in patients with EpCAM^{high} metastatic breast cancer (Schmidt *et al.* 2010). In 2009 the trifunctional antibody Catumaxomab (Removab) gained approval for the European market and is now used in the treatment of patients with malignant ascites (Baeuerle and Gires 2007; Munz *et al.* 2010). However, until now Catumaxomab is the only EpCAM-specific antibody, which is used in the clinics.

1.2.6 EpCAM in esophageal carcinomas

Esophageal cancer is the fifth leading cause of cancer-related deaths worldwide (World-Health-Organization 2008). Both forms, i.e. squamous cell carcinomas deriving from normal squamous esophageal epithelia, as well as adenomatous cell carcinomas, deriving from transformed epithelial cells of the esophagus (Barrett's esophagus), are characterized by early metastatic spread and intrinsic resistance to current systemic chemotherapies (Ilson 2007; Siewert and Ott 2007; Klein and Stoecklein 2009). In consequence, the 5-year survival rate is

comparably low, even if the primary tumor can be removed by surgery, which is the case in only around 15-20% of all patients suffering from esophageal cancer (Mariette *et al.* 2004; Klein and Stoecklein 2009). The bad overall survival rate in this type of carcinoma is also due to the fact that neither adjuvant nor neo-adjuvant therapies are capable of efficiently eradicate esophageal cancer cells (Mariette *et al.* 2007).

Similarly to other squamous epithelia, EpCAM is not expressed in normal squamous epithelium of the esophagus, whereas in the majority of squamous esophageal carcinoma cells a strong *de novo* expression of EpCAM is observable (Winter *et al.* 2003b; Stoecklein *et al.* 2006; Kimura *et al.* 2007). In a study by Stoecklein *et al.* it was shown that high EpCAM expression in squamous esophageal carcinomas correlates with decreases periods of relapse-free and disease-specific survival of the patients (Stoecklein *et al.* 2006). This is in consistence with findings in other cancer types like pancreatic, breast and lung carcinomas (van der Gun *et al.* 2010). However, a study by Kimura *et al.* showed a different picture. Also in this particular study high EpCAM levels were associated with increased carcinogenesis, but EpCAM expression was also correlated with decreased cancer progression and enhanced patient survival (Kimura *et al.* 2007). In a third study by Went *et al.* neither a positive nor a negative impact of EpCAM expression on tumor grade, tumor stage or survival of patients could be found (Philip Went 2008). In contrast to the cells of the normal squamous epithelium, where no EpCAM expression can be observed, columnar epithelial cells of the esophagus are EpCAM-positive (Wong *et al.* 2006; Anders *et al.* 2008). However, this columnar epithelium does not occur in a healthy esophagus but is formed in the context of Barrett's esophagus (BE), a precancerous metaplasia of the esophagus, which predisposes patients to esophageal adenocarcinoma (Fang *et al.* 2013; Spechler 2013). Although cells of esophageal adenocarcinomas are also EpCAM-positive, EpCAM expression could so far not be correlated to any prognostic impact factor in this type of cancer (Kumble *et al.* 1996; Philip Went 2008).

Besides studies in primary tumors, the prognostic impact of EpCAM in esophageal carcinomas was also studied in disseminated tumor cells (DTCs). Hosch *et al.* provided evidence that the occurrence of EpCAM-positive DTCs correlated with a decreased disease free survival of patients. Furthermore, the occurrence of EpCAM-positive cells in lymph nodes was associated with the decrease of both, relapse free and overall survival (Hosch *et al.* 2000).

1.3 Aim of the present study

Understanding the processes involved in cancer formation and progression is essential to provide new therapeutic approaches and drugs to efficiently treat and cure cancer patients. However, although enormous research efforts during the last decades provided scientists and physicians with a detailed understanding of these processes, numerous mechanisms of tumorigenesis still remain elusive. Thereby the formation and outgrowth of metastases, which represent the main reason for cancer related-deaths, are also the least understood mechanisms in the entire process of carcinogenesis.

The epithelial cell adhesion molecule (EpCAM) is a typ I transmembrane protein, which can normally only be found at the basolateral membrane of selected epithelial cells. However, as it is overexpressed in most carcinoma types, it gained attention as prognostic and therapeutic cancer cell marker. Since its discovery in 1979, EpCAM was intensively studied and a participation of the protein in cell adhesion as well as in cell signaling was revealed. Despite this huge research effort, the role of EpCAM in cancer formation and progression is not finally disclosed. Although EpCAM expression was found to be associated with enhanced cancer formation and progression, increased metastatic spread and/or poor clinical outcome in most carcinoma types, there is also evidence that EpCAM can play a role in tumor repression. In some types of cancer, such as esophageal carcinomas, the influence of EpCAM expression on tumor progression is unclear since different studies so far provided contradictory findings. Furthermore, although EpCAM was extensively studied in primary carcinomas, almost nothing is known about its expression and role during further cancer progression, which is odd since EpCAM is the most commonly used antigen to retrieve and detect circulating and disseminated tumor cells. Indeed, there is evidence that EpCAM expression is lost during cancer progression; however the reason for this loss is still unknown.

The present study was performed to learn more about the role of EpCAM in cancer formation, progression and metastases formation and thereby get a deeper understanding of processes involved in carcinogenesis. The ambition was to get an explanation for the finding that EpCAM expression can be associated with both, progression and repression of tumorigenesis, and to shed light onto the questions if and why EpCAM is downregulated at certain stages of carcinogenesis. To do so, squamous esophageal cancer cell lines were used as model system, as esophageal carcinoma is one of the most lethal cancers worldwide, characterized by early metastatic spread and intrinsic resistance to current systemic

chemotherapies (Klein and Stoecklein 2009). Furthermore, the role of EpCAM in this type of cancer is still under debate.

2 MATERIAL

2.1 Chemicals

Table 2. 1: List of chemicals used in the present study.

| Product | Company |
|---|--|
| 3-amino-9-ethylcarbazol | Sigma-Aldrich GmbH, Taufkirchen |
| ABC-Kit Vectastain® Elite® PK6100 | Vector Laboratories, Burlingame (USA) |
| Agarose | Roche, Mannheim |
| Acrylamide, Protogel ultra pure | Schröder Diagnostics, Stuttgart |
| Anorganic salts, acids and bases | Merck KGaA, Darmstadt |
| Antibody dilution buffer | DCS Innovative Diagnostik-Systeme GmbH & Co. KG, Hamburg |
| Ammonium persulfate (APS) | BioRad, Hercules (USA) |
| Aqua dest. | Braun, Melsungen |
| β-Mercaptoethanol | Sigma-Aldrich GmbH, Taufkirchen |
| Bovine serum albumin (BSA) | Sigma-Aldrich GmbH, Taufkirchen |
| Brij L23 solution | Sigma-Aldrich GmbH, Taufkirchen |
| Bromophenol blue | Serva GmbH, Heidelberg |
| Calcein AM | PromoKine/PromoCell GmbH, Heidelberg |
| Dimethyl sulfoxide (DMSO) | Sigma-Aldrich GmbH, Taufkirchen |
| DMEM (4,5g/l glucose/ with L-glutamine) | Biochrom AG, Berlin |
| DMEM (high glucose/ w/o calcium/ w/o L-glutamine) | Life Technologies, Carlsbad (USA) |
| EDTA | Carl Roth GmbH & Co.KG, Karlsruhe |
| EGTA | AppliChem GmbH, Darmstadt |
| Eosin solution 0,5% | Pharmacy Klinikum Großhadern, Munich |
| FACSFlow | Becton Dickinson, Heidelberg |
| FACSSafe | Becton Dickinson, Heidelberg |
| FACSRinse | Becton Dickinson, Heidelberg |
| Fetal calf serum (FCS) | Biochrom AG, Berlin |
| Fibronectin | Biochrom AG, Berlin |
| Gelatine | Sigma-Aldrich GmbH, Taufkirchen |
| Glycine | Serva GmbH, Heidelberg |

| Product | Company |
|--|---------------------------------------|
| Glycerol | Sigma-Aldrich GmbH, Taufkirchen |
| Hematoxylin Gill`s Formula H-3401 | Vector Laboratories, Burlingame (USA) |
| HEPES buffer (1 M) | Biochrom AG, Berlin |
| Hydrogen peroxide (H ₂ O ₂) | Merck KGaA, Darmstadt |
| Kaisers glycerol gelatine | Merck KGaA, Darmstadt |
| Matrigel matrix | Becton Dickinson, Heidelberg |
| Matrigel growth factor reduced matrix | Becton Dickinson, Heidelberg |
| Mayers Hemalaun solution | Merck KGaA, Darmstadt |
| Oligonucleotides | Metabion, International AG, Planegg |
| Organic solvents | Merck, KGaA, Darmstadt |
| Paraformaldehyde | Carl Roth GmbH & Co.KG, Karlsruhe |
| PBS tablets | Invitrogen, Karlsruhe |
| PBS solution | Pharmacy Klinikum Großhadern, Munich |
| Penicillin Streptomycin (Pen Strep) | Biochrom AG, Berlin |
| Proteinase K | Sigma-Aldrich GmbH, Taufkirchen |
| Protein G Sepharose™ 4FastFlow | GE Healthcare, Freiburg |
| Propidium iodide | Sigma-Aldrich GmbH, Taufkirchen |
| Protease Inhibitor Cocktail Complete | Roche, Mannheim |
| Protease Inhibitor Cocktail Complete, EDTA free | Roche, Mannheim |
| Puromycin | Sigma-Aldrich GmbH, Taufkirchen |
| siRNAs | Riboxx, Radebeul |
| Sodiumdodecylsulfat (SDS) | Sigma-Aldrich GmbH, Taufkirchen |
| Temed | BioRad, Hercules (USA) |
| TGFβ 1 | Sigma-Aldrich GmbH, Taufkirchen |
| TissueTek® O.C.T Compound | Sakura Finetek, Staufen |
| Tris-(hydroxymethyl)-aminomethan (TRIS) | Merck KGaA, Darmstadt |
| Triton X-100 | Sigma-Aldrich GmbH, Taufkirchen |
| Trypan blue | Biochrom AG, Berlin |
| Trypsin/ EDTA | Biochrom AG, Berlin |
| Tween 20 | Serva GmbH, Heidelberg |
| Vectashield® with DAPI | Biozol GmbH, Eching |

2.2 Buffer

2.2.1 Cell culture

PBS: 8.0g NaCl, 0.2g KCl, 1.15g Na₂HPO₄, 0.2g KH₂PO₄ to
1l H₂O

Cryopreservation medium: DMEM; 10% DMSO

DMEM/10%FCS: DMEM; 10% FCS; 1% PenStrep

DMEM/1%FCS: DMEM; 1% FCS; 1% PenStrep

DMEM w/o calcium: DMEM w/o calcium; 1% PenStrep; stable glutamine,
HEPES buffer

2.2.2 Flow cytometry

Flow cytometry (FC) buffer: 3% FCS in PBS

Antibody solutions: 1:50 in 50µl FC buffer

Propidium iodide staining solution: 1µg/ml propidium iodide (PI) in FC buffer

2.2.3 Adhesion assay

Plate coating solutions:
6µg/ml fibronectin in adhesion medium
0.2% gelatine in adhesion medium
40µl/ml matrigel in adhesion medium

Cell staining solution: 2µM calcein AM/ ml cell medium w/o FCS

Cell lysis buffer (2x): 4% Triton-X100 in dd. H₂O

2.2.4 Membrane assay

| | |
|--------------------------------|---|
| Homogenisation buffer: | 0.2ml 1M MOPS (pH 7.0), 0.2ml 1M KCl, 0.2ml 100x complete in 19.4ml ddH ₂ O |
| Assay buffer: | 300µl 0.5M sodium nitrate, 10µl 100x complete, 0.5µl 20mM ZnCl ₂ in 689.5µl ddH ₂ O |
| 100x complete: | 1 complete protease inhibitor tablet in 500µl ddH ₂ O |
| Whole cell lysis buffer (10x): | 2 complete protease inhibitor tablets, 1% triton-X100 in 10ml PBS |

2.2.5 SDS-PAGE and western blot

| | |
|-------------------------------------|---|
| Whole cell lysis buffer (2x): | 2 complete protease inhibitor tablets, 1% triton-X100 in 50ml PBS |
| Laemmli buffer (5x): | 62.5mM TRIS pH 6.8, 2% SDS; 10% glycerol, 5% β-mercaptoethanol, 0.001% bromophenol blue |
| Stacking gel (4%): | 13.3ml 30% acrylamide, 16.6ml 2M TRIS pH 6.8, 0.663ml 0.5M EDTA, 69.44ml dd. H ₂ O |
| Resolving gel (15%): | 50ml 30% acrylamide, 16.6ml 2M TRIS pH 8.9, 0.663ml 0.5M EDTA, 32.74 ml dd. H ₂ O |
| Running buffer SDS-PAGE: | 150g TRIS, 720g glycine, 50g SDS to 5l dd. H ₂ O |
| Blotting buffer (10x): | 250mM TRIS, 1.26M glycerol in dd. H ₂ O |
| Western blot washing buffer (PBST): | 8 tablets PBS, 4ml Tween-20 to 4l dd. H ₂ O |

2.3 Molecular kits

Table 2. 2: List of kits used in the present study.

| Product | Company |
|--|-----------------------------------|
| BCA Protein Assay | Pierce, Rockford (USA) |
| Immobilon Western Chemiluminescent HRP substrate | Millipore, Bedford (USA) |
| LightCycler 480 SYBR Green I Master | Roche, Mannheim |
| Lipofectamine™ | Life technologies, Carlsbad (USA) |
| MATra transfection reagent | Iba GmbH, Göttingen |
| Prestained protein marker V | Peqlab, Erlangen |
| QiaShredder | Qiagen, Hilden |
| QuantiTect Reverse Transcription Kit | Qiagen, Hilden |
| RNeasy Mini Kit | Qiagen, Hilden |

2.4 Antibodies

Table 2. 3: List of primary antibodies used in the present study.

| Antibody | Species | Company |
|---------------------------------------|------------------------|--|
| FITC anti-Actin IgG ₁ | mouse, monoclonal | Santa Cruz, Dallas (USA) |
| anti-CK8/18 IgG _{2a} | mouse, monoclonal | Covance Inc., New Jersey (USA) |
| anti-EpCAM (Ber-EP4) IgG ₁ | mouse, monoclonal | Dako Deutschland GmbH, Hamburg |
| anti-EpCAM (C-10) IgG ₁ | mouse, monoclonal | Santa Cruz, Dallas (USA) |
| anti-EpCAM (VU1D9) IgG ₁ | mouse, monoclonal | Cell Signaling Technology, Cambridge (UK) |
| anti-EpICD | guinea pig, polyclonal | Peptide Specialty Laboratories, Heidelberg |
| anti-GFP/YFP IgG _{2a} | mouse, monoclonal | Santa Cruz, Dallas (USA) |
| FICT isotype mouse IgG ₁ | mouse, monoclonal | Diatech, Jesi (Italy) |
| Isotype mouse IgG ₁ | mouse, monoclonal | Dako Deutschland GmbH, Hamburg |
| Isotype mouse IgG _{2a} | mouse, monoclonal | Sigma-Aldrich GmbH, Taufkirchen |

Table 2. 4: List of secondary antibodies used in the present study.

| Antibody | Company |
|--|--|
| ABC-Kit Vectastain® Elite® PK6100 | Vector Laboratories, Burlingame (USA) |
| Alexa 488-conjugated goat-anti-mouse IgG | Mobitec, Göttingen |
| Biotinylated horse-anti-mouse IgG (H&L) | Vector Laboratories, Burlingame (USA) |
| FITC goat-anti-mouse IgG | Jackson ImmunoResearch, West Grove (USA) |
| PO rabbit-anti-guinea pig IgG | Sigma-Aldrich GmbH, Taufkirchen |
| PO goat-anti-maus IgG | Dako Deutschland GmbH, Hamburg |

2.5 Oligonucleotids

2.5.1 qRT-PCR primer

Table 2. 5: List of primers used in the present study.

| Primer | Sequence (in 5`-3` orientation) |
|---------------|--|
| FW_β-actin | ATAGCACAGCCTGGATAGCAACGTAC |
| BW_β-actin | CACCTTCTACAATGAGCTGCGTGTG |
| FW_E-cadherin | TGAGTGTCCCCCGGTATCTTC |
| BW_E-cadherin | CAGTATCAGCCGCTTTCAGATTTT |
| FW_EpCAM | GCAGCTCAGGAAGAATGTG |
| BW_EpCAM | CAGCCAGCTTTGAGCAAATGAC |
| FW_GAPDH | TGCACCACCAACTGCTTAGC |
| BW_GAPDH | GGCATGGACTGTGGTCATGAG |
| FW_N-cadherin | TGGGAATCCGACGAATGG |
| BW_N-cadherin | TGCAGATCGGACCGGATACT |
| FW_RPL13A | CCTGGAGGAGAAGAGGAAAGAGA |
| BW_RPL13A | TTGAGGACCTCTGTGTATTTGTCAA |
| FW_SLUG | AAGCATTTC AACGCCTCCAAA |
| BW_SLUG | GGATCTCTGGTTGTGGTATGACA |
| FW_SNAIL | CCAGTGCCTCGACCACTATG |
| BW_SNAIL | CTGCTGGAAGGTAAACTCTGGATT |
| FW_TWIST 1 | GGGCCGAGACCTAGATGTCATTGT |
| BW_TWIST 1 | CGCCCCACGCCCTGTTTCTT |
| FW_TWIST 2 | CGCGCCAGGAGGAGATTCTGAATGA |

| Primer | Sequence (in 5`-3`orientation) |
|-------------|--------------------------------|
| BW_TWIST 2 | CGCCAACGTTTCGTGGGCTGT |
| FW_Vimentin | CCTTGAACGCAAAGTGGAAT |
| BW_Vimentin | GACATGCTGTTTCCTGAATCTGAG |
| FW_ZEB1 | TTACACCTTTGCATACAGAACCC |
| BW_ZEB1 | TTTACGATTACACCCAGACTGC |
| FW_ZEB2 | CAAGAGGCGCAAACAAGCC |
| BW_ZEB2 | GGTTGGCAATACCGTCATCC |

2.5.2 siRNA

Table 2. 6: List of siRNAs used in the present study.

| siRNA | Sequence |
|----------------------|---------------------------|
| Control (ctrl) siRNA | 5`-UCGUCCGUAUCAUUUCAAU-3` |
| EpCAM siRNA | 5`-UGCCAGUGUACUUCAGUUG-3` |

2.5.3 shRNA

Table 2. 7: List of shRNAs used in the present study.

| shRNA | Sequence |
|----------------------|---|
| Control (ctrl) shRNA | pGIPZ vector V2LHS_17672 (Open Biosystems) |
| EpCAM shRNA I | pGIPZ vector V2LHS_134160 (Open Biosystems) |
| EpCAM shRNA II | pGIPZ vector V2LHS_235265 (Open Biosystems) |
| EpCAM shRNA III | pGIPZ vector V2LHS_134162 (Open Biosystems) |

2.6 Plasmids

Table 2. 8: List of plasmids used in the present study.

| Plasmid | Description |
|-------------------|---------------------------------------|
| 141pCAG-3SIP | CMV, SV40, IRES, puromycin resistance |
| 141pCAG/YFP | YFP in 141pCAG-3SIP |
| 141pCAG/EpICD-YFP | EpICD, YFP tagged in 141pCAG-3SIP |
| 141pCAG/EpCAM-YFP | EpCAM, YFP tagged in 141pCAG-3SIP |

2.7 Cell lines

Table 2. 9: List of cell lines used in the present study.

| Cell line | Description |
|--|---|
| A549 | Human non-small lung cancer cell line |
| A549 - EpCAM-YFP | A549 transfected with 141pCAG/EpCAM-YFP |
| A549 - EpICD-YFP | A549 transfected with 141pCAG/EpICD-YFP |
| A549 - YFP | A549 transfected with 141pCAG/YFP |
| Fibroblasts* | Primary human fibroblast cells |
| Kyse 30 | Human squamous esophageal cancer cell line |
| Kyse 30 - EpCAM-YFP | Kyse 30 transfected with 141pCAG/YFP |
| Kyse 30 - EpICD-YFP | Kyse 30 transfected with 141pCAG/EpICD-YFP |
| Kyse 30 - YFP | Kyse 30 transfected with 141pCAG/EpCAM-YFP |
| Kyse 520 ^{high} / Kyse 520 ^{low} | Human squamous esophageal cancer cell line, cell line shows different expression levels of EpCAM (Kyse 520 ^{high} → high levels of EpCAM Kyse 520 ^{low} → low levels of EpCAM) |
| Kyse 520 ^{high} - ctrl shRNA** | Kyse 520 ^{high} transfected with pGIPZ/ctrl shRNA |
| Kyse 520 ^{high} - EpCAM shRNA** | Kyse 520 ^{high} transfected with pGIPZ/EpCAM shRNA |
| Kyse 520 ^{high} - EpCAM-YFP | Kyse 520 ^{high} transfected with 141pCAG/EpCAMYFP |
| Kyse 520 ^{high} - EpICD-YFP | Kyse 520 ^{high} transfected with 141pCAG/EpICD-YFP |
| Kyse 520 ^{high} - YFP | Kyse 520 ^{high} transfected with 141pCAG/YFP |

* Cells were kindly provided by Andreas Moosmann, Helmholtz Center Munich.

** Cell lines were produced and kindly provided by Christiane Driemel, Universitäts-
klinikum Düsseldorf.

2.8 Consumables

Table 2. 10: List of consumables used in the present study.

| Product | Company |
|---|--|
| 3 MM Whatman paper | Bender & Hobein, Munich |
| 6-well cell culture plate, flat bottom | Nunc, Wiesbaden |
| 96-well cell culture plate, flat bottom | Nunc, Wiesbaden |
| 96-well cell culture plate, round bottom | Nunc, Wiesbaden |
| 96 magnet bar plate | Iba GmbH, Göttingen |
| Cell culture flasks and dishes | Nunc, Wiesbaden |
| Centrifugation tube 15ml/ 50ml | Becton Dickinson, Heidelberg |
| Centrifugation tube 1,5ml (nuclease-free) | Costar, New York (USA) |
| Centrifugation tube 1,5ml/ 2ml | Eppendorf AG, Hamburg |
| Corning® Costar® stripettes | Sigma-Aldrich GmbH, Taufkirchen |
| Cryomold Tissue-Tek®, Biopsy (10x10x5mm) | Sakura Finetek, Staufen |
| Cyto funnel with filter cards | Thermo Scientific, Waltham (USA) |
| Cryo tubes | Becton Dickinson, Heidelberg |
| FACS tubes | Becton Dickinson, Heidelberg |
| Glass flasks | Schott AG, Jena |
| Glass pipettes | Costar, New York (USA) |
| Glass plates | Amersham Bioscience, Glattbrugg (Switzerland) |
| Gloves sempercare latex | Sempermed, Vienna (Austria) |
| Gloves sempercare nitril | Sempermed, Vienna (Austria) |
| Immobilion-P membrane (0.45 µm) | Millipore, Bedford (USA) |
| Microlance 3 / 23G 1.25'' | Becton Dickinson, Heidelberg |
| Microlance 3/ 24G 1'' - Nr. 17, 0.55x25mm | Becton Dickinson, Heidelberg |
| Needle Microlance™ 3 | Millipore, Schwalbach |
| Neubauer chamber | Assistent, Sondheim/Rhön |
| Object slides „Super Frost'' | Nunc, Wiesbaden |
| Parafilm | American National Can, Menasha (USA) |
| Pipette tips | Starlab, Hamburg |
| Quadriperm | Sarstedt, Nümbrecht |

| Product | Company |
|-----------------------------|--|
| Reagent reservoir | Costar, New York (USA) |
| Safe Seal Tips Professional | Biozym Scientific GmbH, Hessisch Oldendorf |
| Scalpel | Feather/ PFM, Cologne |
| Syringe | Braun, Melsungen |
| Sterile filters | Millipore, Wiesbaden |
| Transfection tubes | Becton Dickinson, Heidelberg |

2.9 Equipment

Table 2. 11: List of equipment used in the present study.

| Device | Company |
|---|------------------------------------|
| Autoclave Systec 95 | Systec GmbH, Wettenberg |
| Blotting System Mini trans Blot | BioRad, Hercules (USA) |
| Camera WB750 | Samsung, Seoul (South Korea) |
| Cell Incubator | Heraeus Holding GmbH, Hanau |
| Centifuge Mikro 20 | Hettich Lab Technology, Tuttlingen |
| Centifuge Mikro 22R | Hettich Lab Technology, Tuttlingen |
| Centrifuge Rotanta 46 R | Hettich Lab Technology, Tuttlingen |
| ChemiDoc XRS+ imaging system | BioRad, Hercules (USA) |
| Confocal microscope TCS-SP2 | Leica, Bensheim |
| Cryostat model CM 1900 | Leica, Bensheim |
| Flow cytometer „FACS Calibur“ | Becton Dickinson, Heidelberg |
| Fluorescence microscope „Axiovert 200“ | Carl Zeiss AG, Jena |
| Fluorescence microscope “Olympus BX43F” | Olympus, Tokyo (Japan) |
| Freezer (-20°C, -80°C) | Liebherr, Ochsenhausen |
| Freezer (-80°C) HFU 86-450 | Heraeus, Hanau |
| Fridge (4°C) | Liebherr, Ochsenhausen |
| Light Cyclor 480 System | Roche, Mannheim |
| Magnet stirrer with heat block | Janke & Kunkel, Staufen |
| Microliter pipettes | Gilson Inc., Middleton (USA) |
| Microplate Reader „MRX“ | Dynatech Laboratories, Bad Nauheim |
| Microwave | Sharp Electronics GmbH, Hamburg |

| Device | Company |
|---|----------------------------------|
| Multichannel pipette „Transferpette-8“ | Brand GmbH, Wertheim |
| Nitrogen cooling equipment | Messer Cryotherm, Kirchen/ Sieg |
| Phase contrast microscope “Axiovert 25” | Carl Zeiss AG, Jena |
| pH-meter | WTW, Weilheim |
| Pipetboy® Comfort | Integra Biosciences, Fernwald |
| Power supply E835 | Consort bvba, Turnhout (Belgium) |
| Power supply E865 | Consort bvba, Turnhout (Belgium) |
| Precision scales | Mettler, Gießen |
| Safety cabinet HLB 2448 GS | Heraeus Holding GmbH, Hanau |
| Scales CP 4202 S | Sartorius, Göttingen |
| Scales Mettler PM 4600 | Mettler, Gießen |
| Spectrophotometer „GeneQuantPro“ | GE Healthcare, Solingen |
| Thermocycler Comfort | Eppendorf AG, Hamburg |
| Vertical electrophoresis system miniVE | Hoefer, Holliston (USA) |
| Vortex mixer | IKA Works Inc., Wilmington (USA) |
| Wallac Victor 1420 multilabel counter | PerkinElmer, Waltham (USA) |
| Water bath Exotherm U3e1 | Julabo, Seelbach |

2.10 Software

Table 2. 12: List of software used in the present study.

| Software | Company |
|---------------------------------|---|
| ApE | Wayne Davis (University of Utah), Salt Lake City (USA) |
| BD Cell Quest Pro Version 5.2.1 | Becton Dickinson, Heidelberg |
| Cell Sense Entry Version 1.8.1 | Olympus, Tokyo (Japan) |
| Endnote | Thomson Reuters Corporation, New York (USA) |
| GraphPad Prism 5 | Graphpad Software Inc., La Jolla (USA) |
| Image Lab | BioRad, Hercules (USA) |
| Image J | Wayne Rasband (National Institutes of Health), Bethesda (USA) |
| LAS AF | Leica, Bensheim |
| LightCycler® 480 SW 1.5 | Roche, Mannheim |
| MS Office 2007 | Microsoft, Redmond (USA) |
| Photoshop CS3 | Adobe Systems Inc., San Jose (USA) |
| Revelation 4.2.5 | DYNEX Technologies Inc., Chantilly (USA) |

3 METHODS

3.1 Cell culture

3.1.1 Passaging of cells

Required reagents:

- Dulbecco`s Modified Eagle Medium (DMEM)
- PBS
- Trypsin

All cell lines were cultivated using DMEM complemented with 10% fetal bovine serum and 1% penicillin-streptomycin at 37°C under the atmosphere of 5% CO₂. Selection and maintenance of stably transfected cell lines was achieved by the addition of 1µg/ml puromycin to the medium. For passaging, cells were split every second to third day according to their growth rate. For splitting, cells were washed briefly with PBS and then treated with 3ml trypsin for 10-30min at 37°C. Subsequently, cells were diluted 1:3 to 1:10 in fresh medium.

3.1.2 Counting of cells

Cell numbers were determined in a Neubauer chamber using 20µl of the cell suspension mixed 1:1 with trypan blue to distinguish between living and dead cells. Exact cells numbers were calculated using the following formula:

$$\text{Cells/ml} = 2 \times (\text{cells counted} / \text{number of counted large squares}) \times 10^4$$

3.1.3 Freezing and thawing of cells

Required reagents:

- DMEM
- PBS
- Trypsin
- Cryopreservation medium (DMEM containing 10% DMSO)

For cryopreservation, cells were treated with trypsin as mentioned above. After trypsinisation 9ml DMEM were added to the cells and the suspension then transferred to a 15ml falcon. Cells were then centrifuged for 5min at 280rcf, the supernatant was discarded and the cell pellet resuspended in 1.5ml freezing medium. The suspension was then transferred to a cryotube and stored at -80°C for short term or in liquid nitrogen for long term.

For thawing, cryotubes were briefly incubated at 37°C. The suspension in the tube was mixed with 9ml fresh DMEM in a 15ml tube and centrifuged for 5min at 280rcf to remove DMSO from the medium. Supernatant was discarded and pellet resuspended in 15ml fresh DMEM. The suspension was then transferred into a fresh 75cm² cell culture flask.

3.1.4 Transfection of cells

3.1.4.1 Transient transfection with MATra

Required reagents:

- DMEM
- DMEM w/o FCS
- PBS
- MATra transfection reagent
- siRNA (100pmol/μl)

For transfection with MATra, 1×10^5 - 7×10^5 cells/well were plated in 6-well plates and grown for 24h. Transfection solution was prepared by mixing 2μl siRNA with 500μl DMEM w/o FCS in a transfection tube. Subsequently 2.8μl MATra were added to the mixture, the suspension was mixed by flicking the tube and subsequently incubated for 20min at room temperature. During incubation the medium on the cells was replaced by 1.5ml fresh DMEM containing 10% FCS. The mixture was then added to the cells and the 6-well plates were put on magnetic plates for 15min at 37°C to achieve transfection. Medium was changed 2h after transfection to remove remaining MATra.

3.1.4.2 Generation of stable cell lines

Required reagents:

- DMEM
- DMEM w/o FCS
- PBS
- MATra transfection reagent
- Expression plasmid (1-2 μ g)
- Puromycin (final concentration = 1 μ g/ml)

To create stable cell lines, cells were transfected with MATra as described in 3.1.4.1. 24h after transfection, puromycin was added to the cell medium to select for cells expressing the resistance gene. Cells were cultivated for several weeks in the presence of puromycin and subsequently analyzed by flow cytometry (see 3.1.5), western blot (see 3.3.5) and/or qRT-PCR (see 3.2.3) to ensure the expression of the transfected protein in the whole cell population.

3.1.5 Flow cytometry

Flow cytometry in combination with staining using antigen specific antibodies represents a simple method to analyze the expression of cell surface molecules. In this analysis antigen specific primary and secondary antibodies are used to obtain a fluorescent signal, which is directly proportional to the expression level of the analyzed protein. Furthermore, this method allows the direct measurement of YFP-positive cells and upon staining of cells with propidium iodide (PI) the distinction of living and dead cells.

3.1.5.1 Flow cytometry analysis of membrane proteins

Required reagents:

- PBS
- FC buffer
- Specific primary and secondary antibodies
- Propidium iodide (PI) (1mg/ml)

Note: All centrifugation steps were performed for 5min at 280rcf and room temperature.

For flow cytometry analysis cells were harvested by trypsinisation, washed once with PBS and then incubated in primary antibody (1:50 in 50µl FC buffer) for 15min at room temperature. After centrifugation, the supernatant was discarded and the pellet incubated with secondary antibody (1:50 in 50µl FC buffer) for 15min at room temperature. Cells were then centrifuged and the pellet resuspended in 500µl flow cytometry buffer containing 0.5µl PI. Finally, samples were measured with a BD FACS-Calibur and results analyzed using the Cell Quest Pro (BD) software.

3.1.5.2 Flow cytometry analysis of YFP expressing cells

Required reagents:

- PBS
- FC buffer
- Propidium iodide (PI) (1mg/ml)

Note: All centrifugation steps were performed for 5min at 280rcf and room temperature.

To analyze the expression of YFP, cells were harvested by trypsination, washed once with PBS and were then directly incubated in 500µl FC buffer containing 0.5µl PI. Samples were measured with a BD FACS-Calibur and results analyzed by using the Cell Quest Pro (BD) software.

3.1.6 Cytospin

Cytospin is a method to concentrate cells in suspension and coat these cells on glass slides for further analyses such as immunofluorescence (see 3.4.1) and immunohistochemical staining (see 3.4.2).

Required reagents:

- PBS

Note: All centrifugation steps were performed for 5min at 280rcf at room temperature.

For cytopins, cells were harvested, washed once with PBS, resuspended in 100µl PBS and pipetted into a construction consisting of a cytofunnel, filter paper, and a glass slide. Cells were anchored to the glass slide upon centrifugation, whilst the PBS was drained into the filter paper. Cytofunnel and filter paper were carefully removed from glass slides, which were

then dried over night at room temperature. The next day cells were fixed and stained as described in 3.4.2.

3.1.7 TGF β assay

Required reagents:

- DMEM
- DMEM w/o FCS
- PBS
- TGF β 1

For TGF β assays, cells were plated in 6-well plates (0.5×10^5 cells/ well). On the next day, cell medium was discarded, cells were washed twice with PBS and new medium w/o FCS was added. 24h later, TGF β -1 (10ng/ml) was added to the cells for 72h. Pictures were taken under an Axiovert 25 microscope (Zeiss Q5) with a Samsung WB750 camera. Cells were then harvested and cell surface levels of EpCAM were analyzed upon flow cytometry (see 3.1.5.1). In addition mRNA levels of EpCAM, E-cadherin, N-cadherin and vimentin were assessed using qRT-PCR (see 3.2.3).

3.1.8 Scratch assay

Scratch assay is a method to analyze the migration capacity and velocity of cells. In this assay a wound (scratch) is set into a confluent layer of cells and closure of the scratch is monitored. Although being a simple assay it is mandatory to include proper controls to scratch assays in order to distinguish between cell migration and proliferation.

3.1.8.1 Scratch assay with Kyse 520^{high} and Kyse 520^{low} cells

Required reagents:

- DMEM
- DMEM w/o FCS
- PBS

For scratch assays, cells were seeded in 6-well plates and cultured to a density of 90-100%. Culture medium was then replaced by DMEM w/o FCS and 12-24h later scratches were set in monolayers of cells using a sterile pipette tip. Cells were then washed thrice with PBS and three random sections of two scratches per cell line were marked. Pictures were

taken at different time points under an Axiovert 25 microscope (Zeiss Q5) with a Samsung WB750 camera. To assess the migration velocity, the scratch area at different time points was calculated using the ImageJ software. Further calculations were performed with Microsoft Excel.

Calculations were the following:

$$w_{\text{mean}} = A/a$$

$$t_{\text{migration}} = (w_{\text{mean}}(t_1) - w_{\text{mean}}(t_2))/(\Delta t \cdot 2)$$

w_{mean} = mean width of the scratch (in μm)

A = area of the scratch (in μm^2)

a = length (in μm)

$t_{\text{migration}}$ = migration velocity

$w_{\text{mean}}(t_x)$ = mean distance of the scratch at timepoint x

Δt = time difference

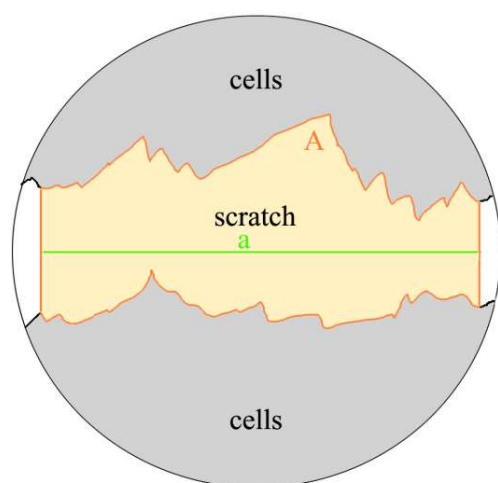


Figure 3. 1: Calculation of the mean width of scratches.

Mean widths of scratches were calculated by dividing the area (A , orange) by the length (a , green) of the scratch.

In parallel 0.5×10^5 cells/well were plated in 6-well plates to address proliferation rates. Cells were treated similarly to scratched cells, were harvested and cell numbers were assessed to rule out effects of proliferation on the closure of scratches. In addition, EpCAM levels were assessed in all samples using flow cytometry (see 3.1.5.1).

3.1.8.2 Scratch assay with siRNA transfected Kyse 30 cells

Required reagents:

- DMEM
- DMEM w/o FCS
- PBS
- siRNA (100pmol/μl)
- MATra transfection reagent

Kyse 30 cells were seeded in 6-well plates and cultured to a density of 80%. Cells were then transfected with either EpCAM-specific or control siRNA as described in 3.1.4.1. 12h after transfection, culture medium was replaced by medium w/o FCS and 8h later scratches were set with a sterile pipette tip. Cells were washed thrice with PBS and three random sections of two scratches per cell line were marked. Pictures were taken at the indicated time points under an Axiovert 25 microscope (Zeiss Q5) with a Samsung WB750 camera. To assess the migration velocity, the scratch area at different time points was calculated using ImageJ software. Further calculations were performed with Microsoft Excel (see 3.1.8.1). Proliferation rates were assessed as abovementioned. EpCAM knock-down was assessed in all samples using flow cytometry (see 3.1.5.1).

3.1.8.3 Fluorescence staining of Kyse 30 and Kyse 520^{low} scratch assays

Required reagents:

- DMEM
- DMEM w/o FCS
- PBS

Cells were seeded on glass slides located in quadriperm dishes, grown to confluency and culture medium was changed to DMEM w/o FCS. 12h later, a scratch was set into the cell monolayer, cells were washed thrice with PBS and migration was allowed for 24h in DMEM w/o FCS. Subsequently, cells were washed with PBS and fixed and stained as described in 3.4.1.

3.1.9 Spheroid formation

3.1.9.1 Basic spheroid formation

Required reagents:

- DMEM
- 1% agarose in PBS
- TissueTek® O.C.T Compound
- Liquid nitrogen

For spheroid formation assays, 96-well plates were coated with 50µl 1% agarose in PBS. After 1-2h, 3×10^4 cells were seeded per well and spheroid formation was allowed for 24-96h. Pictures were taken under an Axiovert 25 microscope (Zeiss Q5) with a Samsung WB750 camera. Thereafter spheroids were harvested, embedded in Tissue-Tek and cryopreserved in liquid nitrogen. Samples were stored at -20°C until further processing (see 3.4.2).

3.1.9.2 Spheroid invasion assay

Required reagents:

- DMEM
- 1% agarose in PBS
- TissueTek® O.C.T Compound
- Liquid nitrogen

For spheroid invasion assays, 96-well plates were coated with 50µl 1% agarose in PBS. After 1-2h, 3×10^4 fibroblast cells were seeded per well and spheroid formation was allowed for 24h. Subsequently, 1×10^4 Kyse 520^{high} or Kyse 520^{low} single cells were added to fibroblast spheroids and invasion was allowed for 48h and 72h. At the indicated time points spheroids were harvested, embedded in Tissue-Tek and frozen in liquid nitrogen. Subsequently, samples were stored at -20°C until further processing.

For immunohistochemical staining, spheroids were cut, fixed and incubated with CK8/18 or EpCAM-specific antibodies (see 3.4.2). Subsequently, pictures of stained spheroid slides were taken under an Olympus BX43F microscope.

3.1.10 Adhesion assay

The adhesion assay is a method to test the adherence of cells to other cells or matrices. To analyze the role of EpCAM in cell adhesion, all adhesion assays were performed without calcium to prevent cell adhesion mediated by cadherins.

3.1.10.1 Cell-matrix adhesion assay w/o calcium

Required reagents:

- DMEM (culture medium)
- DMEM w/o FCS w/o Calcium (adhesion medium)
- PBS
- Matrigel (40 μ l/ml in adhesion medium)
- Calcein AM (1mg/ml)
- Lysis buffer (2% triton X-100 in dd. H₂O)

Note: All centrifugation steps were performed for 5min at 280rcf at room temperature.

For calcium independent cell-matrix adhesion assay, cells were harvested and counted and the required number of cells (1x10⁴ cells/well in a 96-well plate) was plated on 10cm dishes. 24h later, culture medium was discarded, cells were washed 3 times with PBS, 5ml fresh adhesion medium was added and cells let be grown over night. In addition, 96-well plates with flat bottom were coated with 50 μ l matrigel solution over night at 37°C. The next day cells were harvested, washed once with PBS and resuspended in 1-3ml adhesion medium. For cell staining 2 μ l calcein AM per ml medium were added to the cells and samples were incubated for 1h at 37°C. Cells were then washed twice with PBS to get rid of residual calcein AM, were resuspended in adhesion medium and added to 96-well plates (1x10⁴ cells/well). No cells were plated in wells serving as background controls. Cell adhesion was allowed for 2h at 37°C. Thereafter, plates were washed twice with PBS. To do so, 200 μ l PBS were added in each well of another 96-well plate. Subsequently, the sample-containing plate was put onto this second plate and the construction was turned around twice, whereat input control wells were protected from washing upon coverage with parafilm. After washing, cells were lysed upon the addition of lysis buffer to the wells (2x lysis buffer was used for input control wells). Calcein fluorescence was measured on a Wallac Victor 1420 multilabel counter at 485nm/535nm wavelength. Further calculations were performed using Microsoft Excel.

3.1.10.2 Cell-cell adhesion assay w/o calcium

Required reagents:

- DMEM (culture medium)
- DMEM w/o Calcium w/o FCS (adhesion medium)
- PBS
- Calcein AM (1mg/ml)
- Lysis buffer (2% triton X-100 in dd. H₂O)

Note: All centrifugation steps were performed for 5min at 280rcf at room temperature.

For calcium independent cell-cell adhesion assays, cells were plated in 96-well plates with flat bottom (0.5×10^5 cells/well) and were grown over night in culture medium. These cells serve as a confluent matrix at the beginning of the assay. In parallel, additional cells, which were later added to the matrix-containing 96-well plates (1×10^4 cell/well), were plated in 10cm dishes and were grown over night. The next day, all cells were washed 3 times with PBS, and proper amounts of adhesion medium were added. 24h later, 96-well plates were washed once again with PBS and 50 μ l of fresh adhesion medium were added to each well. In parallel, the cells growing in 10cm dishes were harvested and counted. The required number of cells (1×10^4 cells/well) was washed once with PBS and resuspended in 1-3ml adhesion medium. For cell staining, 2 μ l calcein AM per ml medium were added to the cells and cells were incubated for 1h at 37°C. Subsequently, cells were washed twice with PBS to get rid of residual calcein AM, were resuspended in adhesion medium and added to 96-well plates (1×10^4 cells/well). No cells were plated in background control wells. Cell adhesion was allowed for 2h at 37°C. Thereafter, plates were washed twice with PBS. To do so, 200 μ l PBS were added in each well of another 96-well plate. Subsequently, the sample-containing plate was put onto this second plate and the construction was turned around twice, whereat input control wells were protected from washing upon coverage with parafilm. After washing, cells were lysed upon the addition of lysis buffer to the wells (2x lysis buffer was used for input control wells). Calcein fluorescence was measured on a Wallac Victor 1420 multilabel counter at 485nm/535nm wavelength. Further calculations were performed using Microsoft Excel.

3.2 Molecular methods

3.2.1 Isolation of mRNA

For the isolation of total RNA from cells, the RNeasy Mini Kit (Qiagen) with QiaShredder columns (Qiagen) was used according to the manufacturer's protocol. Isolated mRNA was stored at -80°C until further use.

3.2.2 Reverse transcription polymerase chain reaction (RT-PCR)

RT-PCR allows for the conversion of mRNA into cDNA, which subsequently can be used for cloning or qRT-PCR (see 3.2.3). The protein reverse transcriptase (RT) is used for this purpose.

Directly before RT-PCR, the concentration of the total RNA utilized for each experiment was determined with a „GeneQuantPro“ spectrophotometer (GE Healthcare). Subsequently, $1\mu\text{g}$ of the total RNA was added to $2\mu\text{l}$ of gDNA wipeout buffer and the mixture was filled up to $14\mu\text{l}$ with RNase free H_2O . The mixture was heated up to 42°C for 2min to ensure elimination of genomic DNA and then promptly put on ice. For cDNA synthesis, $1\mu\text{l}$ reverse transcriptase, $1\mu\text{l}$ primer mix and $4\mu\text{l}$ Quantiscript RT-buffer were added to the previous solution and the mixture was incubated for 30min at 42°C . As a last step, the sample was heated up to 95°C for 3min to stop the reverse transcription reaction.

Standard reaction procedure:

Mix 1:

| | |
|---------------------------------|------------------------|
| total RNA | $1\mu\text{g}$ |
| gDNA wipeout buffer | $2\mu\text{l}$ |
| RNase free H_2O | add to $14\mu\text{l}$ |

→ put into reaction tube at the beginning

Mix 2:

| | |
|-----------------------------|----------------|
| Quantiscript RT | $1\mu\text{l}$ |
| Quantiscript RT-buffer (5x) | $4\mu\text{l}$ |
| Primer mix | $1\mu\text{l}$ |

→ added to mix 1 later

Standard temperature settings:

| | | |
|-------------------------|---------|----------------------|
| Genomic DNA elimination | 2 min, | 42°C |
| Pause | 1 min, | on ice → add mix 2 |
| RT-PCR reaction | 30 min, | 42°C |
| Stop reaction | 3 min, | 95°C |

After reverse transcription, cDNA samples were stored at -20°C until further use.

3.2.3 Quantitative Real-Time PCR (qRT-PCR)

qRT-PCR allows for the comparison of amounts of specific cDNAs across samples. This is e.g. important to confirm si-/sh-knock-down efficiency, or to compare amounts of specific mRNAs in different parts of an organism or between cell lines.

For qRT-PCR analyses, the LightCycler 480 SYBR Green I Master kit (Qiagen) was used. A mastermix was prepared according to the number of templates and samples to be analyzed. Each sample was analyzed in duplicates.

Standard mastermix (per reaction):

| | |
|-----------------------------|------|
| cDNA (from RT-PCR reaction) | 1µl |
| Primer mix | 2µl |
| SYBR Green master-mix (2x) | 5µl |
| ddH ₂ O | 2µl |
| ----- | |
| Total | 10µl |

Primer mix: Consists of two highly specific primers (each 10µl of a 100µM stock), filled up with 180µl ddH₂O.

2x SYBR Green mastermix (Roche): Contains DNA-polymerase, SYBR-Green and reaction buffer.

Standard reaction setup:

| | |
|--------------------------|--|
| Initial segregation | 10 min, 95°C |
| Segregation | 30 sec, 95°C |
| Annealing and elongation | 60 sec, 72°C → back to step 2, 45 cycles |
| Cooling/Storage | 4°C |

Reaction data were acquired using a Light Cycler 480 device (Roche) and analyzed with LightCycler 480 SW 1.5 (Roche) and Microsoft Excel.

Calculation of different mRNA levels was based on crossing points (Cp) values, which depict the first cycle at which the fluorescence of a sample rises above the background level (Roche 2014). Calculations were performed according to Pfaffl et al., using the $\Delta\Delta C_p$ -method (Pfaffl 2001).

Calculations were the following:

1. Mean of 2 Cp-values: $C_p = (C_{p1} + C_{p2}) / 2$
2. Standardisation to housekeeping gene: $\Delta C_p = C_p - C_{p(\text{Housekeeping gene})}$
3. Calculation of relative gene expression levels:
 - a) Control group (was set to “1.0”): $\Delta\Delta C_{p(\text{control})} = 2^{-(\Delta C_{p(\text{control})} - \Delta C_{p(\text{control})})}$
 - b) Sample group: $\Delta\Delta C_{p(\text{sample})} = 2^{-(\Delta C_{p(\text{sample})} - \Delta C_{p(\text{control})})}$

3.3 Biochemical methods

3.3.1 Membrane assay

Required reagents:

- DMEM
- PBS (ice cold)
- Homogenisation buffer
- Assay buffer
- Whole cell lysis buffer (10x)

Note: After harvesting the cells, all steps were performed at 4°C or on ice.

To generate samples for membrane assays, cells were plated in three 14.5cm dishes and allowed to grow confluent. Subsequently, cell dishes were placed on ice, cells were washed twice with 10ml ice cold PBS, harvested using a cell scraper and transferred to a fresh 15ml reaction tube. Centrifugation was performed thrice for 5min at 280rcf and 4°C, whereat supernatant was discarded, and 5ml fresh PBS was added after each centrifugation step. After these washing steps, cells were homogenized in 3ml homogenisation buffer by douncing them 10 times with a microlance 3/23G 1.25” syringe and subsequently centrifuged for 15min at 1000rcf and 4°C to separate nuclei from the rest of the cells. The supernatant, containing

soluble proteins, membranes and small cell organelles, was split and transferred to two fresh 1.5ml reaction tubes, while the pellet was discarded. Centrifugation was performed for 20min at 16000rcf and 4°C to pellet membranes. To wash the membranes, supernatant was discarded, 500µl homogenisation buffer were added to each reaction tube (not mixed) and samples were centrifuged again for 5min at 16000rcf and 4°C. Finally, membranes were resuspended in 150µl assay buffer and incubated for 16h at 4°C to prevent protein cleavage (0h, control samples) or 37°C to allow protein cleavage (16h samples). Directly after incubation, 20µl 10x lysis buffer were added to each of the samples, which were subsequently processed as described in 3.3.2.

3.3.2 Preparation of whole cell lysates

Required reagents:

- Whole cell lysis buffer (2x)
- PBS
- Laemmli buffer (5x)

To generate samples for whole cell lysates, cells were harvested, washed once with PBS, and centrifuged for 5min at 280rcf and room temperature. The supernatant was discarded and the pellet resuspended in 2x its volume in 2x whole cell lysis buffer (instead of directly lysing the pellet it can also be stored at -80°C for several days). Thereafter, samples were incubated on a rotating platform for 10min at 4°C and subsequently centrifuged for 10min at 16000rpm and 4°C to remove cell debris. Supernatants, which contain solubilized proteins, were transferred into a fresh reaction tube and incubated on ice until subsequent processing. Protein concentration was determined using the BCA-assay (see 3.3.3). In a last step, laemmli buffer was added to the samples. These samples were heated at 95°C for 5min. Protein samples were stored at -20°C until further use.

3.3.3 Determination of protein concentration (BCA assay)

Required reagents:

- BCA assay kit

Protein concentrations were determined using BCA assay kit, according to the manufacturer's protocol. 1µl of the protein samples (10µl in case of membrane assays) were mixed with 99µl (90µl) BCA solution and absorbance at 595nm wavelength was measured with a spectrophotometer („GeneQuantPro“, GE Healthcare). All measurements were performed in duplicates. To calculate protein concentrations, a sample containing a determined concentration of bovine serum albumin (BSA) was used as reference, and background (BG) levels of BCA-only samples were subtracted.

Calculations were performed with Microsoft Excel using the following formula:

$$C_{(\text{sample})} = ((A_{\lambda(\text{sample})} - A_{\lambda(\text{BG})}) / (A_{\lambda(\text{BSA})} - A_{\lambda(\text{BG})})) \times C_{(\text{BSA})}$$

c = protein concentration in mg/ml

A_{λ} = absorbance

3.3.4 Sodium dodecyl sulfate polyacrylamide gel electrophoresis (SDS-PAGE)

Required reagents:

- 10x SDS running buffer
- Resolving gel
- Stacking gel
- APS
- TEMED
- ddH₂O

Resolving gel (15%)

| | |
|--------------------|---------|
| 30% acrylamide | 50ml |
| 2M TRIS pH 8.9 | 16.6ml |
| 0.5µ EDTA | 663µl |
| ddH ₂ O | 32.74ml |

Stacking gel (4%)

| | |
|--------------------|---------|
| 30% acrylamide | 13.3ml |
| 2M TRIS pH 6.8 | 16.6ml |
| 0.5µ EDTA | 663µl |
| ddH ₂ O | 69.44ml |

SDS-PAGE is used to separate polypeptides in a polyacrylamide gel matrix. The separation occurs according to the molecular weight of proteins. Treatment with SDS results in a coverage of proteins with negative charges such that protein size remains as the major parameter of separation. As a result, proteins with a smaller apparent molecular weight migrate faster than those with a higher apparent molecular weight.

Standard SDS-PAGE are comprised of two different types of gels, i.e. a stacking gel, which collects all proteins at the border between the two gel types, and the resolving gel in which the proteins are actually separated. Per gel, 10ml resolving gel (15%) were mixed with 50 μ l APS and 30 μ l TEMED, poured into the gel chamber and covered with ddH₂O to ensure a straight surface. After polymerisation the water was discarded and 2ml of the stacking gel were mixed with 30 μ l APS and 15 μ l TEMED, poured and polymerized on top of the separation gel. Subsequently, same amounts of proteins of whole cell lysate samples (see 3.3.2) were loaded on gels. Gel electrophoresis was conducted for 15min at 15mA and 2h at 30mA in SDS running buffer. Afterwards, gels were used for immunoblotting (see 3.3.5).

3.3.5 Immunoblotting (western blot)

Required reagents:

- Methanol
- 1x blotting buffer
- Blocking solution (5% milk in washing buffer)
- washing buffer (PBST)
- Specific primary and secondary antibodies
- Primary antibody solution (3% BSA in washing buffer)
- Secondary antibody solution (5% milk in washing buffer)
- Chemiluminescent HRP substrate

A wet blot system (Blotting System Mini trans Blot, BioRad) was used for immunoblotting. With this system, polypeptides separated in a polyacrylamide gel can be transferred to a polyvinylidene fluoride (PVDF) membrane. To do so, membranes were first incubated in methanol for 1min and then transferred into blotting buffer. After assembling the system, blotting was conducted for 50min at 100V and room temperature.

After blotting, PVDF membranes were first incubated in blocking solution for minimally 30min at room temperature to prevent unspecific antibody binding. After washing in PBST for 5min, membranes were incubated in primary antibody (diluted in 5ml primary antibody solution) for 1h at room temperature or over night at 4°C. Subsequently, membranes were washed thrice in PBST for 5min and incubated with the appropriate secondary antibody for 45min at room temperature (diluted in 5ml secondary antibody solution). After washing thrice in PBST for 5min, antigen-antibody reactions were revealed upon application of chemiluminescent HRP substrate (Millipore). Protein bands were detected using a ChemiDoc XRS+ imaging system (Biorad) and analyzed using ImageLab (Biorad) and Photoshop (Adobe) software.

3.4 Cell labeling and staining methods

3.4.1 Immunofluorescence

Required reagents:

- Methanol (-20°C)
- PBS
- Paraformaldehyde (PFA)
- Horse serum
- TRIS buffer (0.05M, pH 7.4)
- Specific primary and secondary antibodies

For immunofluorescence staining, cells were plated on glass slides in quadriperm dishes and cultured to the desired confluency. Subsequently, cells were washed thrice with PBS for 5min and fixed with 3.5% PFA for 10min in the dark at 4°C and 5min in the dark at room temperature. Cells were then washed thrice in PBS for 5min, permeabilized using ice cold methanol and blocked with 200µl horse serum (1:200 in TRIS buffer) for 20min at room temperature to prevent unspecific antibody binding. Thereafter, cells were incubated with the first antibody (mouse anti-EpCAM 1:1000 in 200µl TRIS buffer) for 1h at room temperature. After washing thrice with PBS for 5min, cells were incubated with a biotinylated anti-mouse antibody (1:200 in 200µl TRIS buffer) for 30min at room temperature, washed again thrice with PBS for 5min and stained with an Alexa 488-linked anti-biotin antibody (1:500 in 200µl TRIS buffer) until staining was sufficiently strong. Finally, cells were covered with

VectaShield containing DAPI to stain nuclei. Stainings were analyzed using a TCS-SP2 scanning system, a DM-IRB inverted microscope and LAS AF software (Leica).

3.4.2 Immunohistochemistry

Required reagents:

- Methanol (-20°C)
- PBS
- Paraformaldehyde (PFA)
- Horse serum
- TRIS buffer (0.05M, pH 7.4)
- Brij solution (50% Brij in PBS)
- Specific primary and secondary antibodies

Spheroids (see 3.1.9) and tumor explants (see 3.5) were placed in cryomolds, embedded with Tissue Tek and frozen in liquid nitrogen. Frozen samples were processed to serial slices of 4µm thickness with a Cryostat model CM 1900 (Leica) and put on glass slides. Samples were frozen at -20°C until further use.

For immunohistochemical staining, samples were fixed in acetone for 5min at room temperature, followed by fixation with 3.5% PFA for 10min in the dark at 4°C and 5min in the dark at room temperature. Subsequently, endogenous peroxidase activity was blocked upon incubating the samples using 0.03% H₂O₂ in PBS for 10min at room temperature. Sections were washed twice in PBS for 5min at room temperature and incubated with horse serum (1:200 in 200µl TRIS buffer) for 20min at room temperature to prevent unspecific antibody binding. Incubation with first antibody (1:1000 in 200µl TRIS buffer) was performed for 1h at room temperature or over night at 4°C. After washing samples with PBS and Brij solution, sections were incubated with a biotinylated anti-mouse antibody (1:200 in 200µl TRIS buffer) for 30min at RT, washed again with PBS and Brij solution, and subsequently incubated with a peroxidase-labeled avidin–biotin complex. Finally, cells were stained with amino-ethylcarbazole (AEC) as a peroxidase substrate, generating a red-brown staining of the antigen/antibody complexes. Counterstaining was achieved with hematoxylin (blue). Samples were covered with Kaiser's glycerol gelatine and pictures were taken using a Olympus BX43F fluorescence microscope and CellEntry software (Olympus).

3.5 Mouse experiments

Required reagents:

- DMEM w/o FCS
- Growth Factor Reduced BD Matrigel Matrix
- TissueTek® O.C.T Compound
- Liquid nitrogen

Note: All experiments were performed with the approval of the Ethics Commission of the Ludwig Maximilians University Munich (Az.55.2-1-54-2532-101-07) and the Landesamt für Natur, Umwelt und Verbraucherschutz Nordrhein-Westfalen (8.87-50.10.37.09.105).

To analyze *in vivo* growth of tumors, Kyse 520 cells stably transfected with either control or EpCAM-specific shRNA (cell lines kindly provided by Christiane Driemel, Düsseldorf), were injected in 6-8 week old, male NOD SCID mice. Therefore, 5×10^6 cells in 100 μ l DMEM w/o FCS were mixed with 100 μ l Growth Factor Reduced BD Matrigel Matrix and the mixture injected subcutaneously in the right and left flanks of mice using a BD Microlance 3/24G 1`. In addition, another fraction of these cells was used for *in vitro* analyses such as cytospin (see 3.1.6), immunohistochemistry (3.4.2), western blot (see 3.3.5), and qRT-PCR (see 3.2.3). After cell injection, mice were continuously observed for signs of tumor growth. Objective quantitative endpoints for the experiment were a tumor size larger than 20mm, a tumor weight superior to 4g and an animal weight loss superior to 20% of the initial body weight. According to these endpoints but no later than 28 days mice were sacrificed by isofluran inhalation. Formed tumors were explanted, tumor weights were assessed using a precision scale, and tumor tissues were embedded in Tissue Tek and frozen for immunohistochemical analyses (see 3.4.2).

3.6 Statistical analysis

Statistical calculations were performed using Microsoft Excel. The Student's t-Test was applied to calculate the statistical significance of differences between experimental groups. P-values of 0.05 were considered significant. Bars and error bars in histograms represent mean values \pm standard deviation (s.d.) of at least three independent experiments.

4 RESULTS

The formation of metastases is the major reason for cancer related deaths (Sleeman and Steeg 2010; Stoecklein and Klein 2010; Chaffer and Weinberg 2011). Therefore, it is mandatory to identify and analyze mechanisms involved in this process. To form metastases, cancer cells need to loosen from primary tumors, invade the surrounding tissue and intravasate into the blood stream or the lymphatic system upon which they can be allocated to different parts of the body. In the next steps, these circulating tumor cells (CTCs) need to leave the blood or lymphatic system, settle in a secondary organ such as liver, bone or lungs, and resume proliferation (Chaffer and Weinberg 2011). Despite the importance of identifying the processes involved in the different stages of metastasis formation, so far numerous aspects of carcinoma progression remain unexplored.

The epithelial cell adhesion molecule (EpCAM) is known to be overexpressed in most carcinomas (van der Gun *et al.* 2010). Its expression is correlated with increased cell proliferation, formation of larger primary tumors (Maetzel *et al.* 2009) and in the majority of cases a bad prognosis for cancer patients (Spizzo *et al.* 2004; Varga *et al.* 2004; Brunner *et al.* 2008; van der Gun *et al.* 2010). Because of its strong overexpression in carcinomas, EpCAM is used as a marker to identify cancer cells, including CTCs and DTCs (Cohen *et al.* 2006; Criscitiello *et al.* 2010). However, there is evidence that EpCAM is not constantly expressed throughout the whole process of carcinogenesis. It rather seems that EpCAM is highly expressed in primary carcinomas and large metastases, whereas it appears to be downregulated in CTCs, DTCs and micrometastases (Jojovic *et al.* 1998; Rao *et al.* 2005; Gorges *et al.* 2012). These findings suggest a more complex role of EpCAM during the different stages of cancer formation and progression than assumed up to now.

In the present study, esophageal cancer cells were used as model system to get deeper insights into the actual expression of EpCAM during and its influence on tumor formation and progression. These findings shall help to get a better understanding of the processes leading to formation of primary tumors and metastases.

4.1 Cellular systems

4.1.1 Esophageal cancer cell lines Kyse 30 and Kyse 520

To investigate the role of EpCAM during carcinogenesis the esophageal cancer cell lines Kyse 30 and Kyse 520 were used. In a first set of experiments these cell lines were characterized in terms of their morphology and EpCAM expression levels.

Both cell lines showed a typical epithelial morphology (Fig. 4.1 A) and grew in clusters with cobblestone-like appearance (Fig. 4.1 A a-c). However, there were also obvious differences between the cell lines. Kyse 30 cells were larger than Kyse 520 cells, and did not display even cobblestone-like morphology as Kyse 520 cells, but rather included spindle shaped cells (compare Fig. 4.1 A a, d to b, c, e, f). Morphological differences were also observed within the Kyse 520 population. One subpopulation (Kyse 520-1) showed a more round-shaped phenotype and grew in a compacted manner (Fig. 4.1 A b, e), whereas the other (Kyse 520-2) showed a flattened, less compacted phenotype (Fig. 4.1 A c, f). Furthermore, Kyse 520-1 cells had the ability to grow in an anchorage independent way and built up cell piles (Fig. 4.1 A e), which were not observed in case of Kyse 520-2 and Kyse 30 cells, which only grew as single layers (Fig. 4.1 A d, f).

In addition to morphology, EpCAM expression levels of each cell line were assessed using flow cytometry (see 3.1.5.1) and western blot analysis (see 3.3.5). In flow cytometry experiments EpCAM surface expression was analyzed upon incubation of cells with EpCAM-specific as well as isotype antibodies and the measurement of the resulting fluorescence intensities in a FACS-Calibur flow cytometer. All cell lines displayed strong fluorescence signals when incubated with EpCAM-specific antibodies, showing that all cell lines contained high levels of EpCAM at their surfaces (Fig. 4.1 B). However, EpCAM cell surface levels significantly differed between the cell lines. Kyse 520-1 cells showed the highest fluorescence intensities of all analyzed cell lines, displaying a mean fluorescence intensity (MFI) ratio of 288.54, whereas Kyse 30 and Kyse 520-2 cells displayed MFI-ratios of 183.78 and 56.79, respectively (Fig. 4.1 C). In addition to cell surface levels, total protein amounts of EpCAM were measured in whole cell lysates of all cell lines using western blot analysis. Western blot results confirmed data gained in flow cytometry analyses. Kyse 520-1 cells showed the strongest signals in western blot membranes upon incubation with EpCAM-specific antibodies. Compared to Kyse 520-1 cells, EpCAM-specific western blot signals of Kyse 30 and Kyse 520-2 cells were only 50% and 20%, respectively (Fig. 4.1 D). Due to their different

EpCAM levels, Kyse 520 subpopulations from here on are referred as Kyse 520^{high} and Kyse 520^{low} cells.

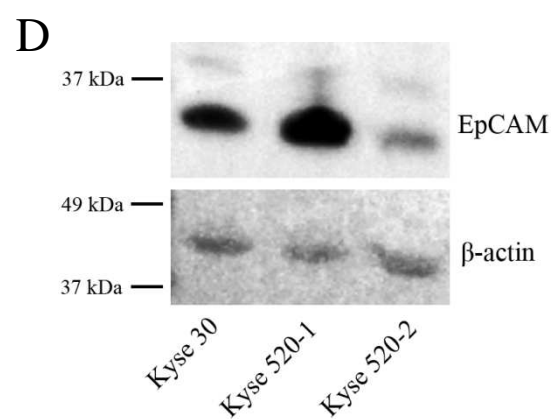
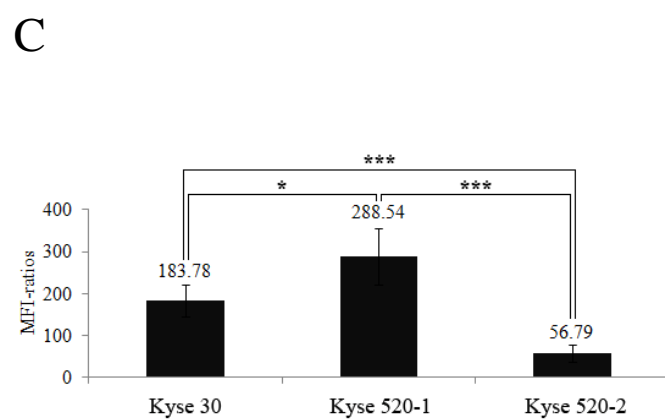
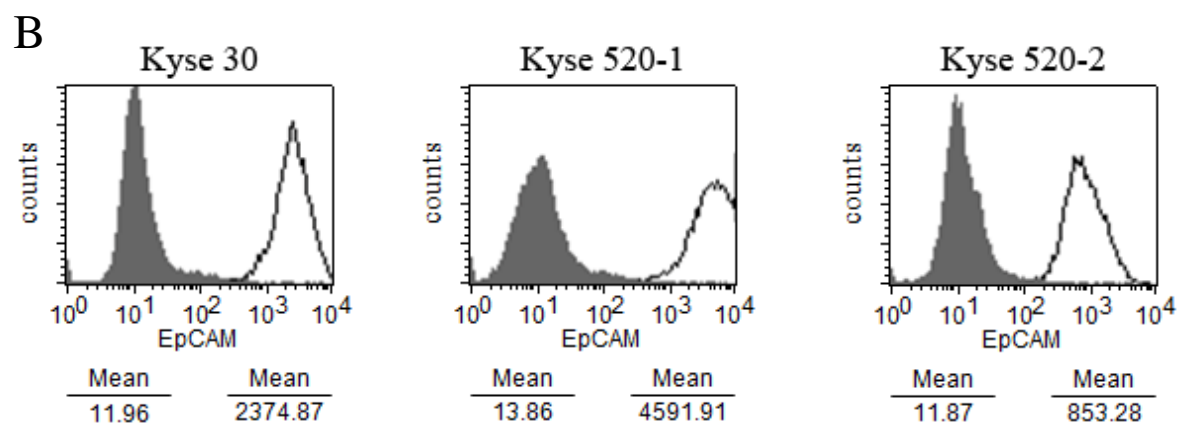
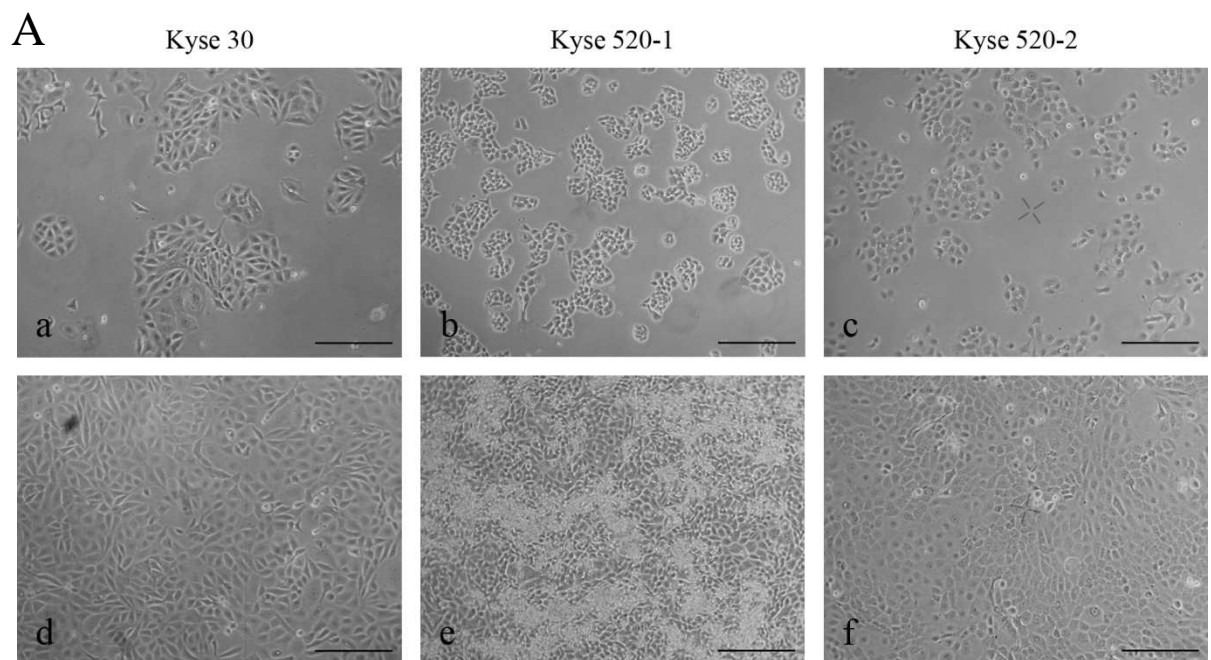


Figure 4. 1: Characterisation of esophageal cancer cell lines.

(A) Morphology of the Kyse cell lines at different densities. Cells were plated in 6-well plates and pictures were taken under an Axiovert 25 microscope (Zeiss) using a Samsung WB750 camera. Bars = 250µm. (B-D) EpCAM levels of different Kyse cell lines. (B) Representative flow cytometry histograms. EpCAM cell surface expression was measured by flow cytometry with EpCAM-specific antibodies (black lined histograms) and isotype controls (filled histograms). (C) Mean fluorescence intensity ratios of EpCAM cell surface expression in different Kyse cell lines are given with standard deviations from three independent experiments. PI was used to exclude dead cells from analyses. (D) Total EpCAM protein levels of different Kyse cell lines in western blot. Whole cell lysates were prepared, equal protein amounts loaded on an SDS gel and transferred to a PVDF membrane. Membrane was incubated with EpCAM-specific antibodies and developed using ECL substrate. β -actin served as control for equal protein loading. P-values: * $p < 0.05$; ** $p < 0.01$; *** $p < 0.001$.

4.1.2 Non-small cell lung cancer cell line A549

Besides esophageal cancer cell lines, the non-small cell lung cancer cell line A549 was used in a set of experiments to get deeper insights into the role of EpCAM in cancer development and progression. Comparably to Kyse cell lines, A549 cells were characterized in terms of their morphology and EpCAM expression levels.

A549 cells displayed an epithelial morphology and grew mainly in clusters (Fig. 4.2 A). However, A549 cells have the ability to grow as single cells and formed clusters which were less compact compared to those of Kyse cell lines (compare Fig. 4.2 A a and Fig. 4.1 A a-c). Furthermore, as was seen in case of Kyse 30 cells, A549 cells sometimes showed a slightly spindle shaped morphology.

EpCAM levels of A549 cells were assessed using flow cytometry and western blot analysis. In contrast to Kyse cell lines, A549 cells generated only weak fluorescence signals in flow cytometry when incubated with EpCAM-specific antibodies (Fig. 4.2 B). EpCAM-specific MFI ratio of A549 cells was 5.33, being only around 2% of the signals generated in Kyse 520^{high} cells (Fig. 4.2 C). These findings were confirmed upon western blot analysis, in which the EpCAM-specific western blot signal of A549 cells was apparently weaker than that of Kyse 520^{high} cells (Fig. 4.2 D).

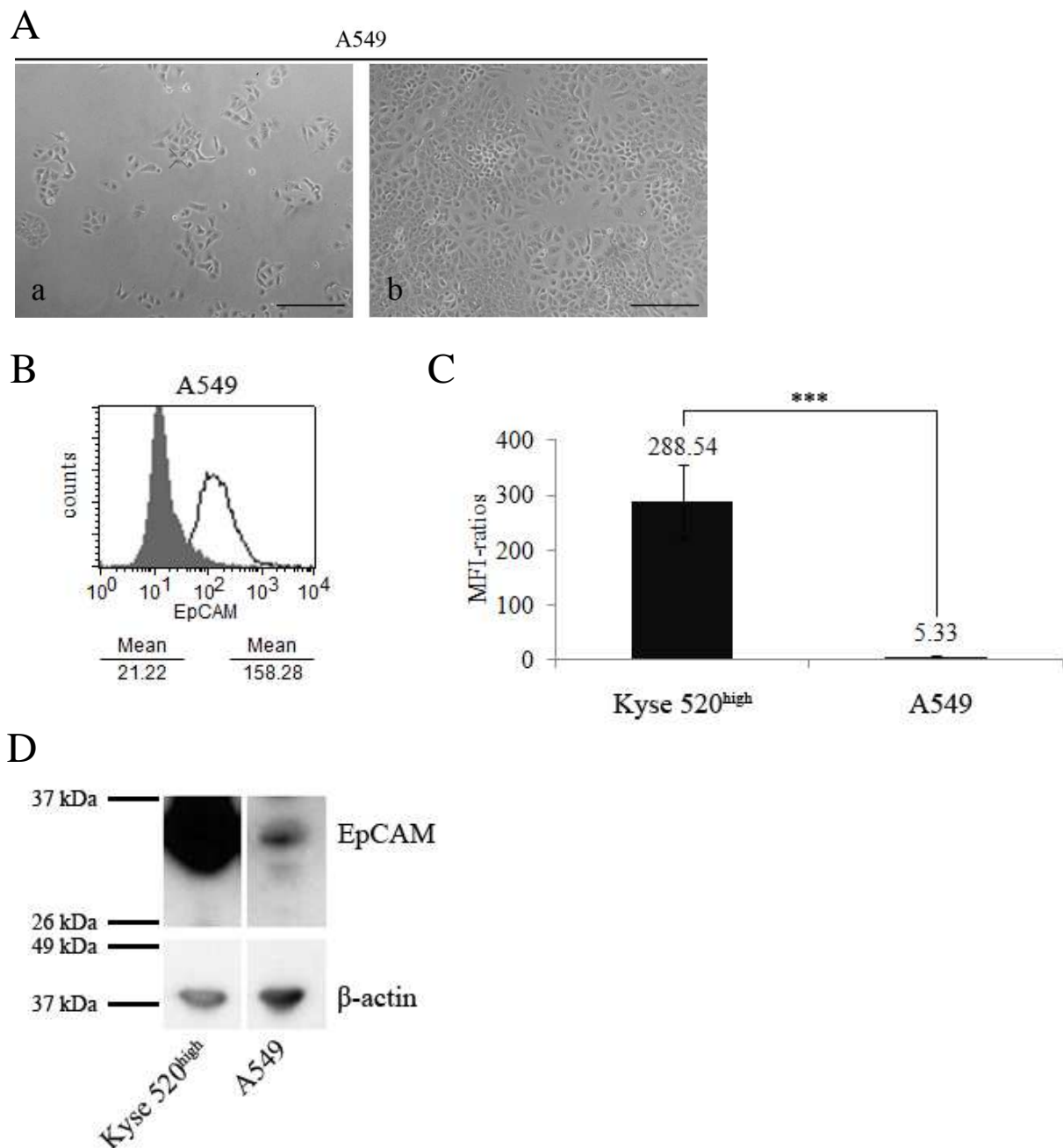


Figure 4. 2: Characterisation of the A549 cell line.

(A) Morphology of A549 cells at different densities. Cells were plated in 6-well plates and pictures were taken under an Axiovert 25 microscope (Zeiss) using a Samsung WB750 camera. Bars = 250 μ m. (B-D) EpCAM level of A549 cells. (B) Representative flow cytometry histogram. EpCAM cell surface expression was measured by flow cytometry with EpCAM-specific antibodies (black lined histograms) and isotype controls (filled histograms). (C) Mean fluorescence intensity ratios of EpCAM cell surface expression in A549 and Kyse 520^{high} cell lines are given with standard deviations from three independent experiments. PI was used to exclude dead cells from the analyses. (D) Total EpCAM protein levels of A549 and Kyse 520^{high} cells in western blot. Whole cell lysates were prepared, equal protein amounts loaded on an SDS gel and transferred to a PVDF membrane. Membrane was incubated with EpCAM-specific antibodies and developed using ECL substrate. β -actin served as control for equal protein loading. P-values: *p < 0.05; ** p < 0.01; *** p < 0.001.

4.1.3 Cell lines stably overexpressing EpCAM

Besides wildtype cells, cell lines stably overexpressing different yellow fluorescent protein (YFP)-fusion constructs were used in the present study to obtain further insights into the function of EpCAM. To create these cell lines, wildtype cells were transfected with a 141pCAG-3SIP vector containing either the full-length EpCAM fused to YFP (EpCAM-YFP), the intracellular part of EpCAM fused to YFP (EpICD-YFP) or YFP only (YFP), which served as reference and control (all constructs were cloned and kindly provided by Matthias Hachmeister, Head and Neck research department, Klinikum Großhadern). MATra transfection reagent was used to introduce the abovementioned constructs into cells (see 3.1.4.1), which were subsequently selected to produce stable transfectants using puromycin, an antibiotic selecting for cells that express the resistance gene of the inserted construct (see 3.1.4.2). After selection, all cell lines were analyzed using flow cytometry (see 3.1.5.2) and western blot (3.3.5) assays to ensure that cell populations stably express the gene of interest from the stably transfected constructs.

Figures 4.3, 4.4 and 4.5 show the results of flow cytometry and western blot analyses of stably transfected A549 (Fig. 4.3), Kyse 30 (Fig. 4.4) and Kyse 520^{high} (Fig. 4.5) cell lines. To see how many percent of stably transfected cells actually express YFP constructs, fluorescence intensity of YFP was analyzed using flow cytometry. Appropriate wildtype cell lines, which do not express YFP, served as controls in these experiments. In all stable transfectants the bulk of cells showed a YFP fluorescence signal (Fig. 4.3 A, Fig. 4.4 A, Fig. 4.5 A, black lines histograms). In case of A549 cells, 99.48% of cells transfected with YFP, 99.01% of cells transfected with EpICD-YFP and 98.60% of cells transfected with EpCAM-YFP showed a fluorescence signal (Fig. 4.3 A). Similar numbers were assessed in stably transfected Kyse 30 cell lines. Here, 99.50% of cells transfected with YFP, 98.75% of cells transfected with EpICD-YFP and 99.94% of cells transfected with EpCAM-YFP displayed fluorescence signals (Fig. 4.4 A). In case of Kyse 520^{high} cells, 88.53% of cells transfected with YFP, 83.18% of cells transfected with EpICD-YFP and 81.96% of cells transfected with EpCAM-YFP showed a fluorescence signal (Fig. 4.5 A). Although all three constructs were expressed in similar proportion of cells, expression strength of each construct differed. A549 cells, stably expressing YFP displayed a mean fluorescence intensity of 4667. EpICD-YFP expressing A549 cells displayed a mean fluorescence intensity of 2277 and EpCAM-YFP expressing cells a mean fluorescence intensity of 2691 (Fig. 4.3 A). In case of Kyse 30 cells, cells transfected with YFP displayed a mean fluorescence intensity of 8372, cells transfected

with EpICD-YFP a mean intensity of 4687 and cells transfected with EpCAM-YFP a mean fluorescence intensity of 4379 (Fig. 4.4 A). Analyses of stable Kyse 520^{high} cells revealed that YFP expressing cells were characterized by a YFP mean fluorescence intensity of 5038, while cells expressing EpICD-YFP displayed a mean fluorescence intensity of 2356 and cells expressing EpCAM-YFP a mean fluorescence intensity of 1038 (Fig. 4.5 A). As abovementioned, all YFP fluorescences were set relative to appropriate wildtype cells, which did not express any YFP protein and therefore served as controls (Fig. 4.3 A, Fig. 4.4 A, Fig. 4.5 A, filled histograms).

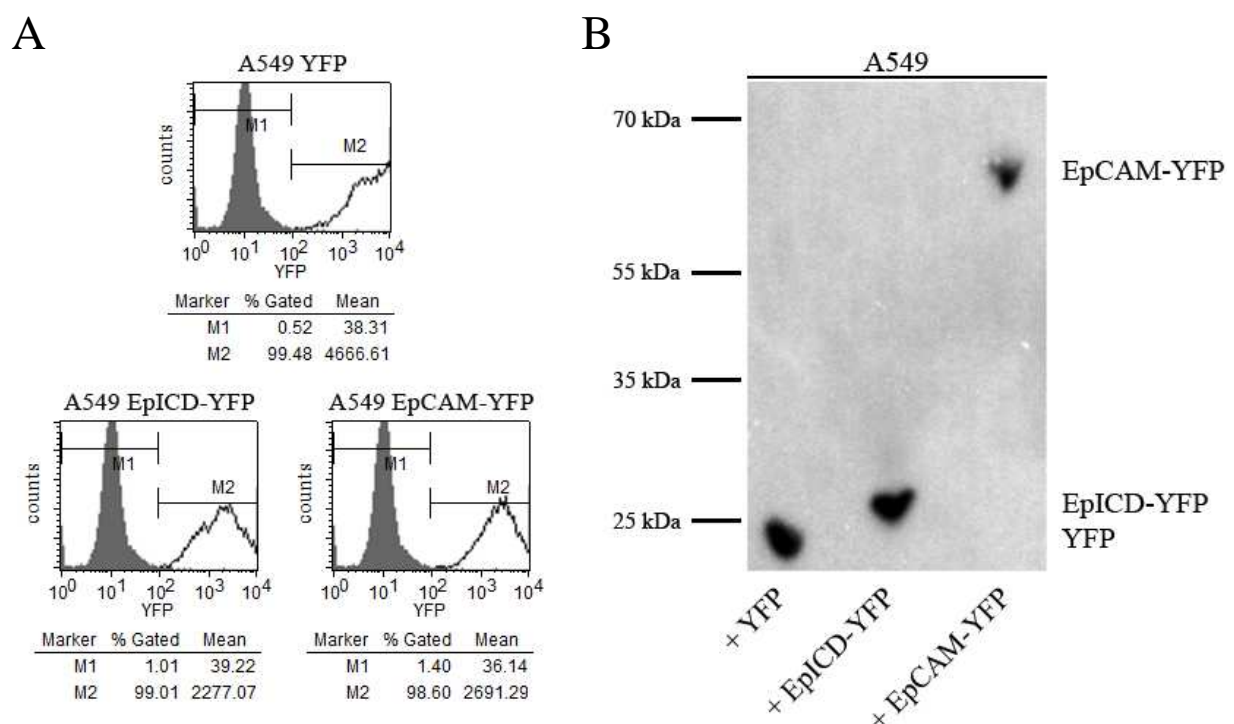


Figure 4. 3: A549 cell lines stably expressing YFP-constructs.

A549 cells were transfected with different YFP constructs and selected using puromycin. After selection, cells were analyzed using flow cytometry and western blot. (A) Flow cytometry analysis of stable A549 cell lines. YFP fluorescence of stable cell lines (black lines histograms) was assessed using flow cytometry. Appropriate wildtype cell lines (filled histograms), which did not express any YFP protein, served as control and were used to set the gates M1 and M2. PI was used to exclude dead cells from the analyses. (B) Western blot analysis of stably transfected A549 cell lines. Whole cell lysates were prepared, equal amounts of proteins were separated in an SDS gel and proteins transferred to a PVDF membrane. Subsequently, membranes were incubated with YFP-specific antibodies and detected using ECL substrate.

Figures 4.3 B, 4.4 B, and 4.5 B show the results of western blot analyses. Equal protein amounts of whole cell lysates from A549 (Fig. 4.3 B), Kyse 30 (Fig. 4.4 B) and Kyse 520^{high} cells (Fig. 4.5 B), stably transfected with YFP, EpICD-YFP or EpCAM-YFP, were loaded on SDS gels and subsequently blotted on PVDF membranes. Membranes were then incubated with YFP-specific antibodies and signals were detected using a ChemiDoc XRS imaging system (BD). Expected molecular weights of the stably expressed proteins were 26.9 kDa (YFP), 30.9 kDa (EpICD-YFP) and 61.9 kDa (EpCAM-YFP). A549, Kyse 30, and Kyse 520^{high} cell lines each showed only one band at the expected positions. No additional or unspecific bands were detected in any of the tested cell lines (Fig. 4.3 B, Fig. 4.4 B, Fig. 4.5 B).

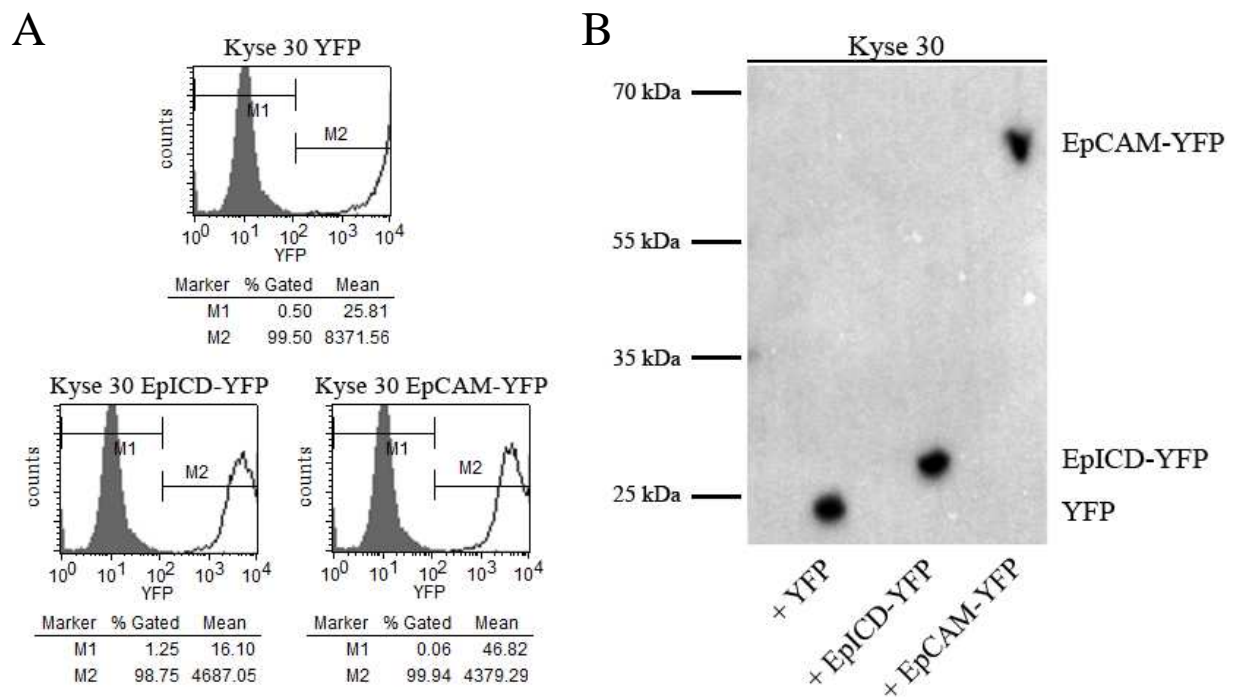


Figure 4. 4: Kyse 30 cell lines stably expressing YFP-constructs.

Kyse 30 cells were transfected with different YFP constructs and selected using puromycin. After selection, cells were analyzed using flow cytometry and western blot. (A) Flow cytometry analysis of stable Kyse 30 cell lines. YFP fluorescence of stable cell lines (black lines histograms) was assessed using flow cytometry. Appropriate wildtype cell lines (filled histograms), which do not express any YFP protein, served as control and were used to set the gates M1 and M2. PI was used to exclude dead cells from the analyses. (B) Western blot analysis of stable transfected Kyse 30 cell lines. Whole cell lysates were prepared, equal amounts of proteins were separated in an SDS gel and proteins transferred to a PVDF membrane. Subsequently, membranes were incubated with YFP-specific antibodies and detected using ECL substrate.

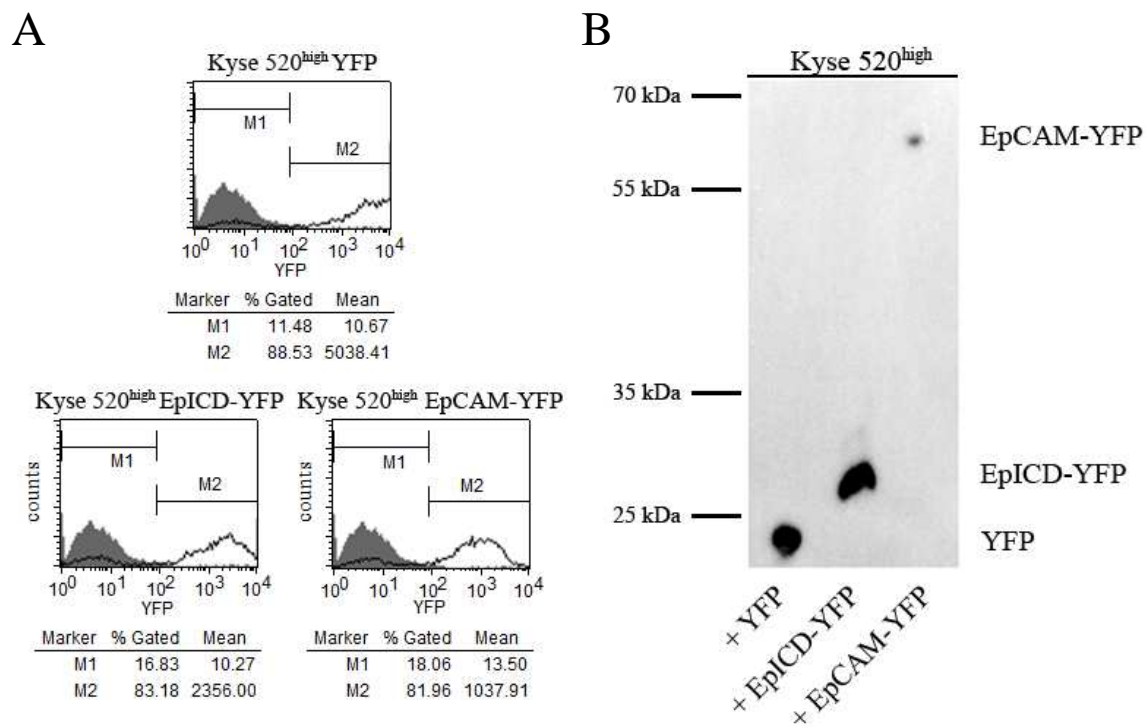


Figure 4. 5: Kyse 520^{high} cell lines stably expressing YFP-constructs.

Kyse 520^{high} cells were transfected with different YFP constructs and selected using puromycin. After selection, cells were analyzed using flow cytometry and western blot. (A) Flow cytometry analysis of stable Kyse 520^{high} cell lines. YFP fluorescence of stable cell lines (black lines histograms) was assessed using flow cytometry. Appropriate wildtype cell lines (filled histograms), which do not express any YFP protein, served as control and were used to set the gates M1 and M2. PI was used to exclude dead cells from the analyses. (B) Western blot analysis of stable transfected Kyse 520^{high} cell lines. Whole cell lysates were prepared, equal amounts of proteins were separated in an SDS gel and proteins transferred to a PVDF membrane. Subsequently, membranes were incubated with YFP-specific antibodies and detected using ECL substrate.

4.2 EpCAM is cleaved in esophageal cancer cell lines

As published in 2009 by Maetzel *et al.*, EpCAM is proteolytically cleaved in HCT-8 and FaDu cells by TACE and presenilin-2 (Maetzel *et al.* 2009). Here, cleavage of EpCAM was assessed in esophageal carcinoma cell lines. To do so, membrane assays (see 3.3.1) were performed in conjunction with subsequent western blot using Kyse 30 and Kyse 520^{high} cells, stably overexpressing EpCAM-YFP (see 4.1.3). Stable cell lines were used instead of wildtype cells because YFP-tagged cleavage products of EpCAM can be visualized more reliably in western blot than cleavage products of wildtype EpCAM. Especially EpICD, with a size of only 4 kDa, is small and labile so that it can hardly be detected in western blot. Membranes from Kyse 30 and Kyse 520^{high} cells were purified as described in 3.3.1 and incubated for 16h at 4°C (0h samples) or 37°C (16h samples). Protein concentrations were assessed using BCA assay (see 3.3.3), and equal protein amounts were loaded on SDS gels and subsequently transferred to a PVDF membrane (see 3.3.5). The membrane was incubated with YFP-specific antibodies in combination with HPR-coupled secondary antibody to detect YFP-tagged EpCAM cleavage products. Expected molecular weights of potential EpCAM cleavage products were ~33 kDa (CTF-YFP), 30.9 kDa (EpICD-YFP) and 26.9 kDa (YFP). Full-length EpCAM-YFP was expected to display an apparent molecular weight of 61.9 kDa.

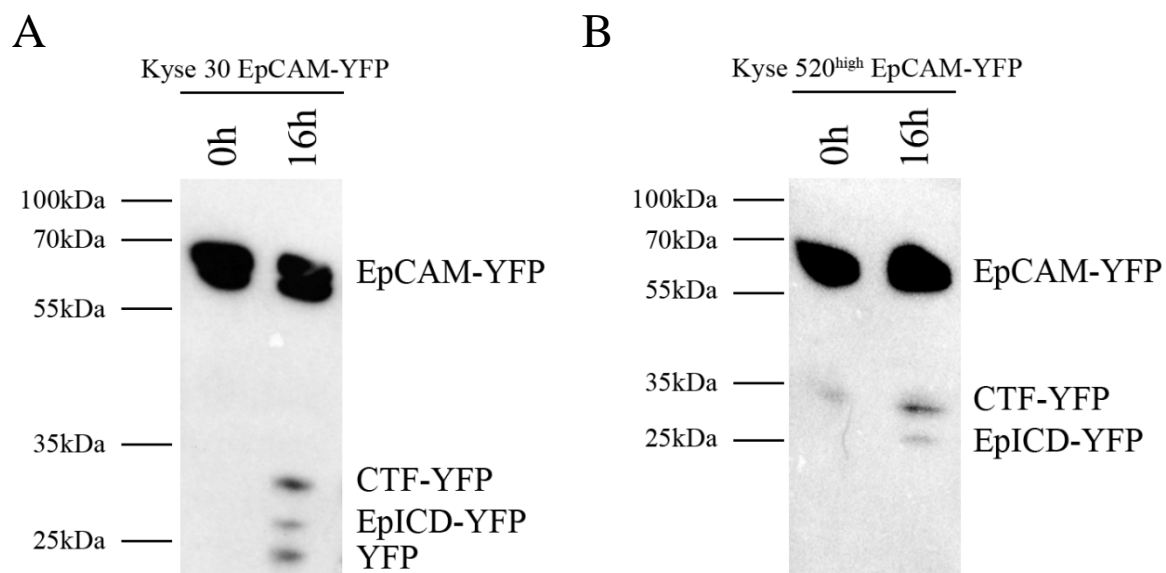


Figure 4. 6: EpCAM is cleaved in Kyse 30 and Kyse 520^{high} cells.

Human esophageal cancer cell lines Kyse 30 and Kyse 520^{high}, stably overexpressing EpCAM-YFP, were used for membrane assay and subsequent western blotting to analyze EpCAM cleavage. Shown are representative blots of Kyse 30 (A) and Kyse 520^{high} (B) samples, incubated with YFP-specific antibody in combination with HPR-coupled secondary antibody.

For Kyse 30 cells only a double-band at the expected height of EpCAM-YFP could be detected in lanes containing 0h samples (Fig. 4.6 A, 0h samples). However, in lanes containing 16h samples, three additional bands, at sizes between 20 and 35kDa, were detectable. These additional bands were located at the expected positions of CTF-YFP, EpICD-YFP and YFP (Fig. 4.6 A, 16h sample). The appearance of a double band at the position of EpCAM-YFP is most likely due to the appearance of different EpCAM glycosylation isoforms (see 1.2.2).

Similar findings were made for Kyse 520^{high} cells. One single band at the expected position of EpCAM-YFP could be detected in lanes containing 0h samples (Fig. 4.6 B, 0h samples), whereas lanes containing 16h samples, displayed two additional bands, at sizes between 20 and 35kDa. These additional bands appeared at the expected positions of CTF-YFP and EpICD-YFP (Fig. 4.6 B, 16h sample).

4.3 EpCAM increases proliferation in esophageal cancer cell lines

EpCAM is a known inducer of proliferation in different cell types and cancer entities (Munz *et al.* 2004; Maetzel *et al.* 2009). Therefore it was tested if EpCAM also impacts on proliferation of esophageal cancer cell lines. To do so, in a first set of experiments Kyse 520^{high} esophageal cancer cells were transfected with either a control or an EpCAM-specific siRNA. To ensure that effects on cell proliferation are not only due to treatment with siRNA, in a second set of experiments proliferation levels of Kyse 520^{high} and Kyse 520^{low} subpopulations, expressing different amounts of EpCAM (see 4.1.1), were compared.

4.3.1 Knock-down of EpCAM decreases proliferation in esophageal cancer cells

To test if depletion of EpCAM has an influence on cell proliferation, Kyse 520^{high} cells were transiently transfected with either a control (ctrl) or an EpCAM-specific siRNA using the MATra transfection system (see 3.1.4.1). After transfection, equal cell numbers were plated in 6-well plates and cells were allowed to grow for 72h in medium containing 10% FCS (normal condition) or 1% FCS (serum starvation). EpCAM knock-down efficiency and proliferation rates were assessed using flow cytometry (see 3.1.5.1) and cell counting (see 3.1.2).

Figure 4.7 sums up the results of three independent experiments. Transfection with EpCAM-specific siRNA led to an average EpCAM knock-down of 51% in the Kyse 520^{high} cells (Fig. 4.7 A-B). Cell numbers were reduced to 71% when cultured with 10% FCS and 58% when cultured with 1% FCS in EpCAM-depleted cells compared to ctrl siRNA transfected cells. Although in both cases proliferation was decreased, observed differences were only significant when assays were performed in the presence of 1% FCS (Fig. 4.7 C).

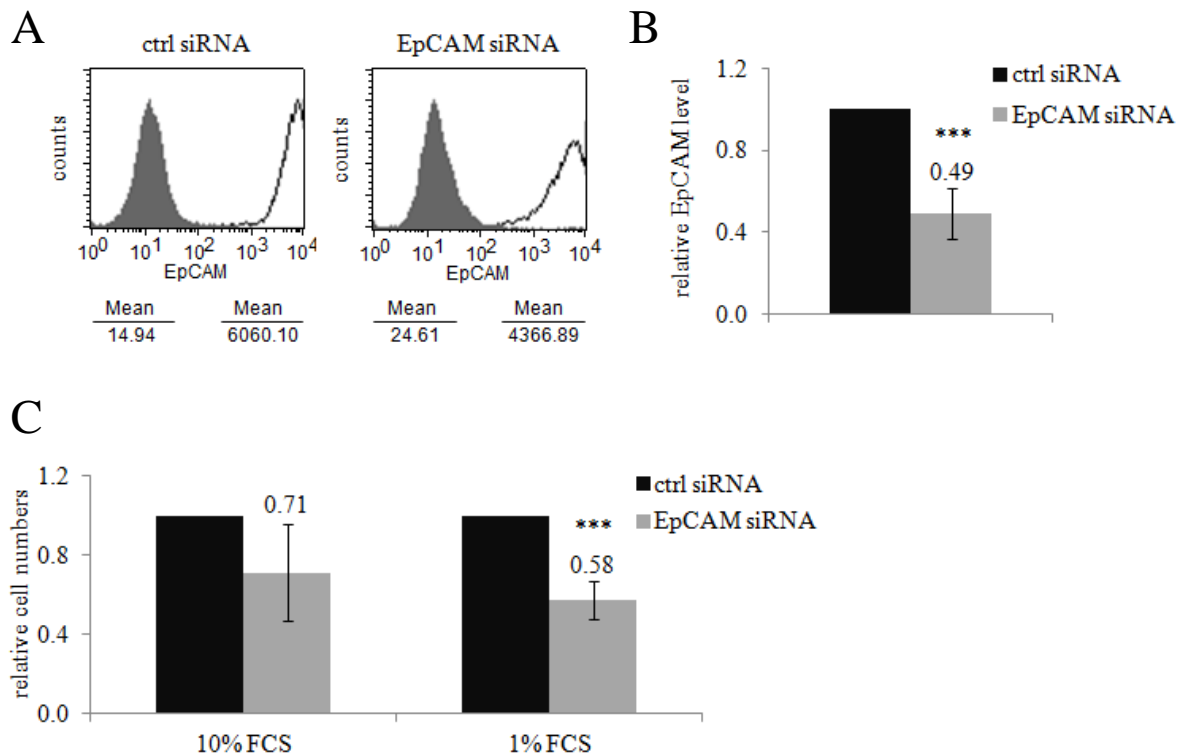


Figure 4. 7: EpCAM knock-down decreases proliferation in Kyse520^{high} cells.

EpCAM expressing Kyse 520^{high} cells were transiently transfected with either a ctrl or an EpCAM-specific siRNA using the MATra transfection system, equal cell numbers were plated in 6-well plates and cells grown for 72h in medium containing 10% or 1% FCS. Knock-down efficiency and relative proliferation rates were assessed using flow cytometry and cell counting. (A) Representative flow cytometry graphs. EpCAM cell surface expression was measured by flow cytometry with EpCAM-specific antibodies (black lined histograms) and isotype controls (filled histograms). (B) Relative mean fluorescence intensity ratios of EpCAM cell surface expression in Kyse 520^{high} cells treated with ctrl siRNA or EpCAM-specific siRNA are given with standard deviations of three independent experiments. Controls are set to “1.0”. (C) Relative cell numbers of Kyse 520^{high} cells treated with either ctrl or EpCAM-specific siRNA. Shown are mean values with standard deviations of three independent experiments. Controls are set to “1.0”. P-values: *p < 0.05; ** p < 0.01; *** p < 0.001.

4.3.2 Kyse 520^{high} cells proliferate faster than Kyse 520^{low} cells

SiRNA-mediated knock-down of EpCAM in Kyse 520^{high} cells resulted in a decrease of proliferation. To ensure that effects on proliferation were not only due to siRNA treatment, the proliferation of Kyse 520 subpopulations (Kyse 520^{high} and Kyse 520^{low}) was analyzed in an independent set of experiments. Kyse 520 subpopulations share the same genetic background and only differ in their EpCAM expression. Hence, potential differences in proliferation of both cell lines can be attributed to EpCAM and associated effects. To analyze proliferation, equal numbers of Kyse 520^{high} and Kyse 520^{low} cells were plated in 6-well plates and grown for 72h in the presence of 1% FCS. EpCAM levels and proliferation rates were assessed using flow cytometry and cell counting.

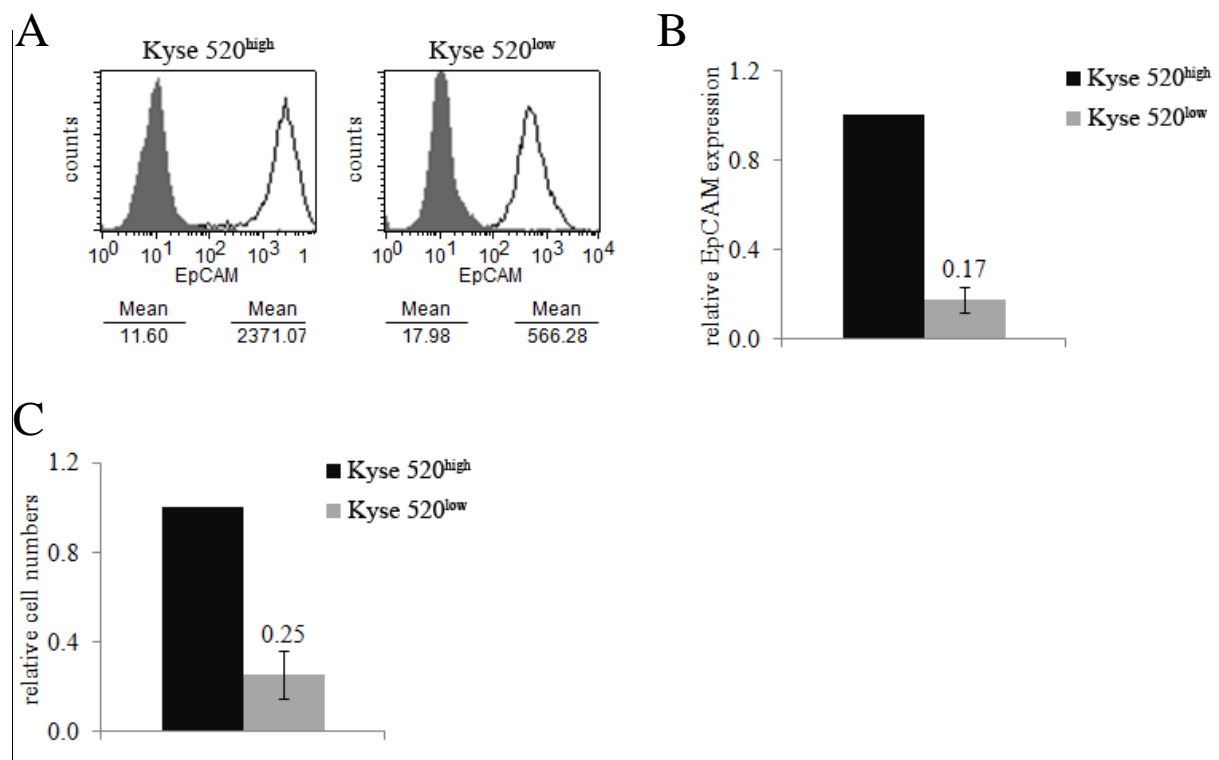


Figure 4. 8: Kyse 520^{high} cells proliferate faster than Kyse 520^{low} cells.

Equal numbers of EpCAM expressing Kyse 520^{high} and Kyse 520^{low} cells were plated in 6-well plates and grown for 72h in the presence of 1% FCS. Cell numbers were counted and EpCAM levels were assessed using flow cytometry. (A) Representative flow cytometry graphs are displayed. EpCAM cell surface expression was measured by flow cytometry with EpCAM-specific antibodies (black lined histograms) and isotype controls (filled histograms). (B) Relative mean fluorescence intensity ratios of EpCAM cell surface expression in Kyse 520^{high} and Kyse 520^{low} cells are given with standard deviations of three independent experiments. Controls are set to “1.0”. (C) Relative cell numbers of Kyse 520^{high} and Kyse 520^{low}. Shown are mean values with standard deviations of three independent experiments. Controls are set to “1.0”. P-values: *p < 0.05; ** p < 0.01; *** p < 0.001.

Flow cytometry data confirmed data already acquired in 4.1.1, demonstrating 5-fold higher EpCAM surface levels in Kyse 520^{high} compared to Kyse 520^{low} cells (Fig. 4.8 A-B). Counting of cell numbers revealed that Kyse 520^{high} cells generated 4-fold more progeny than Kyse 520^{low} cells, which showed on average only 25% of cell numbers counted for Kyse 520^{high} cells (Fig. 4.8 C).

4.4 EpCAM expression enhances tumor growth *in vivo*

Besides enhancing proliferation, EpCAM expression was also associated with formation of larger tumors in *in vivo* mouse model (Maetzel *et al.* 2009). To test if EpCAM has the same effect in esophageal carcinomas, esophageal cancer cells expressing different levels of EpCAM were injected into 6-8 week old, male NOD SCID mice and tumor growth was monitored. Kyse 520 cells, which were stably transfected with either a control (ctrl) or an EpCAM-specific shRNA (cells were produced and kindly provided by Christiane Driemel, Düsseldorf) served as model system in this experiment. After ensuring a potent EpCAM knock-down, 5×10^6 cells from each stable cell line were mixed 1:1 with matrigel, injected into the right (ctrl shRNA) and left (EpCAM shRNA) flanks of the mice (see 3.5) and tumor formation was allowed for a maximum of 28 days. Tumors formed were explanted and analyzed in terms of size and EpCAM expression levels.

Figure 4.9 sums up the results of the experiment. Before injecting into mice, EpCAM levels of ctrl and EpCAM shRNA stable transfectants were analyzed using qRT-PCR (Fig. 4.9 A), western blot (Fig. 4.9 B) and cytospin (Fig. 4.9 D a, c). EpCAM mRNA level was reduced to 5% in Kyse 520 cells stably transfected with EpCAM-specific shRNA compared to control cells, representing a knock-down efficiency of 95% at mRNA level (Fig. 4.9 A). Protein levels of EpCAM were assessed using western blot analysis as well as cytospin with subsequent immunohistochemistry. For western blot, equal protein amounts of ctrl and EpCAM shRNA stable transfectants were loaded on an SDS gel, and transferred to a PVDF membrane, which was incubated with EpCAM-specific antibodies. No EpCAM signal could be detected in lanes containing protein of EpCAM shRNA stable transfectants after an exposure time of 60 sec, whereas a strong, specific signal could be seen in the lane containing the sample of ctrl shRNA transfected cells (Fig. 4.9 B). Results from western blot could be confirmed also in cytospin analysis. Here, Kyse 520 cells stably transfected with EpCAM-specific shRNA displayed a much weaker staining intensity compared to ctrl shRNA transfected cells, when incubated with EpCAM-specific antibodies (Fig. 4.9 D a, c).

After confirming EpCAM knock-down efficiency in EpCAM shRNA stable transfectants, stable cell lines were injected into the right and left flanks of five NOD-SCID mice and tumor growth was allowed for a maximum of 28 days. Tumors formed were explanted and analyzed in terms of size and EpCAM expression. Figure 4.9 C displays the tumor weight of all tumors formed. For both cell lines, tumors had formed in four out of five mice. However, mean weights of the tumors significantly differed, from 0.39g to 0.14g for ctrl and EpCAM shRNA stable transfected cells lines, respectively. In addition to assessing tumor weights, EpCAM expression of the explanted tumors was analyzed using immunohistochemistry (see 3.4.2). Tumors derived from ctrl shRNA transfected cells showed an overall strong expression of EpCAM, reflecting the high levels of EpCAM of cells initially injected into mice (Fig. 4.9 D a-b). However, tumors derived from EpCAM shRNA stable transfectants displayed an unexpectedly high expression of EpCAM, which was in contrast to the low EpCAM levels cells measured before injection into the mice (Fig. 4.9 D c-d). This potential discrepancy was investigated in further detail upon a more precise comparison of EpCAM levels of ctrl and EpCAM shRNA transfected cells before injection, using cytopins, with those of their corresponding tumor explants. To do so, EpCAM expression was classified in four levels: no EpCAM expression (0), weak EpCAM expression (1), intermediate EpCAM expression (2) and strong EpCAM expression (3). Figure 4.9 E displays EpCAM levels of the different samples. In case of ctrl shRNA transfected cells, 0% of tumor cells in cytopin and 0.20% of tumor cells in the explants showed no EpCAM expression, 13.30% and 10.80% of cells displayed a weak, 45.20% and 52.40% an intermediate, and 41.50 and 36.60% a strong expression of EpCAM (Fig. 4.9 E, left panel). Hence, EpCAM levels before and after injection revealed no significant difference. However, in case of EpCAM shRNA stable transfectants, 35.50% of tumor cells in cytopin and 11.70% of tumor cells in the explants displayed no expression of EpCAM, 51.70% and 38.80% of cells showed a weak, 10.90% and 40.30% an intermediate, and 1.90% and 9.20% a strong expression of EpCAM (Fig. 4.9 E, right panel). These results were suggestive of a positive selection of EpCAM expressing cells *in vivo*.

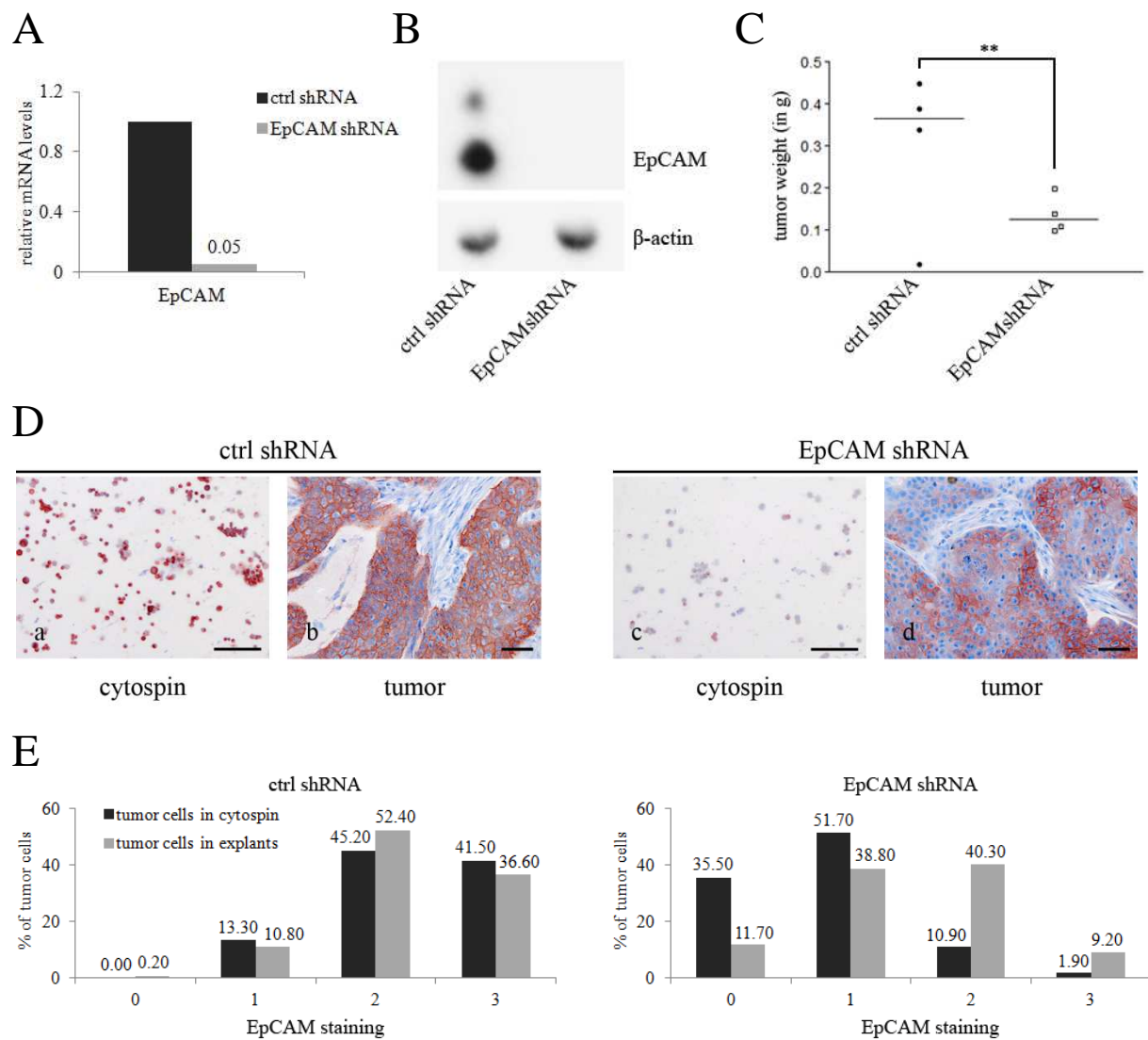


Figure 4. 9: EpCAM expression is correlated to tumor growth *in vivo*.

Ky520 cells were stably transfected with either a ctrl or an EpCAM-specific shRNA and injected into the flanks of 6-8 week old NOD-SCID mice. Tumors formed were explanted and analyzed in terms of size and EpCAM expression. (A) EpCAM levels of ctrl shRNA and EpCAM shRNA stable transfectants were assessed using qRT-PCR with EpCAM-specific primers. β -Actin served as housekeeping gene. Controls are set to "1.0". (B) EpCAM protein levels of ctrl and EpCAM shRNA stable transfected cells were analyzed in western blot with EpCAM-specific antibodies in combination with HRP-conjugated secondary antibody. Shown are expression levels of EpCAM in ctrl and EpCAM shRNA treated cells before inoculation into mice. β -Actin served as control for equal sample loading. (C) Five NOD-SCID mice were injected with ctrl or EpCAM shRNA stable transfectants in the right and left flanks, respectively. Tumor growth was allowed for a maximum of 28 days and weight of tumors was assessed and is given in gram. (D) EpCAM expression was assessed by immunocytochemistry in cytopsin of ctrl and EpCAM-specific shRNA stable transfectants and by immunohistochemistry after xenotransplantation using EpCAM-specific antibodies. Bars (cytopsin) = 200 μ m, bars (explants) = 50 μ m. (E) EpCAM expression was quantified in cytopsin and tumor explants. Staining ranged from 0-3, which represents negative (0), weak (1), intermediate (2), and strong expression (3). Shown are percentages of tumor cells classified from 0-3.

4.5 Reduction of EpCAM correlates with mesenchymal traits

4.5.1 EpCAM is downregulated in migrating cells

The experiments presented so far revealed that EpCAM expression correlated with increased proliferation and tumor formation in esophageal cancer cell lines. These findings are in line with already published data, demonstrating the role of EpCAM in proliferation and tumor formation in different cancer entities (Munz *et al.* 2004; Maetzel *et al.* 2009). However, there is increasing evidence for a dynamic expression of EpCAM throughout the various stages of carcinogenesis, and it appears that EpCAM is downregulated in a proportion of CTCs, DTCs and small metastases (Jojovic *et al.* 1998; Rao *et al.* 2005; Gorges *et al.* 2012). These findings lead to the question, what are the reasons and advantages of EpCAM downregulation in these cells.

At different stages of carcinogenesis, cells need to switch and/or adapt phenotype to allow for further cancer progression. In the first step of cancer formation, cells need to have an epithelial, proliferating phenotype to give rise to a primary tumor. Later, cells have to adopt a mesenchymal phenotype, allowing them to loosen from the primary tumor, and invade into the blood or lymph system and disseminate. This phenotypic switch is termed epithelial-to-mesenchymal transition (EMT). However, in order to enable outgrowth of metastases, this phenotypic change needs to be reversed in a process called mesenchymal-to-epithelial transition (MET) to reactivate the epithelial, proliferative characteristics of cancer cells.

One major result of EMT is the generation of migrating cells with a mesenchymal phenotype. Therefore, the expression of EpCAM was monitored during the migration of Kyse 30 and Kyse 520^{low} cells in scratch assay experiments (see 3.1.8). In these experiments, cells were plated on glass slides, grown to confluency, a scratch was set into the cell monolayer and migration of cells was allowed for 24h. Subsequently, cells were washed with PBS and stained with EpCAM-specific antibody in combination with fluorescence-coupled secondary antibodies (see 3.4.1). Samples were analyzed using a TCS-SP2 confocal microscope (Leica).

Figures 4.10 and 4.11 sum up the results of the experiments. Scratching of cells led to formation of wounds in the cell monolayers as well as to disruption of cells at the borders of the scratches. To close these wounds, cells started to loosen from neighbouring cells and migrated into the wounded area. Figure 4.10 a-c shows a part of the scratch where so far no migration had occurred. Cells in this area displayed the typical EpCAM staining pattern of

epithelial cells, mainly characterized by a strong staining at plasma membranes (Fig. 4.10 a-c). This pattern was also observed in all cells, which did not migrate. However, in migrating cells, the staining pattern of EpCAM was changed. Strong EpCAM signals at the plasma membranes were lost and fluorescence signals were detected in the cytoplasm rather than at cell membranes. In addition, cells furthest away from the initial scratch displayed lowest EpCAM staining (Fig. 4.10 d-m, Fig. 4.11). Changes in staining patterns between migrating and non-migrating cells were found in both, Kyse 30 and Kyse 520^{low} cells.

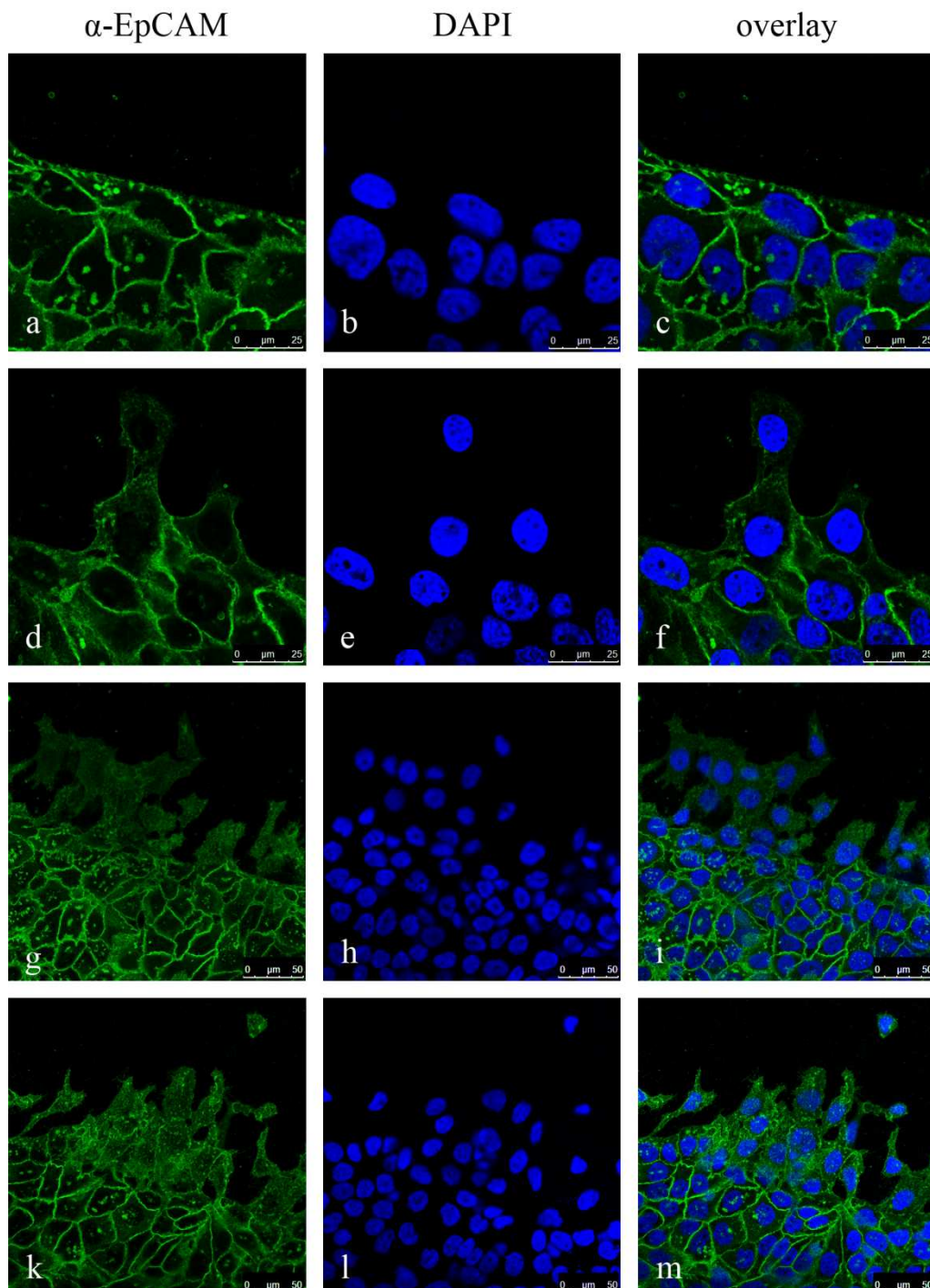
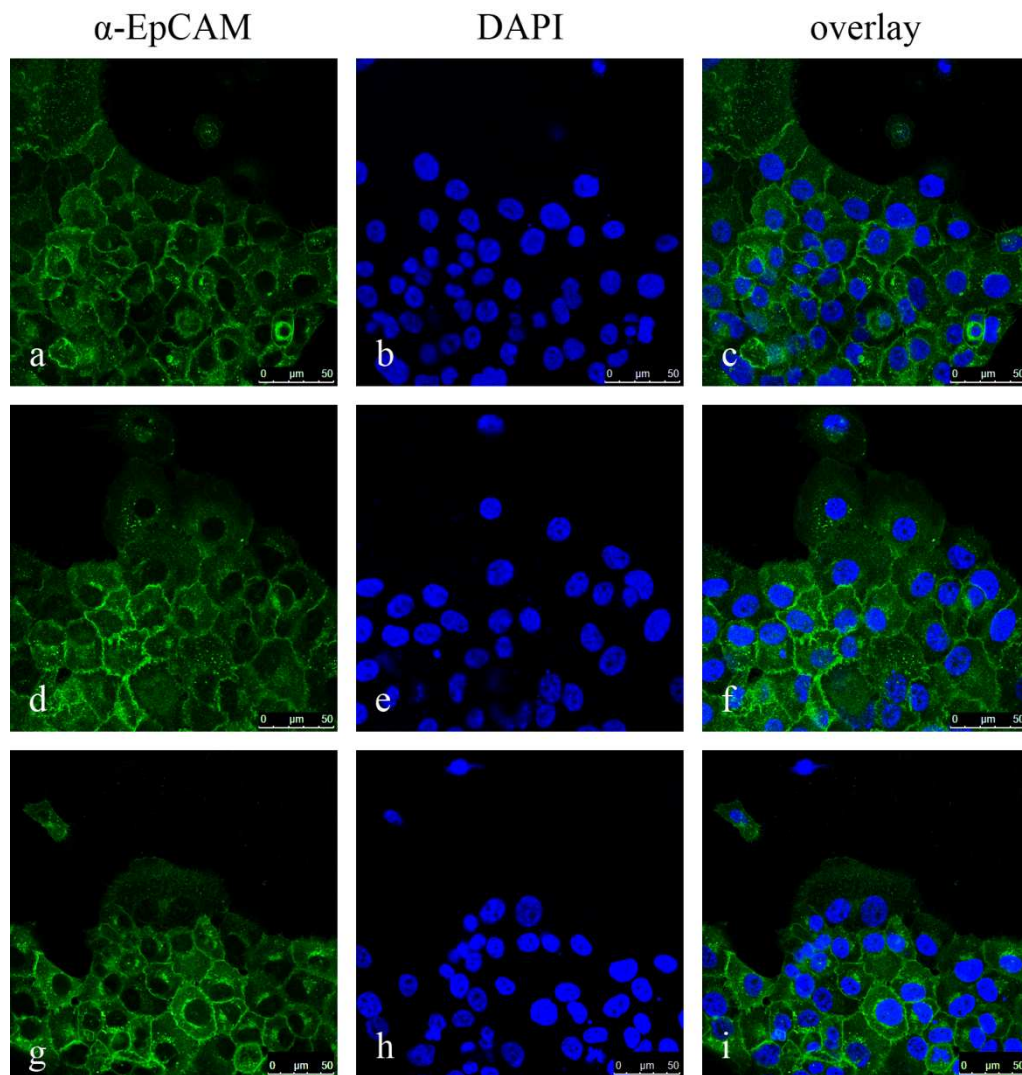


Figure 4. 10: Migrating Kyse 30 cells downregulate EpCAM expression.

Kyse 30 cells were plated on glass slides, grown to density and scratches were set in confluent monolayers. After allowing migration for 24h, cells were washed with PBS, and stained with EpCAM-specific antibody in combination with Alexa488-coupled secondary antibody. Subsequently, cells were embedded with Vectashield, containing DAPI for nuclear staining. Shown are microphotographs of Kyse 30 cells taken under a TCS-SP2 confocal microscope (Leica).

**Figure 4. 11: Migrating Kyse 520^{low} cells downregulate EpCAM expression.**

Kyse 520^{low} cells were plated on glass slides, grown to density and scratches were set in confluent monolayers. After allowing migration for 24h, cells were washed with PBS, and stained with EpCAM-specific antibody in combination with Alexa488-coupled secondary antibody. Subsequently, cells were embedded with Vectashield, containing DAPI for nuclear staining. Shown are microphotographs of Kyse 520^{low} cells taken under a TCS-SP2 confocal microscope (Leica).

4.5.2 Downregulation of EpCAM is associated with increased migration velocity and gain of mesenchymal markers

Previous experiments revealed that migrating cells were characterized by weaker EpCAM staining than non-migrating cells, pointing towards a downregulation of EpCAM in migrating cells. Therefore, in a next set of experiments the impact of EpCAM expression on migration velocity was addressed. For these experiments two model systems were used. On the one hand, Kyse 30 cells were transiently transfected with either control or EpCAM-specific siRNA. On the other hand, naturally occurring Kyse 520^{high} and Kyse 520^{low} cells were included in the experiment. Scratch assays were performed to analyze the migration velocity of these cells (see 3.1.8). It is important to mention that in these experiments it was crucial to add proper controls in order to distinguish between cell migration and proliferation. In addition, experiments were performed under 0% FCS to minimize proliferative effects.

4.5.2.1 Kyse 30 cells migrate faster and show increased vimentin levels upon depletion of EpCAM

Kyse 30 cells were transfected with either control or EpCAM-specific siRNA (see 3.1.4.1). To measure the efficiency of EpCAM knock-down, EpCAM levels were assessed at mRNA and protein levels using qRT-PCR (see 3.2.3) and flow cytometry (see 3.1.5.1), respectively. On average, EpCAM was downregulated to 15% at mRNA (Fig. 4.12 F) and 52% at cell surface level (Fig. 4.12 A-B) in Kyse 30 cells transfected with EpCAM-specific siRNA compared to ctrl cells. Relative cell proliferation rates were assessed by counting cell numbers of the proliferation controls, which were grown under similar conditions as the scratched cells. No significant difference could be observed between proliferation rates of ctrl and EpCAM-depleted Kyse 30 cells when cultured w/o FCS (Fig. 4.12 C).

Figure 4.12 D-E displays the results of cell migration analyses. Representative pictures (Fig. 4.12 D), as well as mean migration velocity data (Fig. 4.12 E), show that cells transfected with EpCAM-specific siRNA migrated faster and closed scratches earlier compared to cells transfected with ctrl siRNA. Consequently, the mean migration velocity of EpCAM-depleted cells was 3.02-fold higher than that of control cells.

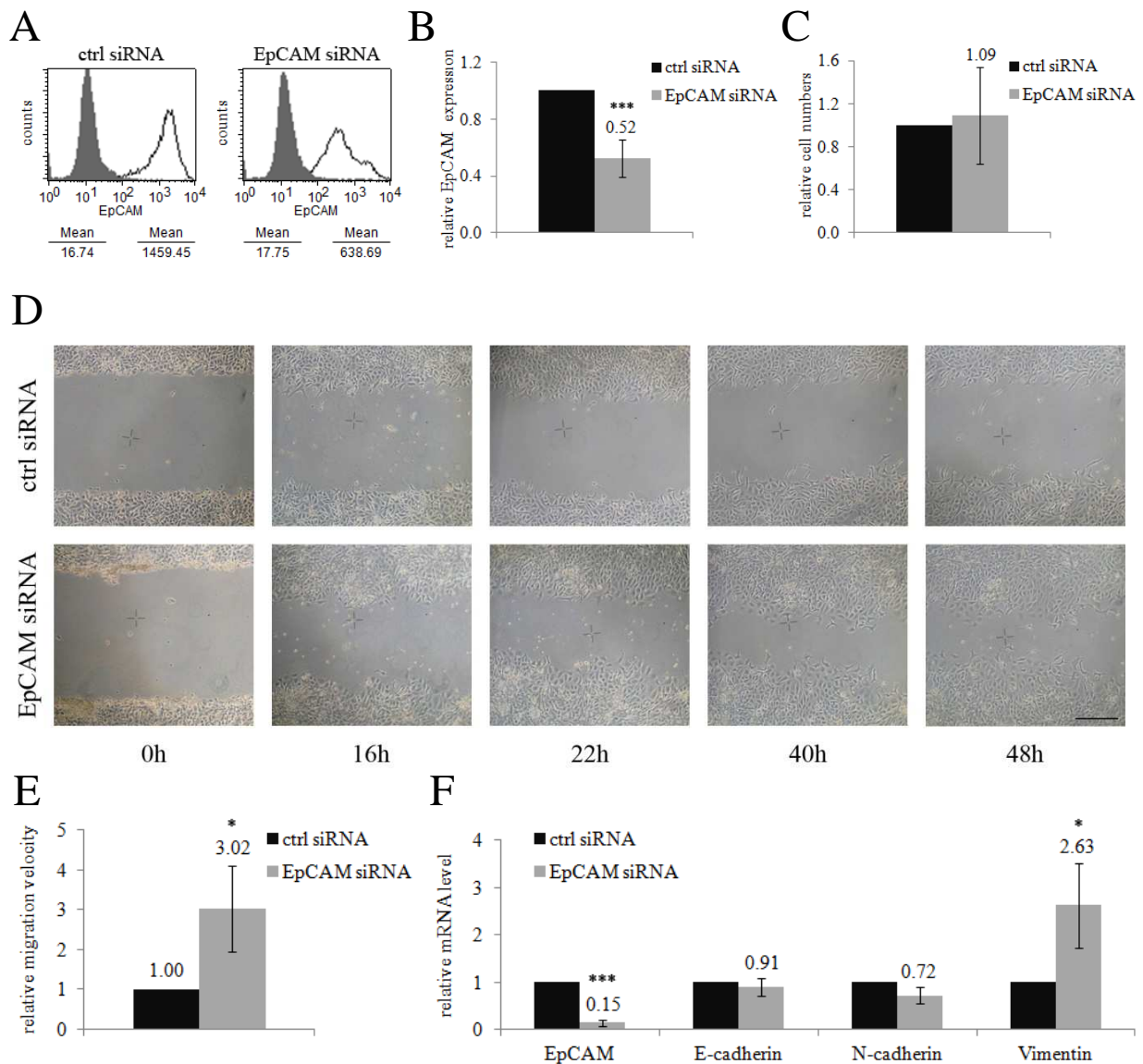


Figure 4.12: Scratch assays with siRNA transfected Kyse 30 cells.

Kyse 30 cells were transiently transfected with either control or EpCAM-specific siRNA, and used in scratch assays under restrictive conditions (0% FCS). (A) Representative flow cytometry graphs. EpCAM cell surface expression was measured by flow cytometry with EpCAM-specific antibodies (black lined histograms) and isotype controls (filled histograms). (B) Relative mean fluorescence intensity ratios of EpCAM cell surface expression in Kyse 30 ctrl siRNA and EpCAM siRNA cells are given with standard deviations from three independent experiments. Controls are set to “1.0”. (C) Control and EpCAM siRNA transfected cells were seeded at equal numbers and cell numbers were determined after completion of the experiments. Shown are mean relative numbers normalized to control treated cells from three independent experiments. Controls are set to “1.0”. (D) Confluent layers of control and EpCAM siRNA transfected cells were scratched and closure of the scratch was assessed over time. Microphotographs were taken at the indicated time points. Bar = 250 μ m. (E) Relative migration velocities of control and EpCAM siRNA transfected cells are given as mean values from three independent experiments with standard deviations. Controls are set to “1.0”. (F) Levels of EpCAM, E-cadherin, N-cadherin and vimentin mRNAs were assessed by qRT-PCR with *GAPDH* as a reference gene. Shown are normalized relative mRNA levels standardized to ctrl siRNA transfected Kyse 30 cells from three independent experiments. P-values: * $p < 0.05$; ** $p < 0.01$; *** $p < 0.001$.

Besides assessing cell numbers and migration velocities, mRNA levels of selected epithelial and mesenchymal markers were measured using qRT-PCR. The epithelial marker E-cadherin showed a relative mRNA level of 91% in EpCAM-depleted cells compared to control cells, whereas mesenchymal markers N-cadherin and vimentin showed relative mRNA levels of 72% and 263% in cells transfected with EpCAM-specific siRNA compared to ctrl siRNA transfected cells (Fig. 4.12 F).

4.5.2.2 Kyse 520^{low} cells migrate faster and show higher levels of mesenchymal markers than Kyse 520^{high} cells

To ensure that differences in migration velocity and EMT marker expression are not due to siRNA treatment in general, naturally occurring Kyse 520^{high} and Kyse 520^{low} cells were used in scratch assays under restrictive conditions (0% FCS), and migration velocity and levels of epithelial and mesenchymal markers were assessed.

EpCAM levels of Kyse 520^{high} and Kyse 520^{low} cells were assessed at mRNA and protein level using qRT-PCR (see 3.2.3) and flow cytometry (see 3.1.5.1), respectively. Kyse 520^{low} cells displayed on average 26% of EpCAM mRNA (Fig. 4.13 F) and 14% of EpCAM cell surface levels (Fig. 4.13 A-B) compared to Kyse 520^{high} cells. Proliferation rate was assessed by counting cells of the proliferation controls after completion of scratch assays. On average Kyse 520^{high} cells showed a more than 4-fold higher cell number compared to Kyse 520^{low} cells (Fig. 4.13 C).

Figure 4.13 D-E shows the results of cell migration analyses. Representative pictures (Fig. 4.13 D) as well as mean migration velocity data (Fig. 4.13 E) show that Kyse 520^{low} cells migrated faster and closed scratches earlier, compared to Kyse 520^{high} cells. Migration velocity of Kyse 520^{low} cells on average was 2.86-fold higher than that of Kyse 520^{high} cells.

Similarly to siRNA transfected Kyse 30 cells, mRNA levels of several EMT markers were assessed in Kyse 520^{high} and Kyse 520^{low} cells using qRT-PCR. The epithelial marker E-cadherin showed comparable mRNA levels in both cell lines. In contrast, mRNA levels of mesenchymal markers N-cadherin and vimentin were 206.85-fold and 257.83-fold higher on average in Kyse 520^{low} compared to Kyse 520^{high} cells (Fig. 4.13 F).

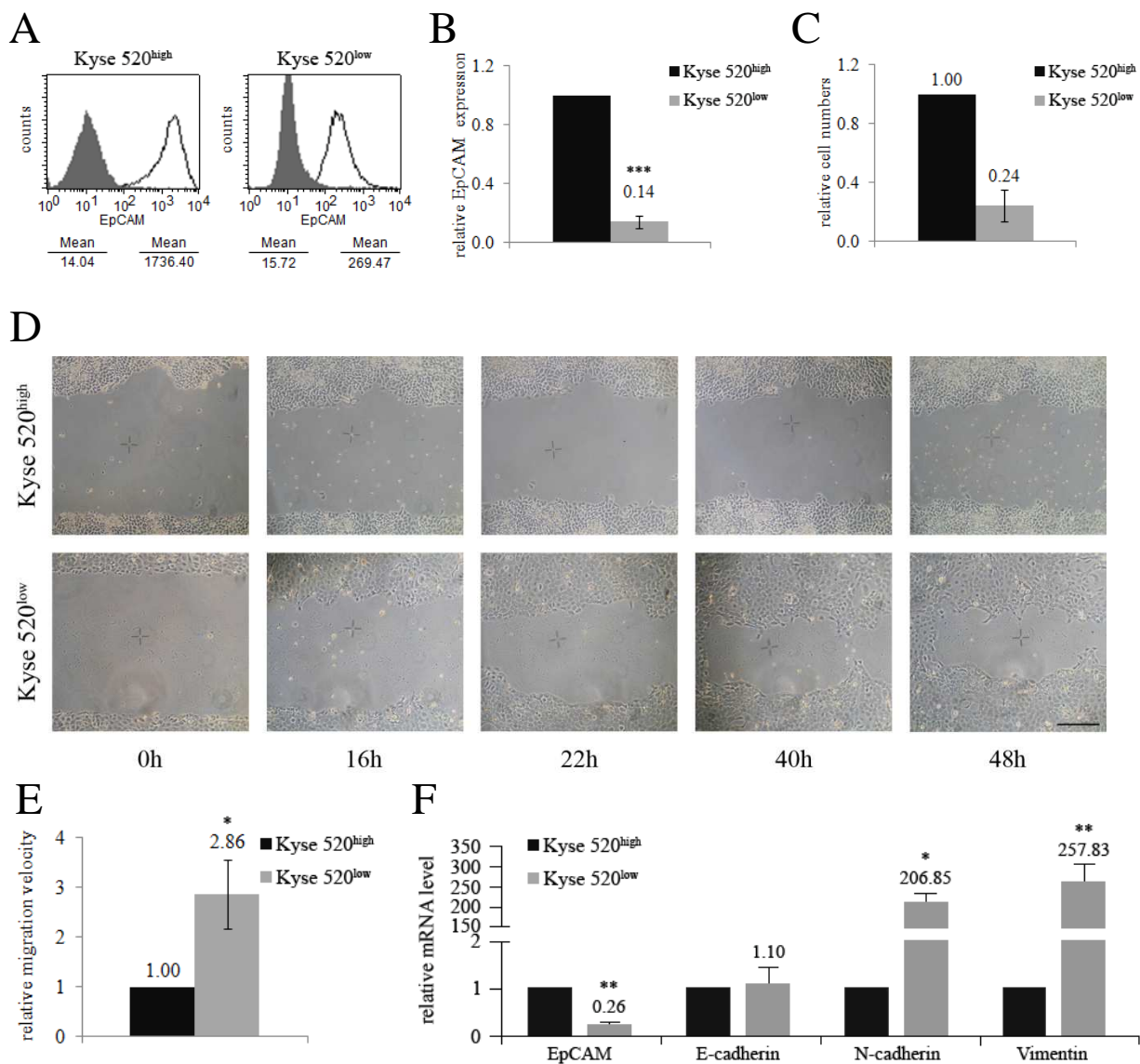


Figure 4.13: Scratch assays with Kyse 520^{high} and Kyse 520^{low} cells.

Kyse 520^{high} and Kyse 520^{low} cells were used in scratch assays under restrictive conditions (0% FCS). (A) Representative flow cytometry graphs. EpCAM cell surface expression was measured by flow cytometry with EpCAM-specific antibodies (black lined histograms) and isotype controls (filled histograms). (B) Relative mean fluorescence intensity ratios of EpCAM cell surface expression in Kyse 520^{high} and Kyse 520^{low} cells are given with standard deviations from three independent experiments. Controls are set to “1.0”. (C) Kyse 520^{high} and Kyse 520^{low} cells were seeded at equal numbers and cell numbers determined after completion of the experiments. Shown are mean relative numbers normalized to Kyse 520^{high} cells from three independent experiments. Controls are set to “1.0”. (D) Confluent layers of Kyse 520^{high} and Kyse 520^{low} cells were scratched and closure of the scratch was assessed over time. Microphotographs were taken at the indicated time points. Bar = 250 μ m. (E) Relative migration velocities of Kyse 520^{high} and Kyse 520^{low} cells are given as mean values from three independent experiments with standard deviations. Controls are set to “1.0”. (F) Levels of EpCAM, E-cadherin, N-cadherin and vimentin mRNAs were assessed by qRT-PCR with *GAPDH* as a reference gene. Shown are normalized relative mRNA levels standardized to Kyse 520^{high} cells from three independent experiments. P-values: * $p < 0.05$; ** $p < 0.01$; *** $p < 0.001$.

4.5.2.3 Migration velocity is enhanced in Kyse 520^{low} cells transfected with EpCAM-specific siRNA

After comparing Kyse 520^{high} and Kyse 520^{low} cells in terms of migration velocity and EMT marker levels, it was tested if the observed differences can be further amplified when Kyse 520^{low} cells are treated with an EpCAM-specific siRNA (see 3.1.4.1). To ensure efficient EpCAM knock-down, EpCAM levels were assessed on mRNA and protein level using qRT-PCR (see 3.2.3) and flow cytometry (see 3.1.5.1), respectively. On average, EpCAM was downregulated to 26% at mRNA (Fig. 4.14 F) and 54% on cell surface level (Fig. 4.14 A-B) in Kyse 520^{low} cells transfected with EpCAM-specific siRNA compared to ctrl cells. Relative cell proliferation rates were assessed by counting cell numbers of the proliferation controls after completion of the scratch assays. Cell numbers were decreased by 26% in Kyse 520^{low} transfected with EpCAM siRNA, compared to ctrl cells when cultured w/o FCS (Fig. 4.14 C).

Figure 4.14 D-E displays the results of cell migration analyses. Representative pictures (Fig. 4.14 D) as well as mean migration velocity data (Fig. 4.14 E) show that cells transfected with EpCAM-specific siRNA migrated faster and closed the scratches earlier compared to cells transfected with ctrl siRNA, whereat the mean migration velocity in EpCAM-depleted cells was 2.79-fold higher than that of control cells.

Besides assessing cell numbers and migration velocities, mRNA levels of selected epithelial and mesenchymal markers were measured using qRT-PCR. The epithelial marker E-cadherin showed a relative mRNA level of 74% in EpCAM-depleted cells compared to control cells, whereas mesenchymal markers N-cadherin and vimentin showed relative mRNA levels of 94% and 163% in cells transfected with EpCAM-specific siRNA compared to ctrl siRNA transfected cells (Fig. 4.14 F).

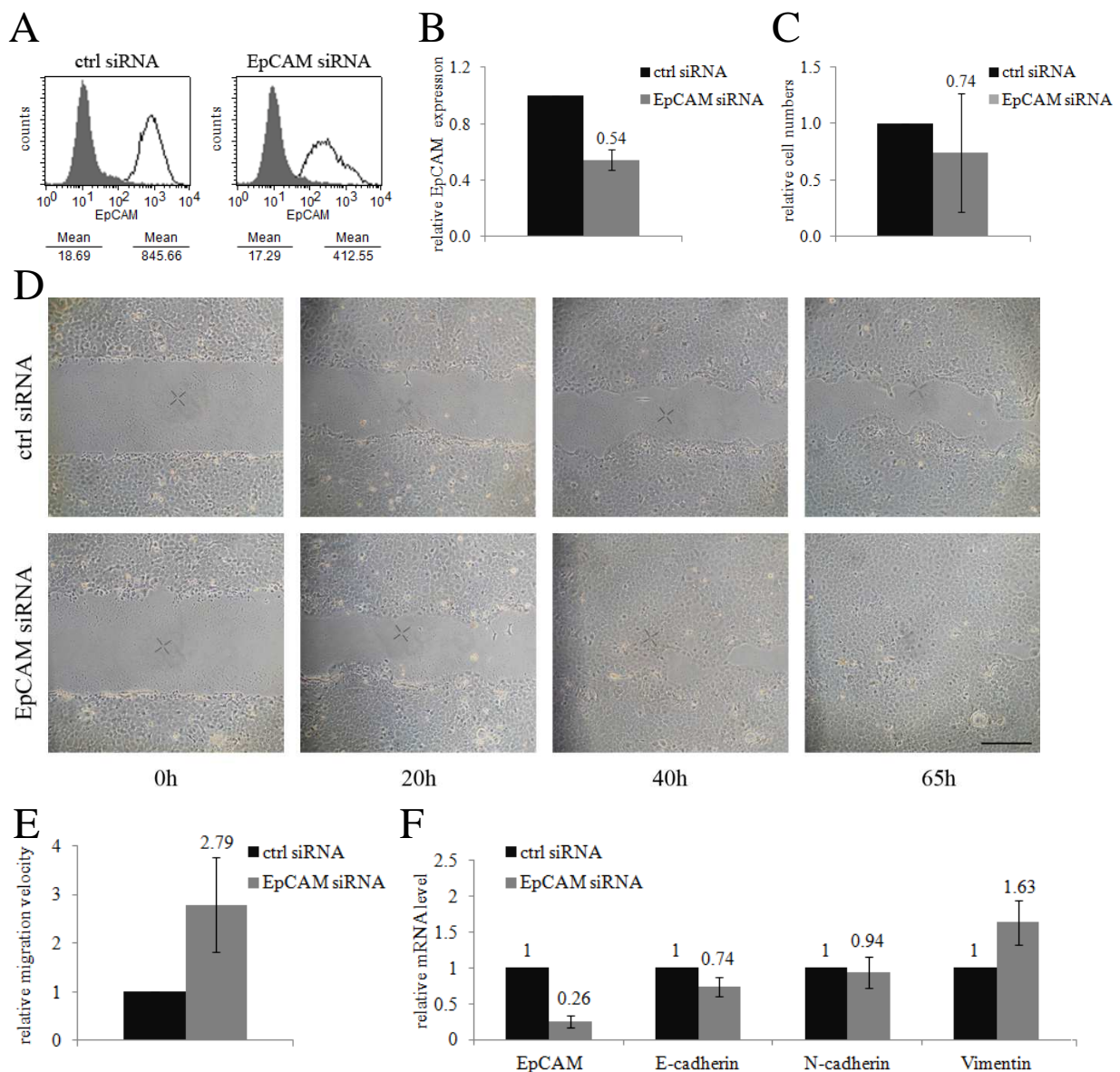


Figure 4. 14: Scratch assays with siRNA transfected Kyse 520^{low} cells.

Kyse 520^{low} cells were transiently transfected with either control or EpCAM-specific siRNA, and used in scratch assays under restrictive conditions (0% FCS). (A) Representative flow cytometry graphs. EpCAM cell surface expression was measured by flow cytometry with EpCAM-specific antibodies (black lined histograms) and isotype controls (filled histograms). (B) Relative mean fluorescence intensity ratios of EpCAM cell surface expression in Kyse 520^{low} ctrl siRNA and EpCAM siRNA cells are given with standard deviations from three independent experiments. Controls are set to “1.0”. (C) Control and EpCAM siRNA transfected cells were seeded at equal numbers and cell numbers were determined after completion of the experiment. Shown are mean relative numbers normalized to control treated cells from three independent experiments. Controls are set to “1.0”. (D) Confluent layers of control and EpCAM siRNA transfected cells were scratched and closure of the scratch was assessed over time. Microphotographs were taken at the indicated time points. Bar = 250µm. (E) Relative migration velocities of control and EpCAM siRNA transfected cells are given as mean values from two independent experiments with standard deviations. Controls are set to “1.0”. (F) Levels of EpCAM, E-cadherin, N-cadherin and vimentin mRNAs were assessed by qRT-PCR with *GAPDH* as a reference gene. Shown are normalized relative mRNA levels standardized to ctrl siRNA transfected Kyse 520^{low} cells from three independent experiments. P-values: *p < 0.05; ** p < 0.01; *** p < 0.001.

4.5.3 Kyse 520 cells with lower levels of EpCAM show higher invasion capacity

Besides migration capacity, the ability to invade into tissues is a known characteristic of metastatic cells (Moustakas and Heldin 2012; Tiwari *et al.* 2012). In order to assess the impact of EpCAM expression on the ability of cells to invade, Kyse 520^{high} and Kyse 520^{low} cells were used in spheroid invasion assay (see 3.1.9.2). In this assay, primary human fibroblast cells were seeded on hardened agarose in 96-well plates and spheroid formation was allowed for 24h. Subsequently, Kyse 520^{high} or Kyse 520^{low} cells were added to spheroids and invasion was allowed for 48 and 72h. At the indicated time points, spheroids were harvested, frozen in liquid nitrogen, processed to 4µm thick sections, and used for immunohistochemical analyses (see 3.4.2). Cells were stained with either EpCAM- or cytokeratin (CK) 8/18-specific antibodies (red stainings) to obtain protein-specific staining. These stainings allowed discrimination between Kyse 520 and fibroblast cells, since fibroblast cells do neither express EpCAM nor the epithelial marker CK8/18, whereas Kyse 520 cells express both proteins. After staining with specific antibodies, spheroid sections were counterstained using hematoxylin (blue staining) to visualize nuclei and cytoplasm of all cells.

Figures 4.15 and 4.16 display the results of these experiments. As can be seen in CK8/18 (Fig. 4.15) and EpCAM stained (Fig. 4.16) sections, almost no cancer cells could be found within fibroblast spheroids after 48 and 72h when Kyse 520^{high} cells were added. Instead of infiltrating the spheroid, Kyse 520^{high} cells formed a ring around the fibroblast spheroids. Only some single Kyse 520^{high} cells could be found centered in fibroblast spheroids (Fig. 4.15 a-d, Fig. 4.16 a-d). In contrast, when Kyse 520^{low} cells were added to the spheroids, high amounts of EpCAM- or CK8/18-positive cells were detected within fibroblast spheroids after 48 and 72h (Fig. 4.15 e-h, Fig. 4.16 e-h).

A detailed look at CK8/18 and EpCAM staining intensities disclosed similar levels of CK8/18 in Kyse 520^{high} and Kyse 520^{low} in all cancer cells of one slide (Fig. 4.15). Similarly, EpCAM expression was steady in Kyse 520^{high} cells throughout samples (Fig. 4.16 a-d). However, in case of Kyse 520^{low} cells, EpCAM staining intensity differed between cells within one spheroid section. Cells, which located at the rim of spheroids, showed a stronger EpCAM staining compared to those, which located further inside the spheroid (Fig. 4.16 e-h).

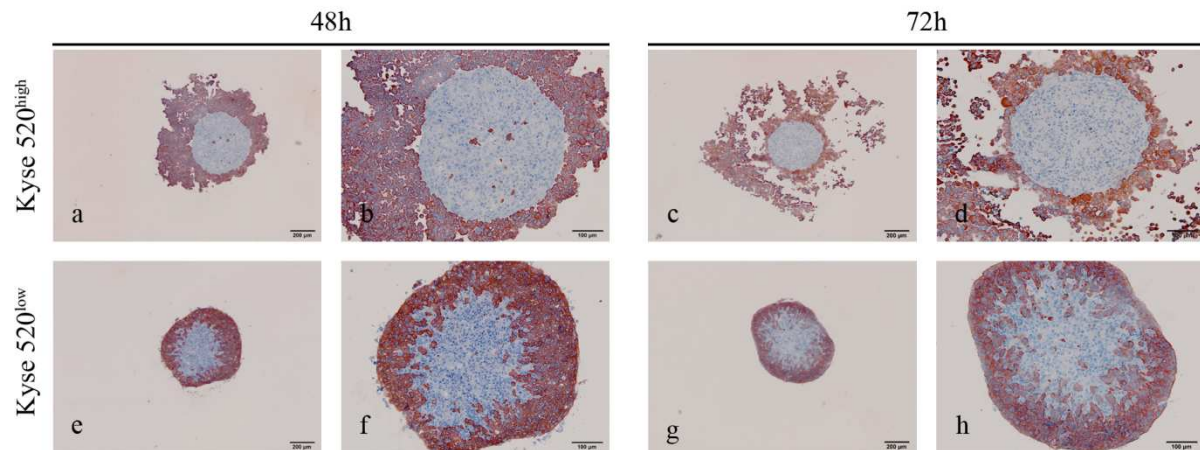


Figure 4. 15: CK8/18 staining of spheroid cryo-sections.

Kyse 520^{high} and Kyse 520^{low} cells were used in spheroid invasion assays. Primary fibroblast cells were grown for 24h on agarose-coated 96-well plates to allow spheroid formation. Subsequently, Kyse 520^{high} or Kyse 520^{low} cells were added and invasion was allowed for 48 and 72h. At the indicated time points, spheroids were harvested, frozen, cut, and stained using immunohistochemistry. Shown are pictures of cryo-sections incubated with CK8/18-specific antibodies (red) and counterstained using hematoxylin (blue).

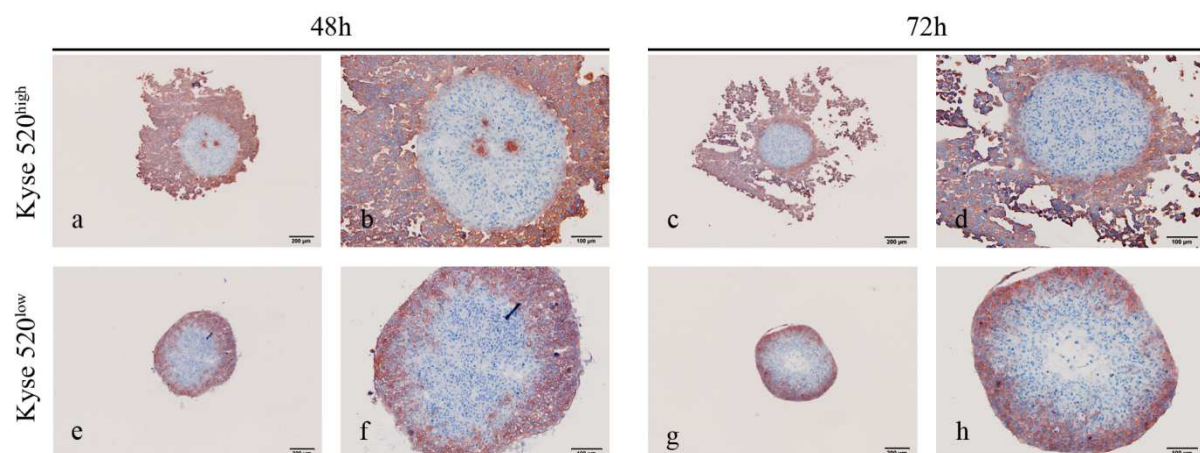


Figure 4. 16: EpCAM staining of spheroid cryo-sections.

Kyse 520^{high} and Kyse 520^{low} cells were used in spheroid invasion assays. Primary fibroblast cells were grown for 24h on agarose-coated 96-well plates to allow spheroid formation. Subsequently, Kyse 520^{high} or Kyse 520^{low} cells were added and invasion was allowed for 48 and 72h. At the indicated time points spheroids were harvested, frozen, cut, and stained using immunohistochemistry. Shown are pictures of cryo-sections incubated with EpCAM-specific antibodies (red) and counterstained using hematoxylin (blue).

4.6 EpCAM is decreased upon induced EMT

The abovementioned experiments demonstrated that cells with lower EpCAM levels migrate faster, invade more efficiently into spheroids, and display increased amounts of mesenchymal markers. These effects could be observed in cells in which EpCAM was depleted using siRNA (see experiments with Kyse 30 and Kyse 520^{low} cells transfected with ctrl or EpCAM-specific siRNA) as well as in cells, which naturally show different EpCAM expression levels (see experiments with Kyse 520^{high} and Kyse 520^{low} cells). As already mentioned, one process during which cells change their phenotype from epithelial to mesenchymal, is the epithelial-to-mesenchymal transition (EMT). Therefore, the effects of an induced EMT on the expression levels of EpCAM were analyzed upon treatment of cells with TGF β (see 3.1.7), a known inducer of EMT.

4.6.1 TGF β treatment of A549 cells

A549 cells were used as control cell line in TGF β assays, because they are known to exhibit TGF β -induced EMT (Kim *et al.* 2007). Therefore, A549 cells represented the ideal cell line to test if and how TGF β treatment affects EpCAM expression. For TGF β assay, cells were plated on 6-well plates and grown under restrictive conditions (0% FCS) for 24h. Subsequently, TGF β was added for 72h. Cells were then analyzed in terms of their morphology, EMT marker expression and EpCAM expression levels.

Figure 4.17 sums up results of TGF β assays conducted with A549 cells. As can be seen in Figure 4.17 A, A549 cells changed their morphology when treated with TGF β . Without TGF β treatment, cells showed a cobblestone-like, epithelial morphology and grew in clusters, whereas they showed a spindle-shaped, mesenchymal morphology and grew as single cells when TGF β was added to the culture medium. Besides morphology, also mRNA levels of typical EMT markers were altered when cells were treated with TGF β . As expected, the mRNA level of the epithelial marker E-cadherin displayed an average decrease to 4%, whereas levels of mesenchymal markers N-cadherin and vimentin on average were increased 3.97-fold and 2.83-fold, in TGF β treated cells compared to control cells, which were treated with buffer only (Fig. 4.17 B).

After ensuring that TGF β treatment induced EMT in A549 cells, mRNA and cell surface levels of EpCAM were assessed upon qRT-PCR and flow cytometry, respectively.

Compared to control cells, cell surface and mRNA levels of EpCAM were decreased to 44% and 16% in TGF β treated cells, respectively (Fig. 4.17 B-D).

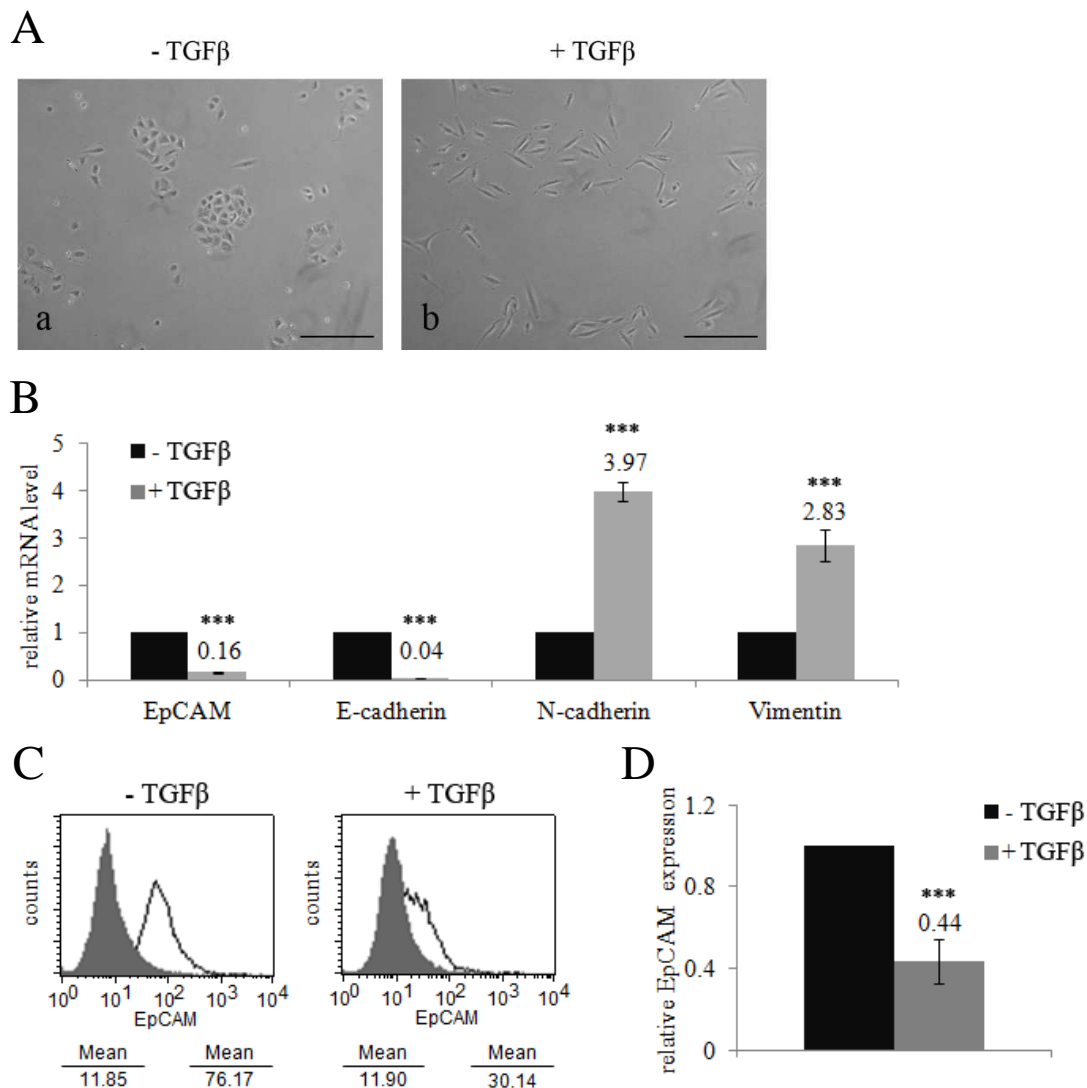


Figure 4. 17: Induction of EMT results in downregulation of EpCAM in A549 cells.

A549 cells were treated with TGF β or buffer only for 72h. Subsequently, morphology, mRNA levels of selected EMT markers, and mRNA and cell surface levels of EpCAM were analyzed. (A) Shown are microphotographs of cells treated with or w/o TGF β taken under a Axiovert 25 microscope (Zeiss) using a Samsung WB750 camera. Bars = 250 μ m. (B) Levels of EpCAM, E-cadherin, N-cadherin and vimentin were assessed upon qRT-PCR with specific primers. *RPL13A* served as a housekeeping gene for standardisation. Shown are mean relative mRNA expression level normalized to untreated cells from three independent experiments with standard deviations. (C) EpCAM cell surface expression was assessed by flow cytometry with EpCAM-specific antibody (black lined histograms) and isotype control antibody (filled histograms). Shown are representative results from three independent experiments. (D) Relative mean fluorescence intensity ratios of EpCAM cell surface expression in cells treated with or w/o TGF β are given with standard deviations from three independent experiments. Controls are set to "1.0". P-values: *p < 0.05; ** p < 0.01; *** p < 0.001.

4.6.2 TGF β treatment of esophageal cancer cell lines

After ensuring that TGF β treatment induces EMT by using A549 cells (see 4.6.1), in a next step TGF β assays were performed with esophageal cancer cell lines Kyse 30 and Kyse 520^{low}. To do so, cells were plated in 6-well plates and grown under restrictive conditions (0% FCS) for 24h. Subsequently, TGF β was added for 72h, and cells analyzed in terms of their morphology, EMT marker levels and EpCAM expression.

4.6.2.1 Effects of TGF β treatment in Kyse 30 cells

Figure 4.18 sums up the results of the TGF β assays conducted with Kyse 30 cells. Similar to A549 cells, a drastic morphological change of Kyse 30 cells was observed upon TGF β treatment. Without TGF β , cells showed a cobblestone-like, epithelial morphology and grew in clusters, whereas they showed a spindle-shaped, mesenchymal morphology and grew as single cells when TGF β was added (Fig. 4.18 A). Besides morphological changes also mRNA levels of typical EMT markers were altered upon TGF β treatment. The mRNA level of the epithelial marker E-cadherin was increased 1.91-fold on average when cells were treated with TGF β . Even stronger upregulation was observed for mesenchymal markers N-cadherin and vimentin, which on average showed 7.82-fold and 3.36-fold increased mRNA levels in TGF β treated cells compared to control cells, which were treated with buffer only (Fig. 4.18 B).

Similar to A549 cells, EpCAM levels were changed upon TGF β -induced EMT in Kyse 30 cells. However, in contrast to A549 cells in which mRNA and cell surface levels of EpCAM were decreased after TGF β treatment (Fig. 4.18 B-D), in Kyse 30 cells only cell surface levels of EpCAM were decreased, whereas mRNA levels revealed slightly increased. On average, EpCAM mRNA levels were increased 1.42-fold (Fig. 4.18 B), whereas cell surface levels were decreased to 53% (Fig. 4.18 D).

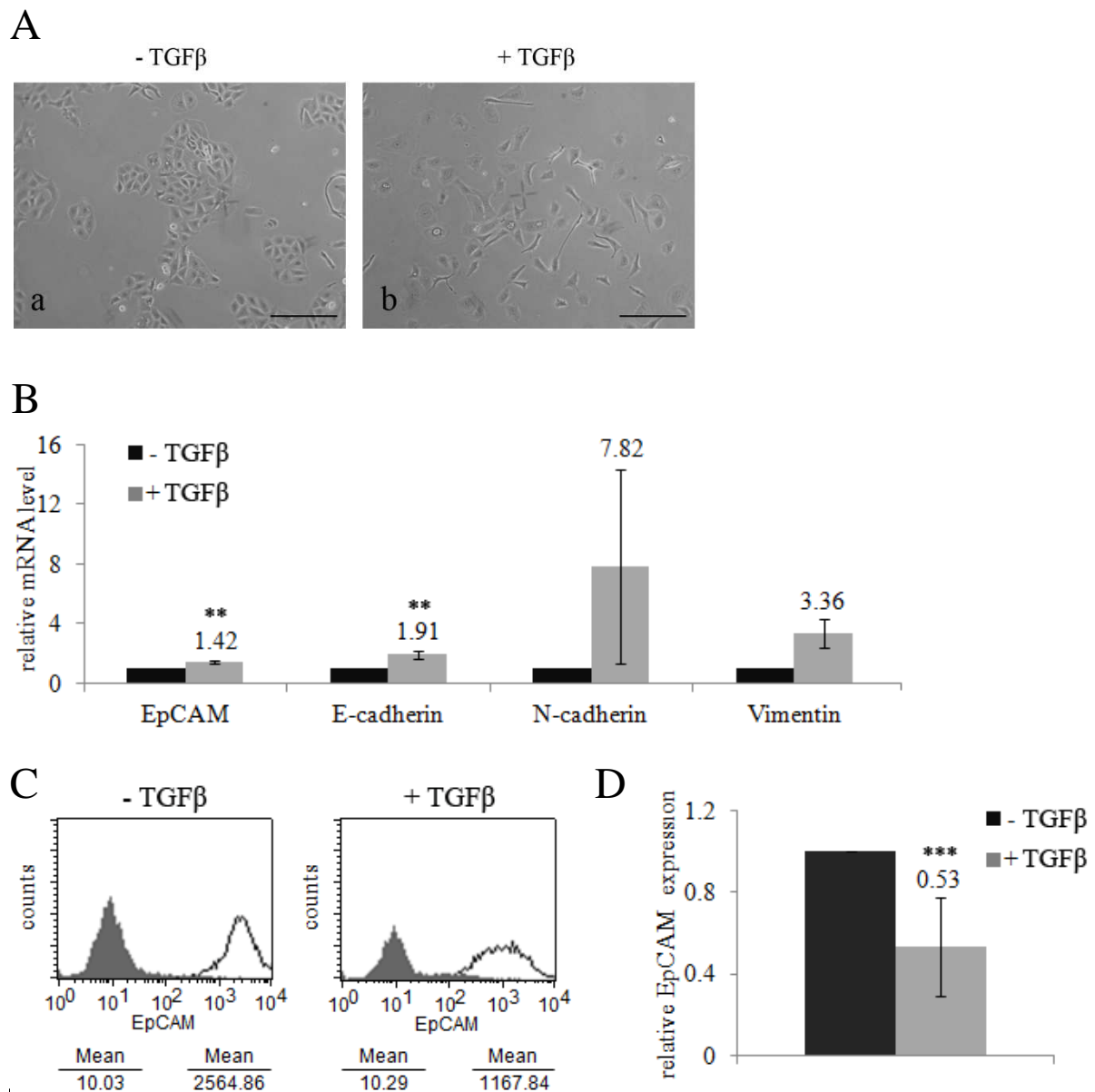


Figure 4. 18: Induction of EMT results in a loss of EpCAM in Kyse 30 cells.

Kyse 30 cells were treated with TGF β or buffer only for 72h. Subsequently, morphology, mRNA levels of selected EMT markers, and mRNA and cell surface levels of EpCAM were analyzed (A) Shown are microphotographs of cells treated with or w/o TGF β taken under a Axiovert 25 microscope (Zeiss) using a Samsung WB750 camera. Bars = 250 μ m. (B) Levels of EpCAM, E-cadherin, N-cadherin and vimentin were assessed upon qRT-PCR with specific primers. *GAPDH* served as a housekeeping gene for standardisation. Shown are mean relative mRNA expression level normalized to untreated cells from three independent experiments with standard deviations. (C) EpCAM cell surface expression was assessed by flow cytometry with EpCAM-specific antibody (black lined histograms) and isotype control antibody (filled histograms). Shown are representative results from three independent experiments. (D) Relative mean fluorescence intensity ratios of EpCAM cell surface expression in cells treated with or w/o TGF β are given with standard deviations from three independent experiments. Controls are set to “1.0”. P-values: *p < 0.05; ** p < 0.01; *** p < 0.001.

4.6.2.2 Effects of TGF β treatment in Kyse 520^{low} cells

Figure 4.19 sums up the results of TGF β assays conducted with Kyse 520^{low} cells. In contrast to A549 and Kyse 30 cells, Kyse 520^{low} cells displayed no morphological changes when treated with TGF β . Cells showed a cobblestone-like, epithelial morphology and grew in clusters no matter if cultured with TGF β or buffer only (Fig. 4.19 A). Although there were no obvious morphological changes, mRNA levels of typical EMT markers were altered in Kyse 520^{low} cells when treated with TGF β . On average, levels of mesenchymal markers N-cadherin and vimentin were increased 1.65-fold and 8.13-fold in TGF β treated cells compared to control cells (Fig. 4.19 B). However, the epithelial marker E-cadherin showed almost no regulation and displayed average mRNA levels of 98% compared to control cells.

Comparably to Kyse 30 cells, TGF β treatment of Kyse 520^{low} cells resulted in a reduction of EpCAM at cell surface but not on mRNA level. On average, EpCAM cell surface levels were decreased to 47% (Fig. 4.19 D), whereas mRNA levels were not regulated (Fig. 4.19 B).

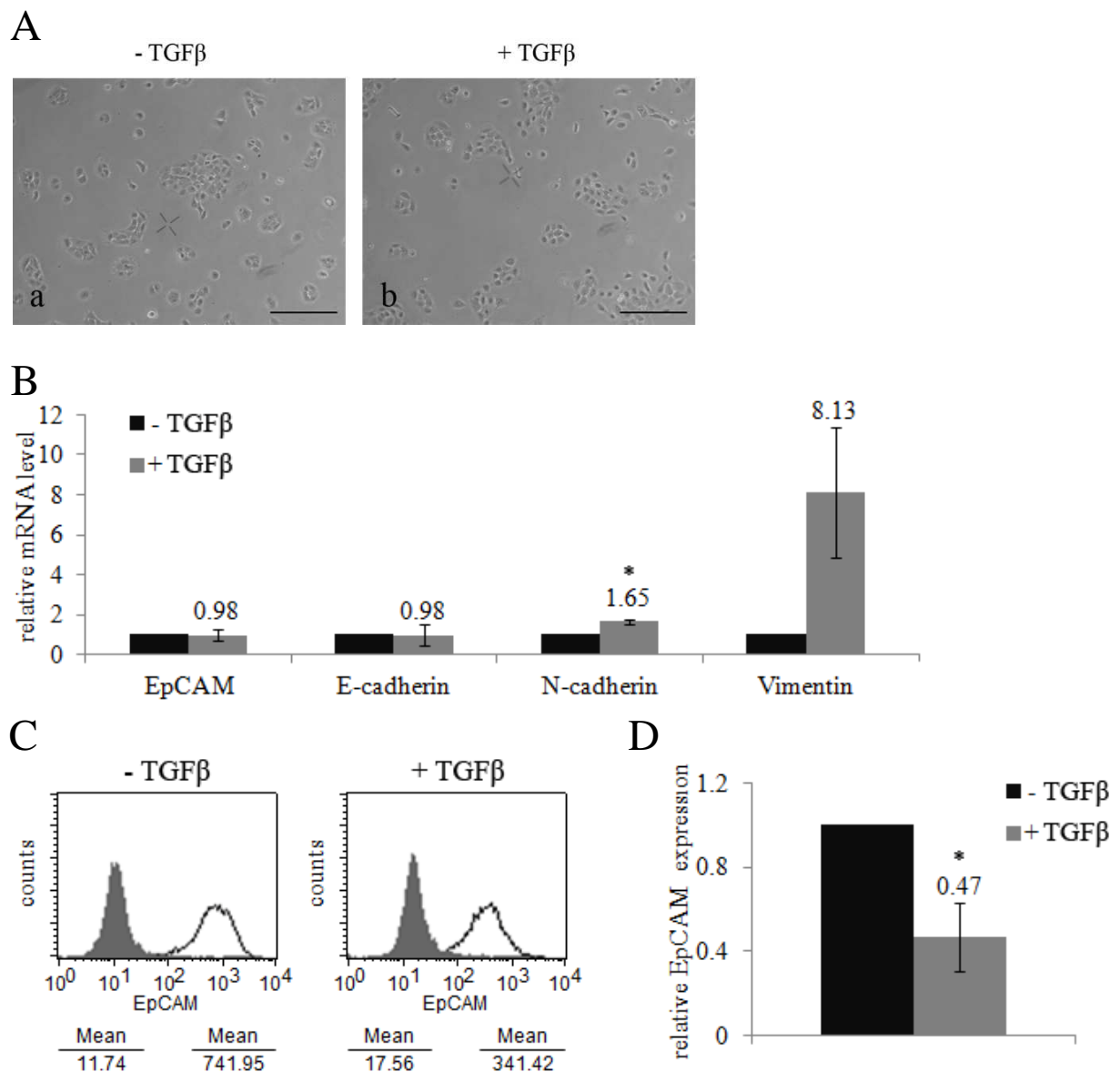


Figure 4. 19: Induction of EMT results in a loss of EpCAM in Kyse 520^{low} cells.

Kyse 520^{low} cells were treated with TGF β or buffer only for 72h. Subsequently, morphology, mRNA levels of selected EMT markers, and mRNA and cell surface levels of EpCAM were analyzed (A) Shown are microphotographs of cells treated with or w/o TGF β taken under a Axiovert 25 microscope (Zeiss) using a Samsung WB750 camera. Bars = 250 μ m. (B) Levels of EpCAM, E-cadherin, N-cadherin and vimentin were assessed upon qRT-PCR with specific primers. *GAPDH* served as a housekeeping gene for standardisation. Shown are mean relative mRNA expression level normalized to untreated cells from three independent experiments with standard deviations. (C) EpCAM cell surface expression was assessed by flow cytometry with EpCAM-specific antibody (black lined histograms) and isotype control antibody (filled histograms). Shown are representative results from three independent experiments. (D) Relative mean fluorescence intensity ratios of EpCAM cell surface expression in cells treated with or w/o TGF β are given with standard deviations from three independent experiments. Controls are set to “1.0”. P-values: *p < 0.05; ** p < 0.01; *** p < 0.001.

4.7 Overexpression of EpCAM is not sufficient to prevent effects of TGF β

Previous experiments showed that treatment with TGF β , which drives cells to undergo EMT, led to a decrease of EpCAM at least at cell surface level (see 4.6). This finding rose the question if, vice versa, an overexpression of EpCAM can prevent effects of TGF β . To answer this question, TGF β assays were performed with A549 and Kyse 30 cells stably overexpressing different YFP constructs (see 4.1.3). A549 and Kyse 30 cells were used because these cell lines showed the strongest reaction upon TGF β treatment in previous experiments. Cell morphology and mRNA levels of EMT markers were used as readout.

4.7.1 EpCAM overexpression does not prevent TGF β -induced EMT in A549 cells

A549 cells stably transfected with YFP (control cell line), EpICD-YFP or EpCAM-YFP were used in TGF β assays (see 3.1.7), and cell morphology and mRNA levels of EMT markers were assessed. As already seen for wildtype cells (Fig. 4.17 A), A549-YFP cells showed a cobblestone-like, epithelial morphology and grew in clusters when treated with buffer only. However, when treated with TGF β , cells changed their morphology towards a spindle-shaped, mesenchymal phenotype and grew as single cells (Fig. 4.20 A a, d). These morphological changes comparably occurred in EpICD-YFP and EpCAM-YFP stably overexpressing A549 cell lines when cells were treated with TGF β (Fig. 4.20 A b-c, e-f).

The analysis of mRNA levels of typical EMT markers using qRT-PCR (see 3.2.3) revealed an average decrease of E-cadherin to 3%, as well as an 11.08-fold and 3.15-fold average increase of N-cadherin and vimentin in YFP overexpressing cells treated with TGF β (Fig. 4.20 B). Similar regulations of EMT markers were found in EpICD-YFP and EpCAM-YFP overexpressing A549 cells when treated with TGF β . Epithelial marker E-cadherin was decreased to 5% and 12% in A549 EpICD-YFP and A549 EpCAM-YFP overexpressing cells, respectively. Mesenchymal markers N-cadherin and vimentin were increased 13.71-fold and 2.82-fold in A549 EpICD-YFP, and 7.26-fold and 2.46-fold in A549 EpCAM-YFP cells (Fig. 4.20 B). Besides, EpCAM mRNA levels were decreased to 13% in YFP and EpICD-YFP overexpressing cells upon TGF β treatment. Only in EpCAM-YFP overexpressing cells EpCAM mRNA level remained almost unchanged when cell were treated with TGF β , showing 88% of the mRNA level in untreated cells (Fig. 4.20 B).

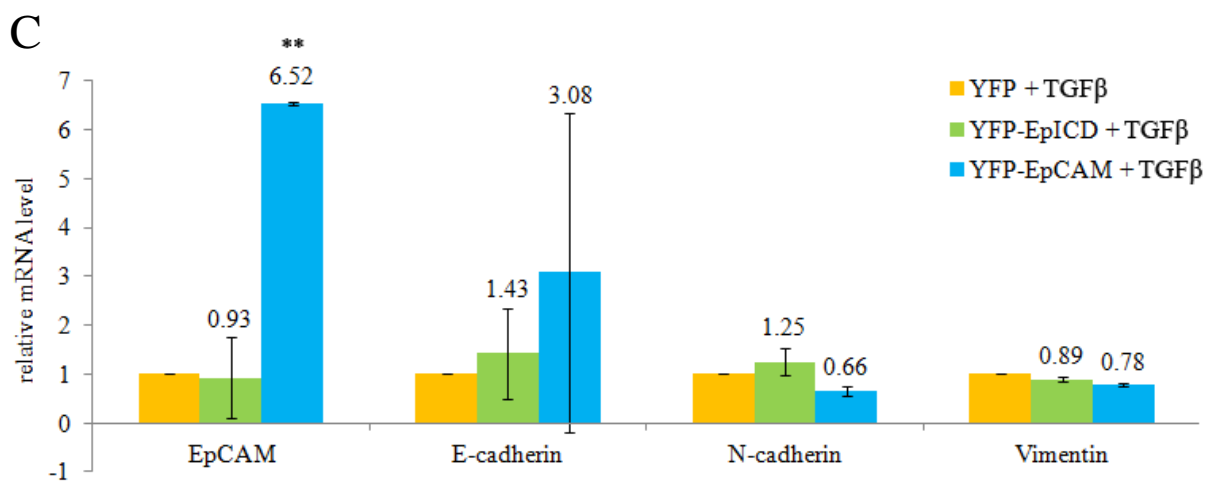
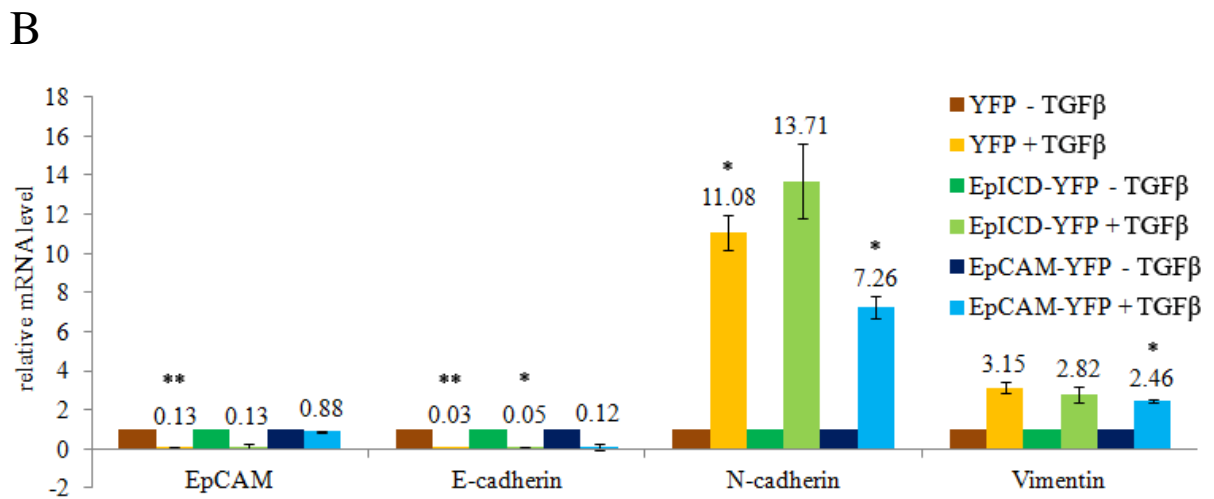
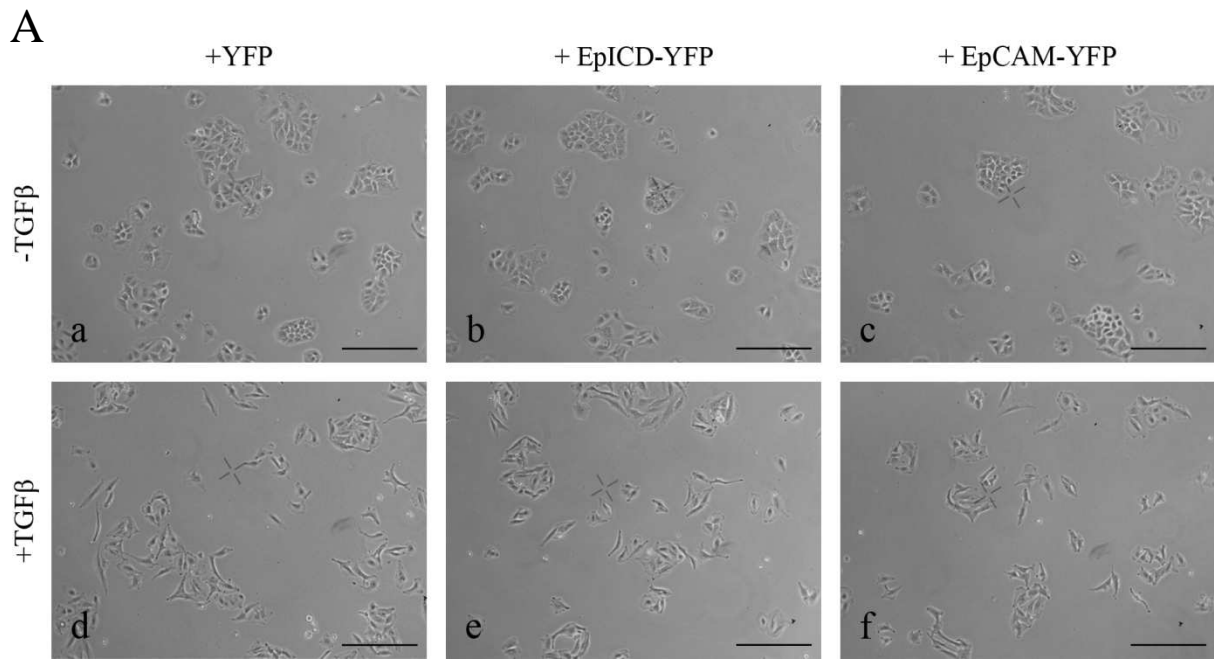


Figure 4. 20: EpCAM overexpression does not prevent effects of TGF β in A549 cells.

A549 cells stably overexpressing YFP, EpICD-YFP or EpCAM-YFP construct were treated with TGF β for 72h. (A) Cell morphology was analyzed in cells grown with or w/o TGF β . Shown are microphotographs taken under an Axiovert 25 microscope (Zeiss) using a WB750 camera (Samsung). Bars = 250 μ m. (B) mRNA levels of EpCAM and EMT markers E-cadherin, N-cadherin and vimentin were assessed in cells treated with and w/o TGF β using qRT-PCR. *RPL13A* served as a house-keeping gene for standardisation. Shown are mean relative mRNA expression levels normalized to untreated cells from two independent experiments with standard deviations. (C) To directly compare the regulation of EMT markers upon TGF β treatment, values of TGF β treated cells (displayed in B) were set relative to each other. Shown are mean relative mRNA expression levels normalized to YFP expressing A549 cells from two independent experiments with standard deviations. P-values: *p < 0.05; ** p < 0.01; *** p < 0.001.

In a next step, EMT marker levels of TGF β treated samples were directly compared to analyze the influence of EpCAM and EpICD overexpression on TGF β treatment. To do so, mRNA data of TGF β treated cells were set relative to each other, whereby YFP overexpressing cells served as control group. For E-cadherin, relative mRNA levels were 1.43-fold higher in EpICD-YFP and 3.08-fold higher in EpCAM-YFP expressing cells compared to YFP expressing cells. In case of N-cadherin, relative mRNA levels were 1.25-fold higher in EpICD-YFP and 34% lower in EpCAM-YFP cells compared to levels in YFP cells. Relative mRNA levels of vimentin were 11% lower in EpICD-YFP and 22% lower in EpCAM-YFP cells compared to YFP cells. However, it must be noted that none of the displayed differences was significant (Fig. 4.20 C).

4.7.2 EpCAM overexpression does not prevent TGF β -induced EMT in Kyse 30 cells

Kyse 30 cells stably transfected with YFP (control cell line), EpICD-YFP or EpCAM-YFP constructs were used in TGF β assays (see 3.1.7). Cell morphology and mRNA levels of different EMT markers were analyzed after 72h of treatment. As already seen in wildtype cells (Fig. 4.18 A), Kyse 30 YFP cells without any treatment showed a mainly cobblestone-like, epithelial morphology and grew in clusters. However, when treated with TGF β , cells changed their morphology towards a spindle-shaped, mesenchymal phenotype and grew as single cells (Fig. 4.21 A a, d). These morphological changes comparably occurred in EpICD-YFP and EpCAM-YFP stably overexpressing Kyse 30 cells when treated with TGF β (Fig. 4.21 A b-c, e-f).

The analysis of mRNA levels of typical EMT markers using qRT-PCR (see 3.2.3), revealed a slight (1.54-fold) increase of the epithelial marker E-cadherin as well as a strong increase of the mesenchymal markers N-cadherin (12.79-fold) and vimentin (24.92-fold) in TGF β treated Kyse 30 YFP cells when compared to untreated cells (Fig. 4.21 B). Similar regulations of EMT markers were observed in case of EpICD-YFP and EpCAM-YFP overexpressing Kyse 30 cells. MRNA levels of the epithelial marker E-cadherin were slightly increased 1.66-fold and 1.22-fold in Kyse 30 EpICD-YFP and Kyse 30 EpCAM-YFP overexpressing cells, respectively. Mesenchymal markers N-cadherin and vimentin were increased 17.16-fold and 45.41-fold in Kyse 30 EpICD-YFP, and 9.26-fold and 28.39-fold in Kyse 30 EpCAM-YFP overexpressing cells (Fig. 4.21 B). As already seen in Kyse 30 wildtype cells, EpCAM mRNA levels were not significantly changed upon TGF β treatment in stable Kyse 30 cells. Compared to untreated cells, EpCAM mRNA levels in TGF β treated cells were upregulated 1.20-fold, 1.64-fold, and 1.41-fold in Kyse 30 YFP, Kyse 30 EpICD-YFP, and Kyse 30 EpCAM-YFP overexpressing cells, respectively (Fig. 4.21 B).

In a next step, EMT marker levels of TGF β treated samples were directly compared to analyze the influence of EpCAM and EpICD overexpression on TGF β treatment. To do so, mRNA data of TGF β treated cells were set relative to each other, whereby YFP overexpressing cells served as control group. In case of E-cadherin, relative mRNA levels were similar in EpICD-YFP and 21% lower in EpCAM-YFP overexpressing cells compared to YFP overexpressing cells. For N-cadherin, relative mRNA levels on average were 1.39-fold higher in EpICD-YFP and 31% lower in EpCAM-YFP cells compared to YFP cells. Relative mRNA levels of vimentin were on average 1.93-fold higher in EpICD-YFP and 1.17-fold higher in EpCAM-YFP cell lines compared to YFP cells. However, it must be noted that none of the displayed differences was significant (Fig. 4.21 C).

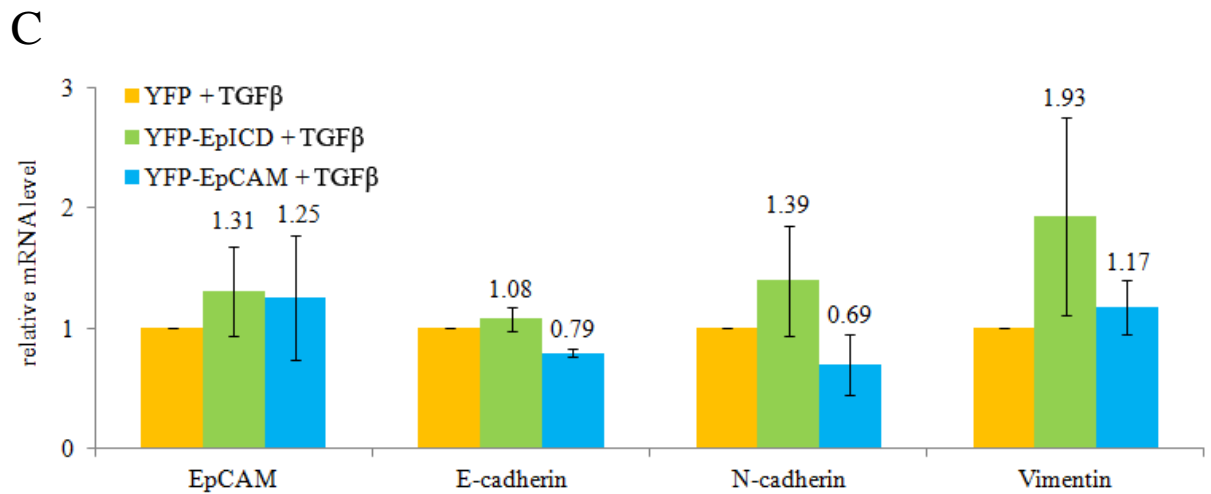
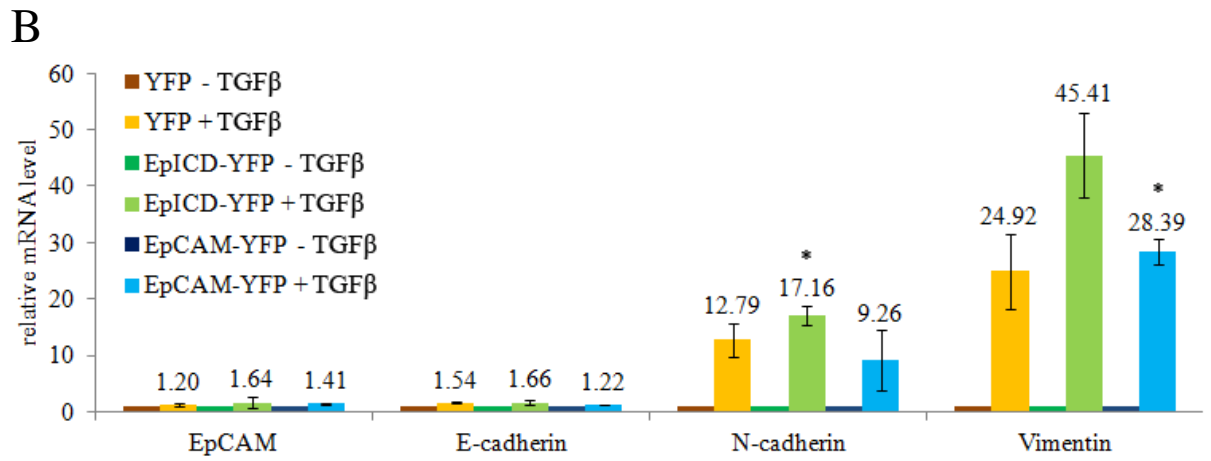
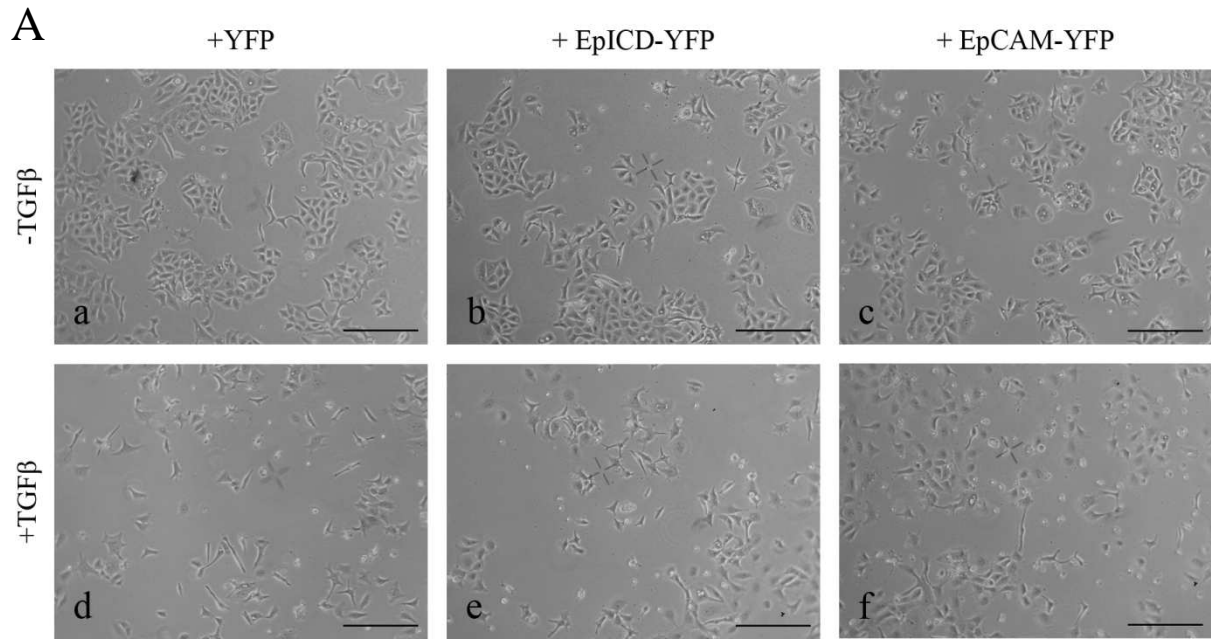


Figure 4. 21: EpCAM overexpression does not prevent effects of TGF β in Kyse 30 cells.

Kyse 30 cells stably overexpressing YFP, EpICD-YFP or EpCAM-YFP construct were treated with TGF β for 72h. (A) Cell morphology was analyzed in cells grown with or w/o TGF β . Shown are microphotographs taken under an Axiovert 25 microscope (Zeiss) using a WB750 camera (Samsung). Bars = 250 μ m. (B) mRNA levels of EpCAM and EMT markers E-cadherin, N-cadherin and vimentin were assessed in cells treated with and w/o TGF β using qRT-PCR. *GAPDH* served as a house-keeping gene for standardisation. Shown are mean relative mRNA expression levels normalized to untreated cells from two independent experiments with standard deviations. (C) To directly compare the regulation of EMT markers upon TGF β treatment, values of TGF β treated cells (displayed in B) were set relative to each other. Shown are mean relative mRNA expression levels normalized to YFP expressing Kyse 30 cells from two independent experiments with standard deviations. P-values: *p < 0.05; ** p < 0.01; *** p < 0.001.

4.8 How does EpCAM sustain the epithelial/ proliferative phenotype?

The experiments presented so far, showed that EpCAM expression in esophageal carcinoma cells correlates with increased cell proliferation *in vitro* as well as with formation of larger tumors in *in vivo* mouse model. In contrast, EpCAM was found downregulated in migrating cells, and cells with lower EpCAM levels showed functional traits of EMT, such as faster migration velocity, higher invasion capacity and increased levels of mesenchymal markers. These findings support the notion that EpCAM plays an active role in sustaining the epithelial, proliferative phenotype of cells. Following studies aimed at understanding the mechanisms underlying this function of EpCAM in esophageal carcinoma.

4.8.1 Analysis of the signaling function of EpCAM

EMT can be induced via various pathways. One of the most common ones is the TGF β signaling pathway (see 1.1.2.3), in which TGF β binds and activates its receptors, subsequently leading to activation of SMAD proteins, and increased expression of transcription factors, like SNAIL, SLUG, TWISTs and ZEBs. These transcription factors eventually induce the expression of mesenchymal markers, like N-cadherin and vimentin, and the repression of epithelial markers like E-cadherin. To test if this pathway is activated upon EpCAM depletion, A549 and Kyse 30 cells were transiently transfected with control or EpCAM-specific siRNA, and mRNA levels of transcription factors involved in EMT were analyzed using qRT-PCR (see 3.2.3). To ensure that the TGF β pathway in principle can be activated in the selected cell lines, mRNA levels of the abovementioned transcription factors were assessed after activating the TGF β pathway upon the addition of TGF β for 72h (see 3.1.7).

4.8.1.1 EpCAM depletion does not activate the TGF β pathway in A549 cells

A549 cells were cultivated with or w/o TGF β for 72h, and mRNA levels of EpCAM and selected transcription factors were assessed using qRT-PCR. Figure 4.22 A sums up the acquired data. EpCAM mRNA levels were decreased to 21% of EpCAM levels found in control cells, when cells were treated with TGF β (similar EpCAM downregulation could already be observed in 4.6.1). In contrast, mRNA levels of transcription factors were mainly increased upon addition of TGF β . Levels of SNAIL, SLUG and ZEB-1 showed an average increase of 1.80-fold, 8.85-fold and 2.14-fold, respectively, reflecting the activation of the TGF β pathway (Fig. 4.22 A). Only TWIST-1 mRNA levels were decreased by 29% when cells were treated with TGF β . Levels of TWIST-2 and ZEB-2 mRNA remained below detection limit.

Knowing that the TGF β pathway can be activated in A549 cells, in the next step these cells were transfected with either control or EpCAM-specific siRNA (see 3.1.4.1). EpCAM knock-down efficiency and mRNA levels of selected transcription factors were assessed 72h after transfection using flow cytometry and qRT-PCR. EpCAM levels were on average decreased to 20% at mRNA (Fig. 4.22 D) and 57% at cell surface (Fig. 4.22 B-C) level, respectively, displaying efficient EpCAM knock-down. MRNA levels of most transcription factors were found decreased in EpCAM siRNA transfected cells. Levels of SLUG, TWIST-1, ZEB-1 and ZEB-2 were reduced to 45%, 89%, 55% and 26%, respectively, in EpCAM depleted cells compared to control cells. Only mRNA levels of SNAIL were slightly increased (1.16-fold) in EpCAM depleted cells. TWIST-2 remained below detection limit (Fig. 4.22 D).

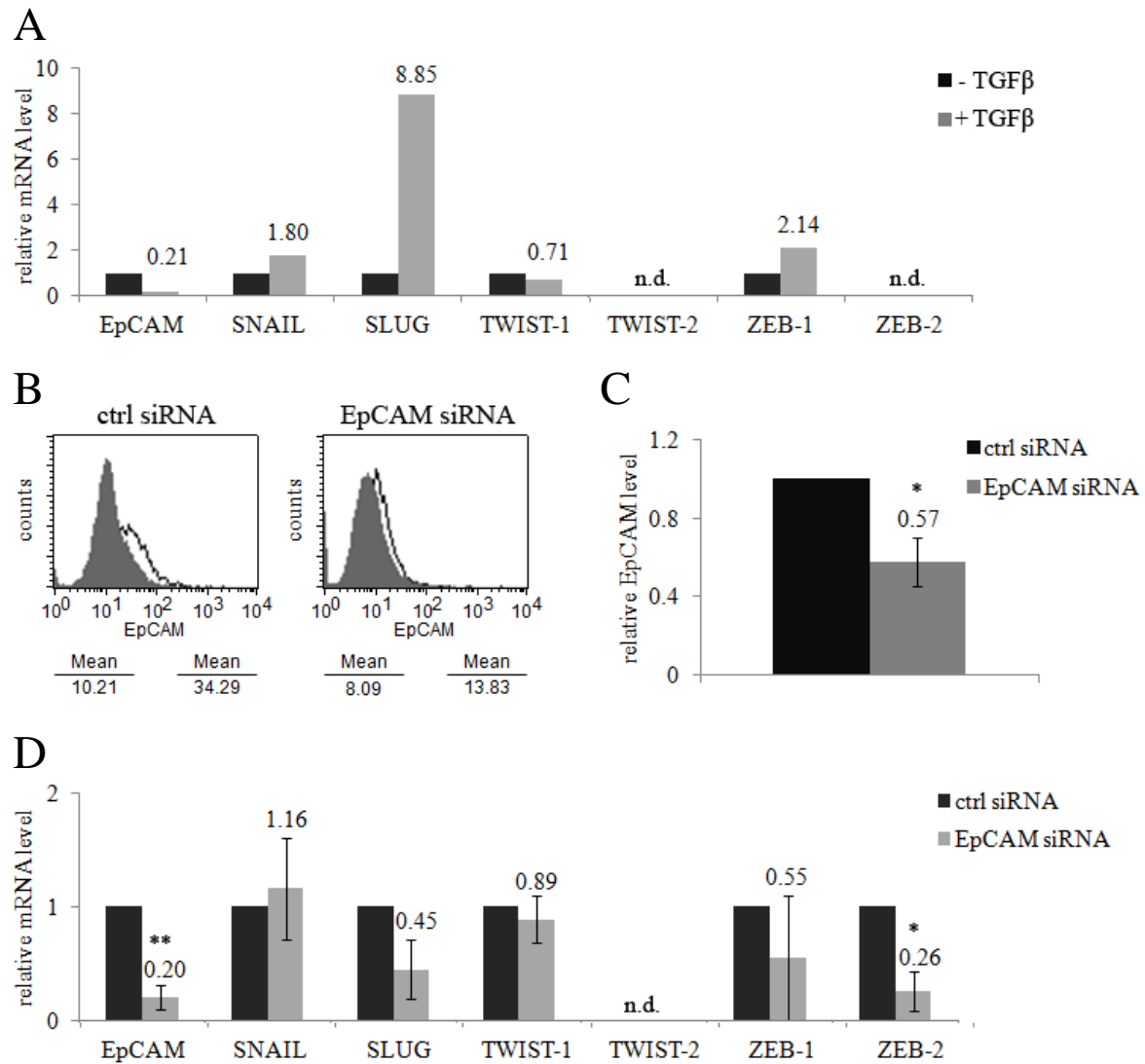


Figure 4. 22: EpCAM knock-down does not induce the TGF β pathway in A549 cells.

(A) A549 cells were cultivated with or w/o TGF β for 72h and mRNA levels of EpCAM and selected transcription factors involved in the TGF β pathway were assessed using qRT-PCR with specific primers. *RPL13A* served as a house-keeping gene for standardisation. Shown are mRNA expression level normalized to untreated cells from one experiment. (B-D) A549 cells were transiently transfected with either control or EpCAM-specific siRNA. 72h after transfection, EpCAM knock-down efficiency as well as mRNA level of transcription factors were analyzed. (B) EpCAM cell surface expression was assessed by flow cytometry with EpCAM-specific antibody (black lined histograms) and isotype antibody (filled histograms). Shown are representative results from three independent experiments. (C) Relative mean fluorescence intensity ratios of EpCAM cell surface expression in cells transfected with ctrl or EpCAM-specific siRNA are given with standard deviations from three independent experiments. Controls are set to “1.0”. (D) MRNA levels of EpCAM and transcription factors involved in TGF β pathway were assessed upon qRT-PCR with specific primers. *RPL13A* served as a house-keeping gene for standardisation. Shown are mean relative mRNA expression levels normalized to ctrl cells from three independent experiments with standard deviations. P-values: * $p < 0.05$; ** $p < 0.01$; *** $p < 0.001$. n.d.; not detectable.

4.8.1.2 EpCAM depletion does not activate the TGF β pathway in Kyse 30 cells

Kyse 30 cells were cultivated with or w/o TGF β for 72h, and mRNA levels of EpCAM and selected transcription factors were assessed using qRT-PCR. Figure 4.23 A sums up the acquired qRT-PCR data. EpCAM mRNA level was increased 1.51-fold, compared to EpCAM level found in control cells, when cells were treated with TGF β (similar EpCAM upregulation could already be observed in 4.6.2.1). Levels of selected transcription factors were increased 7.01-fold (SNAIL), 5.92-fold (SLUG), 1.65-fold (TWIST-1) and 1.27-fold (TWIST-2) in TGF β treated cells compared to control cells, displaying the activation of the TGF β pathway in Kyse 30 cells when treated with TGF β . Levels of ZEB-1 and ZEB-2 remained below detection limit (Fig. 4.23 A).

Knowing that the TGF β pathway can be activated in Kyse 30 cells, in the next step these cells were transfected with either a control or an EpCAM-specific siRNA (see 3.1.4.1). EpCAM knock-down efficiency, as well as mRNA levels of selected transcription factors, was assessed 72h after transfection using flow cytometry and qRT-PCR. EpCAM levels were on average decreased to 8% at mRNA (Fig. 4.23 D) and 26% at cell surface level (Fig. 4.23 B- C), respectively, displaying efficient EpCAM knock-down. MRNA levels of transcription factors were found to be similar or decreased in EpCAM siRNA transfected cells compared to control cells. Mean mRNA levels were 73% (SNAIL), 91% (SLUG), 83% (TWIST-1), 46% (TWIST-2) and 83% (ZEB-1), respectively, in EpCAM-depleted cells. ZEB-2 remained below detection limit (Fig. 4.23 D).

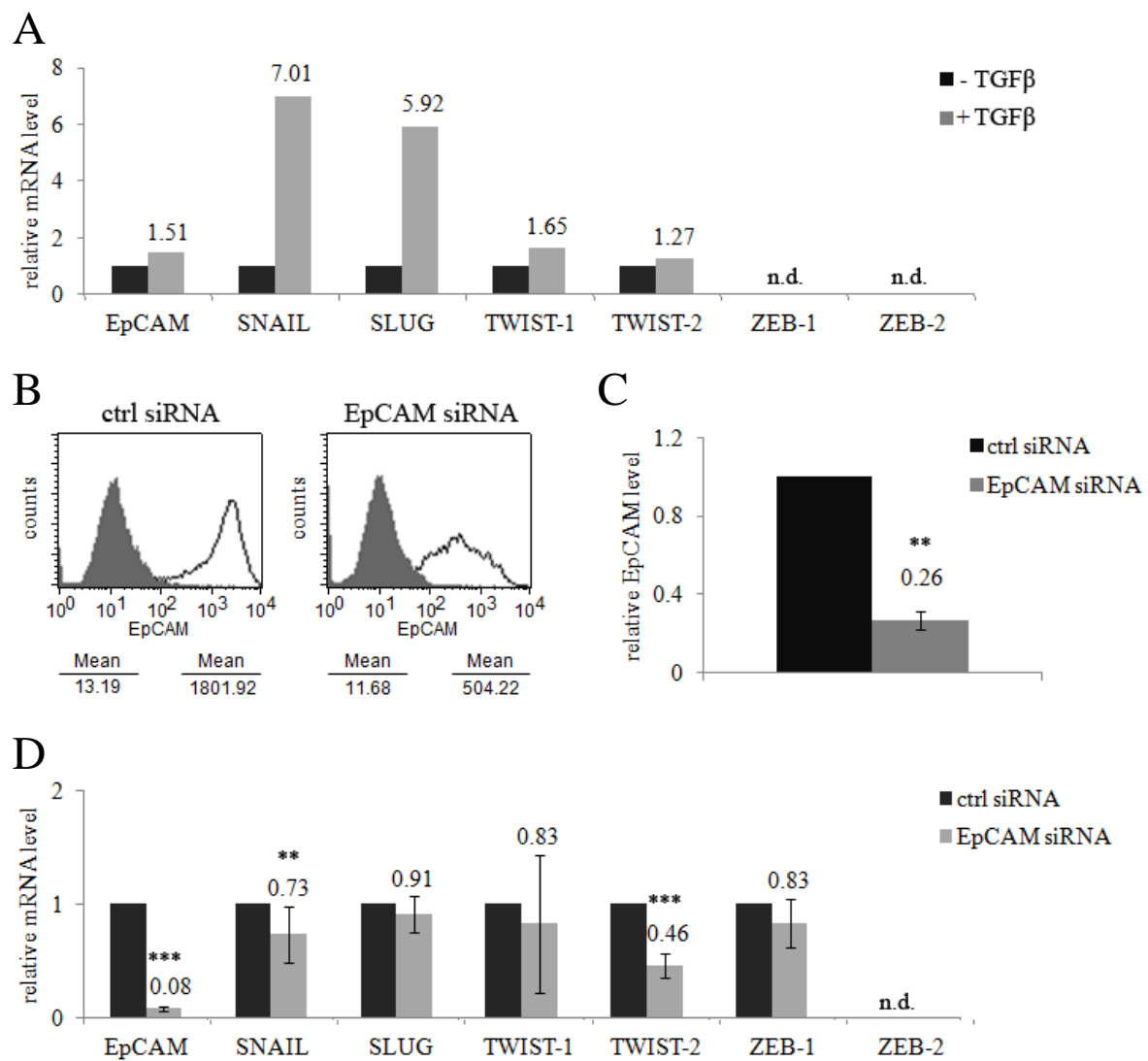


Figure 4. 23: EpCAM knock-down does not induce the TGFβ pathway in Kyse 30 cells.

(A) Kyse 30 cells were cultivated with or w/o TGFβ for 72h and mRNA levels of EpCAM and selected transcription factors involved in TGFβ pathway were assessed using qRT-PCR with specific primers. *GAPDH* served as a house-keeping gene for standardisation. Shown are mRNA expression level normalized to untreated cells from one experiment. (B-D) Kyse 30 cells were transiently transfected with either control or EpCAM-specific siRNA. 72h after transfection, EpCAM knock-down efficiency as well as mRNA level of transcription factors were analyzed. (B) EpCAM cell surface expression was assessed by flow cytometry with EpCAM specific antibody (black lined histograms) and isotype antibody (filled histograms). Shown are representative results from three independent experiments. (C) Relative mean fluorescence intensity ratios of EpCAM cell surface expression in cells transfected with ctrl or EpCAM-specific siRNA are given with standard deviations from three independent experiments. Controls are set to “1.0”. (D) MRNA levels of EpCAM and transcription factors involved in TGFβ pathway were assessed upon qRT-PCR with specific primers. *GAPDH* served as a house-keeping gene for standardisation. Shown are mean relative mRNA expression levels normalized to ctrl cells from three independent experiments with standard deviations. P-values: *p < 0.05; ** p < 0.01; *** p < 0.001. n.d.; not detectable.

4.8.2 Analysis of the adhesive function of EpCAM

EpCAM was characterized as a cell adhesion molecule by Litvinov *et al.* already in 1994 (Litvinov *et al.* 1994a; Litvinov *et al.* 1994b). Experiments presented so far, revealed that reduction of EpCAM expression provides cells with increased migratory and invasive capacities. To find out if this is due to reduced cell adhesion, adhesion assays were performed with siRNA transfected Kyse 30 cells, as well as with Kyse 520^{high} and Kyse 520^{low} cells. Adhesion assays were performed either on a surface consisting of matrigel, which mimics the extracellular matrix (cell-matrix adhesion assays, see 3.1.10.1) or on a surface consisting of a dense cell monolayer (cell-cell adhesion assay, see 3.1.10.2). To ensure that the strong cell contacts provided by cadherins, which are calcium-dependent cell adhesion molecules, do not overlay possible effects of EpCAM knock-down, all adhesion assays were performed without calcium. This included the use of calcium-free medium and the absence of FCS.

4.8.2.1 Cell adhesion is not weakened in EpCAM-depleted Kyse 30 cells

Kyse 30 cells were transiently transfected with either a ctrl or an EpCAM-specific siRNA (see 3.1.4.1), and used in adhesion assays (see 3.1.10). To ensure EpCAM knock-down, cell surface levels of EpCAM were assessed using flow cytometry (see 3.1.5.1). As depicted in Figure 4.24 A-B, EpCAM levels showed an average decrease to 49% in cells transfected with EpCAM-specific siRNA compared to ctrl siRNA transfected cells.

SiRNA treated cells were used for cell-matrix and cell-cell adhesion assays. In cell-matrix adhesion assays, cells were added to matrigel-coated 96-well plates and adhesion was allowed for 2h (see 3.1.10.1). As shown in Figure 4.24 C, on average 7.27% of ctrl siRNA and 11.67% of EpCAM siRNA transfected cells were able to attach to the matrigel-matrix within 2h. These numbers display that on average EpCAM siRNA transfected cells adhered 1.49-times better than ctrl siRNA transfected cells (Fig. 4.24 D).

For cell-cell adhesion assays, transfected cells were first plated on 96-well plates to form a dense monolayer, and subsequently additional cells were allowed to adhere for 2h (see 3.1.10.2). This setting led to four possible combinations: ctrl siRNA cells plated on ctrl siRNA cells, ctrl siRNA cell plated on EpCAM siRNA cells, EpCAM siRNA cells plated on ctrl siRNA cells and EpCAM siRNA cells plated on EpCAM siRNA cells. The results of these experiments are depicted in Figure 4.24 E-F, whereat the caption beneath the diagrams describes the cells, which were used as a feeder layer and the labeling above the graphs

depicts the cells, which were subsequently added. On average 11.26% and 10.87% of the ctrl siRNA treated cells were able to adhere to ctrl and EpCAM siRNA transfected cells respectively, whereas 15.81% and 14.55% of EpCAM-depleted cells were able to adhere to ctrl and EpCAM siRNA transfected cells within 2h (Fig. 4.24 E). Putting these numbers in relation to each other shows that adhesion efficiency was slightly higher when ctrl cells adhered to EpCAM-depleted cells (1.17-fold), when EpCAM-depleted cells adhered to ctrl cells (1.55-fold), and when EpCAM-depleted cells adhered to EpCAM-depleted cells (1.52-fold) compared to the setting when ctrl cells adhered to ctrl cells (Fig. 4.24 F). It must be noted here that ctrl cells represent the cells with the highest EpCAM expression and, furthermore, that none of the observed differences was significant. Hence, EpCAM knock-down did not significantly and measurably influence adhesion of Kyse 30 cells to matrix, nor to each other.

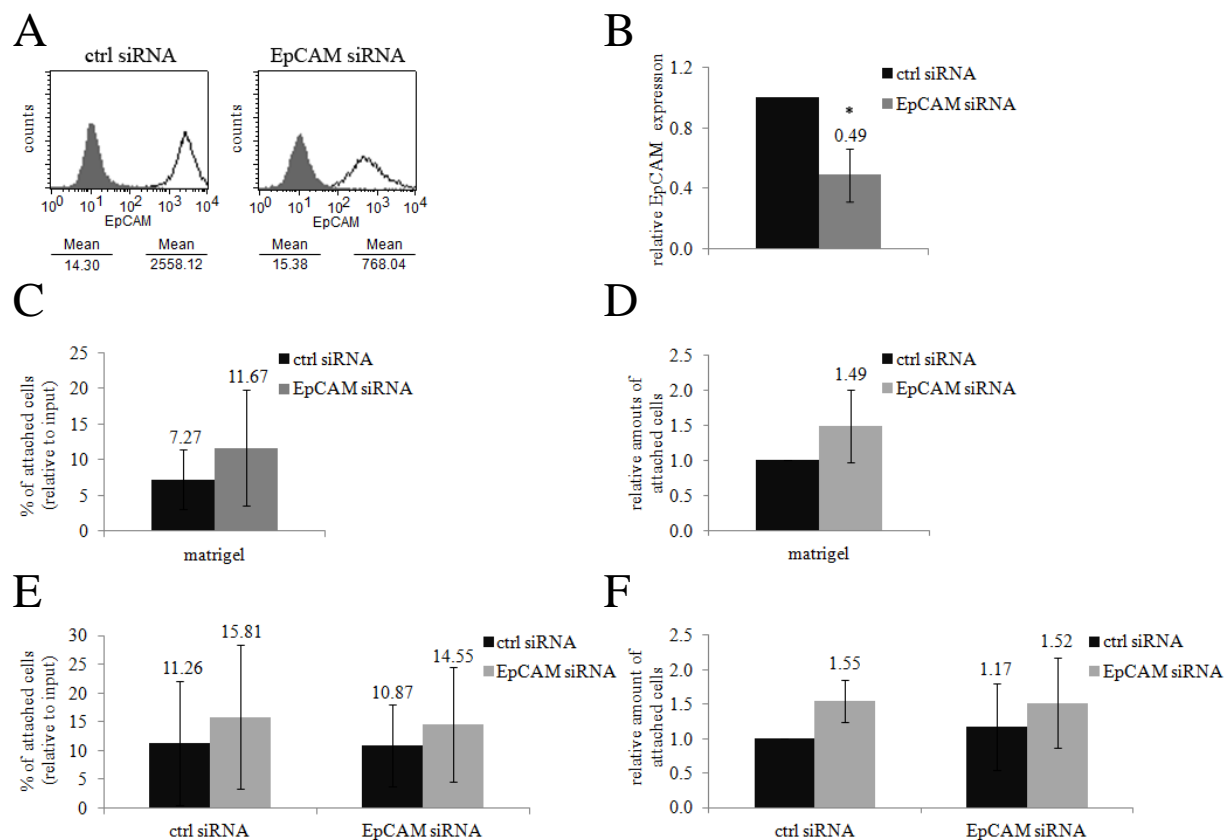


Figure 4.24: Adhesion assays with siRNA transfected Kyse 30 cells.

Kyse 30 cells were transiently transfected with either a ctrl or an EpCAM-specific siRNA, and subsequently used in adhesion assays to analyze the function of EpCAM as cell adhesion molecule in esophageal cancer cells. (A) EpCAM cell surface expression was assessed by flow cytometry with EpCAM-specific antibody (black lined histograms) and isotype control antibody (filled histograms). Shown are representative results from three independent experiments. (B) Relative mean fluorescence intensity ratios of EpCAM cell surface expression in cells transfected with ctrl or EpCAM-specific siRNA are given with standard deviations from three independent experiments. Controls are set to “1.0”. (C-D) Amounts of adherent cells in cell-matrix adhesion assays. (C) Mean percentages of adherent cells transfected with ctrl or EpCAM-specific siRNA are given with standard deviations from three independent experiments. Numbers were calculated relative to input. (D) Relative mean values of adherent cells transfected with ctrl or EpCAM-specific siRNA are given with standard deviations from three independent experiments. Controls are set to “1.0”. (E-F) Amounts of adherent cells in cell-cell adhesion assays. (E) Mean percentages of adherent cells transfected with ctrl or EpCAM-specific siRNA are given with standard deviations from three independent experiments. Numbers were calculated relative to input cells. (F) Relative mean values of adherent cells transfected with ctrl or EpCAM-specific siRNA are given with standard deviations from three independent experiments. Controls are set to “1.0”. P-values: * $p < 0.05$; ** $p < 0.01$; *** $p < 0.001$.

4.8.2.2 EpCAM depletion impacts on cell-matrix but not cell-cell adhesion in Kyse 520 cells

Besides siRNA transfected Kyse 30 cells, Kyse 520^{high} and Kyse 520^{low} cells were used in adhesion assays (see 3.1.10) to obtain a better understanding about the role of EpCAM as an adhesion molecule in esophageal cancer cells.

EpCAM cell surface levels were assessed using flow cytometry (see 3.1.5.1). As depicted in Figure 4.25 A-B, Kyse 520^{low} cells on average displayed more than 4-fold lower EpCAM surface levels than Kyse 520^{high} cells.

Kyse 520^{high} and Kyse 520^{low} cells were used for cell-matrix and cell-cell adhesion assays. In cell-matrix adhesion assays, cells were added to matrigel coated 96-well plates and adhesion was allowed for 2h. As shown in Figure 4.25 C, on average 20.37% of Kyse 520^{high} and 8.15% of Kyse 520^{low} cells were able to attach to the matrigel matrix within 2h. These numbers show that on average Kyse 520^{low} cells adhered 2.38-times worse than Kyse 520^{high} cells (Fig. 4.25 D).

For cell-cell adhesion assays, cells were first plated on 96-well plates to form a dense monolayer, and subsequently additional cells were allowed to adhere for 2h (see 3.1.10.2). This setting led to four possible combinations: Kyse 520^{high} cells plated on Kyse 520^{high} cells, Kyse 520^{high} cell plated on Kyse 520^{low} cells, Kyse 520^{low} cells plated on Kyse 520^{high} cells, and Kyse 520^{low} cells plated on Kyse 520^{low} cells. The results of these experiments are depicted in Figure 4.25 E-F, whereat the caption beneath the diagrams describes the cells, which were used as a feeder layer and the labeling above the graphs depicts the cells, which were subsequently added. On average, 2.66% and 7.15% of the Kyse 520^{high} cells were able to adhere to Kyse 520^{high} and Kyse 520^{low} cells, respectively, whereas 7.56% and 7.95% of Kyse 520^{low} cells were able to adhere on Kyse 520^{high} and Kyse 520^{low} cells within 2h (Fig. 4.25 E).

Putting these numbers relative to each other shows that adhesion efficiency was higher when Kyse 520^{high} cells adhered to Kyse 520^{low} cells (2.25-fold), when Kyse 520^{low} cells adhered to Kyse 520^{high} cells (3.09-fold), and when Kyse 520^{low} cells adhered to Kyse 520^{low} cells (2.64-fold) compared to the setting when Kyse 520^{high} cells adhered to Kyse 520^{high} cells (Fig. 4.25 F). However, it must be noted here that none of the differences was significant. Hence, EpCAM did not significantly and measurably influence adhesion of Kyse 520 cells to each other.

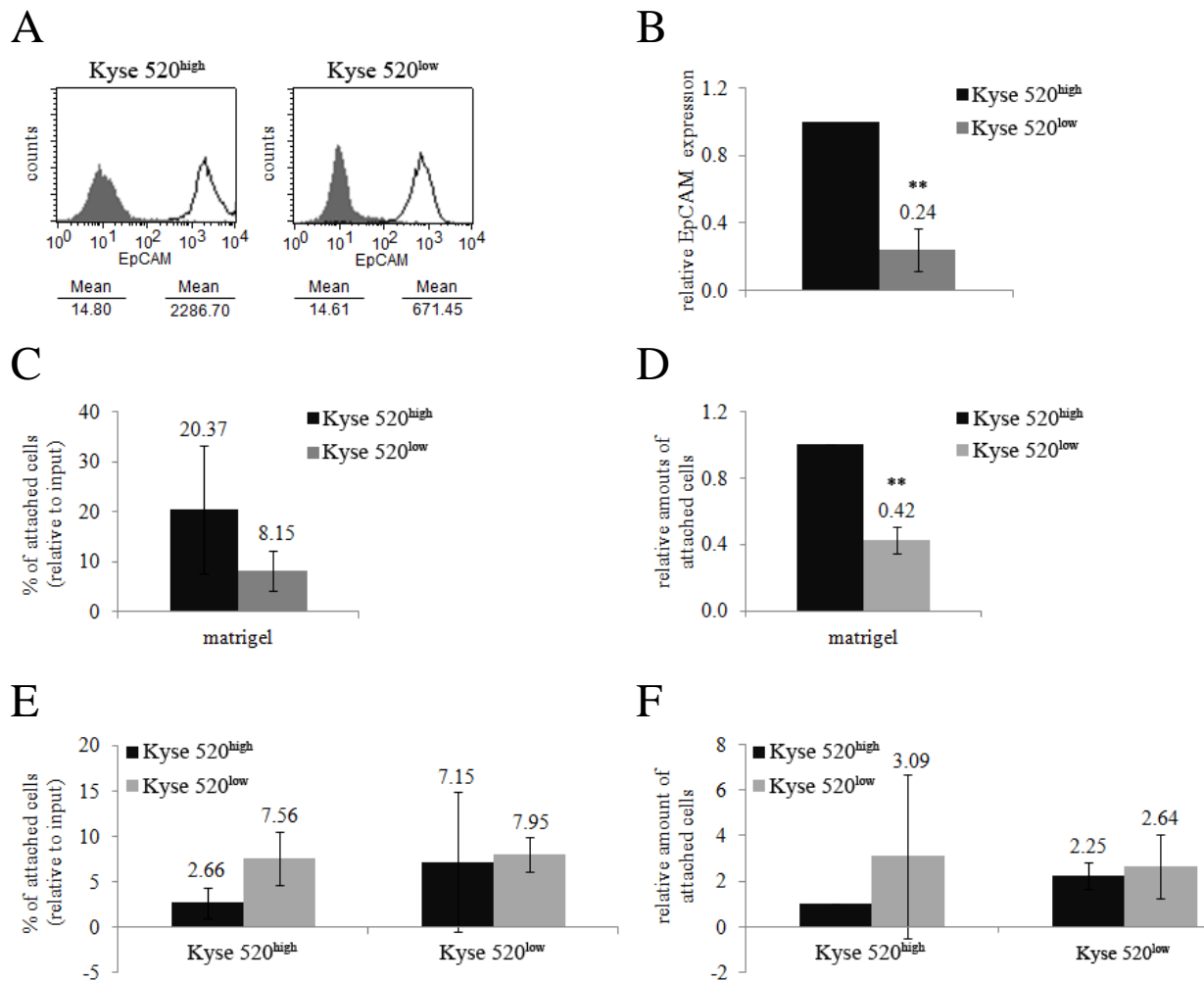


Figure 4. 25: Adhesion assays in Kyse 520^{high} and Kyse 520^{low} cells.

Kyse 520^{high} and Kyse 520^{low} cells were used in adhesion assays to analyze the function of EpCAM as an adhesion molecule in esophageal cancer cells. (A) EpCAM cell surface expression was assessed by flow cytometry with EpCAM-specific antibody (black lined histograms) and isotype control antibody (filled histograms). Shown are representative results from three independent experiments. (B) Relative mean fluorescence intensity ratios of EpCAM cell surface expression in Kyse 520^{high} and Kyse 520^{low} cells are given with standard deviations from three independent experiments. Controls are set to “1.0”. (C-D) Amounts of adherent cells in cell-matrix adhesion assays. (C) Mean percentages of adherent Kyse 520^{high} and Kyse 520^{low} cells are given with standard deviations from three independent experiments. Numbers were calculated relative to input. (D) Relative mean values of adherent Kyse 520^{high} and Kyse 520^{low} cells are given with standard deviations from three independent experiments. Controls are set to “1.0”. (E-F) Amounts of adherent cells in cell-cell adhesion assays. (E) Mean percentages of adherent Kyse 520^{high} and Kyse 520^{low} cells are given with standard deviations from three independent experiments. Numbers were calculated relative to input. (F) Relative mean values of adherent Kyse 520^{high} and Kyse 520^{low} cells are given with standard deviations from three independent experiments. Controls are set to “1.0”. P-values: *p < 0.05; ** p < 0.01; *** p < 0.001.

5 DISCUSSION

Cancer is one of the leading causes of death worldwide, affecting more and more people (Jemal *et al.* 2011; Are *et al.* 2013). Enormous research efforts during the last decades led to a more detailed understanding of the processes which are involved in cancer formation and progression, and provided tumor patients with innovative and more efficient treatment strategies. However, many mechanisms of tumorigenesis are still poorly or not at all understood. Cancer progression mainly starts with only one or a few single cells, which gather mutations enabling the cells to escape from cellular regulatory mechanisms related to cell proliferation, apoptosis and growth control. The mutated cells can thereby proliferate indefinitely and eventually give rise to a primary tumor. As a next step, single cells of the primary tumor start to loosen and migrate away from the tumor bulk, invade into the blood or lymph system and thereby translocate within the body of the cancer patient. Eventually, the cells settle at a secondary site in the body where they again start to proliferate and thereby give rise to metastases, which represent the main cause of cancer related deaths (Sleeman and Steeg 2010; Stoecklein and Klein 2010) (see 1.1.1). To be able to efficiently treat and cure cancer, it is mandatory to have a detailed understanding of all the processes and mechanisms taking action during all the different stages of carcinogenesis, including the role of cancer related proteins.

One of the proteins known to be involved in cancer formation and progression is the epithelial cell adhesion molecule (EpCAM). EpCAM was initially discovered as tumor antigen in 1979 as it induces the selection of specific antibodies upon immunisation of mice with colon carcinoma cells (Herlyn *et al.* 1979). Further studies revealed that EpCAM has an apparent molecular weight of 37-42 kDa, can be glycosylated (Gottlinger *et al.* 1986a; Gottlinger *et al.* 1986b), and consists of three major domains, i.e. a large extracellular domain, a single transmembrane domain as well as a small intracellular domain (Balzar *et al.* 1999b; Gires 2008). EpCAM was described to be a cell adhesion molecule in 1994 (Litvinov *et al.* 1994b; Litvinov *et al.* 1997), while more recent studies revealed a role in cell signaling. The internal part of EpCAM (EpICD) can be shed from the rest of the molecule upon proteolytic cleavage (Maetzel *et al.* 2009) and form a complex with FHL-2 and β -catenin proteins (Martin *et al.* 2002; Labalette *et al.* 2004). Subsequently, this complex can translocate into the nucleus and bind to Lef-1, which enables the activation of EpCAM-specific genes like the oncogenic transcription factor c-myc, the cell cycle related protein cyclin-D1 and the

epidermal fatty acid binding protein (EFABP) (Munz *et al.* 2004; Maetzel *et al.* 2009; Chaves-Perez *et al.* 2013). Compared to normal tissue, in which EpCAM expression can only be found at the basolateral side of plasma membranes of simple, unstratified epithelia (Momburg *et al.* 1987; Litvinov *et al.* 1996), EpCAM is *de novo* or highly overexpressed in almost all carcinoma types (Zorzos *et al.* 1995; Litvinov *et al.* 1996). Its strong expression in cancer compared to appropriate healthy tissues is also the reason why EpCAM became an important prognostic and therapeutic marker (see 1.2.5.3) (Munz *et al.* 2010; van der Gun *et al.* 2010). Besides its role as prognostic marker and in therapy, EpCAM is nowadays also the most frequently used antigen to detect and retrieve circulating (CTCs) and disseminated tumor cells (DTCs) (Cohen *et al.* 2006; Criscitiello *et al.* 2010; Imrich *et al.* 2012). However, although EpCAM is a well-characterized protein, which already has been used in therapeutic approaches (Gires and Bauerle 2010; Munz *et al.* 2010), its role in cancer formation and progression is still not finally understood (van der Gun *et al.* 2010). This is especially true in case of CTCs, DTCs and metastases (see 1.2.4.3). Recent findings of our cooperation partners in Düsseldorf provided evidence that in case of esophageal carcinomas EpCAM is not constantly expressed throughout the various stages of carcinogenesis, but rather shows a dynamic expression. Thereby, primary tumors displayed high EpCAM expression levels, whereas the majority of cognate disseminated tumor cells (DTCs) revealed to be EpCAM-negative (Driemel *et al.* 2013). Similar observations were already published by other groups, including a study by Jojovic *et al.*, describing that large metastases formed by colon cancer cells showed similar staining patterns as primary tumors, while small metastases displayed a loss of EpCAM (Jojovic *et al.* 1998). In addition, in a comparative study of primary tumors and their cognate CTCs, EpCAM expression was found to be 10-fold less in CTCs than in tumors (Rao *et al.* 2005). This led to the postulation that EpCAM expression might be downregulated upon epithelial-to-mesenchymal transition (EMT) (Jojovic *et al.* 1998), an essential process in carcinogenesis during which cells change their phenotype from epithelial to mesenchymal, enabling them to loosen cell contacts and leave their surroundings (see 1.1.2). In contrast, other studies correlated enhanced migration and invasion of cells to high EpCAM levels. One example for this is a study by Osta *et al.*. The group showed that downregulation of EpCAM in breast cancer cells is associated with decreased cell migration and invasion. This led to the assumption that, in case of breast carcinomas, high EpCAM expression is associated with increased metastasis (Osta *et al.* 2004). Additional studies in prostate and colon carcinomas also provided data about a correlation between EpCAM and increased cell invasion and metastasis (Lin *et al.* 2012; Ni *et al.* 2013).

In order to understand how EpCAM contributes to the formation and progression of carcinomas and why it is downregulated or lost at selected stages of carcinogenesis, the effects of EpCAM expression and depletion were analyzed in a set of diverse assays, whereat esophageal cancer cells were used as a model system. The results of these experiments will be subsequently discussed.

5.1 EpCAM expression correlates with increased proliferation and formation of larger tumors

Since an increased proliferation rate is one of the major hallmarks of EpCAM expressing carcinoma cells, the influence of EpCAM on proliferation was also analyzed in esophageal cancer cells. Experiments with esophageal Kyse 520 carcinoma cells, which were transfected with either a control or an EpCAM-specific siRNA, as well as trials with Kyse 520^{high} and Kyse 520^{low} cells, revealed that cells displaying lower levels of EpCAM proliferated less than their counterparts expressing higher levels of EpCAM (see Fig. 4.7 and 4.8). These results are in line with former findings of our own and other groups, which revealed that EpCAM expression is correlated to increased proliferation in colon, pharynx, breast, gastric, lung and pancreatic cancer cells (Munz *et al.* 2004; Osta *et al.* 2004; Maetzel *et al.* 2009; Wenqi *et al.* 2009; Hase *et al.* 2011; Thuma and Zoller 2013). EpCAM induces proliferation via its function as signaling molecule. This function depends is in great parts on regulated intramembrane proteolysis and the release of the intracellular domain EpICD, which eventually leads to activation of genes like cyclin D1 and c-Myc (Maetzel *et al.* 2009; Chaves-Perez *et al.* 2013). Presumably, this signaling cascade is also active in esophageal cancer cells, since experimental data evidenced that EpCAM becomes cleaved and EpICD is formed in Kyse 30 and Kyse 520 cells (see 4.2). However, so far no differences in c-Myc or cyclin D1 mRNA levels could be observed when comparing Kyse 520 cells transfected with a ctrl or an EpCAM-specific siRNA, or Kyse 520^{high} and Kyse 520^{low} cells (data not shown). It is therefore possible that EpCAM regulates a different set of genes in esophageal cancer cells. In any case, further experiments are necessary to elucidate how exactly EpCAM signaling induces proliferation in esophageal carcinomas.

A second finding of these experiments was that effects on proliferation were more pronounced when cells were cultured under restrictive conditions (see Fig. 4.7), indicating that in case of esophageal cancer EpCAM expression has a larger influence in cells growing

under adverse conditions, such as the lack of nutrition. This assumption is supported by former findings of our group showing that effects of EpCAM overexpression in HEK 293 cells are more pronounced under restrictive conditions (Munz *et al.* 2004). Indeed, an absence of nutrition can be found in primary tumors and large metastases, lacking proper angiogenesis and results in the prevention of further tumor growth and progression (Hiratsuka 2011; Leite de Oliveira *et al.* 2011; Barzi and Lenz 2012). It is therefore tempting to speculate that the expression of EpCAM enables cancer cells to survive such conditions until proper nutrition supply is warranted again. However, more experimental data need to be provided to strengthen this hypothesis, including data from other cancer entities grown under non-restrictive and restrictive condition, such as lack of nutrition or hypoxia.

Besides increasing proliferation rates, EpCAM was also found to lead to formation of larger tumors *in vivo*, when esophageal cancer cells are injected subcutaneously into immunodeficient mice (see 4.4). Compared to cells which were stably transfected with a ctrl shRNA, tumors formed from cells stably transfected with an EpCAM-specific shRNA were on average 2.78 times smaller (0.39g compared to 0.14g, see Fig. 4.9 C). Similar observations were made by our cooperation partners in Düsseldorf, who injected Kyse 520 cells, naturally occurring as two subpopulations with different EpCAM levels (Kyse 520^{high} and Kyse 520^{low}), into the flanks of NOD/SCID mice, resulting in the formation of tumors with average weights of 0.35g (Kyse 520^{high} cells) and 0.14g (Kyse 520^{low} cells) (Driemel *et al.* 2013). In addition, a former study of our own group demonstrated that human embryonic kidney cells (HEK 293), stably transfected with an EpCAM-overexpressing construct, led to formation of larger tumors *in vivo* when subcutaneously injected into NOD/SCID mice, than cells stably transfected with a control construct, which barely generated tumors *in vivo* (Maetzel *et al.* 2009).

In contrast to tumor size, tumor occurrence *in vivo* was not influenced by expression of EpCAM in esophageal tumor cells in the present study. In both groups tumors formed in four out of five mice, independently of the EpCAM levels of injected cells (see Fig. 4.9 C). However, when comparing the EpCAM levels of cells before injection with those of their cognate tumor explants, a discrepancy was found for cells stably transfected with EpCAM-specific shRNA (see Fig. 4.9 D-E). In contrast to ctrl shRNA transfected cells, displaying similar percentages of cells expressing no, low, intermediate and high levels of EpCAM in tumor cells before injection and tumor explants, relative numbers of cells expressing intermediate and high levels of EpCAM were substantially increased in tumors formed from

EpCAM-depleted cells compared to the corresponding cells before injection into mice (see Fig. 4.9 D-E). Furthermore, none of the tumors formed by EpCAM-depleted cells was found to be EpCAM-negative, but all tumors showed a certain level of EpCAM expression. These findings suggest a positive selection of EpCAM-expressing cells during cancer formation and growth. Cells expressing high levels of EpCAM seem to have a selection advantage, possibly due to increased proliferation rates and/or survival features, and thereby are able to overgrow the population of cells, which express EpCAM at low levels or do not express EpCAM at all. However, another explanation for the abovementioned findings could be that basically only EpCAM-positive, but not EpCAM-negative cells are capable to induce the formation of esophageal carcinomas. As a consequence, this would imply that epithelial cells of the esophagus, which do not express EpCAM, could never trigger tumor formation. At present, using shRNA or siRNA does not allow for the generation of true knock-out cells, which do not express EpCAM at all. Thus, a definite answer on the actual contribution to tumor formation, especially concerning the absolute necessity of EpCAM expression for this process, cannot be given. In this respect, further experiments should be conducted to address the point, whether EpCAM increases tumor formation or whether it is indispensable. To provide a complete knock-out, the EpCAM gene should be destroyed, using either TALENs (Morbiter *et al.* 2011; Sun and Zhao 2013) or a CRISPR/Cas system in forthcoming studies (Cho *et al.* 2013; Sampson *et al.* 2013).

So far, all results from *in vitro* and *in vivo* experiments, i.e. the positive correlation of EpCAM expression with increased proliferation rates, formation of larger tumors, and the obvious *in vivo* selection for EpCAM-positive cells during tumor growth, support the findings from Stoecklein *et al.* and Went *et al.*, describing EpCAM as a tumor-promoting protein in esophageal cancer, correlated with bad prognosis for survival of patients (Went *et al.* 2004; Stoecklein *et al.* 2006). This is in line with findings in numerous other cancer entities, including lung (Kubuschok *et al.* 1999; Piyathilake *et al.* 2000), breast (Gastl *et al.* 2000; Osta *et al.* 2004; Spizzo *et al.* 2004), prostate (Poczatek *et al.* 1999; Zellweger *et al.* 2005; Ni *et al.* 2013), bladder (Brunner *et al.* 2008), and pancreas (Li *et al.* 2007; Fong *et al.* 2008; Scheunemann *et al.* 2008) carcinomas, in which EpCAM expression is correlated with carcinogenesis, tumor progression, metastases formation and/or shorter survival. However, although in the majority of carcinomas EpCAM seems to be associated with cancer formation and progression, there are some cancer entities, i.e. renal (Seligson *et al.* 2004; Went *et al.* 2005; Klatte *et al.* 2009) and thyroid (Ensinger *et al.* 2006; Ralhan *et al.* 2010a) carcinomas, in which the expression of EpCAM is associated with a protective role. In addition, there are

cancer types, including gastric (Songun *et al.* 2005; Deveci and Deveci 2007; Scheunemann *et al.* 2009), ovarian (Kim *et al.* 2003; Heinzelmann-Schwarz *et al.* 2004; Spizzo *et al.* 2006) and colorectal (Basak *et al.* 1998; Gosens *et al.* 2007; Kuhn *et al.* 2007) carcinomas, for which contradictory studies report on both, a protective and a cancer promoting role of EpCAM, as reviewed by van der Gun *et al.* in 2010 (van der Gun *et al.* 2010). As already mentioned (see 1.2.6), this is also the case for esophageal cancer, as a study by Kimura *et al.*, in contrast to studies by Stoecklein *et al.* and Went *et al.*, described EpCAM as tumor-associated antigen, which is inversely correlated with tumor progression, stimulates an immunological response against cancer cells, increases cell adhesion, and suppresses formation of metastases (Kimura *et al.* 2007). Maybe a closer look at the various stages of carcinogenesis would provide an explanation for these contradictory findings, as it might be that the presence of EpCAM has different effects during the diverse stages of carcinoma progression. One possible explanation could be that EpCAM expression enhances cancer cell proliferation and thereby is associated with tumor growth, but prevents cell migration, maybe by the formation of cell-cell contacts (see 1.2.5.1). Indeed, our collaboration partners provided evidence supporting this hypothesis. On the one hand, they have shown that high EpCAM expression on DTCs is associated with increased occurrence of metastases and reduced overall survival of patients. On the other hand, they found that most of the DTCs were actually EpCAM-negative, although these cells derived from primary tumors expressing high amounts of EpCAM (Driemel *et al.* 2013). This supports the notion that EpCAM is important for the growth of primary tumors and outgrowth of metastases, whereas it is dispensable during migration and invasion of metastasising cells. To learn more about why EpCAM is downregulated in certain carcinoma cells, another set of experiments was performed using esophageal cancer cells as model system (see 4.5 - 4.7). The results of these experiments will be subsequently discussed.

5.2 Loss of EpCAM leads to traits of EMT in esophageal cancer cells

Besides a necessity for proliferation, migration and invasion of cells are essential processes during cancer progression and were therefore analyzed in the present study. By using Kyse 30 and Kyse 520^{low} esophageal cancer cells in scratch assays and subsequently staining them with a combination of EpCAM-specific and fluorochrome-coupled antibodies, it was found that migrating cells display a different EpCAM staining pattern compared to their non-migrating counterparts (see 4.5.1). Non-migrating cells basically displayed a strong

membranous EpCAM staining, with only few fluorescence signals detectable inside the cell (Fig. 4.10, Fig. 4.11). Thereby they reflected the typical EpCAM staining pattern that was already observed in various other carcinoma cells (Denzel *et al.* 2009; Maetzel *et al.* 2009; Lee *et al.* 2012). However, this staining pattern was completely changed in migrating cells. Here, EpCAM fluorescence signals were mainly located in the cytoplasm, whereas membranous staining was almost or totally lost (Fig. 4.10 d-m, Fig. 4.11). Furthermore, a correlation between EpCAM-specific staining intensity and cell migration could be observed, with fluorescence signals being weaker, the further cells had migrated (Fig. 4.10 d-m, Fig. 4.11). This redistribution and loss of fluorescence signals mirrors a change in EpCAM location and expression, apparently essential to allow cells to migrate. Additional experiments should be performed to ascertain if overexpression of EpCAM can interfere with or even prevent cell migration.

The obvious changes in EpCAM distribution and expression raised the question how EpCAM is downregulated in migrating cells. The obtained data suggested a stepwise regulation, whereat in a first step EpCAM is removed from the membrane and relocated into the cytoplasm, and in a second step EpCAM expression is modulated at the protein and, eventually, at the transcriptional level. A recent study from our group provided new data about the regulation of murine and human EpCAM upon RIP. Hachmeister *et al.* reported that not only TACE but also BACE-1 is capable to cleave EpCAM (see 1.2.3). However, as BACE-1 is a sheddase with a pH optimum of 4.5, it is not active at the cell membrane but in acidified cell components such as endosomes and lysosomes (Hachmeister *et al.* 2013). The finding that BACE-1 can cleave EpCAM thus raised the hypothesis that localisation and degradation of EpCAM are partly regulated by endocytosis. Indeed, our group was able to identify specific interactions of EpCAM with proteins associated with clathrin-dependent and -independent endocytosis in a SILAC (stable isotope labeling by/with amino acids in cell culture) interaction study in murine cells (unpublished data). Among the identified interaction partner were the clathrin light chain A (CLTA) and clathrin heavy chain 1 (CLTC) proteins, as well as the adaptor proteins AP2A1 and AP2B1, subunits of the adaptor-protein complex AP-2, which mediates the interaction between clathrins and the target molecules (Traub 2005; McMahon and Boucrot 2011). In addition, flotillin 1 and flotillin 2, which play a role in clathrin-independent endocytosis (Banning *et al.* 2011; Zhao *et al.* 2011), were identified as potential EpCAM interaction partners. Endocytosis would provide a further layer of complexity to the processes, which are involved in EpCAM regulation. Additionally, as endocytosis is a comparatively fast and reversible process (Conner and Schmid 2003;

Sigismund *et al.* 2008; El-Sayed and Harashima 2013), it would enable a quick and reversible turnover of EpCAM at the cell membrane. This, in consequence, would allow a fast adaptation of EpCAM cell surface levels to new environmental and functional requirements. However, further experiments are mandatory to provide evidence if and how endocytosis of EpCAM occurs. As regulation of EpCAM expression could be due to various processes, including EpCAM promoter silencing, regulation of EpCAM-specific transcription factors, and activation of EpCAM-specific miRNAs, additional experiments are necessary to reveal the actual mechanism(s) of EpCAM downregulation in migrating cells.

After finding that EpCAM is redistributed and subsequently downregulated in migrating cells, scratch assays were performed with siRNA transfected Kyse 30 cells to investigate if forced downregulation of EpCAM enhances migration of cells (see 4.5.2.1). Indeed, it was found that EpCAM depletion using an EpCAM-specific siRNA led to an increase of cell migration velocity, confirming the findings obtained in immunofluorescence staining experiments (Fig. 4.12 D-E). Besides the induction of cell migration, upregulation of the mesenchymal marker vimentin could be observed in EpCAM depleted cells when compared to control cells (see Fig. 4.12 F), pointing towards a phenotypic change of cells from an epithelial to a mesenchymal phenotype. To ensure that effects on cells were not only due to transfection with siRNA, experiments were repeated with esophageal Kyse 520^{high} and Kyse 520^{low} cells, which represent naturally occurring variants of one single cell line having the same genetic background but differing in their EpCAM expression levels (see 4.5.2.2). Indeed, experiments performed with Kyse 520 variants confirmed data obtained in scratch assay experiments with siRNA transfected Kyse 30 cells. Compared to Kyse 520^{high} cells, Kyse 520^{low} cells showed a significantly higher migration velocity as well as much higher mRNA levels of the mesenchymal markers N-cadherin and vimentin (see Fig. 4.13 D-F). These differences could be further amplified when Kyse 520^{low} cells were transfected with an EpCAM-specific siRNA (see 4.5.2.3). As in Kyse 30 cells, EpCAM-depleted Kyse 520^{low} cells showed an enhanced migration velocity and increased mRNA levels of vimentin, compared to control cells (see Fig. 4.14 D-F). Furthermore, mRNA levels of E-cadherin were slightly decreased in EpCAM-depleted cells (see Fig. 4.14 F). Taken together, these data led to the assumption that Kyse 520^{high} and Kyse 520^{low} cells not only display two subpopulations with different EpCAM expression levels, but actually represent an epithelial (Kyse 520^{high}) and a more mesenchymal (Kyse 520^{low}) cell type, depending on the expression level of EpCAM. This hypothesis was further confirmed by an experiment performed to analyze the invasive capacity of cells expressing different levels of EpCAM. Kyse 520^{high} and Kyse

520^{low} cells were thereby added to fibroblast spheroids and invasion of the cancer cells was monitored (see 4.5.3). Again, Kyse 520^{low} cells displayed a more mesenchymal phenotype characterized by massive invasion into fibroblast spheroids, whereas invasion of Kyse 520^{high} cells was almost not observable (see Fig. 4.15, Fig. 4.16). Tumor cells with different capacities, concerning epithelial and mesenchymal characteristics, were also described for the case of tumor-inducing cells (TICs). In 2011, Biddle *et al.* reported on two distinct TIC subpopulations. One TIC population was characterized as CD44^{high}/EpCAM^{high} (termed ESA-1 for epithelial specific antigen in this study) and displayed an epithelial phenotype, including high proliferation rates. The second TIC population displayed a CD44^{high}/EpCAM^{low} cell surface phenotype and showed mesenchymal characteristics such as higher levels of mesenchymal markers vimentin and TWIST, reduced expression of epithelial markers E-cadherin and involucrin, slow proliferation rates and a high migratory ability (Biddle *et al.* 2011). Furthermore, Biddle and colleagues observed that CD44^{high}/EpCAM^{high} cells can switch their phenotype to CD44^{high}/EpCAM^{low} and vice versa, indicating a high plasticity of these cell populations (Biddle *et al.* 2011). It is conceivable that such a plasticity and trans-differentiation of TIC populations is central to cancer progression, particularly to processes of metastases formation.

After finding that EpCAM downregulation led to a phenotypic change from epithelial to mesenchymal, it was tested if vice versa induction of EMT led to a decrease of EpCAM expression. Therefore, cells were treated with TGF β , a known inducer of EMT (Moreno-Bueno *et al.* 2009) (see 4.6). To examine effects of TGF β treatment, the non-small lung cancer cell line A549, which is known to react to this kind of treatment (Kasai *et al.* 2005; Kim *et al.* 2007), was used as a control along with esophageal cancer cell lines Kyse 30 and Kyse 520 in the assay. In summary, TGF β treatment led to induction of EMT, revealed by morphologic changes, reduced mRNA levels of the epithelial marker E-cadherin and/or increased mRNA levels of the mesenchymal markers N-cadherin and vimentin, in all three cell lines (see 4.6.1, 4.6.2.1, 4.6.2.2). However, in case of Kyse 520 cells, only Kyse 520^{low} (see 4.6.2.2) but not Kyse 520^{high} cells (data not shown) showed a reaction upon TGF β treatment.

In all cell lines, which showed signs of EMT a downregulation of EpCAM was observed. However, whereas in A549 cell, which showed the most prominent reaction to the treatment with TGF β , EpCAM levels were decreased on both, mRNA and cell surface level (see Fig. 4.17 B-D), in Kyse 30 and Kyse 520^{low} cells EpCAM downregulation was observed

at cell surface levels only, while mRNA levels remained constant (Kyse 520^{low} cells, see Fig. 4.19 B-D) or were even slightly increased (Kyse 30 cells, see Fig. 4.18 B-D). The reason(s) for these differences remain(s) so far unknown. One possibility is that A549 cells react faster to TGF β treatment and thereby showed a more complete change of phenotype. This is supported by the findings that A549 cells not only showed an upregulation of mesenchymal markers, but also a substantial decrease of the epithelial marker E-cadherin, which was not observed in any of the Kyse cell lines. Furthermore, A549 cells showed the most drastic change in cell morphology (see Fig. 4.17 A). If this assumption is true, EpCAM downregulation at mRNA level should also be observable in Kyse cells when treated with TGF β for a longer time period. However, first experiments to verify this hypothesis remained so far inconclusive. Another option to test this hypothesis is to perform TGF β treatment in A549 cells for a shorter time period to see if EpCAM downregulation under these circumstances is only observable at the cell surface, but not the mRNA level.

A second possible explanation for the abovementioned finding is that EpCAM regulation upon EMT induction fundamentally differs in A549 and Kyse cells. From what could be observed in the experiments, EpCAM seems to be regulated at the transcriptional level in A549 cells, whereas regulation takes place at the post-transcriptional and/or posttranslational level in Kyse cells. This means that in A549 cells EMT-dependent EpCAM depletion is due to either a change of the chromatin structure in the *EPCAM* gene or to changes of proteins involved in *EPCAM* gene transcription, eventually leading to a decrease of EpCAM mRNA levels. In contrast, regulation of EpCAM in Kyse cells is either due to impaired EpCAM translation, which could be the result of specific miRNAs' activity, an insufficient transport of the EpCAM protein to the cell membrane or a decreased half-life time of EpCAM at the membrane. From what is known so far, none of the mentioned possibilities can be excluded. It is known that EpCAM expression can be regulated at the epigenetic level by DNA methylation of the *EPCAM* promoter region at exon 1 (Spizzo *et al.* 2007; Tai *et al.* 2007; van der Gun *et al.* 2011) as well as by reduction of activating histone marks in the *EPCAM* gene (Lu *et al.* 2010; van der Gun *et al.* 2011). Other studies report that proteins such as ZEB-1 (Vannier *et al.* 2013), tumor necrosis factor α (TNF α) (Gires *et al.* 2001), the chromatin-remodeling factor Smarcd3/Baf60c (Jordan *et al.* 2013) and the tumor suppressor p53 (Sankpal *et al.* 2009), as well as miRNAs like miR-26a, miR-101 (Bao *et al.* 2012a; Bao *et al.* 2012b) and miR-118 (Ji *et al.* 2011), are involved in *EPCAM* gene regulation. Using miRNA prediction tools, 46 (<http://www.microrna.org>) and 32 (<http://www.microrna.gr/microT-CDS>) miRNAs showing a high probability to bind specifically to EpCAM mRNA

could be found, respectively. However, so far no study could confirm a direct binding of any miRNA to the mRNA of EpCAM. Findings from other studies revealed that glycosylation of EpCAM is associated with the stability of EpCAM at the membrane, whereby glycosylation of asparagin 198 was found to have a stabilising effect (Munz *et al.* 2008). Furthermore, a recent study from our group provided a more detailed insight into the processing of EpCAM in humans and mice. Hachmeister *et al.* could show that EpCAM gets not only cleaved by TACE but also by BACE-1 (Hachmeister *et al.* 2013) a sheddase with a pH optimum of 4.5 that is active in endosomes and lysosomes (Venugopal *et al.* 2008). Therefore it is tempting to speculate that EpCAM can also be regulated by endocytosis and subsequent cleavage by BACE-1 in endosomes and lysosomes (Hachmeister *et al.* 2013). It is essential to find out how exactly EpCAM is downregulated during EMT, and whether or not the mechanisms of downregulation vary in different carcinoma types, as these findings not only provide a more complete picture of EpCAM but also generate insights into processes that occur during EMT. The knowledge about mechanisms underlying the formation of metastases is mandatory in order to interfere with this driving, lethal process of carcinogenesis.

After finding that EpCAM levels were reduced, at least on cell surface, it was analyzed if an overexpression of EpCAM could weaken or even prevent the effects of TGF β induced EMT. To do so, cell lines stably transfected with different EpCAM constructs were used in another set of TGF β experiments. As A549 and Kyse 30 cells showed the strongest effects of EMT induction, these cell lines were also used for the additional TGF β assays. However, this time the cells were overexpressing either YFP-tagged full length EpCAM (EpCAM-YFP), YFP-tagged EpICD (EpICD-YFP) or a control construct (YFP). As in previous experiments cell morphology and EMT marker levels were analyzed to rate the effects of TGF β treatment (see 4.7). The use of different EpCAM overexpression constructs allowed for the discrimination of effects mediated by the adhesive and the signaling function of EpCAM. Effects would be due to the adhesive function of EpCAM if they can only be observed in cells expressing EpCAM-YFP, but not in cells expressing EpICD-YFP, whereas effects due to the signaling function of EpCAM should be observed in EpCAM-YFP and EpICD-YFP overexpressing cells. However, findings from the experiments were rather disappointing, as neither overexpression of EpICD nor full length EpCAM could prevent or significantly influence TGF β induced changes in A549 and Kyse 30 cells. Basically almost no differences could be observed between TGF β treated control cells and TGF β treated cells overexpressing EpCAM constructs in term of cell morphology and EMT marker regulation (see Fig. 4.20, Fig. 4.21). Only in A549 cells, overexpression of EpCAM-YFP correlated with a slightly

reduced downregulation of E-cadherin as well as with a slightly lower upregulation of N-cadherin and vimentin after addition of TGF β compared to control cells (see Fig. 4.20 C), meaning that full length EpCAM in this cell line could somewhat dampen the effects of induced EMT. As no differences were found between the A549 cells overexpressing YFP and those which overexpressed EpICD-YFP, observed effects are most likely due to functions of full-length EpCAM. Although the effects of EpCAM on induction of EMT in A549 cells were only marginal, it should be asked why EpCAM had an effect in A549 but not in Kyse 30 cells. A possible explanation for this might be the diverse strategies for EpCAM downregulation. Maybe downregulation strategies of A549 cells, targeting the *EPCAM* gene are not efficiently working on the exogenous EpCAM construct. This assumption is supported by the finding that EpCAM mRNA levels were not significantly decreased in A549 cells overexpressing EpCAM-YFP when treated with TGF β (see Fig. 4.20 B). This effect should also be visible in EpICD overexpressing cells, however, primers used for qRT-PCR analyses bind on a part of the EpCAM mRNA which is not present in the EpICD construct. In contrast, strategies to deplete EpCAM in Kyse 30 cells might also efficiently work in case of the exogenous EpCAM. However, due to technical limitations cell surface levels of EpCAM could not be detected, making it impossible to draw a final conclusion. To address this question, experiments should be repeated using an experimental setting in which mRNA, total protein, and cell-surface levels of EpCAM can be assessed.

Taken together, experiments discussed in the last two chapters revealed the role of EpCAM in esophageal cancer cells and provided an explanation for the finding that EpCAM is downregulated during certain stages of carcinogenesis. It could be shown that expression of EpCAM is associated with increased proliferation of esophageal cancer cells, as well as with formation of larger tumors and a positive selection of cells in NOD/SCID mouse model. In contrast, EpCAM depletion provides cells with a more mesenchymal phenotype accompanied with increased migratory and invasive potential, and increased levels of mesenchymal markers. During induction of EMT, EpCAM was found to be downregulated. Although EpCAM overexpression alone is not sufficient to prevent effects of induced EMT, EpCAM should not be considered as a mere protein that is downregulated during EMT. Rather EpCAM plays an active role in sustaining the epithelial phenotype in esophageal cancer cells. This hypothesis is also supported by *in vivo* findings of our collaboration partners. By analysing DTCs from esophageal cancer patients, they could correlate high levels of EpCAM on these cells with an increased occurrence of lymph node metastases. However, they also found that the majority of DTCs was actually EpCAM negative, although the cells

derived from primary tumors, which were characterized by a high expression of EpCAM (Driemel *et al.* 2013). These data underlined the significance of EpCAM expression during the outgrowth of primary tumors and metastases, as well as the finding that EpCAM depletion is necessary to provide cells with a mesenchymal phenotype, allowing them to metastasize.

The next chapter will concentrate on the molecular mechanisms underlying the distinct functions of EpCAM during carcinogenesis.

5.3 The mechanism behind – How does EpCAM sustain the epithelial phenotype?

From what is known about EpCAM until now, there are two possibilities how it could sustain the epithelial phenotype of cells. On the one hand, EpCAM-specific signaling might lead to the induction or shut-down of one or more specific pathways. On the other hand, cell contacts formed by the extracellular part of EpCAM could belt cells together and thereby prevent migration and invasion.

The TGF β pathway is an important and well characterized pathway involved in cancer related EMT (Willis and Borok 2007; Tiwari *et al.* 2012) (see 1.1.2.3). To analyze if EpCAM plays a role in regulating this pathway, mRNA levels of key players involved in this pathways, i.e. the transcription factors SNAIL, SLUG, TWIST-1, TWIST-2, ZEB-1 and ZEB-2, were assessed in A549 and Kyse 30 cells, transfected with either a control or an EpCAM-specific siRNA (see 4.8.1). To ensure the functionality of the pathway in the cell lines used, activation of the pathway was tested upon treatment with TGF β . Experiments revealed an induction of the TGF β pathway in both, A549 and Kyse 30 cells, demonstrated by increased mRNA levels of SNAIL, SLUG and ZEB-2 in A549 cells (see Fig. 4.22 A), and increased levels of SNAIL and SLUG in Kyse 30 cells (see Fig. 4.23 A), respectively. However, although the TGF β pathway was shown to be functional in A549 and Kyse 30 cells, no activation could be observed upon EpCAM depletion with a specific siRNA, revealing that EpCAM downregulation is not associated with activation of the TGF β pathway in these cell lines (see Fig. 4.22 B-D, Fig. 4.23 B-D).

Besides the TGF β pathway, many other processes are known to be associated with activation and progression of EMT. Other well known pathways are the mitogen-activated protein kinase (MAPK) pathway (Grotegut *et al.* 2006; Tiwari *et al.* 2012), the

phosphoinositide 3-kinase (PI3-K) pathway (Grille *et al.* 2003; Xia *et al.* 2008) and the Notch signaling pathway (Sahlgren *et al.* 2008). However, all these pathways eventually lead to the induction and expression of SNAIL transcription factor, which could never be observed in case of EpCAM knock-down experiments, making it unlikely that EpCAM sustains the epithelial phenotype of cells by suppressing one of these pathways. Recently, also cyclin D1, a known target of EpCAM signaling (Chaves-Perez *et al.* 2013), was found to play a role in EMT, whereby downregulation of cyclin D1 led to an increased expression of mesenchymal genes and enhanced cell migration (Tobin *et al.* 2011). But although it is tempting to speculate that EpCAM sustains the epithelial phenotype by activating cyclin D1, this is not likely as downregulation of cyclin D1 also induces SLUG expression (Tobin *et al.* 2011), which was never observed in the course of EpCAM downregulation.

Other important factors which are regulated during EMT are matrix metalloproteinases (MMPs) and extracellular matrix proteins. These proteins, which play a role in altering cell-matrix and cell-cell interactions through modulation of integrin- and cadherin functions (Berrier *et al.* 2000), are known to be activated upon hepatocyte growth factor (HGF)- and TGF β signaling (Moustakas and Heldin 2012; Tiwari *et al.* 2012) and also play a role in sustaining EMT upon activation of positive feedback loops (Radisky *et al.* 2005; Billottet *et al.* 2008; Thiery *et al.* 2009). Indeed, matrix metalloproteinase 7 (*MMP7*) was found to be a target of EpCAM, whereat EpICD signaling activates *MMP7* gene expression (Denzel *et al.* 2012). It was shown that EpCAM and *MMP7* were most prominently expressed at the leading edges of head and neck carcinomas. This appears consequential as these parts of the tumor represent the sites of most prominent tissue remodeling (Denzel *et al.* 2012). The substrate spectrum of *MMP7* includes proteins such as collagen, vitronectin, proteoglycans and fibronectin. Additionally, *MMP7* is involved in the proteolytic shedding of ectodomains, whereby it regulates the biological functions of membrane proteins such as heparin-binding epidermal growth factor precursor (proHB-EGF), membrane-bound Fas ligand (FasL) and E-cadherin (Ii *et al.* 2006). Taken together, *MMP7* was found to promote tumor cell proliferation and invasion, as well as apoptosis of cells adjacent to tumor cells, thereby promoting cancer growth and progression (Shiomi and Okada 2003; Ii *et al.* 2006; Chen *et al.* 2013). Upregulation of *MMP7* by EpCAM appears to contradict the findings of this study, which provided evidence that EpCAM is involved in sustaining the epithelial phenotype of cells and prevents cell migration and invasion. However, as already mentioned, in certain types of cancer, including breast, prostate and colon carcinomas, EpCAM expression was also found to be associated with increased tumor invasion and migration (Osta *et al.* 2004; Sankpal

et al. 2009; Lin *et al.* 2012; Ni *et al.* 2013). These functions could be mediated by the EpCAM-associated expression of MMP7 (Denzel *et al.* 2012). However, it remains to be elucidated if EpCAM-mediated expression of MMP7 also plays a role in esophageal carcinomas.

Another expanding field is the regulation of EMT by miRNAs. By now, several miRNAs are known to be involved in this process, including the miR-200 family (Gregory *et al.* 2008; Korpala *et al.* 2008; Park *et al.* 2008), miR-34a (Kim *et al.* 2011a) and miR-192 (Kim *et al.* 2011b), which are found to inhibit EMT, as well as the EMT promoting miRNAs miR-155 (Kong *et al.* 2008), miR-10 (Ma *et al.* 2007) and miR-27 (Zhang *et al.* 2011). EpCAM downregulation was already associated with regulation of miRNAs. Kandalam *et al.* showed in 2012 that in Y79 retinoblastoma cells, depletion of EpCAM correlates with downregulation of miRNAs in the 17-92 miRNA cluster, which is involved in cell viability, proliferation and invasion (Kandalam *et al.* 2012). Still, to find out if EpCAM sustains the epithelial phenotype by regulating miRNAs, further experiments are necessary. One approach could make use of a set of miRNA arrays, comparing the miRNA levels of control and EpCAM-depleted cells as well as those of control and EpCAM-overexpressing cell lines. In combination with qRT-PCR candidate validation, such arrays might provide sound data about EpCAM-regulated miRNAs.

EpCAM is not only known as cell signaling molecule but also as protein mediating homophilic cell-cell adhesions (see 1.2.5.1). By keeping cells in contact, EpCAM could prevent cell scattering, migration and invasion, and thereby sustain the epithelial phenotype. To analyze if EpCAM depletion correlates with a loss of cell adhesion in esophageal cancer cells, Kyse 30 cells transfected with a control or an EpCAM-specific siRNA, as well as Kyse 520^{high} and Kyse 520^{low} cells, were compared in cell adhesion assays (see 4.8.2). Obtained experimental data showed no correlation of EpCAM expression to cell-cell adhesion in Kyse 30 (see Fig. 4.24 E-F) and Kyse 520 cells (Fig. 4.25 E-F). These results were rather unexpected as EpCAM was described and acknowledged as cell-cell adhesion molecule already in 1994 (Litvinov *et al.* 1994a; Litvinov *et al.* 1994b). However, adhesive function of EpCAM was demonstrated by overexpressing the protein in cells which actually showed no EpCAM expression. Only in these cells, EpCAM-mediated formation of intercellular contacts, cell aggregation and homotypic cell sorting, as well as EpCAM-associated suppression of invasive growth was undoubtedly documented (Litvinov *et al.* 1994b). In 1997, another study concerning the adhesive function of EpCAM was published, this time showing that EpCAM expression leads to modulation and abrogation of E-cadherin-mediated

cell-cell contacts (Litvinov *et al.* 1997). Later it was found that EpCAM abrogates E-cadherin-mediated cell adhesions without the involvement of β -catenin, by indirectly disrupting the link between α -catenin and F-actin (Winter *et al.* 2003a). Still, also in these studies experiments were performed in murine fibroblast L-cells, showing no endogenous expression of E-cadherin and EpCAM, or in immortalized mammary epithelial HBL-100 cells line, which express E-cadherin but still are EpCAM-negative. This makes it difficult to judge if the findings of these studies reflect the processes in epithelial cancer cell lines or are just side-products of exogenous EpCAM expression in actually EpCAM-negative cells. However, even if EpCAM influences cadherin-mediated cell adhesion also in the esophageal cancer cells used in this study, this should not play any role as all cell adhesion assays were performed w/o calcium, meaning that cell adhesions formed by the calcium dependent cadherins, including E-cadherin, were annihilated anyway. One possible explanation for the missing link between EpCAM depletion and a loss of cell adhesion in the majority of the performed experiments could be that downregulation of EpCAM was not efficient enough, whereby remaining EpCAM molecules were sufficient to maintain cell-cell adhesion. This hypothesis would be easy to prove by performing cell adhesion assays with epithelial cells in which EpCAM is entirely knocked out. If EpCAM indeed plays an essential role as adhesion molecule, this should lead to a strong impairment of cell adhesion. Other proteins which might interfere with this experiment are members of the carcinoembryonic antigen related cell adhesion molecules (CEACAM) protein family, which belong to the Immunoglobulin (Ig) superfamily (Pavlopoulou and Scorilas 2014). As they are able to form cell adhesions in a calcium independent way (Beauchemin and Arabzadeh 2013; Tchoupa *et al.* 2014) they may mask potential effects of EpCAM depletion. Of course, a second possible explanation for the findings in this assays could be that EpCAM only plays a minor or no role as cell adhesion molecule in (a subset of) epithelial carcinoma cells. However, findings from the second part of the adhesion assay experiments provided evidence that this is rather unlikely. Besides the impact of EpCAM on cell-cell adhesion, also a potential influence of the protein on cell-matrix adhesion was investigated. Thereby, it was observed that EpCAM significantly enhanced cell-matrix adhesion in Kyse 520 cells, whereat on average twice as many Kyse 520^{high} than Kyse 520^{low} cells showed adhesion to a matrigel matrix (Fig. 4.25 C-D). However, as already seen in case of cell-cell adhesion, EpCAM depletion had no influence on cell-matrix adhesion of siRNA transfected Kyse 30 cells (Fig. 4.24 C-D). Further experiments are essential to definitely ensure or reject the role of EpCAM as cell adhesion molecule in

epithelial cells and to get insights into how EpCAM modulates cell contacts provided by other cell adhesion molecules.

Unfortunately, none of the experiments performed in the current study was sufficient to definitely explain how EpCAM sustains the epithelial phenotype in cells. So far it could be shown that EpCAM is most likely not involved in the regulation of the TGF β pathway and that partial downregulation of EpCAM does not impair cell-cell and not always interferes with cell-matrix adhesion. Therefore, more research effort is necessary to understand not only what EpCAM does in the cells, but also how this is realized.

5.4 Conclusion

EpCAM is a well-characterized tumor-associated protein (Imrich *et al.* 2012; Patriarca *et al.* 2012), which is overexpressed in most carcinomas and primarily correlated with a bad prognosis (van der Gun *et al.* 2010). However, although the function of EpCAM is well characterized in primary tumors, so far little is known about its role during alternative stages of carcinogenesis, such as detachment of tumor cells from the primary cancer, migration and invasion of circulating and disseminated tumor cells, and metastatic outgrowth of cells at secondary sites of the body. Furthermore, there is evidence that EpCAM is not stably expressed during all processes of cancer formation and progression, but is rather downregulated in CTCs, DTCs and small metastases (Jojovic *et al.* 1998; Rao *et al.* 2005; Driemel *et al.* 2013). The aim of the current study was to find out how EpCAM expression and repression influence tumor formation and progression during the different stages of carcinogenesis to provide a better understanding of processes essential for cancer development and, thus, treatment.

Initial experiments performed during this study revealed that EpCAM is cleaved in esophageal cancer cells (see 4.2) as it has already been shown for HCT-8, FaDu and EpCAM overexpressing HEK 293 cells (Maetzel *et al.* 2009), implying that EpCAM is functional as cell signaling molecule also in the tested esophageal cell lines. Indeed, further experiments provided evidence that EpCAM expression is associated with enhanced proliferation in the these cells, as downregulation of EpCAM led to decreased proliferation rates (see 4.3.1). Same findings were made when comparing Kyse 520^{high} and Kyse 520^{low} cells, whereby Kyse 520^{low} cells displayed substantial lower cell proliferation rates compared to Kyse 520^{high} cells (see 4.3.2). Furthermore, strong expression of EpCAM was associated with the formation of larger tumors and the provision of a selection advantage *in vivo* (see 4.4). Despite these promoting effects, EpCAM was found to be redistributed into the cytoplasm and eventually downregulated in migrating cells (see 4.5.1). Based on this finding, further experiments were performed in which the effects of a downregulation of EpCAM were assessed. It was shown that low levels of EpCAM correlate with higher cell migration rates (see 4.5.2), enhanced invasive capacity (see 4.5.3) and increased levels of mesenchymal markers (see 4.5.2). Experiments including TGF β treatment of cells revealed furthermore a downregulation of EpCAM in cells forced to undergo EMT (see 4.6), an essential process in carcinoma progression (Chaffer and Weinberg 2011). In addition it could be shown that overexpression of EpCAM alone is not sufficient to prevent the effects of TGF β induced EMT (see 4.7).

Taken together, the experiments reported here revealed a positive correlation of EpCAM expression with cell proliferation and tumor growth of esophageal cancer cells *in vitro* and *in vivo*. These findings are in line with experimental data correlating EpCAM to tumor growth and progression in esophageal carcinomas as well as other cancer types. However, it could also be shown that downregulation of EpCAM alone is sufficient to induce mesenchymal traits, including enhanced migratory and invasive capacity as well as increased levels of mesenchymal markers. Thus, EpCAM must be considered as a molecule substantially participating in sustaining the epithelial phenotype of cells. However, experiments performed so far could not reveal the molecular mechanism(s) underlying this finding, providing only evidence that regulation of the TGF β pathway by EpCAM signaling (see 4.8.1) and EpCAM-mediated cell adhesion (see 4.8.2) do not seem to be involved in this process.

Based on the findings of this study the following model was postulated. High levels of EpCAM are of importance during proliferative phases of carcinogenesis, such as initial growth of the tumor and outgrowth of metastases. However, downregulation of EpCAM is essential to allow for a more quiescent and dormant state of cells, required during phases of circulation and dissemination, to enable cells to detached and migrate away from the primary tumor, and to foster the migration and invasion of cells into the surrounding tissues (Fig. 5.1).

For the first time, this study provides a rationale for the observed differences in EpCAM expression during the various steps of carcinogenesis, including findings in esophageal cancer patients, in which the majority of DTCs was found to be EpCAM-negative, despite primary tumors expressing high levels of EpCAM (Driemel *et al.* 2013). Furthermore, these findings provide an explanation for the dual role of EpCAM in certain cancer types, including esophageal carcinomas (van der Gun *et al.* 2010). Although EpCAM expression often correlates with proliferation of cancer cells and tumor growth, the recently identified role in maintaining an epithelial phenotype suggests that EpCAM expression can also be advantageous for cancer patients, as it inhibits migration and invasion of cells and thereby hinders metastatic spread. The other way round, interfering with EpCAM signaling or shutting down EpCAM expression by using therapeutic drugs, may not only result in slower cell proliferation, but also in induction of mesenchymal phenotype, in the worst case leading to metastatic spread. It is therefore mandatory to understand how EpCAM sustains the epithelial phenotype and inhibits mesenchymal changes. If adhesive functions play a major role in this process, one could think about targeting EpCAM signaling rather than EpCAM

expression itself, to slow down proliferation while preserving cell adhesion. If signaling of EpCAM is responsible for a sustained epithelial phenotype, it would be essential to identify exact pathways involved in this process to be able to develop therapeutics that selectively target pathways leading to enhanced proliferation, but do not interfere with the maintenance of the epithelial phenotype. Anyways, the dual function of EpCAM should be considered in new therapeutic approaches, which include EpCAM as target molecule.

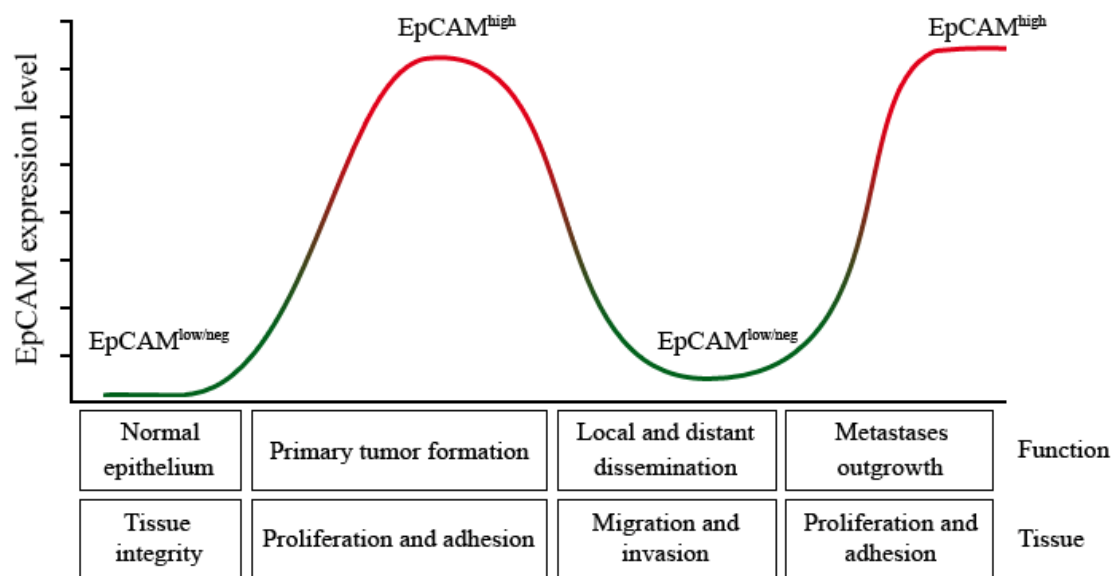


Figure 5. 1: Schematic representation of EpCAM levels throughout tumor progression.

In normal epithelium, EpCAM expression is low or absent and possibly contributes to low level of proliferation in cells close to the basal membrane and to tissue integrity. During tumor formation, EpCAM levels are strongly increased and contribute to cell proliferation. In locally and distantly disseminating tumor cells, EpCAM is substantially reduced and allows for migration and invasion. Disseminated tumor cells that have settled in distant organs to form micrometastases re-express EpCAM strongly to provide proliferative signals

Besides therapeutic implications, findings in this study also question the role of EpCAM as marker for the retrieval of CTCs and DTCs. As EpCAM seems to be frequently downregulated or even lost in migrating cells, it is likely that many CTCs and DTCs lose EpCAM expression. Indeed, in line with our findings, our collaboration partners could demonstrate that the majority of DTCs, deriving from primary esophageal carcinomas, which expressed high levels of EpCAM, is EpCAM negative (Driemel *et al.* 2013). There is increasing evidence that circulating and disseminated tumor cells escape the standard capturing methods due to EpCAM downregulation (Thurm *et al.* 2003; Rao *et al.* 2005; Gorges *et al.* 2012), eventually leading to misinterpretation of CTC and DCT numbers. To reliably detect and capture CTCs and DTCs from patients, it is mandatory to develop novel platforms, which do not only depend on EpCAM, but include other epithelial and also

mesenchymal cell surface markers. Indeed, such a system was recently published by Pecot *et al.* (Pecot *et al.* 2011), while other groups follow another road and working on completely label free methods for CTC detection (Cima *et al.* 2013; Fischer *et al.* 2013).

Finally, it is essential to point out that the findings of this study are most likely not restricted to EpCAM. Special attention should also be paid to other cancer markers associated with tumor growth and progression, including cluster of differentiation (CD) 133 (Irollo and Pirozzi 2013), CD155 (Sadej *et al.* 2014) and CC-motiv-chemokin-receptor 5 (CCR5) (Gonzalez-Martin *et al.* 2012), as their role in cancer could be more complex as it appeared at the first glance. As the current study revealed, it is essential to ask for the role of proteins not only at a single particular stage in cancer progression, but throughout the entire process of tumorigenesis. A lack of consideration of the alternating phenotype of cancer cells may lead to failure of therapeutic strategies, incorrect assessment of cases and, in the worst case, to death of cancer patients. That is why, although this study could provide new insights in the role of EpCAM during carcinogenesis, showed for the first time that EpCAM actively contributes to the maintenance of the epithelial phenotype and provided an explanation for its occasionally dual role in cancer development and progression, further research on EpCAM is absolutely mandatory. As a next step, special focus should be set on revealing the molecular mechanisms that underlie the distinct functions of EpCAM, to find out how EpCAM can be most efficiently used in anti-tumor therapies and to learn more about the mechanisms involved in carcinogenesis. To do so, the establishment of a total EpCAM knock-out cell line is essential. In combination with appropriate wild-type cells, knock-out cell lines can subsequently be used in all abovementioned experiments, including cell-cell and cell-matrix adhesion assays, various signaling studies and *in vivo* assays, and should be able to provide scientists with more clear data than it was possible so far. Besides revealing by which mechanisms EpCAM influences cells, the regulation of EpCAM itself is another important field of research. As already mentioned, our group could recently provide data which suggest a regulation of EpCAM upon endocytosis (Hachmeister *et al.* 2013). Therefore, a set of experiments, including studies with inhibitors specific for clathrin-dependent and/or clathrin-independent endocytosis, should be conducted to ensure that cells actually endocytose EpCAM. Additionally, experiments with labeled EpCAM should be performed in order to assess if endocytosis of EpCAM only leads to degradation of the protein or if it also regulates EpCAM signaling and/or turnover at the cell membrane, as it was observed in case of epithelial growth factor receptor (EGFR) (Sigismund *et al.* 2008) and TGF β -receptors (Di Guglielmo *et al.* 2003).

6 SUMMARY

Cancer is one of the leading causes of death worldwide, affecting more and more people. Although enormous research efforts during the last decades led to a more detailed understanding of processes involved in cancer formation and progression, and provided patients with innovative and more efficient treatment strategies, many mechanisms of tumorigenesis are still poorly understood.

The single span transmembrane protein EpCAM is a well-characterized tumor-associated antigen, which is overexpressed in the vast majority of carcinomas, and correlates with enhanced tumor growth, tumor progression and bad prognosis. Due to these characteristics, EpCAM is used as a prognostic and therapeutic marker, and is currently the most important marker to detect circulating (CTCs) and disseminated (DTCs) tumor cells in cancer patients. The tumor-promoting role of EpCAM is mainly due its signaling function, whereat it activates proteins involved in proliferation, like c-Myc and cyclin D1. However, EpCAM expression is not in all cases correlated with cancer progression. In thyroid and renal carcinomas EpCAM was shown to play a tumor suppressive role maybe due to its function as cell adhesion molecule. Furthermore, controversial findings in oral, gastric, colorectal and esophageal carcinomas associated EpCAM with tumor suppression and progression, pointing towards a dual role of EpCAM in these cancer types. Although the expression and function of EpCAM were intensively studied in cell lines and primary tumors, little is known about its role at alternative stages of carcinogenesis, including the generation of circulating tumor cells, invasion of cancer cells into their surrounding tissue and formation of metastases. In addition, it was found that EpCAM expression is not stable during carcinoma progression but downregulation of EpCAM could be observed in CTCs, DTCs and small metastases.

To find an explanation for the opposing roles of EpCAM in cancer formation and to identify the outcome of EpCAM downregulation during selective stages of carcinogenesis, effects of EpCAM expression and depletion were studied in esophageal cancer cells. Thereby, EpCAM was found to correlate with increased proliferation and the formation of larger tumors. Furthermore, cells expressing high levels of EpCAM seem to have a selection advantage *in vivo*. However, in migrating cells, EpCAM was found to be downregulated and specific EpCAM depletion induced mesenchymal traits in the esophageal cancer cells, including enhanced migratory and invasive capacity, as well as increased levels of mesenchymal markers. Taken together, it was shown that EpCAM expression actively

sustains the epithelial phenotype and downregulation of EpCAM is necessary to provide cells with mesenchymal characteristics.

This study for the first time provides a rationale for the observed downregulation of EpCAM at selective stages of carcinogenesis, and the contradictory findings which associate EpCAM expression with tumor suppression and progression in different types of carcinoma. Further research is necessary to elucidate the molecular mechanisms behind these findings.

7 ZUSAMMENFASSUNG (German summary)

Krebserkrankungen stellen weltweit eine der häufigsten Todesursachen dar und betreffen von Jahr zu Jahr immer mehr Menschen. In den letzten Jahrzehnten wurden die Prozesse, die an der Krebsentstehung und am Verlauf der Krankheit beteiligt sind, immer besser verstanden. Zudem konnte Patienten mit immer neuen und effektiveren Behandlungsstrategien geholfen werden. Trotz dieser bedeutenden Fortschritte, sind viele Mechanismen der Tumorgenese und -progression noch immer wenig verstanden.

Das epithelial exprimierte Transmembranprotein EpCAM ist ein gut charakterisiertes, tumorassoziiertes Molekül, das in der Mehrheit der Karzinome überexprimiert vorliegt. Seine Expression ist meist mit erhöhtem Tumorwachstum, einem schnelleren Krankheitsverlauf und einer schlechteren Prognose verbunden. EpCAM wird als prognostischer und therapeutischer Marker eingesetzt und ist derzeit der wichtigste Marker zur Isolierung und Detektion zirkulierender und disseminierter Tumorzellen in Patienten. Die tumorfördernde Rolle von EpCAM beruht hauptsächlich auf dessen Funktion als Signalmolekül, wobei es Proteine wie c-Myc und cyclin D1 aktiviert, die an der Zellproliferation beteiligt sind und diese aktivieren und verstärken. EpCAM ist jedoch nicht in allen Fällen mit dem Fortschreiten der Tumorerkrankung verbunden. In Karzinomen der Schilddrüse und der Nieren konnte vielmehr eine tumorhemmende Wirkung von EpCAM gezeigt werden, was eventuell auf dessen Rolle als Zelladhäsionsmolekül zurückzuführen ist. Studien, die sich mit Karzinomen in Mund, Magen, Darm und Speiseröhre beschäftigten, kamen zu widersprüchlichen Ergebnissen in Bezug auf EpCAM und assoziierten das Molekül in diesen Karzinomtypen sowohl mit der Förderung als auch mit der Hemmung von Karzinomentstehung und -progression, was auf eine duale Rolle von EpCAM in der Tumorgenese hindeutet. Obwohl die Eigenschaften und Funktionen von EpCAM in Primärtumoren und Zelllinien intensiv studiert wurden, ist wenig über dessen Rolle in weiteren Stadien der Tumorprogression bekannt. Es gibt jedoch Hinweise darauf, dass EpCAM nicht in allen Stadien der Karzinogenese gleichermaßen exprimiert wird. Stattdessen konnte, im Vergleich zu Primärtumoren, eine verminderte Expression in zirkulierenden und disseminierten Zellen, sowie in kleineren Metastasen beobachtet werden.

Um die teilweise widersprüchlichen Funktionen von EpCAM während der Karzinomentstehung und -progression besser zu verstehen und die Folgen einer verminderten EpCAM Expression in bestimmten Phasen der Karzinogenese zu identifizieren, wurden die

Effekte der EpCAM Expression und deren Hemmung in Speiseröhrenkrebszellen untersucht. Dabei konnte gezeigt werden, dass die Expression von EpCAM mit einer erhöhten Proliferationsrate, sowie der Bildung größerer Tumore einhergeht. Zudem wurden Hinweise darauf gefunden, dass Zellen, die EpCAM stark exprimieren, *in vivo* einen Selektionsvorteil besitzen. Dennoch wurde in migrierenden Zellen eine Verminderung der EpCAM Expression beobachtet und eine spezifische Hemmung der EpCAM Expression induzierte mesenchymale Eigenschaften, wie erhöhte Migrations- und Invasionsfähigkeit, sowie eine Erhöhung mesenchymaler Marker. Zusammenfassend konnte gezeigt werden, dass EpCAM aktiv zur Erhaltung des epithelialen Phänotyps in Zellen beiträgt und eine Verminderung der EpCAM Expression notwendig ist um die Ausbildung mesenchymaler Eigenschaften zu ermöglichen. Diese Studie gibt somit erstmals eine Erklärung für die beobachtete Verminderung der EpCAM Expression während selektiver Phasen der Karzinogenese und die scheinbar widersprüchlichen Funktionen von EpCAM als tumorförderndes und -hemmendes Molekül. Weitere Untersuchungen sind notwendig um die, diesen Ergebnissen zugrunde liegenden, molekularen Mechanismen aufzuklären.

APPENDIX

ABBREVIATIONS

| | |
|--------------------|--------------------------------------|
| °C | degree celsius |
| A | adenine |
| aa | amino acids |
| APS | ammoniumpersulfate |
| ATP | adenosine triphosphate |
| bp | base pairs |
| BSA | bovine serum albumin |
| C | cytosine |
| cDNA | complementary DNA |
| CK | cytokeratin |
| CTCs | circulating tumor cells |
| C-term | C-terminus |
| CTF | C-terminal fragment |
| ctrl | control |
| ddH ₂ O | double distilled water |
| DMEM | Dulbecco`s Modified Eagle Medium |
| DMSO | dimethyl sulfoxide |
| DNA | deoxyribonucleic acid |
| dNTP | deoxyribonucleotide triphosphate |
| DTCs | disseminated tumor cells |
| ECL | enhanced chemiluminescence |
| EDTA | ethylene diamine tetraacetic acid |
| EMT | epithelial to mesenchymal transition |
| EpCAM | epithelial cell adhesion molecule |
| EpICD | intracellular domain of EpCAM |
| GFP | green fluorescent protein |
| FACS | fluorescence activated cell sorting |
| FC | flow cytometry |
| FCS | fetal calf serum |
| g | gram |

| | |
|----------------------------------|---|
| G | guanine |
| h | hour |
| H ₂ O | water |
| IH | immunohistochemistry |
| IF | immunofluorescence |
| KH ₂ PO ₄ | potassium dihydrogen phosphate |
| KCl | potassium chloride |
| kDa | kilo Dalton |
| l | litre |
| M | molar |
| mA | milli ampere |
| max | maximal |
| mg | milligram |
| μg | microgram |
| MET | mesenchymal to epithelial transition |
| min | minute |
| ml | millilitre |
| μl | microlitre |
| mM | millimolar |
| μM | micromolar |
| MOPS | 3-(N-Morpholino)propanesulfonic acid, 4-Morpholine- propanesulfonic acid |
| mRNA | messenger RNA |
| n | nano |
| NaCl | sodium chloride |
| Na ₂ HPO ₄ | disodium hydrogen phosphate |
| n.d. | not detectable |
| nm | nanometre |
| N-term | N-terminus |
| OD | optical density |
| PAGE | polyacrylamide gelelectrophoresis |
| PBS | phosphate buffered saline |
| PBST | PBS + Tween-20 |
| PCR | polymerase chain reaction |

| | |
|-------------------|---|
| PI | propidium iodide |
| PFA | paraformaldehyde |
| PVDF | polyvinylidene fluoride |
| qRT-PCR | quantitative Real Time PCR |
| rcf | relative centrifugal force |
| RIP | regulated intramembrane proteolysis |
| RNA | ribonucleic acid |
| rpm | revolutions per minute |
| RT | reverse transcriptase |
| RT-PCR | reverse transcription PCR |
| SDS | sodium dodecyl sulfate |
| SDS-PAGE | sodium dodecyl sulfate polyacrylamide gelelectrophoresis |
| shRNA | short hairpin RNA |
| SILAC | stable isotope labeling by/with amino acids in cell culture |
| siRNA | small interfering RNA |
| T | thymidine |
| TEMED | N,N,N',N'-Tetramethyldiamin |
| TGF β | transforming growth factor β |
| TRIS | tris(hydroxymethyl)aminomethane |
| Triton X-100 | polyethylene glycol p-(1,1,3,3-tetramethylbutyl)-phenyl ether |
| Tween-20 | polyoxyethylen(20)-sorbitan-monolaurat |
| UV | ultraviolet |
| V | volt |
| v/v | volume per volume |
| WB | western blot |
| w/o | without |
| w/v | weight per volume |
| YFP | yellow fluorescent protein |
| ZnCl ₂ | zinc chloride |
| α | alpha |
| β | beta |
| Δ | delta |

LIST OF FIGURES AND TABLES

Table list

| | |
|---|----|
| Table 2. 1: List of chemicals used in the present study..... | 35 |
| Table 2. 2: List of kits used in the present study..... | 39 |
| Table 2. 3: List of primary antibodies used in the present study..... | 39 |
| Table 2. 4: List of secondary antibodies used in the present study..... | 40 |
| Table 2. 5: List of primers used in the present study..... | 40 |
| Table 2. 6: List of siRNAs used in the present study..... | 41 |
| Table 2. 7: List of shRNAs used in the present study..... | 41 |
| Table 2. 8: List of plasmids used in the present study..... | 41 |
| Table 2. 9: List of cell lines used in the present study..... | 42 |
| Table 2. 10: List of consumables used in the present study..... | 43 |
| Table 2. 11: List of equipment used in the present study..... | 44 |
| Table 2. 12: List of software used in the present study..... | 46 |

Figure list

| | |
|--|----|
| Figure 1. 1: Schematic illustration of the current cancer formation models..... | 4 |
| Figure 1. 2: Schematic illustration of basic mechanisms involved in carcinogenesis..... | 6 |
| Figure 1. 3: Schematic illustration of epithelial-to-mesenchymal transition (EMT)..... | 7 |
| Figure 1. 4: Molecular pathways involved in EMT..... | 10 |
| Figure 1. 5: TGF β signaling..... | 12 |
| Figure 1. 6: TGF β -dependent activation of EMT..... | 14 |
| Figure 1. 7: The <i>EPCAM</i> gene..... | 17 |
| Figure 1. 8: The EpCAM protein..... | 20 |
| Figure 1. 9: Amino acid sequence of EpCAM..... | 21 |
| Figure 1. 10: Cleavage and signaling of EpCAM..... | 23 |
| Figure 1. 11: Cleavage and processing of murine EpCAM..... | 24 |
| Figure 3. 1: Calculation of the mean width of scratches..... | 52 |
| Figure 4. 1: Characterisation of esophageal cancer cell lines..... | 69 |
| Figure 4. 2: Characterisation of the A549 cell line..... | 70 |
| Figure 4. 3: A549 cell lines stably expressing YFP-constructs..... | 72 |
| Figure 4. 4: Kyse 30 cell lines stably expressing YFP-constructs..... | 73 |
| Figure 4. 5: Kyse 520 ^{high} cell lines stably expressing YFP-constructs..... | 74 |
| Figure 4. 6: EpCAM is cleaved in Kyse 30 and Kyse 520 ^{high} cells..... | 75 |
| Figure 4. 7: EpCAM knock-down decreases proliferation in Kyse520 ^{high} cells..... | 77 |
| Figure 4. 8: Kyse 520 ^{high} cells proliferate faster than Kyse 520 ^{low} cells..... | 78 |
| Figure 4. 9: EpCAM expression is correlated to tumor growth <i>in vivo</i> | 81 |
| Figure 4. 10: Migrating Kyse 30 cells downregulate EpCAM expression..... | 84 |
| Figure 4. 11: Migrating Kyse 520 ^{low} cells downregulate EpCAM expression..... | 84 |
| Figure 4. 12: Scratch assays with siRNA transfected Kyse 30 cells..... | 86 |
| Figure 4. 13: Scratch assays with Kyse 520 ^{high} and Kyse 520 ^{low} cells..... | 88 |
| Figure 4. 14: Scratch assays with siRNA transfected Kyse 520 ^{low} cells..... | 90 |
| Figure 4. 15: CK8/18 staining of spheroid cryo-sections..... | 92 |

| | |
|--|-----|
| Figure 4. 16: EpCAM staining of spheroid cryo-sections. | 92 |
| Figure 4. 17: Induction of EMT results in downregulation of EpCAM in A549 cells..... | 94 |
| Figure 4. 18: Induction of EMT results in a loss of EpCAM in Kyse 30 cells. | 96 |
| Figure 4. 19: Induction of EMT results in a loss of EpCAM in Kyse 520 ^{low} cells. | 98 |
| Figure 4. 20: EpCAM overexpression does not prevent effects of TGFβ in A549 cells. | 101 |
| Figure 4. 21: EpCAM overexpression does not prevent effects of TGFβ in Kyse 30 cells. ... | 104 |
| Figure 4. 22: EpCAM knock-down does not induce the TGFβ pathway in A549 cells..... | 106 |
| Figure 4. 23: EpCAM knock-down does not induce the TGFβ pathway in Kyse 30 cells. ... | 108 |
| Figure 4. 24: Adhesion assays with siRNA transfected Kyse 30 cells..... | 111 |
| Figure 4. 25: Adhesion assays in Kyse 520 ^{high} and Kyse 520 ^{low} cells..... | 113 |
| Figure 5. 1: Schematic representation of EpCAM levels throughout tumor progression. | 133 |

REFERENCES

- Abdel-Ghany, M.; Cheng, H. C.; Elble, R. C. and Pauli, B. U. (2001). "The breast cancer beta 4 integrin and endothelial human CLCA2 mediate lung metastasis." *J Biol Chem* **276**(27): 25438-25446.
- Ahmed, N.; Maines-Bandiera, S.; Quinn, M. A.; Unger, W. G.; Dedhar, S. and Auersperg, N. (2006). "Molecular pathways regulating EGF-induced epithelio-mesenchymal transition in human ovarian surface epithelium." *Am J Physiol Cell Physiol* **290**(6): C1532-1542.
- Ahmed, S.; Liu, C. C. and Nawshad, A. (2007). "Mechanisms of palatal epithelial seam disintegration by transforming growth factor (TGF) beta3." *Dev Biol* **309**(2): 193-207.
- Akeno, N.; Miller, A. L.; Ma, X. and Wikenheiser-Brokamp, K. A. (2014). "p53 suppresses carcinoma progression by inhibiting mTOR pathway activation." *Oncogene*.
- Aktas, B.; Muller, V.; Tewes, M.; Zeitz, J.; Kasimir-Bauer, S.; Loehberg, C. R.; Rack, B.; Schneeweiss, A. and Fehm, T. (2011). "Comparison of estrogen and progesterone receptor status of circulating tumor cells and the primary tumor in metastatic breast cancer patients." *Gynecol Oncol* **122**(2): 356-360.
- Alberti, S.; Nutini, M. and Herzenberg, L. A. (1994). "DNA methylation prevents the amplification of TROP1, a tumor-associated cell surface antigen gene." *Proc Natl Acad Sci U S A* **91**(13): 5833-5837.
- Alix-Panabieres, C.; Riethdorf, S. and Pantel, K. (2008). "Circulating tumor cells and bone marrow micrometastasis." *Clin Cancer Res* **14**(16): 5013-5021.
- Amirian, E. S.; Adler-Storthz, K. and Scheurer, M. E. (2013). "Associations between human herpesvirus-6, human papillomavirus and cervical cancer." *Cancer Lett* **336**(1): 18-23.
- Anders, M.; Sarbia, M.; Grotzinger, C.; Meining, A.; Hofler, H.; Wiedenmann, B. and Rosch, T. (2008). "Expression of EpCam and villin in Barrett's esophagus and in gastric cardia." *Dis Markers* **24**(6): 287-292.
- Angelow, S.; Ahlstrom, R. and Yu, A. S. (2008). "Biology of claudins." *Am J Physiol Renal Physiol* **295**(4): F867-876.
- Ansieau, S.; Courtois-Cox, S.; Morel, A. P. and Puisieux, A. (2011). "Fail-safe program escape and EMT: a deleterious partnership." *Semin Cancer Biol* **21**(6): 392-396.
- Are, C.; Rajaram, S.; Are, M.; Raj, H.; Anderson, B. O.; Chaluvarya Swamy, R.; Vijayakumar, M.; Song, T.; Pandey, M.; Edney, J. A. and Cazap, E. L. (2013). "A review of global cancer burden: trends, challenges, strategies, and a role for surgeons." *J Surg Oncol* **107**(2): 221-226.
- Bauerle, P. A. and Gires, O. (2007). "EpCAM (CD326) finding its role in cancer." *Br J Cancer* **96**(3): 417-423.
- Balzar, M.; Bakker, H. A.; Briaire-de-Bruijn, I. H.; Fleuren, G. J.; Warnaar, S. O. and Litvinov, S. V. (1998). "Cytoplasmic tail regulates the intercellular adhesion function of the epithelial cell adhesion molecule." *Mol Cell Biol* **18**(8): 4833-4843.
- Balzar, M.; Briaire-de Bruijn, I. H.; Rees-Bakker, H. A.; Prins, F. A.; Helfrich, W.; de Leij, L.; Riethmuller, G.; Alberti, S.; Warnaar, S. O.; Fleuren, G. J. and Litvinov, S. V. (2001). "Epidermal growth factor-like repeats mediate lateral and reciprocal interactions of Ep-CAM molecules in homophilic adhesions." *Mol Cell Biol* **21**(7): 2570-2580.
- Balzar, M.; Prins, F. A.; Bakker, H. A.; Fleuren, G. J.; Warnaar, S. O. and Litvinov, S. V. (1999a). "The structural analysis of adhesions mediated by Ep-CAM." *Exp Cell Res* **246**(1): 108-121.
- Balzar, M.; Winter, M. J.; de Boer, C. J. and Litvinov, S. V. (1999b). "The biology of the 17-1A antigen (Ep-CAM)." *J Mol Med (Berl)* **77**(10): 699-712.
- Banning, A.; Tomasovic, A. and Tikkanen, R. (2011). "Functional aspects of membrane association of reggie/flotillin proteins." *Curr Protein Pept Sci* **12**(8): 725-735.
- Bao, B.; Ali, S.; Banerjee, S.; Wang, Z.; Logna, F.; Azmi, A. S.; Kong, D.; Ahmad, A.; Li, Y.; Padhye, S. and Sarkar, F. H. (2012a). "Curcumin analogue CDF inhibits pancreatic tumor growth by switching on suppressor microRNAs and attenuating EZH2 expression." *Cancer Res* **72**(1): 335-345.
- Bao, B.; Wang, Z.; Ali, S.; Ahmad, A.; Azmi, A. S.; Sarkar, S. H.; Banerjee, S.; Kong, D.; Li, Y.; Thakur, S. and Sarkar, F. H. (2012b). "Metformin inhibits cell proliferation, migration and invasion by attenuating CSC function mediated by deregulating miRNAs in pancreatic cancer cells." *Cancer Prev Res (Phila)* **5**(3): 355-364.

- Barolo, S. (2006). "Transgenic Wnt/TCF pathway reporters: all you need is Lef?" *Oncogene* **25**(57): 7505-7511.
- Barron, D. A. and Rowley, D. R. (2012). "The reactive stroma microenvironment and prostate cancer progression." *Endocr Relat Cancer* **19**(6): R187-204.
- Barzi, A. and Lenz, H. J. (2012). "Angiogenesis-related agents in esophageal cancer." *Expert Opin Biol Ther* **12**(10): 1335-1345.
- Basak, S.; Speicher, D.; Eck, S.; Wunner, W.; Maul, G.; Simmons, M. S. and Herlyn, D. (1998). "Colorectal carcinoma invasion inhibition by CO17-1A/GA733 antigen and its murine homologue." *J Natl Cancer Inst* **90**(9): 691-697.
- Beauchemin, N. and Arabzadeh, A. (2013). "Carcinoembryonic antigen-related cell adhesion molecules (CEACAMs) in cancer progression and metastasis." *Cancer Metastasis Rev* **32**(3-4): 643-671.
- Becker, S.; Solomayer, E.; Becker-Pergola, G.; Wallwiener, D. and Fehm, T. (2007). "Primary systemic therapy does not eradicate disseminated tumor cells in breast cancer patients." *Breast Cancer Res Treat* **106**(2): 239-243.
- Behrens, J.; Lowrick, O.; Klein-Hitpass, L. and Birchmeier, W. (1991). "The E-cadherin promoter: functional analysis of a G.C-rich region and an epithelial cell-specific palindromic regulatory element." *Proc Natl Acad Sci U S A* **88**(24): 11495-11499.
- Bergsagel, P. L.; Victor-Kobrin, C.; Timblin, C. R.; Trepel, J. and Kuehl, W. M. (1992). "A murine cDNA encodes a pan-epithelial glycoprotein that is also expressed on plasma cells." *J Immunol* **148**(2): 590-596.
- Berrier, A. L.; Mastrangelo, A. M.; Downward, J.; Ginsberg, M. and LaFlamme, S. E. (2000). "Activated R-ras, Rac1, PI 3-kinase and PKCepsilon can each restore cell spreading inhibited by isolated integrin beta1 cytoplasmic domains." *J Cell Biol* **151**(7): 1549-1560.
- Biddle, A.; Liang, X.; Gammon, L.; Fazil, B.; Harper, L. J.; Emich, H.; Costea, D. E. and Mackenzie, I. C. (2011). "Cancer stem cells in squamous cell carcinoma switch between two distinct phenotypes that are preferentially migratory or proliferative." *Cancer Res* **71**(15): 5317-5326.
- Billottet, C.; Tuefferd, M.; Gentien, D.; Rapinat, A.; Thiery, J. P.; Broet, P. and Jouanneau, J. (2008). "Modulation of several waves of gene expression during FGF-1 induced epithelial-mesenchymal transition of carcinoma cells." *J Cell Biochem* **104**(3): 826-839.
- Bonnomet, A.; Brysse, A.; Tachsidis, A.; Waltham, M.; Thompson, E. W.; Polette, M. and Gilles, C. (2010). "Epithelial-to-mesenchymal transitions and circulating tumor cells." *J Mammary Gland Biol Neoplasia* **15**(2): 261-273.
- Bort, R.; Signore, M.; Tremblay, K.; Martinez Barbera, J. P. and Zaret, K. S. (2006). "Hex homeobox gene controls the transition of the endoderm to a pseudostratified, cell emergent epithelium for liver bud development." *Dev Biol* **290**(1): 44-56.
- Bremer, E.; Kuijlen, J.; Samplonius, D.; Walczak, H.; de Leij, L. and Helfrich, W. (2004a). "Target cell-restricted and -enhanced apoptosis induction by a scFv:sTRAIL fusion protein with specificity for the pancarcinoma-associated antigen EGP2." *Int J Cancer* **109**(2): 281-290.
- Bremer, E.; Samplonius, D.; Kroesen, B. J.; van Genne, L.; de Leij, L. and Helfrich, W. (2004b). "Exceptionally potent anti-tumor bystander activity of an scFv:sTRAIL fusion protein with specificity for EGP2 toward target antigen-negative tumor cells." *Neoplasia* **6**(5): 636-645.
- Breuhahn, K.; Baeuerle, P. A.; Peters, M.; Prang, N.; Tox, U.; Kohne-Volland, R.; Dries, V.; Schirmacher, P. and Leo, E. (2006). "Expression of epithelial cellular adhesion molecule (EpCAM) in chronic (necro-)inflammatory liver diseases and hepatocellular carcinoma." *Hepatol Res* **34**(1): 50-56.
- Brown, D. M. and Ruoslahti, E. (2004). "Metadherin, a cell surface protein in breast tumors that mediates lung metastasis." *Cancer Cell* **5**(4): 365-374.
- Brown, R. L.; Reinke, L. M.; Damerow, M. S.; Perez, D.; Chodosh, L. A.; Yang, J. and Cheng, C. (2011). "CD44 splice isoform switching in human and mouse epithelium is essential for epithelial-mesenchymal transition and breast cancer progression." *J Clin Invest* **121**(3): 1064-1074.
- Brunner, A.; Prelog, M.; Verdorfer, I.; Tzankov, A.; Mikuz, G. and Ensinger, C. (2008). "EpCAM is predominantly expressed in high grade and advanced stage urothelial carcinoma of the bladder." *J Clin Pathol* **61**(3): 307-310.

- Cao, Q.; Yu, J.; Dhanasekaran, S. M.; Kim, J. H.; Mani, R. S.; Tomlins, S. A.; Mehra, R.; Laxman, B.; Cao, X.; Kleer, C. G.; Varambally, S. and Chinnaiyan, A. M. (2008). "Repression of E-cadherin by the polycomb group protein EZH2 in cancer." *Oncogene* **27**(58): 7274-7284.
- Chaffer, C. L. and Weinberg, R. A. (2011). "A perspective on cancer cell metastasis." *Science* **331**(6024): 1559-1564.
- Chambers, A. F.; Groom, A. C. and MacDonald, I. C. (2002). "Dissemination and growth of cancer cells in metastatic sites." *Nat Rev Cancer* **2**(8): 563-572.
- Chao, Y. L.; Shepard, C. R. and Wells, A. (2010). "Breast carcinoma cells re-express E-cadherin during mesenchymal to epithelial reverting transition." *Mol Cancer* **9**: 179.
- Chaves-Perez, A.; Mack, B.; Maetzel, D.; Kremling, H.; Eggert, C.; Harreus, U. and Gires, O. (2013). "EpCAM regulates cell cycle progression via control of cyclin D1 expression." *Oncogene* **32**(5): 641-650.
- Chen, S. H.; Hung, W. C.; Wang, P.; Paul, C. and Konstantopoulos, K. (2013). "Mesothelin binding to CA125/MUC16 promotes pancreatic cancer cell motility and invasion via MMP-7 activation." *Sci Rep* **3**: 1870.
- Cho, S. W.; Kim, S.; Kim, J. M. and Kim, J. S. (2013). "Targeted genome engineering in human cells with the Cas9 RNA-guided endonuclease." *Nat Biotechnol* **31**(3): 230-232.
- Chong, J. M. and Speicher, D. W. (2001). "Determination of disulfide bond assignments and N-glycosylation sites of the human gastrointestinal carcinoma antigen GA733-2 (CO17-1A, EGP, KS1-4, KSA, and Ep-CAM)." *J Biol Chem* **276**(8): 5804-5813.
- Cima, I.; Wen Yee, C.; Iliescu, F. S.; Min Phy, W.; Hon Lim, K.; Iliescu, C. and Han Tan, M. (2013). "Label-free isolation of circulating tumor cells in microfluidic devices: Current research and perspectives." *Biomicrofluidics* **7**(1): 11810.
- Cirulli, V.; Crisa, L.; Beattie, G. M.; Mally, M. I.; Lopez, A. D.; Fannon, A.; Ptasznik, A.; Inverardi, L.; Ricordi, C.; Deerinck, T.; Ellisman, M.; Reisfeld, R. A. and Hayek, A. (1998). "KSA antigen Ep-CAM mediates cell-cell adhesion of pancreatic epithelial cells: morphoregulatory roles in pancreatic islet development." *J Cell Biol* **140**(6): 1519-1534.
- Cirulli, V.; Ricordi, C. and Hayek, A. (1995). "E-cadherin, NCAM, and EpCAM expression in human fetal pancreata." *Transplant Proc* **27**(6): 3335.
- Cohen, S. J.; Alpaugh, R. K.; Gross, S.; O'Hara, S. M.; Smirnov, D. A.; Terstappen, L. W.; Allard, W. J.; Bilbee, M.; Cheng, J. D.; Hoffman, J. P.; Lewis, N. L.; Pellegrino, A.; Rogatko, A.; Sigurdson, E.; Wang, H.; Watson, J. C.; Weiner, L. M. and Meropol, N. J. (2006). "Isolation and characterization of circulating tumor cells in patients with metastatic colorectal cancer." *Clin Colorectal Cancer* **6**(2): 125-132.
- Conner, S. D. and Schmid, S. L. (2003). "Regulated portals of entry into the cell." *Nature* **422**(6927): 37-44.
- Criscitello, C.; Sotiriou, C. and Ignatiadis, M. (2010). "Circulating tumor cells and emerging blood biomarkers in breast cancer." *Curr Opin Oncol* **22**(6): 552-558.
- Dale, J. K.; Malapert, P.; Chal, J.; Vilhais-Neto, G.; Maroto, M.; Johnson, T.; Jayasinghe, S.; Trainor, P.; Herrmann, B. and Pourquie, O. (2006). "Oscillations of the snail genes in the presomitic mesoderm coordinate segmental patterning and morphogenesis in vertebrate somitogenesis." *Dev Cell* **10**(3): 355-366.
- Dan, Y. Y.; Riehle, K. J.; Lazaro, C.; Teoh, N.; Haque, J.; Campbell, J. S. and Fausto, N. (2006). "Isolation of multipotent progenitor cells from human fetal liver capable of differentiating into liver and mesenchymal lineages." *Proc Natl Acad Sci U S A* **103**(26): 9912-9917.
- Dave, N.; Guaita-Esteruelas, S.; Gutarra, S.; Frias, A.; Beltran, M.; Peiro, S. and de Herreros, A. G. (2011). "Functional cooperation between Snail1 and twist in the regulation of ZEB1 expression during epithelial to mesenchymal transition." *J Biol Chem* **286**(14): 12024-12032.
- Davies, J. A. (1996). "Mesenchyme to epithelium transition during development of the mammalian kidney tubule." *Acta Anat (Basel)* **156**(3): 187-201.
- de Boer, C. J.; van Krieken, J. H.; Janssen-van Rhijn, C. M. and Litvinov, S. V. (1999). "Expression of Ep-CAM in normal, regenerating, metaplastic, and neoplastic liver." *J Pathol* **188**(2): 201-206.
- Deng, B.; Li, Y.; Zhang, Y.; Bai, L. and Yang, P. (2013). "Helicobacter pylori infection and lung cancer: a review of an emerging hypothesis." *Carcinogenesis* **34**(6): 1189-1195.

- Denzel, S.; Mack, B.; Eggert, C.; Massoner, P.; Stocklein, N.; Kemming, D.; Harreus, U. and Gires, O. (2012). "MMP7 is a target of the tumour-associated antigen EpCAM." *Int J Exp Pathol* **93**(5): 341-353.
- Denzel, S.; Maetzel, D.; Mack, B.; Eggert, C.; Barr, G. and Gires, O. (2009). "Initial activation of EpCAM cleavage via cell-to-cell contact." *BMC Cancer* **9**: 402.
- Derynck, R. and Zhang, Y. E. (2003). "Smad-dependent and Smad-independent pathways in TGF-beta family signalling." *Nature* **425**(6958): 577-584.
- Deveci, M. S. and Deveci, G. (2007). "Prognostic value of p53 protein and MK-1 (a tumor-associated antigen) expression in gastric carcinoma." *Gastric Cancer* **10**(2): 112-116.
- Di Guglielmo, G. M.; Le Roy, C.; Goodfellow, A. F. and Wrana, J. L. (2003). "Distinct endocytic pathways regulate TGF-beta receptor signalling and turnover." *Nat Cell Biol* **5**(5): 410-421.
- Di Paolo, C.; Willuda, J.; Kubetzko, S.; Lauffer, I.; Tschudi, D.; Waibel, R.; Pluckthun, A.; Stahel, R. A. and Zangemeister-Wittke, U. (2003). "A recombinant immunotoxin derived from a humanized epithelial cell adhesion molecule-specific single-chain antibody fragment has potent and selective antitumor activity." *Clin Cancer Res* **9**(7): 2837-2848.
- Dick, F. A. and Rubin, S. M. (2013). "Molecular mechanisms underlying RB protein function." *Nat Rev Mol Cell Biol* **14**(5): 297-306.
- Driemel, C.; Kremling, H.; Schumacher, S.; Will, D.; Wolters, J.; Lindenlauf, N.; Mack, B.; Baldus, S. A.; Hoya, V.; Pietsch, J. M.; Panagiotidou, P.; Raba, K.; Vay, C.; Vallbohmer, D.; Harreus, U.; Knoefel, W. T.; Stoecklein, N. H. and Gires, O. (2013). "Context-dependent adaption of EpCAM expression in early systemic esophageal cancer." *Oncogene* **33**: 4904-4915
- Dudas, M.; Li, W. Y.; Kim, J.; Yang, A. and Kaartinen, V. (2007). "Palatal fusion - where do the midline cells go? A review on cleft palate, a major human birth defect." *Acta Histochem* **109**(1): 1-14.
- Dykxhoorn, D. M.; Wu, Y.; Xie, H.; Yu, F.; Lal, A.; Petrocca, F.; Martinvalet, D.; Song, E.; Lim, B. and Lieberman, J. (2009). "miR-200 enhances mouse breast cancer cell colonization to form distant metastases." *PLoS One* **4**(9): e7181.
- Edwards, D. R.; Handsley, M. M. and Pennington, C. J. (2008). "The ADAM metalloproteinases." *Mol Aspects Med* **29**(5): 258-289.
- El-Sayed, A. and Harashima, H. (2013). "Endocytosis of Gene Delivery Vectors: From Clathrin-dependent to Lipid Raft-mediated Endocytosis." *Mol Ther* **21**(6): 1118-1130.
- Ensinger, C.; Kremser, R.; Prommegger, R.; Spizzo, G. and Schmid, K. W. (2006). "EpCAM overexpression in thyroid carcinomas: a histopathological study of 121 cases." *J Immunother* **29**(5): 569-573.
- Fallot, G.; Neuveut, C. and Buendia, M. A. (2012). "Diverse roles of hepatitis B virus in liver cancer." *Curr Opin Virol* **2**(4): 467-473.
- Fang, Y.; Chen, X.; Bajpai, M.; Verma, A.; Das, K. M.; Souza, R. F.; Garman, K. S.; Donohoe, C. L.; O'Farrell, N. J.; Reynolds, J. V. and Dvorak, K. (2013). "Cellular origins and molecular mechanisms of Barrett's esophagus and esophageal adenocarcinoma." *Ann N Y Acad Sci* **1300**: 187-199.
- Fields, A. L.; Keller, A.; Schwartzberg, L.; Bernard, S.; Kardinal, C.; Cohen, A.; Schulz, J.; Eisenberg, P.; Forster, J. and Wissel, P. (2009). "Adjuvant therapy with the monoclonal antibody Edrecolomab plus fluorouracil-based therapy does not improve overall survival of patients with stage III colon cancer." *J Clin Oncol* **27**(12): 1941-1947.
- Fischer, J. C.; Niederacher, D.; Topp, S. A.; Honisch, E.; Schumacher, S.; Schmitz, N.; Zacarias Fohrding, L.; Vay, C.; Hoffmann, I.; Kasprowicz, N. S.; Hepp, P. G.; Mohrmann, S.; Nitz, U.; Stresemann, A.; Krahn, T.; Henze, T.; Griebisch, E.; Raba, K.; Rox, J. M.; Wenzel, F.; Sproll, C.; Janni, W.; Fehm, T.; Klein, C. A.; Knoefel, W. T. and Stoecklein, N. H. (2013). "Diagnostic leukapheresis enables reliable detection of circulating tumor cells of nonmetastatic cancer patients." *Proc Natl Acad Sci U S A* **110**(41): 16580-16585.
- Flatmark, K.; Guldvik, I. J.; Svensson, H.; Fleten, K. G.; Florenes, V. A.; Reed, W.; Giercksky, K. E.; Fodstad, O. and Andersson, Y. (2013). "Immunotoxin targeting EpCAM effectively inhibits peritoneal tumor growth in experimental models of mucinous peritoneal surface malignancies." *Int J Cancer* **133**(6): 1497-1506.

- Fong, D.; Steurer, M.; Obrist, P.; Barbieri, V.; Margreiter, R.; Amberger, A.; Laimer, K.; Gastl, G.; Tzankov, A. and Spizzo, G. (2008). "Ep-CAM expression in pancreatic and ampullary carcinomas: frequency and prognostic relevance." *J Clin Pathol* **61**(1): 31-35.
- Foulds, L. (1954). "The experimental study of tumor progression: a review." *Cancer Res* **14**(5): 327-339.
- Fu, Q.; He, C. and Mao, Z. R. (2013). "Epstein-Barr virus interactions with the Bcl-2 protein family and apoptosis in human tumor cells." *J Zhejiang Univ Sci B* **14**(1): 8-24.
- Gallorini, M.; Cataldi, A. and di Giacomo, V. (2012). "Cyclin-dependent kinase modulators and cancer therapy." *BioDrugs* **26**(6): 377-391.
- Gastl, G.; Spizzo, G.; Obrist, P.; Dunser, M. and Mikuz, G. (2000). "Ep-CAM overexpression in breast cancer as a predictor of survival." *Lancet* **356**(9246): 1981-1982.
- Ghosh, A. K.; Brindisi, M. and Tang, J. (2012). "Developing beta-secretase inhibitors for treatment of Alzheimer's disease." *J Neurochem* **120** Suppl 1: 71-83.
- Gires, O. (2008). "EPCAM (tumor-associated calcium signal transducer 1)." *Genet Cytogenet Oncol Haematol* (February 2008).
<http://AtlasGeneticsOncology.org/Genes/TACSTD1ID42459ch2p21.html>.
- Gires, O. (2012). "EpCAM in hepatocytes and their progenitors." *J Hepatol* **56**(2): 490-492.
- Gires, O. and Bauerle, P. A. (2010). "EpCAM as a target in cancer therapy." *J Clin Oncol* **28**(15): e239-240; author reply e241-232.
- Gires, O.; Eskofier, S.; Lang, S.; Zeidler, R. and Munz, M. (2003). "Cloning and characterisation of a 1.1 kb fragment of the carcinoma-associated epithelial cell adhesion molecule promoter." *Anticancer Res* **23**(4): 3255-3261.
- Gires, O.; Kieu, C.; Fix, P.; Schmitt, B.; Munz, M.; Wollenberg, B. and Zeidler, R. (2001). "Tumor necrosis factor alpha negatively regulates the expression of the carcinoma-associated antigen epithelial cell adhesion molecule." *Cancer* **92**(3): 620-628.
- Goel, S.; Bauer, R. J.; Desai, K.; Bulgaru, A.; Iqbal, T.; Strachan, B. K.; Kim, G.; Kaubisch, A.; Vanhove, G. F.; Goldberg, G. and Mani, S. (2007). "Pharmacokinetic and safety study of subcutaneously administered weekly ING-1, a human engineer monoclonal antibody targeting human EpCAM, in patients with advanced solid tumors." *Ann Oncol* **18**(10): 1704-1707.
- Gonzalez-Martin, A.; Mira, E. and Manes, S. (2012). "CCR5 as a potential target in cancer therapy: inhibition or stimulation?" *Anticancer Agents Med Chem* **12**(9): 1045-1057.
- Gonzalez, B.; Denzel, S.; Mack, B.; Conrad, M. and Gires, O. (2009). "EpCAM is involved in maintenance of the murine embryonic stem cell phenotype." *Stem Cells* **27**(8): 1782-1791.
- Gordon, K. J. and Blobel, G. C. (2008). "Role of transforming growth factor-beta superfamily signaling pathways in human disease." *Biochim Biophys Acta* **1782**(4): 197-228.
- Gorges, T. M.; Tinhofer, I.; Drosch, M.; Rose, L.; Zollner, T. M.; Krahn, T. and von Ahsen, O. (2012). "Circulating tumour cells escape from EpCAM-based detection due to epithelial-to-mesenchymal transition." *BMC Cancer* **12**: 178.
- Gosens, M. J.; van Kempen, L. C.; van de Velde, C. J.; van Krieken, J. H. and Nagtegaal, I. D. (2007). "Loss of membranous Ep-CAM in budding colorectal carcinoma cells." *Mod Pathol* **20**(2): 221-232.
- Goss, P. E. and Chambers, A. F. (2010). "Does tumour dormancy offer a therapeutic target?" *Nat Rev Cancer* **10**(12): 871-877.
- Gottlinger, H.; Johnson, J. and Riethmuller, G. (1986a). "Biochemical and epitope analysis of the 17-1A membrane antigen." *Hybridoma* **5** Suppl 1: S29-37.
- Gottlinger, H. G.; Funke, I.; Johnson, J. P.; Gokel, J. M. and Riethmuller, G. (1986b). "The epithelial cell surface antigen 17-1A, a target for antibody-mediated tumor therapy: its biochemical nature, tissue distribution and recognition by different monoclonal antibodies." *Int J Cancer* **38**(1): 47-53.
- Graff, J. R.; Herman, J. G.; Lapidus, R. G.; Chopra, H.; Xu, R.; Jarrard, D. F.; Isaacs, W. B.; Pitha, P. M.; Davidson, N. E. and Baylin, S. B. (1995). "E-cadherin expression is silenced by DNA hypermethylation in human breast and prostate carcinomas." *Cancer Res* **55**(22): 5195-5199.
- Greaves, M. and Maley, C. C. (2012). "Clonal evolution in cancer." *Nature* **481**(7381): 306-313.
- Gregory, P. A.; Bert, A. G.; Paterson, E. L.; Barry, S. C.; Tsykin, A.; Farshid, G.; Vadas, M. A.; Khew-Goodall, Y. and Goodall, G. J. (2008). "The miR-200 family and miR-205 regulate

- epithelial to mesenchymal transition by targeting ZEB1 and SIP1." *Nat Cell Biol* **10**(5): 593-601.
- Grille, S. J.; Bellacosa, A.; Upson, J.; Klein-Szanto, A. J.; van Roy, F.; Lee-Kwon, W.; Donowitz, M.; Tsiachlis, P. N. and Larue, L. (2003). "The protein kinase Akt induces epithelial mesenchymal transition and promotes enhanced motility and invasiveness of squamous cell carcinoma lines." *Cancer Res* **63**(9): 2172-2178.
- Groot Koerkamp, B.; Rahbari, N. N.; Buchler, M. W.; Koch, M. and Weitz, J. (2013). "Circulating tumor cells and prognosis of patients with resectable colorectal liver metastases or widespread metastatic colorectal cancer: a meta-analysis." *Ann Surg Oncol* **20**(7): 2156-2165.
- Grotegut, S.; von Schweinitz, D.; Christofori, G. and Lehenbre, F. (2006). "Hepatocyte growth factor induces cell scattering through MAPK/Egr-1-mediated upregulation of Snail." *EMBO J* **25**(15): 3534-3545.
- Guerra, E.; Lattanzio, R.; La Sorda, R.; Dini, F.; Tiboni, G. M.; Piantelli, M. and Alberti, S. (2012). "mTrop1/Epcam knockout mice develop congenital tufting enteropathy through dysregulation of intestinal E-cadherin/beta-catenin." *PLoS One* **7**(11): e49302.
- Guillot, C. and Lecuit, T. (2013). "Mechanics of epithelial tissue homeostasis and morphogenesis." *Science* **340**(6137): 1185-1189.
- Hachmeister, M.; Bobowski, K. D.; Hogle, S.; Dislich, B.; Fukumori, A.; Eggert, C.; Mack, B.; Kremling, H.; Sarrach, S.; Coscia, F.; Zimmermann, W.; Steiner, H.; Lichtenthaler, S. F. and Gires, O. (2013). "Regulated intramembrane proteolysis and degradation of murine epithelial cell adhesion molecule mEpCAM." *PLoS One* **8**(8): e71836.
- Hall, J. M.; Lee, M. K.; Newman, B.; Morrow, J. E.; Anderson, L. A.; Huey, B. and King, M. C. (1990). "Linkage of early-onset familial breast cancer to chromosome 17q21." *Science* **250**(4988): 1684-1689.
- Hanahan, D. and Coussens, L. M. (2012). "Accessories to the crime: functions of cells recruited to the tumor microenvironment." *Cancer Cell* **21**(3): 309-322.
- Hase, T.; Sato, M.; Yoshida, K.; Girard, L.; Takeyama, Y.; Horio, M.; Elshazley, M.; Oguri, T.; Sekido, Y.; Shames, D. S.; Gazdar, A. F.; Minna, J. D.; Kondo, M. and Hasegawa, Y. (2011). "Pivotal role of epithelial cell adhesion molecule in the survival of lung cancer cells." *Cancer Sci* **102**(8): 1493-1500.
- Hay, E. D. (1995). "An overview of epithelio-mesenchymal transformation." *Acta Anat (Basel)* **154**(1): 8-20.
- Heinzelmann-Schwarz, V. A.; Gardiner-Garden, M.; Henshall, S. M.; Scurry, J.; Scolyer, R. A.; Davies, M. J.; Heinzelmann, M.; Kalish, L. H.; Bali, A.; Kench, J. G.; Edwards, L. S.; Vanden Bergh, P. M.; Hacker, N. F.; Sutherland, R. L. and O'Brien, P. M. (2004). "Overexpression of the cell adhesion molecules DDR1, Claudin 3, and Ep-CAM in metaplastic ovarian epithelium and ovarian cancer." *Clin Cancer Res* **10**(13): 4427-4436.
- Hemler, M. E. (2001). "Specific tetraspanin functions." *J Cell Biol* **155**(7): 1103-1107.
- Hemler, M. E. (2013). "Tetraspanin proteins promote multiple cancer stages." *Nat Rev Cancer* **14**(1): 49-60.
- Herlyn, M.; Steplewski, Z.; Herlyn, D. and Koprowski, H. (1979). "Colorectal carcinoma-specific antigen: detection by means of monoclonal antibodies." *Proc Natl Acad Sci U S A* **76**(3): 1438-1442.
- Hiratsuka, S. (2011). "Vasculogenesis, angiogenesis and special features of tumor blood vessels." *Front Biosci (Landmark Ed)* **16**: 1413-1427.
- Hosch, S.; Kraus, J.; Scheunemann, P.; Izbicki, J. R.; Schneider, C.; Schumacher, U.; Witter, K.; Speicher, M. R. and Pantel, K. (2000). "Malignant potential and cytogenetic characteristics of occult disseminated tumor cells in esophageal cancer." *Cancer Res* **60**(24): 6836-6840.
- Ii, M.; Yamamoto, H.; Adachi, Y.; Maruyama, Y. and Shinomura, Y. (2006). "Role of matrix metalloproteinase-7 (matrilysin) in human cancer invasion, apoptosis, growth, and angiogenesis." *Exp Biol Med (Maywood)* **231**(1): 20-27.
- Iizasa, H.; Nanbo, A.; Nishikawa, J.; Jinushi, M. and Yoshiyama, H. (2012). "Epstein-Barr Virus (EBV)-associated gastric carcinoma." *Viruses* **4**(12): 3420-3439.
- Iison, D. H. (2007). "Surgery after primary chemoradiotherapy in squamous cancer of the esophagus: is the photon mightier than the sword?" *J Clin Oncol* **25**(10): 1155-1156.

- Imrich, S.; Hachmeister, M. and Gires, O. (2012). "EpCAM and its potential role in tumor-initiating cells." *Cell Adh Migr* **6**(1): 30-38.
- Irollo, E. and Pirozzi, G. (2013). "CD133: to be or not to be, is this the real question?" *Am J Transl Res* **5**(6): 563-581.
- Ito, S.; Nakanishi, H.; Ikehara, Y.; Kato, T.; Kasai, Y.; Ito, K.; Akiyama, S.; Nakao, A. and Tatematsu, M. (2001). "Real-time observation of micrometastasis formation in the living mouse liver using a green fluorescent protein gene-tagged rat tongue carcinoma cell line." *Int J Cancer* **93**(2): 212-217.
- Iwano, M.; Plieth, D.; Danoff, T. M.; Xue, C.; Okada, H. and Neilson, E. G. (2002). "Evidence that fibroblasts derive from epithelium during tissue fibrosis." *J Clin Invest* **110**(3): 341-350.
- Jemal, A.; Bray, F.; Center, M. M.; Ferlay, J.; Ward, E. and Forman, D. (2011). "Global cancer statistics." *CA Cancer J Clin* **61**(2): 69-90.
- Ji, J.; Yamashita, T. and Wang, X. W. (2011). "Wnt/beta-catenin signaling activates microRNA-181 expression in hepatocellular carcinoma." *Cell Biosci* **1**(1): 4.
- Jiang, P.; Du, W. and Yang, X. (2013). "p53 and regulation of tumor metabolism." *J Carcinog* **12**: 21.
- Johannessen, M.; Moller, S.; Hansen, T.; Moens, U. and Van Ghelue, M. (2006). "The multifunctional roles of the four-and-a-half-LIM only protein FHL2." *Cell Mol Life Sci* **63**(3): 268-284.
- Jojovic, M.; Adam, E.; Zangemeister-Wittke, U. and Schumacher, U. (1998). "Epithelial glycoprotein-2 expression is subject to regulatory processes in epithelial-mesenchymal transitions during metastases: an investigation of human cancers transplanted into severe combined immunodeficient mice." *Histochem J* **30**(10): 723-729.
- Jordan, N. V.; Prat, A.; Abell, A. N.; Zawistowski, J. S.; Sciaky, N.; Karginova, O. A.; Zhou, B.; Golitz, B. T.; Perou, C. M. and Johnson, G. L. (2013). "SWI/SNF chromatin-remodeling factor Smarcd3/Baf60c controls epithelial-mesenchymal transition by inducing Wnt5a signaling." *Mol Cell Biol* **33**(15): 3011-3025.
- Kala, R.; Peek, G. W.; Hardy, T. M. and Tollefsbol, T. O. (2013). "MicroRNAs: an emerging science in cancer epigenetics." *J Clin Bioinforma* **3**(1): 6.
- Kalluri, R. and Weinberg, R. A. (2009). "The basics of epithelial-mesenchymal transition." *J Clin Invest* **119**(6): 1420-1428.
- Kandam, M. M.; Beta, M.; Maheswari, U. K.; Swaminathan, S. and Krishnakumar, S. (2012). "Oncogenic microRNA 17-92 cluster is regulated by epithelial cell adhesion molecule and could be a potential therapeutic target in retinoblastoma." *Mol Vis* **18**: 2279-2287.
- Kasai, H.; Allen, J. T.; Mason, R. M.; Kamimura, T. and Zhang, Z. (2005). "TGF-beta1 induces human alveolar epithelial to mesenchymal cell transition (EMT)." *Respir Res* **6**: 56.
- Kasper, M.; Behrens, J.; Schuh, D. and Muller, M. (1995). "Distribution of E-cadherin and Ep-CAM in the human lung during development and after injury." *Histochem Cell Biol* **103**(4): 281-286.
- Katz, L. H.; Li, Y.; Chen, J. S.; Munoz, N. M.; Majumdar, A.; Chen, J. and Mishra, L. (2013). "Targeting TGF-beta signaling in cancer." *Expert Opin Ther Targets* **17**(7): 743-760.
- Keirsebilck, A.; Bonne, S.; Staes, K.; van Hengel, J.; Nollet, F.; Reynolds, A. and van Roy, F. (1998). "Molecular cloning of the human p120ctn catenin gene (CTNND1): expression of multiple alternatively spliced isoforms." *Genomics* **50**(2): 129-146.
- Kenny, P. A. (2007). "TACE: a new target in epidermal growth factor receptor dependent tumors." *Differentiation* **75**(9): 800-808.
- Kerosuo, L. and Bronner-Fraser, M. (2012). "What is bad in cancer is good in the embryo: importance of EMT in neural crest development." *Semin Cell Dev Biol* **23**(3): 320-332.
- Kim, J. H.; Herlyn, D.; Wong, K. K.; Park, D. C.; Schorge, J. O.; Lu, K. H.; Skates, S. J.; Cramer, D. W.; Berkowitz, R. S. and Mok, S. C. (2003). "Identification of epithelial cell adhesion molecule autoantibody in patients with ovarian cancer." *Clin Cancer Res* **9**(13): 4782-4791.
- Kim, J. H.; Jang, Y. S.; Eom, K. S.; Hwang, Y. I.; Kang, H. R.; Jang, S. H.; Kim, C. H.; Park, Y. B.; Lee, M. G.; Hyun, I. G.; Jung, K. S. and Kim, D. G. (2007). "Transforming growth factor beta1 induces epithelial-to-mesenchymal transition of A549 cells." *J Korean Med Sci* **22**(5): 898-904.
- Kim, K. K.; Kugler, M. C.; Wolters, P. J.; Robillard, L.; Galvez, M. G.; Brumwell, A. N.; Sheppard, D. and Chapman, H. A. (2006). "Alveolar epithelial cell mesenchymal transition develops in

- vivo during pulmonary fibrosis and is regulated by the extracellular matrix." *Proc Natl Acad Sci U S A* **103**(35): 13180-13185.
- Kim, N. H.; Kim, H. S.; Li, X. Y.; Lee, I.; Choi, H. S.; Kang, S. E.; Cha, S. Y.; Ryu, J. K.; Yoon, D.; Fearon, E. R.; Rowe, R. G.; Lee, S.; Maher, C. A.; Weiss, S. J. and Yook, J. I. (2011a). "A p53/miRNA-34 axis regulates Snail1-dependent cancer cell epithelial-mesenchymal transition." *J Cell Biol* **195**(3): 417-433.
- Kim, T.; Veronese, A.; Pichiorri, F.; Lee, T. J.; Jeon, Y. J.; Volinia, S.; Pineau, P.; Marchio, A.; Palatini, J.; Suh, S. S.; Alder, H.; Liu, C. G.; Dejean, A. and Croce, C. M. (2011b). "p53 regulates epithelial-mesenchymal transition through microRNAs targeting ZEB1 and ZEB2." *J Exp Med* **208**(5): 875-883.
- Kimura, H.; Kato, H.; Faried, A.; Sohda, M.; Nakajima, M.; Fukai, Y.; Miyazaki, T.; Masuda, N.; Fukuchi, M. and Kuwano, H. (2007). "Prognostic significance of EpCAM expression in human esophageal cancer." *Int J Oncol* **30**(1): 171-179.
- Klatte, T.; Pantuck, A. J.; Said, J. W.; Seligson, D. B.; Rao, N. P.; LaRochelle, J. C.; Shuch, B.; Zisman, A.; Kabbinar, F. F. and Belldegrun, A. S. (2009). "Cytogenetic and molecular tumor profiling for type 1 and type 2 papillary renal cell carcinoma." *Clin Cancer Res* **15**(4): 1162-1169.
- Klein, C. A. and Stoecklein, N. H. (2009). "Lessons from an aggressive cancer: evolutionary dynamics in esophageal carcinoma." *Cancer Res* **69**(13): 5285-5288.
- Kong, W.; Yang, H.; He, L.; Zhao, J. J.; Coppola, D.; Dalton, W. S. and Cheng, J. Q. (2008). "MicroRNA-155 is regulated by the transforming growth factor beta/Smad pathway and contributes to epithelial cell plasticity by targeting RhoA." *Mol Cell Biol* **28**(22): 6773-6784.
- Kopp, H. G.; Avecilla, S. T.; Hooper, A. T. and Rafii, S. (2005). "The bone marrow vascular niche: home of HSC differentiation and mobilization." *Physiology (Bethesda)* **20**: 349-356.
- Korpak, M.; Lee, E. S.; Hu, G. and Kang, Y. (2008). "The miR-200 family inhibits epithelial-mesenchymal transition and cancer cell migration by direct targeting of E-cadherin transcriptional repressors ZEB1 and ZEB2." *J Biol Chem* **283**(22): 14910-14914.
- Krawczyk, N.; Banys, M.; Hartkopf, A.; Hagenbeck, C.; Melcher, C. and Fehm, T. (2013). "Circulating tumour cells in breast cancer." *Ecancermedicallscience* **7**: 352.
- Kubuschok, B.; Passlick, B.; Izbicki, J. R.; Thetter, O. and Pantel, K. (1999). "Disseminated tumor cells in lymph nodes as a determinant for survival in surgically resected non-small-cell lung cancer." *J Clin Oncol* **17**(1): 19-24.
- Kuhn, S.; Koch, M.; Nubel, T.; Ladwein, M.; Antolovic, D.; Klingbeil, P.; Hildebrand, D.; Moldenhauer, G.; Langbein, L.; Franke, W. W.; Weitz, J. and Zoller, M. (2007). "A complex of EpCAM, claudin-7, CD44 variant isoforms, and tetraspanins promotes colorectal cancer progression." *Mol Cancer Res* **5**(6): 553-567.
- Kumble, S.; Omary, M. B.; Fajardo, L. F. and Triadafilopoulos, G. (1996). "Multifocal heterogeneity in villin and Ep-CAM expression in Barrett's esophagus." *Int J Cancer* **66**(1): 48-54.
- Kunavisarut, T.; Kak, I.; Macmillan, C.; Ralhan, R. and Walfish, P. G. (2012). "Immunohistochemical analysis based Ep-ICD subcellular localization index (ESLI) is a novel marker for metastatic papillary thyroid microcarcinoma." *BMC Cancer* **12**: 523.
- Labalette, C.; Renard, C. A.; Neuveut, C.; Buendia, M. A. and Wei, Y. (2004). "Interaction and functional cooperation between the LIM protein FHL2, CBP/p300, and beta-catenin." *Mol Cell Biol* **24**(24): 10689-10702.
- Laks, D. R.; Visnyei, K. and Kornblum, H. I. (2010). "Brain tumor stem cells as therapeutic targets in models of glioma." *Yonsei Med J* **51**(5): 633-640.
- Lapidot, T.; Sirard, C.; Vormoor, J.; Murdoch, B.; Hoang, T.; Caceres-Cortes, J.; Minden, M.; Paterson, B.; Caligiuri, M. A. and Dick, J. E. (1994). "A cell initiating human acute myeloid leukaemia after transplantation into SCID mice." *Nature* **367**(6464): 645-648.
- Le Naour, F.; Andre, M.; Greco, C.; Billard, M.; Sordat, B.; Emile, J. F.; Lanza, F.; Boucheix, C. and Rubinstein, E. (2006). "Profiling of the tetraspanin web of human colon cancer cells." *Mol Cell Proteomics* **5**(5): 845-857.
- Lee, E.; Hong, Y.; Choi, J.; Haam, S.; Suh, J. S.; Huh, Y. M. and Yang, J. (2012). "Highly selective CD44-specific gold nanorods for photothermal ablation of tumorigenic subpopulations generated in MCF7 mammospheres." *Nanotechnology* **23**(46): 465101.

- Lee, J. H.; Jang, S. I.; Yang, J. M.; Markova, N. G. and Steinert, P. M. (1996). "The proximal promoter of the human transglutaminase 3 gene. Stratified squamous epithelial-specific expression in cultured cells is mediated by binding of Sp1 and ets transcription factors to a proximal promoter element." *J Biol Chem* **271**(8): 4561-4568.
- Lei, Z.; Maeda, T.; Tamura, A.; Nakamura, T.; Yamazaki, Y.; Shiratori, H.; Yashiro, K.; Tsukita, S. and Hamada, H. (2012). "EpCAM contributes to formation of functional tight junction in the intestinal epithelium by recruiting claudin proteins." *Dev Biol.* **371**(2):136-145
- Leite de Oliveira, R.; Hamm, A. and Mazzone, M. (2011). "Growing tumor vessels: more than one way to skin a cat - implications for angiogenesis targeted cancer therapies." *Mol Aspects Med* **32**(2): 71-87.
- Leopold, P. L.; Vincent, J. and Wang, H. (2012). "A comparison of epithelial-to-mesenchymal transition and re-epithelialization." *Semin Cancer Biol* **22**(5-6): 471-483.
- Li, C.; Heidt, D. G.; Dalerba, P.; Burant, C. F.; Zhang, L.; Adsay, V.; Wicha, M.; Clarke, M. F. and Simeone, D. M. (2007). "Identification of pancreatic cancer stem cells." *Cancer Res* **67**(3): 1030-1037.
- Lin, C. W.; Liao, M. Y.; Lin, W. W.; Wang, Y. P.; Lu, T. Y. and Wu, H. C. (2012). "Epithelial Cell Adhesion Molecule Regulates Tumor Initiation and Tumorigenesis via Activating Reprogramming Factors and Epithelial-Mesenchymal Transition Genes Expression in Colon Cancer." *J Biol Chem.*
- Linnenbach, A. J.; Wojcierowski, J.; Wu, S. A.; Pyrc, J. J.; Ross, A. H.; Dietzschold, B.; Speicher, D. and Koprowski, H. (1989). "Sequence investigation of the major gastrointestinal tumor-associated antigen gene family, GA733." *Proc Natl Acad Sci U S A* **86**(1): 27-31.
- Lipschutz, J. H. (1998). "Molecular development of the kidney: a review of the results of gene disruption studies." *Am J Kidney Dis* **31**(3): 383-397.
- Litvinov, S. V.; Bakker, H. A.; Gourevitch, M. M.; Velders, M. P. and Warnaar, S. O. (1994a). "Evidence for a role of the epithelial glycoprotein 40 (Ep-CAM) in epithelial cell-cell adhesion." *Cell Adhes Commun* **2**(5): 417-428.
- Litvinov, S. V.; Balzar, M.; Winter, M. J.; Bakker, H. A.; Briaire-de Bruijn, I. H.; Prins, F.; Fleuren, G. J. and Warnaar, S. O. (1997). "Epithelial cell adhesion molecule (Ep-CAM) modulates cell-cell interactions mediated by classic cadherins." *J Cell Biol* **139**(5): 1337-1348.
- Litvinov, S. V.; van Driel, W.; van Rhijn, C. M.; Bakker, H. A.; van Krieken, H.; Fleuren, G. J. and Warnaar, S. O. (1996). "Expression of Ep-CAM in cervical squamous epithelia correlates with an increased proliferation and the disappearance of markers for terminal differentiation." *Am J Pathol* **148**(3): 865-875.
- Litvinov, S. V.; Velders, M. P.; Bakker, H. A.; Fleuren, G. J. and Warnaar, S. O. (1994b). "Ep-CAM: a human epithelial antigen is a homophilic cell-cell adhesion molecule." *J Cell Biol* **125**(2): 437-446.
- Lo, H. W.; Hsu, S. C.; Xia, W.; Cao, X.; Shih, J. Y.; Wei, Y.; Abbruzzese, J. L.; Hortobagyi, G. N. and Hung, M. C. (2007). "Epidermal growth factor receptor cooperates with signal transducer and activator of transcription 3 to induce epithelial-mesenchymal transition in cancer cells via up-regulation of TWIST gene expression." *Cancer Res* **67**(19): 9066-9076.
- LoBuglio, A.; Saleh, M.; Braddock, J.; Lampkin, T.; Khor, S.; Wissel, P. and al., e. (1997). "A phase I trial of the humanized anti-EGP40 monoclonal antibody 3622W94." *Proc am Soc Clin Oncol* **16**:436.
- Lu, T. Y.; Lu, R. M.; Liao, M. Y.; Yu, J.; Chung, C. H.; Kao, C. F. and Wu, H. C. (2010). "Epithelial cell adhesion molecule regulation is associated with the maintenance of the undifferentiated phenotype of human embryonic stem cells." *J Biol Chem* **285**(12): 8719-8732.
- Lujambio, A. and Lowe, S. W. (2012). "The microcosmos of cancer." *Nature* **482**(7385): 347-355.
- Luzzi, K. J.; MacDonald, I. C.; Schmidt, E. E.; Kerkvliet, N.; Morris, V. L.; Chambers, A. F. and Groom, A. C. (1998). "Multistep nature of metastatic inefficiency: dormancy of solitary cells after successful extravasation and limited survival of early micrometastases." *Am J Pathol* **153**(3): 865-873.
- Ma, L.; Teruya-Feldstein, J. and Weinberg, R. A. (2007). "Tumour invasion and metastasis initiated by microRNA-10b in breast cancer." *Nature* **449**(7163): 682-688.
- Maaser, K. and Borlak, J. (2008). "A genome-wide expression analysis identifies a network of EpCAM-induced cell cycle regulators." *Br J Cancer* **99**(10): 1635-1643.

- Maetzel, D.; Denzel, S.; Mack, B.; Canis, M.; Went, P.; Benk, M.; Kieu, C.; Papior, P.; Baeuerle, P. A.; Munz, M. and Gires, O. (2009). "Nuclear signalling by tumour-associated antigen EpCAM." *Nat Cell Biol* **11**(2): 162-171.
- Manning, A. L. and Dyson, N. J. (2012). "RB: mitotic implications of a tumour suppressor." *Nat Rev Cancer* **12**(3): 220-226.
- Mariette, C.; Piessen, G.; Balon, J. M.; Van Seuning, I. and Triboulet, J. P. (2004). "Surgery alone in the curative treatment of localised oesophageal carcinoma." *Eur J Surg Oncol* **30**(8): 869-876.
- Mariette, C.; Piessen, G. and Triboulet, J. P. (2007). "Therapeutic strategies in oesophageal carcinoma: role of surgery and other modalities." *Lancet Oncol* **8**(6): 545-553.
- Martin, B.; Schneider, R.; Janetzky, S.; Waibler, Z.; Pandur, P.; Kuhl, M.; Behrens, J.; von der Mark, K.; Starzinski-Powitz, A. and Wixler, V. (2002). "The LIM-only protein FHL2 interacts with beta-catenin and promotes differentiation of mouse myoblasts." *J Cell Biol* **159**(1): 113-122.
- Mathias, R. A.; Gopal, S. K. and Simpson, R. J. (2012). "Contribution of cells undergoing epithelial-mesenchymal transition to the tumour microenvironment." *J Proteomics*.
- Maziak, W. (2013). "The waterpipe: an emerging global risk for cancer." *Cancer Epidemiol* **37**(1): 1-4.
- McLaughlin, P. M. J.; Trzpis, M.; Kroesen, B.-J.; Helfrich, W.; Terpstra, P.; Dokter, W. H. A.; Ruiters, M. H. J.; de Leij, L. F. M. H. and Harmsen, M. C. (2004). "Use of the EGP-2//Ep-CAM promoter for targeted expression of heterologous genes in carcinoma derived cell lines." *Cancer Gene Ther* **11**(9): 603-612.
- McMahon, H. T. and Boucrot, E. (2011). "Molecular mechanism and physiological functions of clathrin-mediated endocytosis." *Nat Rev Mol Cell Biol* **12**(8): 517-533.
- Medici, D.; Hay, E. D. and Olsen, B. R. (2008). "Snail and Slug promote epithelial-mesenchymal transition through beta-catenin-T-cell factor-4-dependent expression of transforming growth factor-beta3." *Mol Biol Cell* **19**(11): 4875-4887.
- Meh, P.; Pavsic, M.; Turk, V.; Baici, A. and Lenarcic, B. (2005). "Dual concentration-dependent activity of thyroglobulin type-1 domain of testican: specific inhibitor and substrate of cathepsin L." *Biol Chem* **386**(1): 75-83.
- Mihelic, M. and Turk, D. (2007). "Two decades of thyroglobulin type-1 domain research." *Biol Chem* **388**(11): 1123-1130.
- Mishra, R. (2013). "Cell cycle-regulatory cyclins and their deregulation in oral cancer." *Oral Oncol* **49**(6): 475-481.
- Moldenhauer, G.; Momburg, F.; Moller, P.; Schwartz, R. and Hammerling, G. J. (1987). "Epithelium-specific surface glycoprotein of Mr 34,000 is a widely distributed human carcinoma marker." *Br J Cancer* **56**(6): 714-721.
- Molina, F.; Bouanani, M.; Pau, B. and Granier, C. (1996). "Characterization of the type-1 repeat from thyroglobulin, a cysteine-rich module found in proteins from different families." *Eur J Biochem* **240**(1): 125-133.
- Momburg, F.; Moldenhauer, G.; Hammerling, G. J. and Moller, P. (1987). "Immunohistochemical study of the expression of a Mr 34,000 human epithelium-specific surface glycoprotein in normal and malignant tissues." *Cancer Res* **47**(11): 2883-2891.
- Mongroo, P. S. and Rustgi, A. K. (2010). "The role of the miR-200 family in epithelial-mesenchymal transition." *Cancer Biol Ther* **10**(3): 219-222.
- Morales, A. V.; Acloque, H.; Ocana, O. H.; de Frutos, C. A.; Gold, V. and Nieto, M. A. (2007). "Snail genes at the crossroads of symmetric and asymmetric processes in the developing mesoderm." *EMBO Rep* **8**(1): 104-109.
- Morbiter, R.; Elsaesser, J.; Hausner, J. and Lahaye, T. (2011). "Assembly of custom TALE-type DNA binding domains by modular cloning." *Nucleic Acids Res* **39**(13): 5790-5799.
- Moreno-Bueno, G.; Peinado, H.; Molina, P.; Olmeda, D.; Cubillo, E.; Santos, V.; Palacios, J.; Portillo, F. and Cano, A. (2009). "The morphological and molecular features of the epithelial-to-mesenchymal transition." *Nat Protoc* **4**(11): 1591-1613.
- Mosolits, S.; Markovic, K.; Frodin, J. E.; Virving, L.; Magnusson, C. G.; Steinitz, M.; Fagerberg, J. and Mellstedt, H. (2004). "Vaccination with Ep-CAM protein or anti-idiotypic antibody induces Th1-biased response against MHC class I- and II-restricted Ep-CAM epitopes in colorectal carcinoma patients." *Clin Cancer Res* **10**(16): 5391-5402.

- Moustakas, A. and Heldin, C. H. (2012). "Induction of epithelial-mesenchymal transition by transforming growth factor beta." Semin Cancer Biol.
- Moustakas, A.; Pardali, K.; Gaal, A. and Heldin, C. H. (2002). "Mechanisms of TGF-beta signaling in regulation of cell growth and differentiation." Immunol Lett **82**(1-2): 85-91.
- Muller, V.; Stahmann, N.; Riethdorf, S.; Rau, T.; Zabel, T.; Goetz, A.; Janicke, F. and Pantel, K. (2005). "Circulating tumor cells in breast cancer: correlation to bone marrow micrometastases, heterogeneous response to systemic therapy and low proliferative activity." Clin Cancer Res **11**(10): 3678-3685.
- Munz, M.; Fellingner, K.; Hofmann, T.; Schmitt, B. and Gires, O. (2008). "Glycosylation is crucial for stability of tumour and cancer stem cell antigen EpCAM." Front Biosci **13**: 5195-5201.
- Munz, M.; Kieu, C.; Mack, B.; Schmitt, B.; Zeidler, R. and Gires, O. (2004). "The carcinoma-associated antigen EpCAM upregulates c-myc and induces cell proliferation." Oncogene **23**(34): 5748-5758.
- Munz, M.; Murr, A.; Kvesic, M.; Rau, D.; Mangold, S.; Pflanz, S.; Lumsden, J.; Volkland, J.; Fagerberg, J.; Riethmuller, G.; Ruttinger, D.; Kufer, P.; Baeuerle, P. A. and Raum, T. (2010). "Side-by-side analysis of five clinically tested anti-EpCAM monoclonal antibodies." Cancer Cell Int **10**: 44.
- Munz, M.; Zeidler, R. and Gires, O. (2005). "The tumour-associated antigen EpCAM upregulates the fatty acid binding protein E-FABP." Cancer Lett **225**(1): 151-157.
- Nakajima, Y.; Yamagishi, T.; Hokari, S. and Nakamura, H. (2000). "Mechanisms involved in valvuloseptal endocardial cushion formation in early cardiogenesis: roles of transforming growth factor (TGF)-beta and bone morphogenetic protein (BMP)." Anat Rec **258**(2): 119-127.
- Nakaya, Y. and Sheng, G. (2008). "Epithelial to mesenchymal transition during gastrulation: an embryological view." Dev Growth Differ **50**(9): 755-766.
- Nakaya, Y.; Sukowati, E. W.; Wu, Y. and Sheng, G. (2008). "RhoA and microtubule dynamics control cell-basement membrane interaction in EMT during gastrulation." Nat Cell Biol **10**(7): 765-775.
- Nalivaeva, N. N. and Turner, A. J. (2013). "The amyloid precursor protein: a biochemical enigma in brain development, function and disease." FEBS Lett **587**(13): 2046-2054.
- National Cancer Institute, h. w. c. g. c. f. S.-T. m., Date: 10.2.2014 (2014). "Fact Sheet: Metastatic Cancer."
- NCBI (2014). "EPCAM epithelial cell adhesion molecule [Homo sapiens (human)] - Gene ID: 4072."
- Ng, V. Y.; Ang, S. N.; Chan, J. X. and Choo, A. B. (2010). "Characterization of epithelial cell adhesion molecule as a surface marker on undifferentiated human embryonic stem cells." Stem Cells **28**(1): 29-35.
- Ni, J.; Cozzi, P.; Hao, J.; Beretov, J.; Chang, L.; Duan, W.; Shigdar, S.; Delprado, W.; Graham, P.; Bucci, J.; Kearsley, J. and Li, Y. (2013). "Epithelial cell adhesion molecule (EpCAM) is associated with prostate cancer metastasis and chemo/radioresistance via the PI3K/Akt/mTOR signaling pathway." Int J Biochem Cell Biol **45**(12): 2736-2748.
- Nieto, M. A. (2011). "The ins and outs of the epithelial to mesenchymal transition in health and disease." Annu Rev Cell Dev Biol **27**: 347-376.
- Nomura, T. and Katunuma, N. (2005). "Involvement of cathepsins in the invasion, metastasis and proliferation of cancer cells." J Med Invest **52**(1-2): 1-9.
- Novinec, M.; Kordis, D.; Turk, V. and Lenarcic, B. (2006). "Diversity and evolution of the thyroglobulin type-1 domain superfamily." Mol Biol Evol **23**(4): 744-755.
- Nowell, P. C. (1976). "The clonal evolution of tumor cell populations." Science **194**(4260): 23-28.
- Nubel, T.; Preobraschenski, J.; Tuncay, H.; Weiss, T.; Kuhn, S.; Ladwein, M.; Langbein, L. and Zoller, M. (2009). "Claudin-7 regulates EpCAM-mediated functions in tumor progression." Mol Cancer Res **7**(3): 285-299.
- O'Flaherty, J. D.; Barr, M.; Fennell, D.; Richard, D.; Reynolds, J.; O'Leary, J. and O'Byrne, K. (2012). "The cancer stem-cell hypothesis: its emerging role in lung cancer biology and its relevance for future therapy." J Thorac Oncol **7**(12): 1880-1890.
- Osta, W. A.; Chen, Y.; Mikhitarian, K.; Mitas, M.; Salem, M.; Hannun, Y. A.; Cole, D. J. and Gillanders, W. E. (2004). "EpCAM is overexpressed in breast cancer and is a potential target for breast cancer gene therapy." Cancer Res **64**(16): 5818-5824.

- Padua, D. and Massague, J. (2009). "Roles of TGFbeta in metastasis." *Cell Res* **19**(1): 89-102.
- Panwar, A.; Batra, R.; Lydiatt, W. M. and Ganti, A. K. (2014). "Human papilloma virus positive oropharyngeal squamous cell carcinoma: a growing epidemic." *Cancer Treat Rev* **40**(2): 215-219.
- Papageorgis, P.; Lambert, A. W.; Ozturk, S.; Gao, F.; Pan, H.; Manne, U.; Alekseyev, Y. O.; Thiagalingam, A.; Abdolmaleky, H. M.; Lenburg, M. and Thiagalingam, S. (2010). "Smad signaling is required to maintain epigenetic silencing during breast cancer progression." *Cancer Res* **70**(3): 968-978.
- Park, S. M.; Gaur, A. B.; Lengyel, E. and Peter, M. E. (2008). "The miR-200 family determines the epithelial phenotype of cancer cells by targeting the E-cadherin repressors ZEB1 and ZEB2." *Genes Dev* **22**(7): 894-907.
- Patriarca, C.; Macchi, R. M.; Marschner, A. K. and Mellstedt, H. (2012). "Epithelial cell adhesion molecule expression (CD326) in cancer: a short review." *Cancer Treat Rev* **38**(1): 68-75.
- Pauli, C.; Munz, M.; Kieu, C.; Mack, B.; Breinl, P.; Wollenberg, B.; Lang, S.; Zeidler, R. and Gires, O. (2003). "Tumor-specific glycosylation of the carcinoma-associated epithelial cell adhesion molecule EpCAM in head and neck carcinomas." *Cancer Lett* **193**(1): 25-32.
- Pavlopoulou, A. and Scorilas, A. (2014). "A comprehensive phylogenetic and structural analysis of the carcinoembryonic antigen (CEA) gene family." *Genome Biol Evol* **6**(6): 1314-1326.
- Pecot, C. V.; Bischoff, F. Z.; Mayer, J. A.; Wong, K. L.; Pham, T.; Bottsford-Miller, J.; Stone, R. L.; Lin, Y. G.; Jaladurgam, P.; Roh, J. W.; Goodman, B. W.; Merritt, W. M.; Pircher, T. J.; Mikolajczyk, S. D.; Nick, A. M.; Celestino, J.; Eng, C.; Ellis, L. M.; Deavers, M. T. and Sood, A. K. (2011). "A novel platform for detection of CK+ and CK- CTCs." *Cancer Discov* **1**(7): 580-586.
- Pericleous, M.; Mandair, D. and Caplin, M. E. (2013). "Diet and supplements and their impact on colorectal cancer." *J Gastrointest Oncol* **4**(4): 409-423.
- Person, A. D.; Klewer, S. E. and Runyan, R. B. (2005). "Cell biology of cardiac cushion development." *Int Rev Cytol* **243**: 287-335.
- Pfaffl, M. W. (2001). "A new mathematical model for relative quantification in real-time RT-PCR." *Nucleic Acids Res* **29**(9): e45.
- Philip Went, S. D., Daniel Schöpf, Holger Moch, and Gilbert Spizzo (2008). "Expression and prognostic significance of EpCAM." *J. Cancer Mol.* **3**: 169-174.
- Pino, M. S.; Balsamo, M.; Di Modugno, F.; Mottolose, M.; Alessio, M.; Melucci, E.; Milella, M.; McConkey, D. J.; Philippar, U.; Gertler, F. B.; Natali, P. G. and Nistico, P. (2008). "Human Mena+11a isoform serves as a marker of epithelial phenotype and sensitivity to epidermal growth factor receptor inhibition in human pancreatic cancer cell lines." *Clin Cancer Res* **14**(15): 4943-4950.
- Piyathilake, C. J.; Frost, A. R.; Weiss, H.; Manne, U.; Heimbürger, D. C. and Grizzle, W. E. (2000). "The expression of Ep-CAM (17-1A) in squamous cell cancers of the lung." *Hum Pathol* **31**(4): 482-487.
- Poczatek, R. B.; Myers, R. B.; Manne, U.; Oelschlager, D. K.; Weiss, H. L.; Bostwick, D. G. and Grizzle, W. E. (1999). "Ep-Cam levels in prostatic adenocarcinoma and prostatic intraepithelial neoplasia." *J Urol* **162**(4): 1462-1466.
- Radisky, D. C.; Levy, D. D.; Littlepage, L. E.; Liu, H.; Nelson, C. M.; Fata, J. E.; Leake, D.; Godden, E. L.; Albertson, D. G.; Nieto, M. A.; Werb, Z. and Bissell, M. J. (2005). "Rac1b and reactive oxygen species mediate MMP-3-induced EMT and genomic instability." *Nature* **436**(7047): 123-127.
- Ralhan, R.; Cao, J.; Lim, T.; Macmillan, C.; Freeman, J. L. and Walfish, P. G. (2010a). "EpCAM nuclear localization identifies aggressive thyroid cancer and is a marker for poor prognosis." *BMC Cancer* **10**: 331.
- Ralhan, R.; He, H. C.; So, A. K.; Tripathi, S. C.; Kumar, M.; Hasan, M. R.; Kaur, J.; Kashat, L.; MacMillan, C.; Chauhan, S. S.; Freeman, J. L. and Walfish, P. G. (2010b). "Nuclear and cytoplasmic accumulation of Ep-ICD is frequently detected in human epithelial cancers." *PLoS One* **5**(11): e14130.
- Rao, C. G.; Chianese, D.; Doyle, G. V.; Miller, M. C.; Russell, T.; Sanders, R. A., Jr. and Terstappen, L. W. (2005). "Expression of epithelial cell adhesion molecule in carcinoma cells present in blood and primary and metastatic tumors." *Int J Oncol* **27**(1): 49-57.

- Riesenberg, R.; Buchner, A.; Pohla, H. and Lindhofer, H. (2001). "Lysis of prostate carcinoma cells by trifunctional bispecific antibodies (alpha EpCAM x alpha CD3)." J Histochem Cytochem **49**(7): 911-917.
- Riethmuller, G.; Holz, E.; Schlimok, G.; Schmiegel, W.; Raab, R.; Hoffken, K.; Gruber, R.; Funke, I.; Pichlmaier, H.; Hirche, H.; Buggisch, P.; Witte, J. and Pichlmayr, R. (1998). "Monoclonal antibody therapy for resected Dukes' C colorectal cancer: seven-year outcome of a multicenter randomized trial." J Clin Oncol **16**(5): 1788-1794.
- Riethmuller, G.; Schneider-Gadicke, E.; Schlimok, G.; Schmiegel, W.; Raab, R.; Hoffken, K.; Gruber, R.; Pichlmaier, H.; Hirche, H.; Pichlmayr, R. and et al. (1994). "Randomised trial of monoclonal antibody for adjuvant therapy of resected Dukes' C colorectal carcinoma. German Cancer Aid 17-1A Study Group." Lancet **343**(8907): 1177-1183.
- Roche, (2014). "LightCycler ® 480 Instrument Operator's Manual Software Version 1.5; Stand 21.2.2014." http://icob.sinica.edu.tw/pubweb/Core%20Facilities/Data/R401-core/LightCycler480%20II_Manual_V1.5.pdf
- Rothenpieler, U. W. and Dressler, G. R. (1993). "Pax-2 is required for mesenchyme-to-epithelium conversion during kidney development." Development **119**(3): 711-720.
- Sadej, R.; Grudowska, A.; Turczyk, L.; Kordek, R. and Romanska, H. M. (2014). "CD151 in cancer progression and metastasis: a complex scenario." Lab Invest **94**(1): 41-51.
- Sahai, E. (2007). "Illuminating the metastatic process." Nat Rev Cancer **7**(10): 737-749.
- Sahlgren, C.; Gustafsson, M. V.; Jin, S.; Poellinger, L. and Lendahl, U. (2008). "Notch signaling mediates hypoxia-induced tumor cell migration and invasion." Proc Natl Acad Sci U S A **105**(17): 6392-6397.
- Saito, R. A.; Watabe, T.; Horiguchi, K.; Kohyama, T.; Saitoh, M.; Nagase, T. and Miyazono, K. (2009). "Thyroid transcription factor-1 inhibits transforming growth factor-beta-mediated epithelial-to-mesenchymal transition in lung adenocarcinoma cells." Cancer Res **69**(7): 2783-2791.
- Sampson, T. R.; Saroj, S. D.; Llewellyn, A. C.; Tzeng, Y. L. and Weiss, D. S. (2013). "A CRISPR/Cas system mediates bacterial innate immune evasion and virulence." Nature.
- Sankpal, N. V.; Willman, M. W.; Fleming, T. P.; Mayfield, J. D. and Gillanders, W. E. (2009). "Transcriptional repression of epithelial cell adhesion molecule contributes to p53 control of breast cancer invasion." Cancer Res **69**(3): 753-757.
- Sankpal, U. T.; Pius, H.; Khan, M.; Shukoor, M. I.; Maliakal, P.; Lee, C. M.; Abdelrahim, M.; Connelly, S. F. and Basha, R. (2012). "Environmental factors in causing human cancers: emphasis on tumorigenesis." Tumour Biol **33**(5): 1265-1274.
- Sansal, I. and Sellers, W. R. (2004). "The biology and clinical relevance of the PTEN tumor suppressor pathway." J Clin Oncol **22**(14): 2954-2963.
- Savagner, P.; Valles, A. M.; Jouanneau, J.; Yamada, K. M. and Thiery, J. P. (1994). "Alternative splicing in fibroblast growth factor receptor 2 is associated with induced epithelial-mesenchymal transition in rat bladder carcinoma cells." Mol Biol Cell **5**(8): 851-862.
- Savagner, P.; Yamada, K. M. and Thiery, J. P. (1997). "The zinc-finger protein slug causes desmosome dissociation, an initial and necessary step for growth factor-induced epithelial-mesenchymal transition." J Cell Biol **137**(6): 1403-1419.
- Scheunemann, P.; Stoecklein, N. H.; Hermann, K.; Rehders, A.; Eisenberger, C. F.; Knoefel, W. T. and Hosch, S. B. (2009). "Occult disseminated tumor cells in lymph nodes of patients with gastric carcinoma. A critical appraisal of assessment and relevance." Langenbecks Arch Surg **394**(1): 105-113.
- Scheunemann, P.; Stoecklein, N. H.; Rehders, A.; Bidde, M.; Metz, S.; Peiper, M.; Eisenberger, C. F.; Schulte Am Esch, J.; Knoefel, W. T. and Hosch, S. B. (2008). "Occult tumor cells in lymph nodes as a predictor for tumor relapse in pancreatic adenocarcinoma." Langenbecks Arch Surg **393**(3): 359-365.
- Schmidt, M.; Scheulen, M. E.; Dittrich, C.; Obrist, P.; Marschner, N.; Dirix, L.; Ruttinger, D.; Schuler, M.; Reinhardt, C. and Awada, A. (2010). "An open-label, randomized phase II study of adecatumumab, a fully human anti-EpCAM antibody, as monotherapy in patients with metastatic breast cancer." Ann Oncol **21**(2): 275-282.
- Schnell, U.; Cirulli, V. and Giepmans, B. N. (2013). "EpCAM: Structure and function in health and disease." Biochim Biophys Acta. **1828** (8): 1989-2001

- Schon, M. P.; Schon, M.; Klein, C. E.; Blume, U.; Bisson, S. and Orfanos, C. E. (1994). "Carcinoma-associated 38-kD membrane glycoprotein MH 99/KS 1/4 is related to proliferation and age of transformed epithelial cell lines." *J Invest Dermatol* **102**(6): 987-991.
- Schon, M. P.; Schon, M.; Mattes, M. J.; Stein, R.; Weber, L.; Alberti, S. and Klein, C. E. (1993). "Biochemical and immunological characterization of the human carcinoma-associated antigen MH 99/KS 1/4." *Int J Cancer* **55**(6): 988-995.
- Schuettengruber, B.; Chourout, D.; Vervoort, M.; Leblanc, B. and Cavalli, G. (2007). "Genome regulation by polycomb and trithorax proteins." *Cell* **128**(4): 735-745.
- Seligson, D. B.; Pantuck, A. J.; Liu, X.; Huang, Y.; Horvath, S.; Bui, M. H.; Han, K. R.; Correa, A. J.; Eeva, M.; Tze, S.; Beldegrun, A. S. and Figlin, R. A. (2004). "Epithelial cell adhesion molecule (KSA) expression: pathobiology and its role as an independent predictor of survival in renal cell carcinoma." *Clin Cancer Res* **10**(8): 2659-2669.
- Selkoe, D. J. and Wolfe, M. S. (2007). "Presenilin: running with scissors in the membrane." *Cell* **131**(2): 215-221.
- Semenza, G. L. (2013). "Cancer-stromal cell interactions mediated by hypoxia-inducible factors promote angiogenesis, lymphangiogenesis, and metastasis." *Oncogene* **32**(35): 4057-4063.
- Sheen, Y. Y.; Kim, M. J.; Park, S. A.; Park, S. Y. and Nam, J. S. (2013). "Targeting the Transforming Growth Factor-beta Signaling in Cancer Therapy." *Biomol Ther (Seoul)* **21**(5): 323-331.
- Shiomi, T. and Okada, Y. (2003). "MT1-MMP and MMP-7 in invasion and metastasis of human cancers." *Cancer Metastasis Rev* **22**(2-3): 145-152.
- Shipitsin, M.; Campbell, L. L.; Argani, P.; Weremowicz, S.; Bloushtain-Qimron, N.; Yao, J.; Nikolskaya, T.; Serebryiskaya, T.; Beroukhim, R.; Hu, M.; Halushka, M. K.; Sukumar, S.; Parker, L. M.; Anderson, K. S.; Harris, L. N.; Garber, J. E.; Richardson, A. L.; Schnitt, S. J.; Nikolsky, Y.; Gelman, R. S. and Polyak, K. (2007). "Molecular definition of breast tumor heterogeneity." *Cancer Cell* **11**(3): 259-273.
- Si-Tayeb, K.; Lemaigre, F. P. and Duncan, S. A. (2010). "Organogenesis and development of the liver." *Dev Cell* **18**(2): 175-189.
- Siewert, J. R. and Ott, K. (2007). "Are squamous and adenocarcinomas of the esophagus the same disease?" *Semin Radiat Oncol* **17**(1): 38-44.
- Sigismund, S.; Argenzio, E.; Tosoni, D.; Cavallaro, E.; Polo, S. and Di Fiore, P. P. (2008). "Clathrin-mediated internalization is essential for sustained EGFR signaling but dispensable for degradation." *Dev Cell* **15**(2): 209-219.
- Sivagnanam, M.; Mueller, J. L.; Lee, H.; Chen, Z.; Nelson, S. F.; Turner, D.; Zlotkin, S. H.; Pencharz, P. B.; Ngan, B. Y.; Libiger, O.; Schork, N. J.; Lavine, J. E.; Taylor, S.; Newbury, R. O.; Kolodner, R. D. and Hoffman, H. M. (2008). "Identification of EpCAM as the gene for congenital tufting enteropathy." *Gastroenterology* **135**(2): 429-437.
- Sleeman, J. and Steeg, P. S. (2010). "Cancer metastasis as a therapeutic target." *Eur J Cancer* **46**(7): 1177-1180.
- Song, L. B.; Li, J.; Liao, W. T.; Feng, Y.; Yu, C. P.; Hu, L. J.; Kong, Q. L.; Xu, L. H.; Zhang, X.; Liu, W. L.; Li, M. Z.; Zhang, L.; Kang, T. B.; Fu, L. W.; Huang, W. L.; Xia, Y. F.; Tsao, S. W.; Li, M.; Band, V.; Band, H.; Shi, Q. H.; Zeng, Y. X. and Zeng, M. S. (2009). "The polycomb group protein Bmi-1 represses the tumor suppressor PTEN and induces epithelial-mesenchymal transition in human nasopharyngeal epithelial cells." *J Clin Invest* **119**(12): 3626-3636.
- Song, M. S.; Salmena, L. and Pandolfi, P. P. (2012). "The functions and regulation of the PTEN tumour suppressor." *Nat Rev Mol Cell Biol* **13**(5): 283-296.
- Songun, I.; Litvinov, S. V.; van de Velde, C. J.; Pals, S. T.; Hermans, J. and van Krieken, J. H. (2005). "Loss of Ep-CAM (CO17-1A) expression predicts survival in patients with gastric cancer." *Br J Cancer* **92**(9): 1767-1772.
- Spechler, S. J. (2013). "Barrett esophagus and risk of esophageal cancer: a clinical review." *JAMA* **310**(6): 627-636.
- Spizzo, G.; Gastl, G.; Obrist, P.; Fong, D.; Haun, M.; Grunewald, K.; Parson, W.; Eichmann, C.; Millinger, S.; Fiegl, H.; Margreiter, R. and Amberger, A. (2007). "Methylation status of the Ep-CAM promoter region in human breast cancer cell lines and breast cancer tissue." *Cancer Lett* **246**(1-2): 253-261.

- Spizzo, G.; Went, P.; Dirnhofer, S.; Obrist, P.; Moch, H.; Baeuerle, P. A.; Mueller-Holzner, E.; Marth, C.; Gastl, G. and Zeimet, A. G. (2006). "Overexpression of epithelial cell adhesion molecule (Ep-CAM) is an independent prognostic marker for reduced survival of patients with epithelial ovarian cancer." *Gynecol Oncol* **103**(2): 483-488.
- Spizzo, G.; Went, P.; Dirnhofer, S.; Obrist, P.; Simon, R.; Spichtin, H.; Maurer, R.; Metzger, U.; von Castelberg, B.; Bart, R.; Stopatschinskaya, S.; Kochli, O. R.; Haas, P.; Mross, F.; Zuber, M.; Dietrich, H.; Bischoff, S.; Mirlacher, M.; Sauter, G. and Gastl, G. (2004). "High Ep-CAM expression is associated with poor prognosis in node-positive breast cancer." *Breast Cancer Res Treat* **86**(3): 207-213.
- Stingl, J.; Eaves, C. J.; Zandieh, I. and Emerman, J. T. (2001). "Characterization of bipotent mammary epithelial progenitor cells in normal adult human breast tissue." *Breast Cancer Res Treat* **67**(2): 93-109.
- Stoecklein, N. H. and Klein, C. A. (2010). "Genetic disparity between primary tumours, disseminated tumour cells, and manifest metastasis." *Int J Cancer* **126**(3): 589-598.
- Stoecklein, N. H.; Siegmund, A.; Scheunemann, P.; Luebke, A. M.; Erbersdobler, A.; Verde, P. E.; Eisenberger, C. F.; Peiper, M.; Rehders, A.; Esch, J. S.; Knoefel, W. T. and Hosch, S. B. (2006). "Ep-CAM expression in squamous cell carcinoma of the esophagus: a potential therapeutic target and prognostic marker." *BMC Cancer* **6**: 165.
- Strnad, J.; Hamilton, A. E.; Beavers, L. S.; Gamboa, G. C.; Apelgren, L. D.; Taber, L. D.; Sportsman, J. R.; Bumol, T. F.; Sharp, J. D. and Gadski, R. A. (1989). "Molecular cloning and characterization of a human adenocarcinoma/epithelial cell surface antigen complementary DNA." *Cancer Res* **49**(2): 314-317.
- Strobl-Mazzulla, P. H. and Bronner, M. E. (2012). "Epithelial to mesenchymal transition: new and old insights from the classical neural crest model." *Semin Cancer Biol* **22**(5-6): 411-416.
- Strutz, F.; Zeisberg, M.; Ziyadeh, F. N.; Yang, C. Q.; Kalluri, R.; Muller, G. A. and Neilson, E. G. (2002). "Role of basic fibroblast growth factor-2 in epithelial-mesenchymal transformation." *Kidney Int* **61**(5): 1714-1728.
- Sun, N. and Zhao, H. (2013). "Transcription activator-like effector nucleases (TALENs): a highly efficient and versatile tool for genome editing." *Biotechnol Bioeng* **110**(7): 1811-1821.
- Szala, S.; Froehlich, M.; Scollon, M.; Kasai, Y.; Steplewski, Z.; Koprowski, H. and Linnenbach, A. J. (1990). "Molecular cloning of cDNA for the carcinoma-associated antigen GA733-2." *Proc Natl Acad Sci U S A* **87**(9): 3542-3546.
- Tai, K. Y.; Shiah, S. G.; Shieh, Y. S.; Kao, Y. R.; Chi, C. Y.; Huang, E.; Lee, H. S.; Chang, L. C.; Yang, P. C. and Wu, C. W. (2007). "DNA methylation and histone modification regulate silencing of epithelial cell adhesion molecule for tumor invasion and progression." *Oncogene* **26**(27): 3989-3997.
- Takahashi, R. U.; Miyazaki, H. and Ochiya, T. (2014). "The role of microRNAs in the regulation of cancer stem cells." *Front Genet* **4**: 295.
- Takes, R. P.; Baatenburg de Jong, R. J.; Wijffels, K.; Schuurin, E.; Litvinov, S. V.; Hermans, J. and van Krieken, J. H. (2001). "Expression of genetic markers in lymph node metastases compared with their primary tumours in head and neck cancer." *J Pathol* **194**(3): 298-302.
- Tan, B. T.; Park, C. Y.; Ailles, L. E. and Weissman, I. L. (2006). "The cancer stem cell hypothesis: a work in progress." *Lab Invest* **86**(12): 1203-1207.
- Tan, G. J.; Peng, Z. K.; Lu, J. P. and Tang, F. Q. (2013). "Cathepsins mediate tumor metastasis." *World J Biol Chem* **4**(4): 91-101.
- Tan, Y. J. (2011). "Hepatitis B virus infection and the risk of hepatocellular carcinoma." *World J Gastroenterol* **17**(44): 4853-4857.
- Tarmann, T.; Dohr, G.; Schiechl, H.; Barth, S. and Hartmann, M. (1990). "Immunohistochemical detection of an epithelial membrane protein in rat embryos at different stages of development." *Acta Anat (Basel)* **137**(2): 141-145.
- Taube, J. H.; Herschkowitz, J. I.; Komurov, K.; Zhou, A. Y.; Gupta, S.; Yang, J.; Hartwell, K.; Onder, T. T.; Gupta, P. B.; Evans, K. W.; Hollier, B. G.; Ram, P. T.; Lander, E. S.; Rosen, J. M.; Weinberg, R. A. and Mani, S. A. (2010). "Core epithelial-to-mesenchymal transition interactome gene-expression signature is associated with claudin-low and metaplastic breast cancer subtypes." *Proc Natl Acad Sci U S A* **107**(35): 15449-15454.

- Tchoupa, A. K.; Schuhmacher, T. and Hauck, C. R. (2014). "Signaling by epithelial members of the CEACAM family - mucosal docking sites for pathogenic bacteria." *Cell Commun Signal* **12**: 27.
- Tewes, M.; Aktas, B.; Welt, A.; Mueller, S.; Hauch, S.; Kimmig, R. and Kasimir-Bauer, S. (2009). "Molecular profiling and predictive value of circulating tumor cells in patients with metastatic breast cancer: an option for monitoring response to breast cancer related therapies." *Breast Cancer Res Treat* **115**(3): 581-590.
- Thampoe, I. J.; Ng, J. S. and Lloyd, K. O. (1988). "Biochemical analysis of a human epithelial surface antigen: differential cell expression and processing." *Arch Biochem Biophys* **267**(1): 342-352.
- Thiery, J. P. (2002). "Epithelial-mesenchymal transitions in tumour progression." *Nat Rev Cancer* **2**(6): 442-454.
- Thiery, J. P.; Acloque, H.; Huang, R. Y. and Nieto, M. A. (2009). "Epithelial-mesenchymal transitions in development and disease." *Cell* **139**(5): 871-890.
- Thuma, F. and Zoller, M. (2013). "EpCAM-associated claudin-7 supports lymphatic spread and drug-resistance in rat pancreatic cancer." *Int J Cancer* **133**(4): pages 855–866
- Thurm, H.; Ebel, S.; Kentenich, C.; Hensen, A.; Riethdorf, S.; Coith, C.; Wallwiener, D.; Braun, S.; Oberhoff, C.; Janicke, F. and Pantel, K. (2003). "Rare expression of epithelial cell adhesion molecule on residual micrometastatic breast cancer cells after adjuvant chemotherapy." *Clin Cancer Res* **9**(7): 2598-2604.
- Timms, B. G. (2008). "Prostate development: a historical perspective." *Differentiation* **76**(6): 565-577.
- Tiwari, N.; Gheldof, A.; Tatari, M. and Christofori, G. (2012). "EMT as the ultimate survival mechanism of cancer cells." *Semin Cancer Biol* **22**(3): 194-207.
- Tjensvoll, K.; Nordgard, O. and Smaaland, R. (2014). "Circulating tumor cells in pancreatic cancer patients: methods of detection and clinical implications." *Int J Cancer* **134**(1): 1-8.
- Tobin, N. P.; Sims, A. H.; Lundgren, K. L.; Lehn, S. and Landberg, G. (2011). "Cyclin D1, Id1 and EMT in breast cancer." *BMC Cancer* **11**: 417.
- Traub, L. M. (2005). "Common principles in clathrin-mediated sorting at the Golgi and the plasma membrane." *Biochim Biophys Acta* **1744**(3): 415-437.
- Trzpis, M.; Bremer, E.; McLaughlin, P. M.; de Leij, L. F. and Harmsen, M. C. (2008). "EpCAM in morphogenesis." *Front Biosci* **13**: 5050-5055.
- Trzpis, M.; McLaughlin, P. M.; de Leij, L. M. and Harmsen, M. C. (2007a). "Epithelial cell adhesion molecule: more than a carcinoma marker and adhesion molecule." *Am J Pathol* **171**(2): 386-395.
- Trzpis, M.; Popa, E. R.; McLaughlin, P. M.; van Goor, H.; Timmer, A.; Bosman, G. W.; de Leij, L. M. and Harmsen, M. C. (2007b). "Spatial and temporal expression patterns of the epithelial cell adhesion molecule (EpCAM/EGP-2) in developing and adult kidneys." *Nephron Exp Nephrol* **107**(4): e119-131.
- Tsubura, A.; Senzaki, H.; Sasaki, M.; Hilgers, J. and Morii, S. (1992). "Immunohistochemical demonstration of breast-derived and/or carcinoma-associated glycoproteins in normal skin appendages and their tumors." *J Cutan Pathol* **19**(1): 73-79.
- van der Gun, B. T.; de Groote, M. L.; Kazemier, H. G.; Arendzen, A. J.; Terpstra, P.; Ruiters, M. H.; McLaughlin, P. M. and Rots, M. G. (2011). "Transcription factors and molecular epigenetic marks underlying EpCAM overexpression in ovarian cancer." *Br J Cancer* **105**(2): 312-319.
- van der Gun, B. T.; Melchers, L. J.; Ruiters, M. H.; de Leij, L. F.; McLaughlin, P. M. and Rots, M. G. (2010). "EpCAM in carcinogenesis: the good, the bad or the ugly." *Carcinogenesis* **31**(11): 1913-1921.
- Vanharanta, S. and Massague, J. (2013). "Origins of metastatic traits." *Cancer Cell* **24**(4): 410-421.
- Vannier, C.; Mock, K.; Brabletz, T. and Driever, W. (2013). "Zeb1 regulates E-cadherin and Epcam expression to control cell behavior in early zebrafish development." *J Biol Chem*.
- Varga, M.; Obrist, P.; Schneeberger, S.; Muhlmann, G.; Felgel-Farnholz, C.; Fong, D.; Zitt, M.; Brunhuber, T.; Schafer, G.; Gastl, G. and Spizzo, G. (2004). "Overexpression of epithelial cell adhesion molecule antigen in gallbladder carcinoma is an independent marker for poor survival." *Clin Cancer Res* **10**(9): 3131-3136.
- Vassar, R.; Kovacs, D. M.; Yan, R. and Wong, P. C. (2009). "The beta-secretase enzyme BACE in health and Alzheimer's disease: regulation, cell biology, function, and therapeutic potential." *J Neurosci* **29**(41): 12787-12794.

- Venugopal, C.; Demos, C. M.; Rao, K. S.; Pappolla, M. A. and Sambamurti, K. (2008). "Beta-secretase: structure, function, and evolution." *CNS Neurol Disord Drug Targets* **7**(3): 278-294.
- Villasenor, A.; Chong, D. C.; Henkemeyer, M. and Cleaver, O. (2010). "Epithelial dynamics of pancreatic branching morphogenesis." *Development* **137**(24): 4295-4305.
- Vincent, T.; Neve, E. P.; Johnson, J. R.; Kukalev, A.; Rojo, F.; Albanell, J.; Pietras, K.; Virtanen, I.; Philipson, L.; Leopold, P. L.; Crystal, R. G.; de Herreros, A. G.; Moustakas, A.; Pettersson, R. F. and Fuxe, J. (2009). "A SNAIL1-SMAD3/4 transcriptional repressor complex promotes TGF-beta mediated epithelial-mesenchymal transition." *Nat Cell Biol* **11**(8): 943-950.
- Warzecha, C. C.; Jiang, P.; Amirikian, K.; Dittmar, K. A.; Lu, H.; Shen, S.; Guo, W.; Xing, Y. and Carstens, R. P. (2010). "An ESRP-regulated splicing programme is abrogated during the epithelial-mesenchymal transition." *EMBO J* **29**(19): 3286-3300.
- Warzecha, C. C.; Sato, T. K.; Nabet, B.; Hogenesch, J. B. and Carstens, R. P. (2009). "ESRP1 and ESRP2 are epithelial cell-type-specific regulators of FGFR2 splicing." *Mol Cell* **33**(5): 591-601.
- Weissenstein, U.; Schumann, A.; Reif, M.; Link, S.; Toffol-Schmidt, U. D. and Heusser, P. (2012). "Detection of circulating tumor cells in blood of metastatic breast cancer patients using a combination of cytokeratin and EpCAM antibodies." *BMC Cancer* **12**: 206.
- Wendt, M. K.; Tian, M. and Schiemann, W. P. (2012). "Deconstructing the mechanisms and consequences of TGF-beta-induced EMT during cancer progression." *Cell Tissue Res* **347**(1): 85-101.
- Wenqi, D.; Li, W.; Shanshan, C.; Bei, C.; Yafei, Z.; Feihu, B.; Jie, L. and Daiming, F. (2009). "EpCAM is overexpressed in gastric cancer and its downregulation suppresses proliferation of gastric cancer." *J Cancer Res Clin Oncol* **135**(9): 1277-1285.
- Went, P.; Dirnhofer, S.; Salvisberg, T.; Amin, M. B.; Lim, S. D.; Diener, P. A. and Moch, H. (2005). "Expression of epithelial cell adhesion molecule (EpCam) in renal epithelial tumors." *Am J Surg Pathol* **29**(1): 83-88.
- Went, P.; Vasei, M.; Bubendorf, L.; Terracciano, L.; Tornillo, L.; Riede, U.; Kononen, J.; Simon, R.; Sauter, G. and Baeuerle, P. A. (2006). "Frequent high-level expression of the immunotherapeutic target Ep-CAM in colon, stomach, prostate and lung cancers." *Br J Cancer* **94**(1): 128-135.
- Went, P. T. H.; Lugli, A.; Meier, S.; Bundi, M.; Mirlacher, M.; Sauter, G. and Dirnhofer, S. (2004). "Frequent EpCam protein expression in human carcinomas." *Human Pathology* **35**(1): 122-128.
- Willis, B. C. and Borok, Z. (2007). "TGF-beta-induced EMT: mechanisms and implications for fibrotic lung disease." *Am J Physiol Lung Cell Mol Physiol* **293**(3): L525-534.
- Winter, M. J.; Cirulli, V.; Briaire-de Bruijn, I. H. and Litvinov, S. V. (2007). "Cadherins are regulated by Ep-CAM via phosphatidylinositol-3 kinase." *Mol Cell Biochem* **302**(1-2): 19-26.
- Winter, M. J.; Nagelkerken, B.; Mertens, A. E.; Rees-Bakker, H. A.; Briaire-de Bruijn, I. H. and Litvinov, S. V. (2003a). "Expression of Ep-CAM shifts the state of cadherin-mediated adhesions from strong to weak." *Exp Cell Res* **285**(1): 50-58.
- Winter, M. J.; Nagtegaal, I. D.; van Krieken, J. H. and Litvinov, S. V. (2003b). "The epithelial cell adhesion molecule (Ep-CAM) as a morphoregulatory molecule is a tool in surgical pathology." *Am J Pathol* **163**(6): 2139-2148.
- Wong, C. W.; Song, C.; Grimes, M. M.; Fu, W.; Dewhirst, M. W.; Muschel, R. J. and Al-Mehdi, A. B. (2002). "Intravascular location of breast cancer cells after spontaneous metastasis to the lung." *Am J Pathol* **161**(3): 749-753.
- Wong, N. A.; Warren, B. F.; Piris, J.; Maynard, N.; Marshall, R. and Bodmer, W. F. (2006). "EpCAM and gpA33 are markers of Barrett's metaplasia." *J Clin Pathol* **59**(3): 260-263.
- Wooster, R.; Neuhausen, S. L.; Mangion, J.; Quirk, Y.; Ford, D.; Collins, N.; Nguyen, K.; Seal, S.; Tran, T.; Averill, D. and et al. (1994). "Localization of a breast cancer susceptibility gene, BRCA2, to chromosome 13q12-13." *Science* **265**(5181): 2088-2090.
- World-Health-Organization (2008). "THE GLOBAL BURDEN OF DISEASE 2004 UPDATE; http://www.who.int/healthinfo/global_burden_disease/GBD_report_2004update_full.pdf."
- World-Health-Organization (2013). "Regional estimates for 2000-2011 - CAUSE-SPECIFIC MORTALITY - Global summary estimates; http://www.who.int/healthinfo/global_burden_disease/estimates_regional/en/index.html".

- Wroblewski, L. E. and Peek, R. M., Jr. (2013). "Helicobacter pylori in gastric carcinogenesis: mechanisms." *Gastroenterol Clin North Am* **42**(2): 285-298.
- Wu, C. J.; Mannan, P.; Lu, M. and Udey, M. C. (2013). "Epithelial cell adhesion molecule (EpCAM) regulates claudin dynamics and tight junctions." *J Biol Chem* **288**(17): 12253-12268.
- Wu, K. J. and Yang, M. H. (2011). "Epithelial-mesenchymal transition and cancer stemness: the Twist1-Bmi1 connection." *Biosci Rep* **31**(6): 449-455.
- Xia, N.; Thodeti, C. K.; Hunt, T. P.; Xu, Q.; Ho, M.; Whitesides, G. M.; Westervelt, R. and Ingber, D. E. (2008). "Directional control of cell motility through focal adhesion positioning and spatial control of Rac activation." *FASEB J* **22**(6): 1649-1659.
- Yamashita, T.; Budhu, A.; Forgues, M. and Wang, X. W. (2007). "Activation of Hepatic Stem Cell Marker EpCAM by Wnt- β -Catenin Signaling in Hepatocellular Carcinoma." *Cancer Res* **67**(22): 10831-10839.
- Yang, J. and Weinberg, R. A. (2008). "Epithelial-mesenchymal transition: at the crossroads of development and tumor metastasis." *Dev Cell* **14**(6): 818-829.
- Yang, L.; Lin, C. and Liu, Z. R. (2006). "P68 RNA helicase mediates PDGF-induced epithelial mesenchymal transition by displacing Axin from beta-catenin." *Cell* **127**(1): 139-155.
- Yoon, S. M.; Gerasimidou, D.; Kuwahara, R.; Hytiroglou, P.; Yoo, J. E.; Park, Y. N. and Theise, N. D. (2011). "Epithelial cell adhesion molecule (EpCAM) marks hepatocytes newly derived from stem/progenitor cells in humans." *Hepatology* **53**(3): 964-973.
- Yu, Z.; Pestell, T. G.; Lisanti, M. P. and Pestell, R. G. (2012). "Cancer stem cells." *Int J Biochem Cell Biol* **44**(12): 2144-2151.
- Yunta, M. and Lazo, P. A. (2003). "Tetraspanin proteins as organisers of membrane microdomains and signalling complexes." *Cell Signal* **15**(6): 559-564.
- Zavadil, J. and Bottinger, E. P. (2005). "TGF-beta and epithelial-to-mesenchymal transitions." *Oncogene* **24**(37): 5764-5774.
- Zeisberg, M.; Shah, A. A. and Kalluri, R. (2005). "Bone morphogenic protein-7 induces mesenchymal to epithelial transition in adult renal fibroblasts and facilitates regeneration of injured kidney." *J Biol Chem* **280**(9): 8094-8100.
- Zeisberg, M.; Yang, C.; Martino, M.; Duncan, M. B.; Rieder, F.; Tanjore, H. and Kalluri, R. (2007). "Fibroblasts derive from hepatocytes in liver fibrosis via epithelial to mesenchymal transition." *J Biol Chem* **282**(32): 23337-23347.
- Zellweger, T.; Ninck, C.; Bloch, M.; Mirlacher, M.; Koivisto, P. A.; Helin, H. J.; Mihatsch, M. J.; Gasser, T. C. and Bubendorf, L. (2005). "Expression patterns of potential therapeutic targets in prostate cancer." *Int J Cancer* **113**(4): 619-628.
- Zhang, Z.; Liu, S.; Shi, R. and Zhao, G. (2011). "miR-27 promotes human gastric cancer cell metastasis by inducing epithelial-to-mesenchymal transition." *Cancer Genet* **204**(9): 486-491.
- Zhao, F.; Zhang, J.; Liu, Y. S.; Li, L. and He, Y. L. (2011). "Research advances on flotillins." *Virology* **8**: 479.
- Zorzos, J.; Zizi, A.; Bakiras, A.; Pectasidis, D.; Skarlos, D. V.; Zorzos, H.; Elemenoglou, J. and Likourinas, M. (1995). "Expression of a cell surface antigen recognized by the monoclonal antibody AUA1 in bladder carcinoma: an immunohistochemical study." *Eur Urol* **28**(3): 251-254.

PUBLICATIONS

During my work as PhD student I was able to contribute to the following publications.

First authorship

Context-dependent adaption of EpCAM expression in early systemic esophageal cancer.

Driemel C*, Kremling H*, Schumacher S, Will D, Wolters J, Lindenlauf N, Mack B, Baldus SA, Hoya V, Pietsch JM, Panagiotidou P, Raba K, Vay C, Vallböhmer D, Harréus U, Knoefel WT, Stoecklein NH, Gires O.

Oncogene. 2013 Oct 21.; PMID: 24141784; doi: 10.1038/onc.2013.441.

*Both authors contributed equally to this work and are listed in alphabetical order.

Co-authorships

Regulated intramembrane proteolysis and degradation of murine epithelial cell adhesion molecule mEpCAM.

Hachmeister M, Bobowski KD, Hogl S, Dislich B, Fukumori A, Eggert C, Mack B, Kremling H, Sarrach S, Coscia F, Zimmermann W, Steiner H, Lichtenthaler SF, Gires O. PLoS One. 2013 Aug 29;8(8):e71836.; PMID: 24009667; doi:10.1371/journal.pone.0071836.

EpCAM regulates cell cycle progression via control of cyclin D1 expression.

Chaves-Pérez A, Mack B, Maetzel D, Kremling H, Eggert C, Harréus U, Gires O. Oncogene. 2013 Jan 31;32(5):641-50.; PMID: 22391566; doi: 10.1038/onc.2012.75. Epub 2012 Mar 5.

ACKNOWLEDGEMENTS

First of all I want to thank my supervisor Prof. Dr. Olivier Gires, for giving me the chance to work in his lab and providing me with the interesting and challenging project of my PhD thesis. Thank you very much for your great supervision, for always taking time to discuss and for all the things I could learn from you during the last years.

A special Thank you! to my colleagues Sannia Sarrach, Carola Eggert, Matthias Hachmeister, Brigitte Mack, Gisela Kranz, Elisabeth Pfrogner, Darko Libl, Petra Massoner, Martina Rami, Karolina Bobowski and all the other people of the Head and Neck research department. I am sure that I will never ever find such great colleagues like you. I want to thank you for the wonderful time I could spend with you, for all your help and advice, for all the things I could learn from you and for all the fun we had together.

Special thanks again to Piri, Gisela and Darko for providing the best immunofluorescence and -histochemistry samples. We would be lost without you! Piri, I will always miss you when I will use a confocal microscope.

Of course I also want to thank our cooperation partners in Düsseldorf, especially Christiane Driemel and Prof. Dr. Nikolas Stoecklein. Thank you for all your help and support, for discussions and brainstorming. Christiane, although we never met, it was a pleasure to work with you.

I want to thank all the friends I had and have in my life, especially my best friend Sabrina, who stands by my side for I don't know how long and never let me down. Another special thanks to Kathi, Betti, Rike and Maike who together with me faced the joy and suffering of studying biology. I wish I could see all of you much more often!

Special thanks also to my whole family, including all my aunts, uncles, cousins and all the other people who were, are or will be a part of this big, crazy family. What would I do without you? Of course I especially want to thank my parents and my sister for all their love, help and support during my whole life, for always believing in me and for giving me the freedom to do the things that I love.

Finally, I want to thank Kevin. I really don't know what I should write as you mean so much to me that it is impossible to put all these things in a few words. Thank you so much for being my love and my friend, for always backing me up, never letting me down, for giving me strength and courage to make my way and of course for enduring my grumbling. Thank you for sharing your life with me.

Thank you all!